University of Cyprus

DEPARTMENT OF BIOLOGICAL SCIENCES

PATTERNS OF PHENOTYPIC AND GENETIC VARIATION IN *POGONIULUS* TINKERBIRDS AND THEIR ROLE IN INTERACTIONS AT CONTACT ZONES

NWANKWO EMMANUEL CHIBUIKE

A Dissertation Submitted to the University of Cyprus in Partial Fulfillment of the Requirements for the Degree of Doctor of Philosophy

MAY 2018

VALIDATION PAGE

Doctoral Candidate: Nwankwo Emmanuel Chibuike

Doctoral Dissertation Title: PATTERNS OF PHENOTYPIC AND GENETIC VARIATION IN *POGONIULUS* TINKERBIRDS AND THEIR ROLE IN INTERACTIONS AT CONTACT ZONES

The present Doctoral Dissertation was submitted in partial fulfillment of the requirements for the Degree of Doctor of Philosophy at the ***Department of*** *Biological Sciences and was approved on the 9th of May by the members of the* ***Examination Committee****.*

Examination Committee:

Research Supervisor: Alexander Kirschel, Assitant Professor_____

(Name, position and signature)

Committee Member: Anna Papadopoulou, Assitant Professor _____

(Name, position and signature)

Committee Member: Spyros Sfendourakis, Associate Professor

(Name, position and signature)

Committee Member: Claire Doutrelant**,** Assitant Professor

(Name, position and signature)

Committee Member: Jérôme Fuchs**,** Assitant Professor

(Name, position and signature)

DECLARATION OF DOCTORAL CANDIDATE

The present doctoral dissertation was submitted in partial fulfillment of the requirements for the degree of Doctor of Philosophy of the University of Cyprus. It is a product of original work of my own, unless otherwise mentioned through references, notes, or any other statements.

Nwankwo Emmanuel Chibuike

……..

Περίληψη

Τα όρια των ειδών καθορίζονται κυρίως βάσει των φαινοτυπικών χαρακτηριστικών ή της μοριακής φυλογενετικής αλλά τα πρότυπα δεν είναι πάντοτε σταθερά. Επίσης, τέτοιες μεθόδοι μπορεί να αγνοήσουν το ρόλο των χαρακτηριστικών που είναι σημαντικά στην αναπαραγωγική απομόνωση. Εδώ, συγκρίνω τα πρότυπα διαφοροποίησης μερικών φαινοτυπικών (μορφολογία, φτέρωμα, τραγούδι) και γενετικών (μιτοχονδριακό και πυρηνικό DNA) χαρακτήρων και τους συγκρίνω με πειράματα που εξετάζουν την έκταση στην οποία χαρακτήρες σημαντικοί στην αναγνώριση των ειδών, αναγνωρίζονται μεταξύ των πληθυσμών. Πρώτα απ'όλα, εξετάζω ένα πρότυπο στο *Pogoniulus bilineatus* στην ανατολική Αφρική, όπου η ταχεία απόκλιση τραγουδιών μεταξύ των υποειδών είναι ασύμφωνη με τη φυλογενετική απόσταση. Παρά τον μικρότερο χρόνο απόκλισης, τα *P. b. fischeri* από την Κένυα και τη Ζανζιβάρη διαφέρουν δραματικά στο τραγούδι από το *P. b. bilineatus*. Αντίθετα, το *P. b. conciliator*, το οποίο απέκλινε πολύ πιο πρίν από τους άλλους δύο πληθυσμούς, μοιράζεται ακόμη το ίδιο τραγούδι με το *bilineatus*. Έχοντας δείξει πώς ο φαινότυπος και ο γονότυπος μπορούν να διαδραματίσουν κάποιο ρόλο στα όρια των ειδών, στη συνέχεια επικεντρώθηκα σε ένα ζευγάρι ειδών *Pogoniulus* που έχουν αποκλίνει για ακόμα μεγαλύτερο χρονικό διάστημα και που συναντώνται σε μια σειρά ζωνών επαφής στην υποσαχάρια Αφρική, το οποίο μας επιτρέπει να καθορίσουμε πώς η μεταβολή του φαινοτύπου και του γονοτύπου μπορεί να επηρεάσει την έκταση στην οποία αναγνωρίζουν το ένα το άλλο ως ξεχωριστά είδη. Διαπίστωσα λοιπόν ότι παρά τα 10 εκατομμύρια χρόνια απόκλισης στο μιτοχονδριακό DNA και τις διακριτές διαφορές στο φτέρωμα της κεφαλής, τα *P. pusillus* και τα *P. chrysoconus* στη νότια Αφρική υβριδίζονται εκτενώς, όπως αποκαλύφθηκε και από τις αναλύσεις των μικροδορυφορικών δεικτών. Τα τραγούδια των δύο ειδών στη νότια Αφρική συγκλίνουν στη ζώνη επαφής, όπως συμβαίνει και στην Τανζανία, αλλά παραμένουν διακριτά στην Κένυα και την Αιθιοπία. Οι γονιδιωματικές αναλύσεις των δεδομένων RADseq δείχνουν την διείσδυση των SNP στην Τανζανία, καθώς και στη νότια Αφρική, αλλά ελάχιστες ή καθόλου ενδείξεις διεισδυτικού υβριδισμού στην Κένυα. Ο ρόλος του τραγουδιού στη ρύθμιση της αναπαραγωγικής απομόνωσης υποστηρίζεται από πειράματα αναπαραγωγής τραγουδιών που δείχνουν ότι και τα δύο είδη ξεχωρίζουν το τραγούδι τους από το τραγούδι των άλλων ειδών στην Κένυα, αλλά όχι στην Τανζανία και τη νότια Αφρική. Τα δεδομένα από το RADseq χρησιμοποιήθηκαν επίσης για τον εντοπισμό περιοχών του γονιδιώματος που διέπουν τον κόκκινο και κίτρινο χρωματισμό στο φτέρωμα του μπροστινού μέρους της κεφαλής. Μια Genome Wide Association Study (GWAS) έδειξε τρία γονίδια που ελέγχουν ειδικά την

χρωστική των οφθαλμών (HPS4), την οπτική μάθηση (NDRG4) και την ανίχνευση ερεθισμάτων φωτός που εμπλέκονται στην οπτική αντίληψη (CACNA2D4) καθώς επίσης και αρκετά γονίδια που είναι γνωστό ότι ελέγχουν τη μορφολογική ανάπτυξη, αλλά δεν εντοπίστηκαν υποψήφια γονίδια που κωδικοποιούν πρωτεΐνες που συνδέονται άμεσα με το χρωματισμό του φτερώματος όπως σε άλλα είδη, δίνοντας μας την ευκαιρία για μελλοντική έρευνα. Ωστόσο, αυτή η έρευνα υποδηλώνει ότι η απόκλιση στο τραγούδι διαδραματίζει κρίσιμο ρόλο στην αναπαραγωγική απομόνωση και ότι σε μια μελλοντική έρευνα θα πρέπει να διερευνηθούν οι παράγοντες που οδηγούν στην απόκλιση του τραγουδιού καθώς επίσης και τα γονίδια που διέπουν κληρονομικούς χαρακτήρες του τραγουδιού.

Abstract

Species limits are most typically determined based on phenotypic characters or molecular phylogenetics, but patterns are not always congruent. Also, such methods might ignore the role of traits important in reproductive isolation. Here I compared patterns of variation in several phenotypic (morphology, plumage and song) and genotypic (mitochondrial and nuclear DNA) characters and compared them with experiments testing the extent to which characters important in species recognition are recognised among populations. Firstly, I examined a pattern in yellow-rumped tinkerbird *Pogoniulus bilineatus* in East Africa, where rapid song divergence between subspecies is discordant with phylogenetic distance. In spite of the shorter divergence time, *P. b. fischeri* from Kenya and Zanzibar differ dramatically in song from nominate *bilineatus*. By contrast, *P. b. conciliator*, diverged long before from the other two populations, yet shares the same song with nominate *bilineatus*. Having demonstrated how phenotype and genotype might play a role in species limits, I then focused on a species pair of *Pogoniulus* tinkerbirds that have been diverging for yet longer, and that meet in a series of contact zones in sub-Saharan Africa, allowing us to determine how variation in phenotype and genotype might affect the extent to which they recognise one another as separate species. I found that in spite of circa 10 my of divergence in mitochondrial DNA, and distinct differences in forecrown plumage, *P. pusillus* and *P. chrysoconus* in Southern Africa hybridise extensively, as revealed by microsatellite analyses. Songs of the two species in Southern Africa converge at the contact zone, as they do in Tanzania, but they remain distinct in Kenya and Ethiopia. Genomic analyses of RADseq data show introgression of SNPs in Tanzania, as well as in Southern Africa, but little or no evidence of introgressive hybridisation in Kenya. The role of song in mediating reproductive isolation is supported by playback experiments that show that both species discriminate between their song and the other species' song in Kenya, but not in Tanzania and Southern Africa. RADseq data were also used to identify regions of the genome underlying red and yellow pigmentation in forecrown feathers. A Genome wide association study recovered three genes that specifically control for eye pigmentation (HPS4), visual learning (NDRG4) and detection of light stimulus involved in visual perception (CACNA2D4) and several genes known to control morphological development, but no candidate protein coding genes directly linked to feather pigmentation in other species had been identified, which highlights an avenue for future research. Nevertheless, this research suggests song divergence plays a critical role in mediating reproductive isolation, and further work should also explore the factors driving divergence in song and the genes underlying heritable song characters.

Acknowledgments

I thank M. Phumlile (All Out Africa), Mr Mandla (Mbuluzi Game Reserve), Mr Azi (APLORI), J. Roberts and K. Solomon for assistance in the field, A. Monadjem, L. and N. Baker, B. Finch, D. Turner, N. Cordeiro, F. Dowsett-Lemaire, R. Dowsett, C. Jackson, and J. Gijsbertsen for logistical assistance and/or discussion, the following museums (and their staff) for access to their collections: Natural History Museum of Los Angeles County (K. Garrett), the British Museum of Natural History (M. Adams), the National Museum of Natural History, the Peabody Museum of Yale University, the Museum of Natural Science of Louisiana State University, the Donald R. Dickey Collection of the University of California, Los Angeles, the Museum of Vertebrate Zoology at University of California Berkeley and the Zoological Museum of the University of Copenhagen (J. Fjeldså), and J. Fuchs (MNHN) and J. Bolding Kristensen (ZMUC) for samples. I thank the Kenya National Council for Science and Technology (NCST), the National Museums of Kenya, the National Environment Management Authority (NEMA) of Kenya, Tanzania Wildlife Research Institute (TAWIRI), the Tanzania Commission for Science and Technology (COSTECH), Tanzania National Parks (TANAPA), Tanzania Conservation Resource Centre (TCRC) for assistance with research permits. I thank Ghana Wildlife Society (Japhet Roberts) for providing the documents I needed for my research in Ghana and providing me with useful information on the potential locations to trap tinkerbirds and broadbills within Ghana. I also thank Hilary Edwards (Mananga Golf Club) and Alan Howlands (IYSIS, Swaziland) for helping me with logistics during my field work within Swaziland. My friends, Chief Benson Chizubem Gem and Rennie Kufakunensu, you were always there to listen to my complaints and to make me smile even when I am stressed out. Prof. Hilary Edeoga (MOUAU), Prof A. U. Ezealor (MOUAU) and Prof. Manu Shiiwua (APLPORI, UNIJOS), Prof. M. C. Dike (MOUAU) and Prof. Emmanuel Nzegbule (MOUAU) provided me with all the support I needed from Nigeria in preparation for my doctoral

programm at the University of Cyprus. Pastor Branislav Mirilov, Pastor Kim Papaioannou, Elder Valerie Fidelia and the community of Seventh Day Adventist Community in Cyprus, you all made Saturday a day I look forward throughout the week. Will I forget to mention Gift Nwankwo? Gift was always checking on me and will never forget to ask, “have you eaten today?” Elder Moses Nwankwo and Deaconess Victoria Nwankwo, your parental care and prayer supported me through these year though I was far way from home. My sublings, Godswill, Godspower, Godstime, Blessing and Marvelous, thank you so much for your encouragements. The Seveth Day Adventist Community in Umudike and Elder and Deaconess E. O. Akoma, thank you so much for asking how I was faring all these years.

I am grateful to Dr Spyros Sfendourakis and Dr Vasilis Promponas for their suggestions and contribution at the proposal stage of this research and providing help in bioinformatics software installation, Dr Anna Papadopoulou for helping out with GenBank data submission, comments that improved my document and chairing my examination committee, Dr Paris Skourides and his lab members for helping out with laboratory tools. Professor Constantinos Deltas allowed me to do my microsatellite analysis in his lab and Dr Antonis Kirmizes gave me the permission to use the Nanodrop equipment in his lab to determine the concentration of my extracted genomic DNA samples. Athanasios Karageorgos helped me immensely with some of my lab work and also with Andreas Iannou. Chryso Pallari was very helpful in sequence alignment and pointing me in the right direction with the use of MrBayes for phylogenetic Bayesian analysis. I am also thankful to Andreas Demetriou for being a great friend during my stay at the University and providing my lab reagents. Eliana Hadjiantoni exposed me to necessary skills in working with several lab equipment and DNA extraction/amplification protocols. Michaella Moysi did aid in getting import permits for some of the samples loaned by different museums. I also thank Dr Alan Breslford for supporting in

the ddRadseq laboratory analysis together with his student Daniel Pierce. Alan also provided useful ideas during the analysis of the Radseq data.

I am very indebted to my supervisor, Dr Alexander N. G. Kirschel for allowing me to study in his laboratory as a PhD student. You did provide me with the supports I needed at the different stages of my research. I will need as many pages as the whole of my thesis to describe all the support, however, one would always find the traces of it across the entire document.

My coming to the University of Cyprus and my survival were like a tree jointly planted by Dr Manu Shiiwua and Professor Augustine Ezealor, Phil Hall watered the tree by providing every necessary manure and water required for proper growth and development of the tree and Dr A. P. Leventis was the source of the nutrients and water. This work was supported by the A.P. Leventis Ornithological Research Institute and a Marie Curie Reintegration Grant.

PATTERNS OF PHENOTYPIC AND GENETIC VARIATION IN *POGONIULUS* TINKERBIRDS AND THEIR ROLE IN INTERACTIONS AT CONTACT ZONES

TABLE OF CONTENTS

LIST OF TABLES

Chapter One

Chapter Two

Chapter Three

Chapter Four

APPENDIX TO CHAPTER THREE

APPENDIX TO CHAPTER FOUR

LIST OF FIGURES

APPENDIX TO CHAPTER TWO

APPENDIX TO CHAPTER THREE

Figure A1. Distributions of tetrahedral x, y, z colour cordinates for crown, breast and belly plumage patches against latitude shows a variety of patterns, with convergence and divergence in different measures towards the contact zone.

Figure A2. Distributions of tetrahedral x, y, z colour cordinates for throat, wing and rump plumage patches against latitude shows a variety of patterns, with convergence and divergence in different measures towards the contact zone.

CHAPTER ONE

INTRODUCTION

Rapid divergence in signals associated with mate choice and interactions among related species at contact zone dependent themselves on environmental factors play an important role in the generation and maintenance of biodiversity both at local and global spatial scales. It therefore becomes very important to identify the specific diverging signals that contribute or determine the maintenance of premating reproductive isolation. Identifying divergent signals important in maintaining reproductive isolation will contribute immensely to our understanding of the processes driving signal divergence and the roles they play in speciation and co-existence of species. One of the central foci of ecological studies involve studying the processes that occur at the population, community and ecosystem levels with a specific focus on biodiversity (Boughman 2001, 2002; Rundle et al. 2005, Tobias et al 2010). Over decades, ecologists have studied the mechanisms of speciation ranging from divergence in phenotypic and genetic traits to responses to environmental gradients (Endler 1995, Kirkpatrick and Barton 1997, Lee 2002, Kawecki and Ebert 2004, Gienapp et al. 2008, Sexton et al. 2009).

Species delimitation and species concepts

Species constitute the basic biotic units of every ecological community. Several methods have been used in delimiting what constitutes a species such that as many as 22 species concepts were reviewed by Mayden (1997). de Queiroz (2007) synthesized a common ground across the alternative species concepts, initially felt to be irreconcilable, in the form of the unified species concept. Under the unified species concept, species are separately evolving metapopulation lineages. Previous species concepts therefore provide different lines of evidences applicable to evaluating lineage separation known as secondary species criteria. The present study provides

lines of evidence for divergence between metapopulations of *Pogoniulus* tinkerbirds based on genetic, recognition, ecological and phenotypic (song, plumage and body size) accumulated differences among the populations. It is pertinent to mention that the accumulation of the mentioned secondary species criteria among the metapopulations does not necessarily occur at the same time nor follow specific sequence or order during the events of speciation. Evolutionary processes that can lead to speciation include natural selection (including sexual selection), mutation, gene flow and genetic drift. These evolutionary processes influence at different degrees the genotypic, phenotypic and behavioural characters of the populations. Over time, the recognition of individuals from diverging populations as potential reproductive mates may break down leading to reproductive isolation.

Association between audio-visual signals and environmental characteristics

Ranging from fish (Endler 1980), to reptiles (Leal and Fleishman 2002) and birds (Marchetti 1993) there is much evidence of associations between audio-visual signals and environmental characteristics of the specific habitats where these signals are produced by the species. Studies on signal variation across wide geographic ranges where there are variations in habitat characteristics, have shown that spatial variation in signals could be driven by differences in climatic conditions, elevation, ambient noise (Kirschel et al 2009b) but also character displacement through interactions between related species (Grether et al. 2009, Kirschel et al. 2009a, Tobias and Seddon 2009). Furthermore, while acoustic adaptation may involve signal structure adapting to vegetation density (Wiley and Richards 1978), Tobias et al (2010) proposed as an alternative, that such signal variation might instead be an outcome of an evolutionary response of habitat-related selection on body size. The implication of such evidence is that speciation could result from divergent selection on signals important in mate selection resulting from habitat heterogeneity (Kirschel et al. 2011). Tobias et al (2010) further

provided evidence for the role of ecological adaptation of acoustic signals in promoting reproductive isolation. Comparative studies on behavioural evolution and speciation have effectively used bird song as a model system (reviewed in Slabbekoorn and Smith 2002b, Wilkins et al 2013). For example, Mason et al. (2016) compared the rates of evolution between two distantly related lineages of passerine birds in the Neotropics (one oscine clade with learned song (Traupidea) and one suboscine clade with innate song) based on an analysis of a combination of bioacoustics and phylogenetic data. They found faster rates of evolution among the thraupids with learned song relative to furnarids with presumed innate song and suggested that behavioural traits involved in mate choice and territoriality contribute to macroevolutionary patterns of species richness. It therefore becomes important to empirically determine the extent of discordance between divergence in phenotypic and genetic traits of avian species with innate songs. *Pogoniulus* tinkerbirds provide an opportunity to carry out such a study in nature as they occur along environmental gradients, have variation in phenotypic traits between populations that can be unambiguously quantifiable, and have contact regions where closely related species interact.

Song is a key trait used by birds in choosing their mates (Endler 1992; Price 1998). Divergence in bird song has been reported by Slabbekoorn and Smith (2002a) to be driven by habitat differences. Further evidence in the divergence of song characteristics accounted for by habitat have been observed by Wiley 1991; Kirschel et al. 2009a; Tobias et al. 2010 among others). Typically, tropical forest bird songs are more tonal with low frequency features relative to open habitat bird songs (Wiley and Richards 1982; Slabbekoorn et al. 2002). In the effort to maximize propagation of acoustic signals, birds adapt their vocalizations to the physical structure of their habitat (Rothstein and Fleischer 1987; Brown and Handford 1998; Daniel and Blumstein 1998; Seddon 2005) and birds prefer habitats that enhance the transmission of their songs (Luther 2009; Tobias et al. 2010a). The ability of birds to adjust the frequency of their

songs to accommodate the fluctuating noise conditions has been observed in several studies (Tumer and Brainard 2007; Halfwerk and Slabbekoorn 2009; Gross et al. 2010 but see Nemeth et al. 2013).

Based on the 'Acoustic Adaptation Hypothesis' (Morton 1975, Hansen 1979), it is believed that selection dependent on habitat structure determines the pattern of avian acoustic characteristics (Boncoraglio and Saino 2007). Considering the effect of habitat structure on avian acoustic characteristics, it is important to measure several environmental and biotic factors of habitats within which avian song studies are being carried out. For example, the song of green hylia (*Hylia prasina*) was reported in Kirschel et al (2009a) to vary with elevation and tree cover, as well as ambient noise.

Evolution of reproductive isolation

The evolution of reproductive isolation between closely related lineages and the persistence of isolating barriers may be the outcome of the interplay between phenotypic differentiation and sexual selection (Coyne and Orr 2004). But that does not imply that every form of phenotypic differentiation between lineages will lead to the emergence of reproductive barriers. As such, identifying specific phenotypic traits and genomic regions that are introgressed or not introgressed upon secondary contact between closely related species within a contact zone becomes very important to our understanding of the evolutionary process involved in maintaining species boundaries. In the event of secondary contact between previously isolated lineages, we would expect the interaction between them, if hybridization takes place, to lead to exchange of genes and ultimately the homogenizing of genomes. Genetic recombination between species undergoing hybridization might lead to the occurrence of individuals with intermediate phenotypic and changes in allele frequencies. Hybrid zones between previously isolated lineages provide a natural laboratory for the investigation of the effects of gene flow

between lineages under secondary contact and its consequences on biodiversity. One of the consequences of hybridisation include collapsing of previously isolated lineages into one lineage evidence of which have been reported in threespine stickleback *Gasterosteus aculeatus* (Taylor et al. 2006, Gow et al 2006, Behm et al. 2009, Harrison and Larson 2014, Wu 2001), and in Darwin's finches (Kleindorfer et al 2014) and ravens (Kearns et al. 2018). The ecology of interacting species may also play a role in the persistence of species boundaries even under secondary contact. Persistence of species boundaries under secondary contact will be more effective if there is convergence of ecological gradient from habitats in allopatry to sympatry of the respective species leading to the hybrids being more adapted and show higher fitness at the habitat in sympatry relative their parental populations.

Modes of speciation

Speciation is the process through which new biological species emerge from a common ancestor over generations (Grant and Grant 2006). The various modes of speciation include allopatric, peripatric, parapatric and sympatric speciation, which are generally based on different extents of isolation.

Allopatric speciation occurs when a species range splits into two or more geographically isolated sub-populations. Through dissimilar selective pressures and/or genetic drift, via mutations the respective populations undergo genotypic and/or phenotypic divergence. These forces drive divergence between populations to the extent that they are assumed to have become reproductively isolated and expected to no longer exchange genes following secondary contact.

Peripatric speciation is a sub-form of allopatric speciation in which new species emerge from smaller peripheral populations following a founder event of dispersal from the main population. In this form of speciation genetic drift is usually the driving force. Peripatric

speciation was proposed by Ernst Mayr (1982) as an explanation for speciation among birds of the Malay Archipelago, but evidence for this mode of speciation is limited.

Parapatric speciation is a form of speciation driven by differential landscape-dependent selection pressure. With reduced gene flow between two populations, the presence of strong differential selection may impede assimilation and different species may emerge over many generations. Interbreeding between the populations may result in reduced fitness of heterozygote individuals, which can drive the evolution of premating isolating behaviours or mechanisms that prevent interbreeding.

Sympatric speciation involves the emergence of two or more descendant species from a single ancestral species within the same geographical location, thus without any separation from the ancestral species' geographic range. The basic condition for sympatric speciation include genotypic adaptation to different resources in which the limited resources generate frequency-dependent selection. A typical example of this form of speciation is that of cichlids of East Africa inhabiting the Rift Valley lakes, specifically Lake Victoria, Lake Malawi and Lake Tanganyika. Over 800 described species have been known to diversify from the same ancestral fish *Oryzias latipes* over generations (Takeda 2008). Sympatric speciation is also thought to have led to the tremendous diversification of the crustaceans of the Siberia's Lake Baikal (Jeffery et al. 2016).

Role of ecology in species divergence

Ecology is important in explaining the patterns of diversification of organisms (Wiens and Donoghue 2004, Edwards et al. 2005, Erwin 2011). Ecological speciation may result from natural selection in populations under varying environmental conditions (Endler 1977; Rundle et al. 2005, Schluter 2001, 2009). Greater levels of divergence have been found in phenotypic traits across an environmental gradient than between isolated sites within the same habitat

(Slabbekoorn and Smith 2002a; Kirschel et al. 2011). The divergence-with-gene-flow hypothesis posits that divergence occurs in spite of gene flow between populations under different habitat conditions (Rice and Hostert 1993). Recent molecular studies provide evidence on the consistency of genomic divergence with phenotypic traits under selection pressures (Mullen and Hoekstra 2008; Freedman et al. 2010; Michel et al. 2010).

The emergence of a premating isolation mechanism can result in assortative mating (Coyne and Orr 2004) and in relation to mate choice and species recognition may also determine the extent of divergence between populations. Acoustic displays play an important role in advertisement for the attraction of mates, competition for mates and territories (Bradbury and Vehrencamp 1998). Species recognition and mate choice are known to be influenced by variation in acoustic signals produced by birds of the same or different species (Collins 2004; Catchpole and Slater 2003). The spectral and temporal properties of acoustic signals of birds have been found to vary geographically and have been shown to influence the relative response levels between males and females (ten Cate et al. 2002; Gil and Gahr 2002; Riebel 2009). Learned songs in songbirds differ culturally between populations and may subsequently affect gene flow due to variation in successful territorial establishment and mate attraction (Ellers and Slabbekoorn 2003). This might be regulated by the interplay between variation in the song of the males and female preferences (Brenowitz and Beecher 2005).

Some of the factors recognized by Sexton and colleagues (2009) to influence species' range limits include Allee effects, gene swamping and competitive exclusion. They based their conclusions on theoretical modelling and recommended empirical studies focus on determining the role of phenotypic and genetic variation in the evolution of range limits with or without environmental heterogeneity. Genetic variation with little environmental heterogeneity is evident in the pattern of distribution found in three subspecies of yellow-rumped tinkerbirds (*Pogoniulus bilineatus bilineatus, P. b. fischeri* and *P. b. conciliator*) described in Chapter 2.

Despite the similarity in their habitats there is a distinct range pattern of *P. b. fischeri* in coastal Kenya and on the island of Zanzibar and *P. b. bilineatus* and *P. b. conciliator* in coastal and montane Tanzania respectively. The distribution of yellow-fronted tinkerbird (*Pogoniulus chrysoconus*) and red-fronted tinkerbird (*Pogoniulus pusillus*) across sub-Saharan Africa provides a great opportunity for studying evolutionary processes that may maintain species boundaries under secondary contact between closely related species. What is interesting about the distribution of *P. chrysoconus* and *P. pusillus* is that they can be found occurring in parapatry at contact zones in at least four regions in Africa, which include Ethiopia, Kenya and Uganda, Tanzania and in Southern Africa (specifically in South Africa and Swaziland).

Next-generation sequencing as a tool in avian genomic study

Recent avian evolutionary studies have been based on genomic analyses, which allow the study of numerous loci using thousands of genetic markers. One of the common methods used to obtain such genomic data is Next-generation sequencing. Based on genome-wide analysis, Stryjewski and Sorenson (2017) demonstrated the importance of multi-locus recombination of ancestral genetic variation in generating phenotypic novelty and diversity. Similar analyses have been extensively used in identifying the genomic regions that control for pigmentation and colour patterns among birds (Toews 2017, Cuthill et al. 2017, Brelsford et al. 2017), as well as other vertebrates (Nachman et al 2003), invertebrates (Bastide et al 2013), and plants (Arabidopsis Genome Initiative 2000, Kahawara 2013).

Study species and their distribution

Tinkerbirds (also known as tinker-barbets) belong to the genus *Pogoniulus* of the Lybiidae family and Piciformes order (Short and Horne 2001). They are widely distributed in tropical regions of Africa and occur in a wide range of habitats from lowland rainforest to dry savanna

at various altitudes. There are nine recognised species of tinkerbirds (including *Pogoniulus makawai* that is still debated) with several subspecies, which are listed in Table 1 with their distribution. Adult yellow-fronted tinkerbirds have black upperparts heavily streaked with yellow and white, with a strong black and white face pattern and a yellow forecrown patch. Its rump is lemon yellow, while the underparts range from yellow to whitish. Adult red-fronted tinkerbirds are distinguished from yellow-fronted by the red colour of the forecrown patch and a more golden wing panel. Tinkerbirds are sexually monomorphic, but young yellow-fronted and red-fronted tinkerbirds have a differentiating dark crown that lacks the distinctive yellow or red forecrown.

Yellow-rumped tinkerbirds (*Pogoniulus bilineatus*) typically occupy savanna woodland, forest edge, gallery forest and secondary forest at elevations up to 2500m above sea level while yellow-fronted and red-fronted tinkerbird typically occupy more open acacia woodland, but in different parts of their range each species can be found in tall forest. They are vocal and conspicuous species that occur singly or in pairs. The calls of Yellow-rumped tinkerbirds are usually in bursts of four to six notes relative to the prolonged calls of the red-fronted and yellow-fronted tinkerbirds. The diet of Yellow-rumped tinkerbirds is usually composed of a variety of fruits, including figs, fruits and vegetables. Food material are ingested whole and the undigested materials such as seed pits are regurgitated. Occasionally they feed on small insects, such as ants, cicadas, dragonflies, crickets, locusts, beetles, moths and mantis. The habitat preference of the yellow-rumped tinkerbird include canopy and mid-stratum of coastal and riparian forest, moist thickets, and montane forest (Irwin 1981). They are also observed in abundance in areas with high population of figs *Ficus* spp. (Maclean 1993), in denser and moister vegetation types (Fry et al. 1988).

Yellow-rumped, yellow-fronted and red-fronted tinkerbirds are primary cavity nesters, excavating cavities in dead branches between September-March (Maclean 1993). Their clutch

size is about 2-4 eggs that are incubated for 13-15 days. Nesting responsibilities are shared by both parents, which have been observed to place sticky mistletoe seeds around their nest entrance, assumed to deter predators. Yellow-rumped tinkerbird distribution overlaps with that of red-fronted tinkerbird especially in the coastal regions of southern KwaZulu-Natal, however, red-fronted tinkerbird prefers relatively less humid and open habitat (Fry et al. 1988).

Table 1. Tinkerbird species and their distributions across Africa.

Common Name	**Scientific name**	**Distribution**
Speckled tinkerbird	*Pogoniulus scolopaceus*	Angola, Benin, Cameroon, Central African Republic, Republic of the Congo, Democratic Republic of the Congo, Ivory Coast, Equatorial Guinea, Gabon, Ghana, Guinea, Liberia, Nigeria, Sierra Leone, Togo, and Uganda.
Western tinkerbird	*Pogoniulus coryphaea*	Angola, Cameroon, Democratic Republic of the Congo, Nigeria, Rwanda, Burundi and Uganda.
Moustached tinkerbird	*Pogoniulus leucomystax*	Kenya, Tanzania, Zanzibar, Malawi, Mozambique and Zambia.
Green tinkerbird	*Pogoniulus simplex*	Kenya, Malawi, Mozambique, Tanzania and Zanzibar.
Red-rumped tinkerbird	*Pogoniulus atroflavus*	Angola, Cameroon, Central African Republic, Republic of the Congo, Democratic Republic of the Congo, Ivory Coast, Equatorial Guinea, Gabon, Ghana, Guinea, Liberia, Nigeria, Senegal, Sierra Leone, and Uganda.

Yellow-throated tinkerbird	*Pogoniulus subsulphureus*	Angola, Benin, Cameroon, Bioko Island, Central African Republic, Republic of the Congo, Democratic Republic of the Congo, Ivory Coast, Equatorial Guinea, Gabon, Ghana, Guinea, Liberia, Nigeria, Sierra Leone, and Uganda.
Yellow-rumped tinkerbird	*Pogoniulus bilineatus*	Angola, Benin, Burundi, Cameroon, Central African Republic, Republic of the Congo, Democratic Republic of the Congo, Ivory Coast, Equatorial Guinea, Gabon, Gambia, Ghana, Guinea, Guinea-Bissau, Kenya, Liberia, Malawi, Nigeria, Rwanda, Senegal, Sierra Leone, South Africa, South Sudan, Swaziland, Tanzania, Togo, Uganda, and Zambia.
White-chested tinkerbird	*Pogoniulus makawai*	Zambia
Yellow-fronted tinkerbird	*Pogoniulus chrysoconus*	Angola, Benin, Botswana, Burkina Faso, Burundi, Cameroon, Central African Republic, Chad, Republic of the Congo, Democratic Republic of the Congo, Côte d'Ivoire, Ethiopia, Gambia, Ghana, Guinea, Guinea-Bissau, Kenya, Malawi, Mali, Mauritania, Mozambique, Namibia, Niger, Nigeria, Rwanda, Senegal, South Africa, South Sudan, Sudan, Swaziland, Tanzania, Togo, Uganda, Zambia and Zimbabwe

Red-fronted tinkerbird	*Pogoniulus pusillus*	Eritrea, Ethiopia, Kenya, Mozambique, Somalia, South Africa, South Sudan, Sudan, Swaziland, Tanzania and Uganda

Aim and Objectives

The overall aim of the study was to investigate how the extent of phenotypic and genetic differences between related species might affect the magnitude and direction of displacement between them when they come together in coexistence.

The specific objectives for the research were to:

1. Investigate variation in *Pogoniulus* tinkerbirds focusing on variation in song based on analyses from field recordings, variation in plumage and morphology from measurements of museum specimens and at contact zones in the field.

2. Determine the extent to which phenotypic and genetic differences influence interactions at contact zones among *Pogoniulus* tinkerbirds.

3. Measure and control for phenotypic variation explained by environmental gradients, genetic differentiation and geographic distance.

Each of the specific objectives mentioned above formed a section in this thesis, some of which are already published in peer-reviewed scientific journals while others are in the verge of being submitted for publication.

Specific projects

Chapter 2 focuses on the phylogeography of three subspecies of *Pogoniulus bilineatus* ranging from East Africa to Southern Africa.

In Chapter 3, I investigate the extent of introgressive hybridization in tinkerbird species in Southern Africa that have been diverging for millions of years.

Chapter 4 involves an investigation into differential patterns of phenotypic and genomic variation in interacting *Pogoniulus* tinkerbirds across four independent contact zones.

Brief description of the methods

For each of the projects, bird songs were recorded in the field at the different locations, using mist nets of different sizes birds were trapped for morphological measurement and collection of DNA samples (feather and blood samples). The trapped individual birds were handled with care and safely released into their respective habitats after sample collection in the field. Playback experiments were also performed for each of the species in the field which involved recording the behavioural responses of the focal individuals to conspecific and heterospecific songs. Plumage coloration of the distinguishing body patches of the species were obtained by measuring the reflectance of the feather samples collected from the rump patch for Yellow-rumped tinkerbird and fore crown patch for Red-fronted and Yellow-fronted tinkerbirds. The collected blood samples were preserved in Queens lysis buffer in 1.5ml cryovial tubes. The geographical coordinates of each location where samples were collected were recorded using Garmin GPS units. To obtain the vegetative characteristics of the surveyed locations, Moderate Resolution Imaging Radiometer raster files at 250 m resolution (MODIS/Terra Vegetation Indices 16-Day L3 Global 250m) from 2010 were used to extract vegetation continuous field (VCF) and enhanced vegetation index (EVI) data for coordinates of the field locations in ArcGIS 10.1 (ESRI, 2012). In addition to the samples we collected from the field, we also collected morphometric and plumage reflectance measurement from museums material, either loaned or handled on site (by Dr. A. Kirschel).

Spectral and temporal properties of songs recorded were measured in Raven 1.4 software (Charif et al. 2010) and the resultant data were used in statistical analyses to determine the extent of variation in song explained by genetic differences and environmental factors (elevation, latitude, longitude).

Molecular samples were analysed in the laboratory by extracting the whole genomic DNA from the blood, tissue and feather samples using Qiagen and Macherey Nagel DNA extraction kits. Specific nuclear and mitochondrial genes were amplified using PCR (polymerase chain reaction) method on the Applied Biosystems Veriti Thermal Cycler based on the specific requirements of the primers used for each of the genes. The PCR samples were sequenced by Macrogen Incorporated. We also obtained genomic data for the study on chapter four using Restriction site associated DNA (RAD) markers based on next generation sequencing technique. Some of the software used for genetic analysis include jModelTest for selection of evolutionary models used in phylogenetic reconstruction, MEGA and Bioedit used in DNA sequence alignment and annotation, RaxML and IQ-tree used in phylogenetic reconstruction based on maximum likelihood method (ML), RevBayes used in Bayesian Inference of phylogenetic trees, Figtree used in visualizing phylogenetic trees, STRUCTURE (Pritchard et al. 2000) for Bayesian admixture analysis, CLUster Matching and Permutation Program for averaging across iterations (CLUMPP, Jakobsson and Rosenberg 2007), Structure Harvester (Earl and Vonholdt 2012) for selection of the best K value for population structure analysis, VCFtools (Danecek et al. 2011) and PLINK (Chang et al. 2015) for filtering and summary statistics of RADseq data, and R Statistical packages used in various sections of the research as summarised in Table 2. Other analysis performed on the sequenced and genomic data are described in each of the chapters. Statistical analyses were performed in R 3.3.0 (R Core Team 2017) and above depending on the latest version available at the time of each section of the project. Some statistical analyses were performed in Stata 11 (StataCorp 2015).

Phylogenetic relationship of *Pogoniulus* genus

To explore the phylogenetic relationships within the genus *Pogoniulus*, we performed a molecular phylogenetic analysis on genes sequenced from DNA extracted from a blood samples from our field collections and tissue samples from Museums collections (NHM in Tring, ZMUC, FMNH, MNHN) and fieldwork performed as part of previous (Kirschel *et al.* 2009a) and ongoing studies including outgroup samples from GenBank. Genomic DNA was extracted using the protocol for the DNeasy blood and tissue kit (Qiagen, West Sussex, UK). Two mitochondrial genes, cytochrome *b* and ATPase subunit 6/8, and one nuclear DNA gene, Myoglobin were amplified and sequenced for 81 samples. PCR reactions were completed using Qiagen HotStarTaq Master Mix in ABI 2720 thermal cyclers (Applied Biosystems, Foster City, CA). PCR products were visualized in 2% Agarose gel (with 2.5 µl Ethidium Bromide) and purified through the Qiagen Mini-elute kit. PCR-amplification of DNA from fresh tissue or blood samples was performed using published primers (for cytochrome *b*, L14841 Kocher *et al.* 1989 and H4a Harshman 1994; for ATPase 6/8, CO2GQL and C03HMH Eberhard and Bermingham 2004; for Myoglobin intron-2, Myo2 Haslewood et al. 1998 and Myo3F Slade et al. 1993). We added six outgroup sequences for *Tricholaema diadematata*, *Lybius dubius* (GenBank: B39244), *Picumnus cirratus* (GenBank: AY165819.1), *Ramphastos toco* (GenBank: AY959852), *Sasia ochracea* (GenBank: NC028019) and *Melanerpes carolinus* (GenBank: U89192.1).

We determined the best partitioning schemes and corresponding nucleotide substitution models for each of the genes using PartitionFinder2 (Lanfear *et al.*, 2016). The data-set blocks were predefined a priori based on the genes. The corrected Akaike information criterion (AICc) and the 'greedy' algorithm with branch-lengths estimated as unlinked were used to search for the best-fit scheme. Phylogenetic analyses were conducted using Bayesian phylogenetic

reconstruction based on the combined loci of the mitochondrial genes and nuclear gene with the model partitioning restricted to the genes (ATPase/Myo: GTR+I+G; Cyt-*b*: GTR+G).

Divergence times of the Bayesian Inference tree were estimated in RevBayes 1.0.7 (Hohna et al., 2016) using 5.38 m.y.a. (mean = 35 mya, sd = ± 9, max = 65.38) as a minimum age limit for the ancestor of the *Pogoniulus* tinkerbirds based on a Late Miocene *Pogoniulus* fossil at Kohfidisch Austria (Mlíkovský 2002). The divergence time boundaries were selected to include time of divergence from previous studies (see Paton et al. 2002, Nahum et al. 2003) between the distant species whose sequences were included in the analysis as outgroups (*Picumnus cirratus* AY165819.1, *Ramphastos toco* AY959852, *Sasia ochracea* NC028019 and *Melanerpes carolinus* U89192.1). We used a relaxed uncorrelated lognormal clock model and a stochastic node for the mean rate of each partition to range from 0.007-0.01 (mean = 0.0088, sd = 0.0006, min = 0.007, max = 0.01). The sampling probability was set to the ratio of the tips and the estimated total number of described bird species in the Lybiidae (52, del Hoyo et. al. 2017) and we ran the burn-in phase of the Monte Carlo sampler for 105 iterations under two independent replicates using 13 different moves in a random move schedule with 102 moves per iteration and a tuning interval of 250. The main phase of the MCMC analysis was run for one million generations sampling every 100 generations under two independent runs and the same random moves as in the burn-in phase. Convergence from the independent runs and ESS values were evaluated in Tracer 1.6 (Rambaut et al. 2014). The final tree was produced from the generated trees by compiling a maximum posteriori tree using a burn-in of 20%.

The Bayesian phylogenetic tree showed the divergence of *Pogoniulus* tinkerbirds from their recent ancestor may have occurred around 20.75 MYA (Figure 1). *P. pusillus* and *P. p affinis* were monophyletic while *P. chrysoconus* was paraphyletic. We also recovered *P. makawai* to be nested within the *P. bilineatus leucolaimus* clade consistent with findings in Kirschel et al. (2018). The phylogenetic relationships among *P. b. bilineatus*, *P. b conciliator*

and *P. b. fischeri* show nominate *bilineatus* being more closely related to *fischeri* than to *conciliator*. *P. corypheaus* and *P leucomystax* are sister groups and both share a recent common ancestor with *P. simplex*.

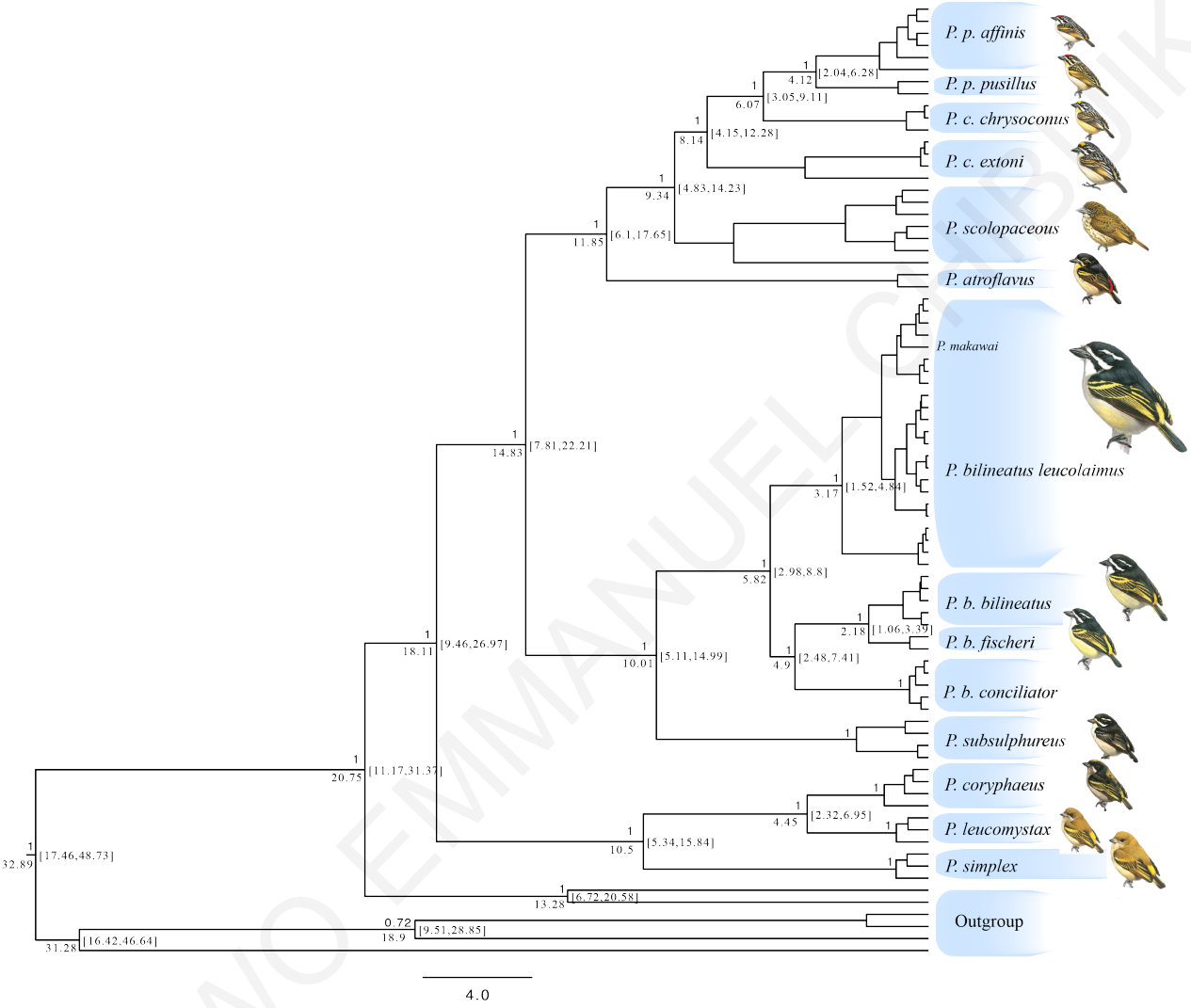

Figure 1. Bayesian phylogenetic reconstruction of *Pogoniulus* genus based on two mitochondrial genes (cyt *b*: 1027 bp, ATPase: 832 bp) and one nuclear gene (Myo: 697 bp). The values above node edges correspond to Posterior probabilities, below the node edges are the average divergence times and in front of the nodes are 95% high posterior density of the the divergence ages. The scale corresponds to divergence time in MY. The size of the pictures of the species are not scaled. The divergence of the genus from their recent ancestor appear to have occurred around 20.75 [11.17-31.37] MYA.

References

ARABIDOPSIS GENOME INITIATIVE, 2000. Analysis of the genome sequence of the flowering plant Arabidopsis thaliana. *Nature*, **408**(6814), p.796.

BASTIDE, H., BETANCOURT, A., NOLTE, V., TOBLER, R., STÖBE, P., FUTSCHIK, A. and SCHLÖTTERER, C., 2013. A genome-wide, fine-scale map of natural pigmentation variation in Drosophila melanogaster. *PLoS genetics*, **9**(6), p.e1003534.

BEHM, J.E., IVES, A.R. and BOUGHMAN, J.W., 2009. Breakdown in postmating isolation and the collapse of a species pair through hybridization. *The American Naturalist*, **175**(1), pp.11-26.

BONCORAGLIO, G. and SAINO, N., 2007. Habitat structure and the evolution of bird song: a meta-analysis of the evidence for the acoustic adaptation hypothesis. *Functional Ecology,* **21**(1), pp. 134-142.

BOUGHMAN, J. W. 2001. Divergent sexual selection enhances reproductive isolation in sticklebacks. *Nature* **411**:944–948.

BOUGHMAN, J. W. 2002. How sensory drive can promote speciation. *Trends in Ecology and Evolution*. **17**:571–577.

BRENOWITZ, E.A. and BEECHER, M.D., 2005. Song learning in birds: diversity and plasticity, opportunities and challenges. *Trends in neurosciences*, **28**(3), pp.127-132.

BRADBURY, J.W. and VEHRENCAMP, S.L., 2000. Economic models of animal communication. *Animal behaviour*, **59**(2), pp.259-268.

BRELSFORD, A., TOEWS, D.P. and IRWIN, D.E., 2017. Admixture mapping in a hybrid zone reveals loci associated with avian feather coloration. *Proc. R. Soc. B*, **284**(1866), p.20171106.

BROWN, A.H., FELDMAN, M.W. and NEVO, E., 1980. Multilocus Structure of Natural Populations of HORDEUM SPONTANEUM. *Genetics,* **96**(2), pp. 523-536.

CATCHPOLE, C.K. and SLATER, P.J., 2003. *Bird song: biological themes and variations*. Cambridge University press.

CHANG, C.C., CHOW, C.C., TELLIER, L.C., VATTIKUTI, S., PURCELL, S.M. and LEE, J.J., 2015. Second-generation PLINK: rising to the challenge of larger and richer datasets. *Gigascience*, **4**(1), p.7.

CHARIF, R.A., STRICKMAN, L.M. and WAACK, A.M., 2010. *Raven Pro 1.4 User's Manual*. The Cornell Lab of Ornithology, Ithaca, NY.

COLLINS, S. 2004. Vocal fighting and flirting: the functions of birdsong. Pp. 39–79 in P. Marler and H. Slabbekoorn, eds. Nature's music: the science of birdsong. *Elsevier*, San Diego, CA.

COYNE, J. A., and ORR H.A., 2004. *Speciation*. Sinauer Associates, Sunderland, MA.

CUTHILL, I.C., ALLEN, W.L., ARBUCKLE, K., CASPERS, B., CHAPLIN, G., HAUBER, M.E., HILL, G.E., JABLONSKI, N.G., JIGGINS, C.D., KELBER, A. and MAPPES, J., 2017. The biology of color. *Science*, *357*(6350), p.eaan0221.

DANECEK, P., AUTON, A., ABECASIS, G., ALBERS, C.A., BANKS, E., DEPRISTO, M.A., HANDSAKER, R.E., LUNTER, G., MARTH, G.T., SHERRY, S.T. and MCVEAN, G. 2011. The variant call format and VCFtools. *Bioinformatics*, **27**:2156–2158.

DANIEL, J.C. and T BLUMSTEIN, D., 1998. A test of the acoustic adaptation hypothesis in four species of marmots. *Animal Behaviour,* **56**(6), pp. 1517-1528.

DEL HOYO, J., ELLIOTT, A., SARGATAL, J., CHRISTIE, D.A. and DE JUANA, E. (eds.). *Handbook of the Birds of the World Alive*. Lynx Edicions, Barcelona. (retrieved from https://www.hbw.com/node/467072 on 19 December 2017).

De QUEIROZ, K., 2007. Species concepts and species delimitation. *Systematic biology*, **56**(6), pp.879-886.

EARL, D.A. and VONHOLDT, B.M., Conservation Genetics Resources; 2011. *STRUCTURE HARVESTER: a website and program for visualizing STRUCTURE output and implementing the Evanno method.*

EBERHARD, J. R., and BERMINGHAM, E., 2004. Phylogeny and biogeography of the *Amazona ochrocephala* (Aves: Psittacidae) complex. *Auk,* **121**: 318-332.

EDWARDS, S.V., KINGAN, S.B., CALKINS, J.D., BALAKRISHNAN, C.N., JENNINGS, W.B., SWANSON, W.J. and SORENSON, M.D., 2005. Speciation in birds: genes, geography, and sexual selection. *Proceedings of the National Academy of Sciences*, **102**(suppl 1), pp.6550-6557.

ELLERS, J. and SLABBEKOORN, H., 2003. Song divergence and male dispersal among bird populations: a spatially explicit model testing the role of vocal learning. *Animal Behaviour*, **65**(4), pp.671-681.

ENDLER, J.A., 1977. *Geographic variation, speciation, and clines* (No. 10). Princeton University Press.

ENDLER J.A., 1980. Natural selection on color patterns in *Poecilia reticulata* *Evolution*, **34**:pp.76-91

ENDLER, J.A., 1992. Signals, signal conditions, and the direction of evolution. *The American Naturalist*, **139**, pp.S125-S153.

ENDLER, J.A., 1995. Multiple-trait coevolution and environmental gradients in guppies. *Trends in ecology and evolution*, **10**(1), pp.22-29.

ERWIN, D.H., LAFLAMME, M., TWEEDT, S.M., SPERLING, E.A., PISANI, D. and PETERSON, K.J., 2011. The Cambrian conundrum: early divergence and later ecological success in the early history of animals. *Science*, **334**(6059), pp.1091-1097.

FREEDMAN, A.H., THOMASSEN, H.A., BUERMANN, W. and SMITH, T.B., 2010. Genomic signals of diversification along ecological gradients in a tropical lizard. *Molecular Ecology*, **19**(17), pp.3773-3788.

FRY, C.H., KEITH, S. and URBAN, E.K., 1988. The birds of Africa. Vol. 3: parrots to woodpeckers.

GIENAPP, P., TEPLITSKY, C., ALHO, J.S., MILLS, J.A. and MERILÄ, J., 2008. Climate change and evolution: disentangling environmental and genetic responses. *Molecular ecology*, **17**(1), pp.167-178.

GIL, D. and GAHR, M., 2002. The honesty of bird song: multiple constraints for multiple traits. *Trends in Ecology and Evolution*, **17**(3), pp.133-141.

GOW, J.L., PEICHEL, C.L. and TAYLOR, E.B., 2006. Contrasting hybridization rates between sympatric three-spined sticklebacks highlight the fragility of reproductive barriers between evolutionarily young species. *Molecular ecology*, **15**(3), pp.739-752.

GRANT, P.R. and GRANT, B.R., 2006. Species before speciation is complete. *Annals of the Missouri Botanical Garden*, **93**(1), pp.94-102.

GRETHER, G.F., LOSIN, N., ANDERSON, C.N. and OKAMOTO, K. 2009. The role of interspecific interference competition in character displacement and the evolution of competitor recognition. *Biological Review,* **84**: 617–635.

GROSS, K., PASINELLI, G. and KUNC, H.P., 2010. Behavioral plasticity allows short-term adjustment to a novel environment. *The American Naturalist,* **176**(4), pp. 456-464.

HALFWERK, W. and SLABBEKOORN, H., 2009. A behavioural mechanism explaining noise-dependent frequency use in urban birdsong. *Animal Behaviour,* **78**(6), pp. 1301-1307.

HANSEN, E.M., 1979. Sexual and vegetative incompatibility reactions in Phellinus weirii. *Canadian journal of Botany,* **57**(15), pp. 1573-1578.

HARRISON, R.G. and LARSON, E.L., 2014. Hybridization, introgression, and the nature of species boundaries. *Journal of Heredity*, **105**(S1), pp.795-809.

HARSHMAN, J. 1994. Reweaving the tapestry: What can we learn from Sibley and Ahlquist (1990)? *Auk,* **111**: 377-388.

HESLEWOOD, M.M., ELPHINSTONE, M.S., TIDEMANN, S.C. and BAVERSTOCK, P.R., 1998. Myoglobin intron variation in the Gouldian Finch *Erythrura gouldiae* assessed by temperature gradient gel electrophoresis. *Electrophoresis*, **19**(2), pp.142-151.

HÖHNA, S., LANDIS, M.J., HEATH, T.A., BOUSSAU, B., LARTILLOT, N., MOORE, B.R., HUELSENBECK, J.P. and RONQUIST, F. 2016. RevBayes: Bayesian phylogenetic inference using graphical models and an interactive model-specification language. *Syst. Biol.* **65**: 726-36.

IRWIN, H.P.A., 1981. A simple omnidirectional sensor for wind-tunnel studies of pedestrian-level winds. *Journal of wind engineering and industrial aerodynamics*, **7**(3), pp.219-239.

JAKOBSSON, M. and ROSENBERG, N.A., 2007. CLUMPP: a cluster matching and permutation program for dealing with label switching and multimodality in analysis of population structure. *Bioinformatics*, **23**(14), pp.1801-1806.

JEFFERY, N.W., YAMPOLSKY, L. and GREGORY, T.R., 2016. Nuclear DNA content correlates with depth, body size, and diversification rate in amphipod crustaceans from ancient Lake Baikal, Russia. *Genome*, **60**(4), pp.303-309.

KAWAHARA, Y., DE LA BASTIDE, M., HAMILTON, J.P., KANAMORI, H., MCCOMBIE, W.R., OUYANG, S., SCHWARTZ, D.C., TANAKA, T., WU, J.,

ZHOU, S. and CHILDS, K.L., 2013. Improvement of the *Oryza sativa* Nipponbare reference genome using next generation sequence and optical map data. *Rice*, **6**(1), p.4.

KEARNS, A.M., RESTANI, M., SZABO, I., SCHRØDER-NIELSEN, A., KIM, J.A., RICHARDSON, H.M., MARZLUFF, J.M., FLEISCHER, R.C., JOHNSEN, A. and OMLAND, K.E., 2018. Genomic evidence of speciation reversal in ravens. *Nature communications*, **9**(1), p.906.

KAWECKI, T.J. and EBERT, D., 2004. Conceptual issues in local adaptation. *Ecology letters*, **7**(12), pp.1225-1241.

KIRSCHEL, A.N., BLUMSTEIN, D.T. and SMITH, T.B., 2009a. Character displacement of song and morphology in African tinkerbirds. *Proceedings of the National Academy of Sciences*, **106**(20), pp.8256-8261.

KIRSCHEL, A.N.G., BLUMSTEIN, D.T., COHEN, R.E., BUERMANN, W., SMITH, T.B. and SLABBEKOORN, H. 2009b. Birdsong tuned to the environment: green hylia song varies with elevation, tree cover, and noise. *Behavioural Ecology,* **20**: 1089–1095.

KIRSCHEL A. N. G. H. SLABBEKOORN, D. T. BLUMSTEIN, R. E. COHEN, S. R. DE KORT, W. BUERMANN, and T. B. SMITH., 2011. Testing alternative hypotheses for evolutionary diversification in an African songbird: rainforest refugia versus ecological gradients. *Evolution*. **65**, pp. 3162–3174.

KIRSCHEL, A.N., NWANKWO, E.C. and GONZALEZ, J.C.T., 2018. Investigation of the status of the enigmatic White-chested Tinkerbird Pogoniulus makawai using molecular analysis of the type specimen. *Ibis*. https://doi.org/10.1111/ibi.12597

KIRKPATRICK, M. and BARTON, N.H., 1997. Evolution of a species' range. *The American Naturalist*, **150**(1), pp.1-23.

KLEINDORFER, S., O'CONNOR, J.A., DUDANIEC, R.Y., MYERS, S.A., ROBERTSON, J. and SULLOWAY, F.J., 2014. Species collapse via hybridization in Darwin's tree finches. *The American Naturalist*, **183**(3), pp.325-341.

KOCHER, T.D., THOMAS, W.K., MEYER, A., EDWARDS, S. V, PÄÄBO, S., VILLABLANCA, F.X., *et al*. 1989. Dynamics of mitochondrial DNA evolution in animals: amplification and sequencing with conserved primers. *Proceedings of the National Academic Sciences of the United State of America,* **86**: 6196–6200.

LANFEAR, R., FRANDSEN, P.B., WRIGHT, A.M., SENFELD, T. and CALCOTT, B., 2016. PartitionFinder 2: new methods for selecting partitioned models of evolution for molecular and morphological phylogenetic analyses. *Molecular Biology and Evolution*, **34**(3), pp.772-773.

LEAL, M. and FLEISHMAN, L.J., 2002. Evidence for habitat partitioning based on adaptation to environmental light in a pair of sympatric lizard species. *Proceedings of the Royal Society of London B: Biological Sciences*, **269**(1489):351-359.

LEE, C.E., 2002. Evolutionary genetics of invasive species. *Trends in ecology and evolution*, **17**(8):386-391.

LUTHER, D., 2009. The influence of the acoustic community on songs of birds in a neotropical rain forest. *Behavioral Ecology,* **20**(4), pp. 864-871.

MACLEAN, G. L. 1993. *Roberts' birds of Southern Africa.* 6th edition. Trustees of the John Voelcker Bird Book Fund, Cape Town.

MARCHETTI, K. 1993 Dark habitats and bright birds illustrate the role of the environment in species divergence. Nature **362**, 149–152.

MASON, N.A., BURNS, K.J., TOBIAS, J.A., CLARAMUNT, S., SEDDON, N. and DERRYBERRY, E.P., 2016. Song evolution, speciation, and vocal learning in passerine birds. *Evolution*. 1–27

MAYDEN R. L., 1999, Consilience and a hierarchy of species concepts: Advances toward closure on the species puzzle, *Journal of Nematology*, vol. **31**:95-116.

MAYR, E., 1982. Speciation and macroevolution. *Evolution*, **36**(6):1119-1132.

MULLEN, L.M. and HOEKSTRA, H.E., 2008. Natural selection along an environmental gradient: a classic cline in mouse pigmentation. *Evolution*, **62**(7), pp.1555-1570.

MICHEL, A.P., SIM, S., POWELL, T.H., TAYLOR, M.S., NOSIL, P. and FEDER, J.L., 2010. Widespread genomic divergence during sympatric speciation. *Proceedings of the National Academy of Sciences*, **107**(21), pp.9724-9729.

MLÍKOVSKÝ J. 2002. *Cenozoic birds of the world*. Part 1: Europe. Praha: Ninox Press.

MORTON, E.S., 1975. Ecological sources of selection on avian sounds. *The American Naturalist,* **109**(965), pp. 17-34.

NACHMAN, M.W., 2002. Variation in recombination rate across the genome: evidence and implications. *Current opinion in genetics and development*, **12**(6), pp.657-663.

NACHMAN, M.W., HOEKSTRA, H.E. and D'AGOSTINO, S.L., 2003. The genetic basis of adaptive melanism in pocket mice. *Proceedings of the National Academy of Sciences of the United States of America,* **100**(9), pp. 5268-5273.

NAHUM, L.A., PEREIRA, S.L., CAMPOS FERNANDES, F.M.D., RUSSO MATIOLI, S. and WAJNTAL, A., 2003. Diversification of Ramphastinae (Aves, Ramphastidae) prior to the Cretaceous/Tertiary boundary as shown by molecular clock of mtDNA sequences. *Genetics and Molecular Biology*, **26**(4), pp.411-418.

NEMETH, E., PIERETTI, N., ZOLLINGER, S.A., GEBERZAHN, N., PARTECKE, J., MIRANDA, A.C. and BRUMM, H., 2013. Bird song and anthropogenic noise: vocal constraints may explain why birds sing higher-frequency songs in cities. *Proc. R. Soc. B*, **280**(1754):2012-2798.

PATON, T., HADDRATH, O. and BAKER, A.J., 2002. Complete mitochondrial DNA genome sequences show that modern birds are not descended from transitional shorebirds. *Proceedings of the Royal Society of London B: Biological Sciences*, **269**(1493), pp.839-846.

PRICE, T., 1998. Sexual selection and natural selection in bird speciation. *Philosophical Transactions of the Royal Society B: Biological Sciences*, **353**(1366), pp.251-260.

PRITCHARD, J.K., STEPHENS, M. and DONNELLY, P., 2000. Inference of population structure using multilocus genotype data. *Genetics,* **155**(2), pp. 945-959.

RAMBAUT, A., SUCHARD, M., XIE, W. and DRUMMOND, A. 2014. Tracer v. 1.6. Institute of Evolutionary Biology, University of Edinburgh.

R DEVELOPMENT CORE TEAM. 2017. *R: A Language and Environment for Statistical Computing* (R Foundation for Statistical Computing, Vienna).

RICE, W.R. and HOSTERT, E.E., 1993. Laboratory experiments on speciation: what have we learned in 40 years? *Evolution*, **47**(6), pp.1637-1653.

RIEBEL, K., 2009. Song and female mate choice in zebra finches: a review. *Advances in the Study of Behavior*, **40**, pp.197-238.

ROTHSTEIN, S.I. and FLEISCHER, R.C., 1987. Vocal dialects and their possible relation to honest status signalling in the brown-headed cowbird. *Condor*, pp. 1-23.

RUNDLE, H.D., NAGEL, L., BOUGHMAN, J.W. and SCHLUTER, D., 2000. Natural selection and parallel speciation in sympatric sticklebacks. *Science*, **287**(5451), pp.306-308.

RUNDLE, H. D., S. F. CHENOWETH, P. DOUGHTY, and M. W. BLOWS. 2005. Divergent selection and the evolution of signal traits and mating preferences. *PLoS Biol*. **3**:e368.

SEDDON, N., 2005. Ecological adaptation and species recognition drives vocal evolution in neotropical suboscine birds. *Evolution,* **59**(1), pp. 200-215.

SEXTON, J.P., MCINTYRE, P.J., ANGERT, A.L. and RICE, K.J., 2009. Evolution and ecology of species range limits. *Annual Review of Ecology, Evolution, and Systematics*, **40**.

SLABBEKOORN, H., J. ELLERS, and T. B. SMITH. 2002. Birdsong and sound transmission: the benefits of reverberations. *Condor* **104**, pp. 564–573.

SLABBEKOORN, H. and SMITH, T.B., 2002a. Habitat-dependent song divergence in the little greenbul: an analysis of environmental selection pressures on acoustic signals. *Evolution*, **56**(9), pp.1849-1858.

SLABBEKOORN, H. and SMITH, T.B. 2002b. Bird song, ecology and speciation. *Philosophical Transactions of the Royal Society of London B: Biological,* **357**: 493–503.

SLADE, R.W., MORITZ, C., HEIDEMAN, A. and HALE, P.T., 1993. Rapid assessment of single-copy nuclear DNA variation in diverse species. *Molecular Ecology*, **2**(6), pp.359-373.

SCHLUTER, D., 2001. Ecology and the origin of species. *Trends in ecology and evolution*, *16*(7), pp.372-380.

SCHLUTER, D., 2009. Evidence for ecological speciation and its alternative. *Science*, **323**(5915), pp.737-741.

SHORT, L. and HORNE, J.F., 2001. *Toucans, barbets, and honeyguides: Ramphastidae, Capitonidae and Indicatoridae* (Vol. 8). Oxford University Press.

SNELL-ROOD, E.C. and BADYAEV, A.V., 2008. Ecological gradient of sexual selection: elevation and song elaboration in finches. *Oecologia*, *157*(3), pp.545-551.

STATACORP, L. P. 2015. Stata 11. TX, USA: StataCorp LP.

STRYJEWSKI, K.F. and SORENSON, M.D., 2017. Mosaic genome evolution in a recent and rapid avian radiation. *Nature ecology and evolution*, 1(12), p.1912.

TAKEDA, H., 2008. Draft genome of the medaka fish: a comprehensive resource for medaka developmental genetics and vertebrate evolutionary biology. *Development, growth and differentiation*, **50**(s1).

TAYLOR, E.B., BOUGHMAN, J.W., GROENENBOOM, M., SNIATYNSKI, M., SCHLUTER, D. and GOW, J.L., 2006. Speciation in reverse: morphological and genetic evidence of the collapse of a three-spined stickleback (Gasterosteus aculeatus) species pair. *Molecular Ecology*, **15**(2), pp.343-355.

TEN CATE, C., SLABBEKOORN, H. and BALLINTIJN, M.R., 2002. Birdsong and male—male competition: causes and consequences of vocal variability in the collared dove (*Streptopelia decaocto*). In *Advances in the Study of Behavior* (Vol. 31, pp. 31-75). Academic Press.

TOBIAS, J.A. and SEDDON, N. 2009. Signal design and perception in Hypocnemis antbirds: evidence for convergent evolution via social selection. *Evolution,* **63**: 3168–3189.

TOBIAS, J.A., ABEN, J., BRUMFIELD, R.T., DERRYBERRY, E.P., HALFWERK, W., SLABBEKOORN, H. and SEDDON, N., 2010a. Song divergence by sensory drive in Amazonian birds. *Evolution*, **64**(10), pp.2820-2839.

TOBIAS, J.A., SEDDON, N., SPOTTISWOODE, C.N., PILGRIM, J.D., FISHPOOL, L.D.C. and COLLAR, N.J. 2010b. Quantitative criteria for species delimitation. *Ibis,* **152**: 724–746.

TOEWS, D.P., HOFMEISTER, N.R. and TAYLOR, S.A., 2017. The evolution and genetics of carotenoid processing in animals. *Trends in Genetics,* **33**(3), pp. 171-182.

TOEWS, D.P., TAYLOR, S.A., VALLENDER, R., BRELSFORD, A., BUTCHER, B.G., MESSER, P.W. and LOVETTE, I.J., 2016. Plumage genes and little else distinguish the genomes of hybridizing warblers. *Current Biology*, **26**(17), pp.2313-2318.

TUMER, E.C. and BRAINARD, M.S., 2007. Performance variability enables adaptive plasticity of 'crystallized'adult birdsong. *Nature,* **450**(7173), pp. 1240.

WIENS, J.J. and DONOGHUE, M.J., 2004. Historical biogeography, ecology and species richness. *Trends in ecology and evolution*, *19*(12), pp.639-644.

WILEY, R.H., 1991. Associations of song properties with habitats for territorial oscine birds of eastern North America. *The American Naturalist*, **138**(4), pp.973-993.

WILEY, R.H. and RICHARDS, D.G., 1978. Physical constraints on acoustic communication in the atmosphere: implications for the evolution of animal vocalizations. *Behavioral Ecology and Sociobiology*, **3**(1), pp.69-94.

WILEY, R. H., and D. G. RICHARDS. 1982. Adaptations for acoustic communication in birds: sound transmission and signal detection. Pp. 131–181 in D. E. Kroodsma and E. H. Miller, eds. Acoustic communication in birds. Vol. 1. Academic Press, New York.

WILKINS, M.R., SEDDON, N. and SAFRAN, R.J. 2013. Evolutionary divergence in acoustic signals: causes and consequences. *Trends in Ecology and Evolution,* **28**: 156–166.

WU, C.I., 2001. The genic view of the process of speciation. *Journal of Evolutionary Biology*, **14**(6), pp.851-865.

CHAPTER TWO

Rapid song divergence leads to discordance between genetic distance and phenotypic characters important in reproductive isolation

(The work in this chapter has been published: NWANKWO, E. C., PALLARI, C. T., HADJIOANNOU, L., IOANNOU, A., MULWA, R. K., AND KIRSCHEL, A. N. G., 2018. Rapid song divergence leads to discordance between genetic distance and phenotypic characters important in reproductive isolation. *Ecology and Evolution*, 8:716–731.)

Abstract

The criteria for species delimitation in birds have long been debated, and several recent studies have proposed new methods for such delimitation. On one side, there is a large consensus of investigators who believe that the only evidence that can be used to delimit species is molecular phylogenetics, and with increasing numbers of markers to gain better support, whereas on the other, there are investigators adopting alternative approaches based largely on phenotypic differences, including in morphology and communication signals. Yet, these methods have little to say about rapid differentiation in specific traits shown to be important in reproductive isolation. Here, we examine variation in phenotypic (morphology, plumage, and song) and genotypic (mitochondrial and nuclear DNA) traits among populations of yellow-rumped tinkerbird *Pogoniulus bilineatus* in East Africa. Strikingly, song divergence between the *P. b. fischeri* subspecies from Kenya and Zanzibar and *P. b. bilineatus* from Tanzania is discordant with genetic distance, having occurred over a short time frame, and playback experiments show that adjacent populations of *P. b. bilineatus* and *P. b. fischeri* do not recognize one another's songs. While such rapid divergence might suggest a founder event following invasion of Zanzibar, molecular evidence suggests otherwise, with insular *P. b. fischeri* nested within mainland *P. b. fischeri*. Populations from the Eastern Arc Mountains are genetically more distant yet share the same song with *P. b. bilineatus* from Coastal Tanzania and Southern Africa, suggesting they would interbreed. We believe investigators ought to examine potentially rapid divergence in traits important in species recognition and sexual selection when

delimiting species, rather than relying entirely on arbitrary quantitative characters or molecular markers.

Introduction

Historically, species delimitation was based on morphological differences identified among specimens of organisms by natural historians and collectors (Linnaeus 1758; Agardh 1852). Over time, several alternative species concepts had been proposed, and Ernst Mayr's Biological Species Concept (BSC), focusing on the ability of different groups to interbreed (Mayr 1963), gained much favour. However, because related groups of organisms are commonly distributed allopatrically, delimitation of species using the BSC has seldom been tested in nature (Lagache et al. 2013). Because species diversification results from cumulative changes in heritable traits among populations, molecular phylogenetics have become the most commonly used methodology for species delimitation, with phylogenies reflecting evolutionary histories, and accordingly the phylogenetic species concept (PSC) has prevailed in recent times, especially in studies on birds (Cracraft 1992; Barrowclough et al. 2016). Fine scale phylogeographic studies have used one or more genes, often mitochondrial genes, to establish patterns of historical biogeography. But, mitochondrial gene trees are not always congruent with species trees (Moore 1995; Rokas et al. 2003; Edwards et al. 2005), often because of mito-nuclear discordance (Toews and Brelsford 2012). More recent studies have incorporated nuclear genes to determine the extent of concordance with faster-evolving mitochondrial genes, or even orders of magnitude more markers via next-generation sequencing methods (NGS) such as double-digest Restriction Associated DNA sequencing (ddRADseq) and hybrid enrichment (reviewed in Lemmon and Lemmon 2013).

While phylogeographic studies might reveal to a greater or lesser extent how long populations have been evolving in isolation, they reveal little with regards to which diverging characters lead to reproductive isolation and speciation. Divergence in characters that lead to reproductive isolation could occur at a much faster rate than the mutation rate of many markers used in phylogenetic studies (Mallet 2005; but see Winger and Bates 2015), such as in a gene affecting visual or acoustic communication signals that affect mate choice or species recognition. An alternative approach for species delimitation was proposed by Tobias et al. (2010), based on a calibration of phenotypic differences of a set of 58 species pairs occurring in sympatry, and applying that calibration to species in allopatry. The study has stimulated a heated debate between its authors and proponents (e.g. Collar et al. 2016) and PSC supporters (e.g. Remsen 2015), though neither system addresses the issue of reproductive isolation among species.

Rapid divergence in characters leading to reproductive isolation between populations could be driven by natural selection, by adaptation to differences between their constituent environments (Dynesius and Jansson 2000), or sexual selection (Gavrilets 2000), or even by genetic drift resulting from a founder event. Mayr (1947, 1982) championed the role of drift driving 'genetic revolutions' in his definition of peripatric speciation, the process he proposed to explain divergence in phenotypic characters in island populations following dispersal from the mainland. If such rapid speciation can occur in such circumstances, how does it correspond with genetic divergence in a group of related organisms?

In birds, song, colour pattern, and morphology are important signals in conspecific interaction (Clayton 1990; Andersson 1994; Candolin 2003; Partan and Marler 2005). Over time, divergence in these traits across populations can lead to positive assortative mating with corresponding divergence in the recognition of those traits (Price 1998), and consequently reproductive isolation. Studies using experiments with taxidermic mount presentations and

song playback have shown how divergence in phenotypic traits might lead to species recognition failure, including in plumage and song (e.g. Uy et al. 2009). There is also much evidence of increased body size (e.g. gigantism) between island populations and populations on the mainland (Murphy 1938). Body size is negatively correlated with song frequency in birds (Wallschlager 1980; Ryan and Brenowitz 1985; Seddon 2005), and bill shape with song pace (Podos 2001), and divergence in these morphological traits could lead to distinct song differences affecting mate choice or species recognition.

Little is known regarding the extent to which such phenotypic divergence corresponds to genetic divergence among populations with varying extents of genetic isolation. In the present study we examined the patterns of diversification between populations of yellow-rumped tinkerbird (*Pogoniulus bilineatus*) with the specific objective of comparing variation in song characteristics and song recognition, morphology and plumage, and genetic differentiation between populations of the subspecies *P. bilineatus bilineatus* (hereafter *bilineatus*) and *P. bilineatus fischeri* (hereafter *fischeri*) in Eastern to Southern Africa. We focused on these subspecies because they had been reported to emit distinctly different vocalisations (e.g. Stevenson and Fanshawe 2002). We thus wanted to investigate the possibility that divergence in song could have resulted from a founder event following dispersal to island populations, and specifically Zanzibar, and compare patterns of phenotypic variation with genetic divergence among populations. The aim of the study is thus to understand the mode of speciation between the two subspecies, and the extent to which phenotypic divergence corresponds with genetic differentiation. In addition to *fischeri* from coastal Kenya and Zanzibar (specifically Unguja island) and *bilineatus* from Coastal Tanzania southwards to eastern South Africa, we also included populations from the lower Eastern Arc Mountains in the study. Some recent studies on other species from these mountains have revealed high levels of differentiation (Bowie et al. 2004; Bowie and Fjeldså 2005; Burgess et al. 2007; Fjeldså et al. 2012). A subspecies of

yellow-rumped tinkerbird *P. b. conciliator* (hereafter *conciliator*) was described from the Uluguru Mountains within the Eastern Arc Mountains by Friedmann (1929), but subsequently synonymised with *fischeri* (Short and Horne 2002); yet the morphological traits that led Friedmann (1929) to originally describe it as different mean it is worth investigating in the context of differential patterns of phenotypic and genetic divergence among regional populations.

We hypothesised that because song is considered an innate character in Piciformes (Kirschel et al. 2009a), variation in song, along with heritable morphological characters, should be concordant with patterns of population genetic structure and phylogeny. We thus examined patterns of song variation in the field and tested the extent to which variation was detectable to different populations using playback experiments, and examined patterns of variation in morphology and plumage in museum specimens, while collecting DNA samples in the field for molecular phylogenetic and population genetic analyses.

Materials and Methods

Field recordings and song analyses

We examined variation in acoustic signal characteristics in 67 yellow-rumped tinkerbird from East to Southern Africa. Songs were recorded in the field at 25 sites in Kenya and Tanzania, including Zanzibar, between July 2011 and March 2014, and in Swaziland in March 2015, using a Marantz PMD 661 (Marantz Corporation, Kanagawa, Japan) solid-state digital recorder with a Sennheiser MKH-8020 microphone housed in a Telinga Universal parabolic reflector, or a Sennheiser MKH-8050 directional microphone housed in a Rycote Modular Windshield WS 9 Kit, at 16 bits and a 48 kHz sampling rate. Raven 1.4 software was used for sound analyses (Charif et al. 2010). Five songs per recording were measured and mean values calculated. The following parameters were measured: Peak frequency (Hz), delta time (s), last

pulse duration, inter-note interval (gap) and number of pulses. The rate of each song was computed using the formula below (from Kirschel et al. 2009a):

$$R = \frac{(NP-1)}{(DT-LC)}$$

where R= Rate of song

NP = Number of pulses

DT = Delta time

LC = Last pulse duration

Playback experiment

For the playback experiments, we used synthetically produced playbacks as stimuli, to prevent pseudoreplication associated with authentic recordings (McGregor et al. 1992). This method permits testing specifically for the effect of differences in frequency and rate between the two subspecies' songs and avoids motivational, signal-to-noise ratio, geographic population, background noise, or other differences inherent in field recordings (McGregor et al. 1992). For the *fischeri* stimulus we took mean values from 21 recordings collected from four populations in Kenya in 2011/2012. For *bilineatus* we used 10 recordings collected from 10 populations in Tanzania in 2013. Mean song frequency and rate from all the recordings for each subspecies were used to produce the synthetic playback stimuli using Audacity (Audacity, v. 1.3.3, 2011). Some experiments were performed using an alternative *bilineatus* synthetic stimulus, e.g., for experiments in Kenya in 2012 prior to obtaining recordings of *bilineatus* from Tanzania in 2013 to produce the stimulus, and in those cases, we used a previously prepared synthetic stimulus for *P. bilineatus* based on recordings from Uganda (Kirschel et al. 2009a). The Uganda song-based stimulus was prepared using a song frequency and rate well within the range of variation of recordings used to prepare the *bilineatus* from Tanzania stimulus.

Playback experiments were performed on 16 individuals (five in Tanzania, eight in Zanzibar and three in Kenya). Each paired playback experiment lasted twelve minutes, during which two sets of stimuli were presented. For each individual we placed a speaker and playback recorder within 30 m of the location of the focal bird. In all cases distances were estimated to the nearest meter and behavioural data were recorded during the playback experiment. The playback stimuli consisted of one min silence pre-playback, two min playback of the first song stimulus and one min silence post-playback. The focal bird's singing behaviour was recorded during the pre-playback silence and then during stimulus playback and in the post-playback silence to allow for testing of the effect of playback on song behaviour. A further four minutes of silence was observed before initiating the second experiment of the pair. Six variables were selected to characterise behavioural responses (see Table 1). The six variables were reduced to a single variable by Factor Analysis of Mixed Data (FAMD, Pages, 2004). This method calculated principal components accounting for both continuous and categorical variables. The first principal component was used to test for significant variation in responses to playbacks using a generalized linear model.

Table 1. Behavioural variables used to measure response of focal individuals to song playback.

Variable	**Description**
Latency to flight toward speaker (L)(sec)	Time until the focal bird flew toward the playback speaker, recorded in seconds.
Total time spent (T_t)(sec)	Total time spent by the bird within 20m for the entire playback experiment.
Number of songs before playback (NS_{bp})	Number of songs emitted by the focal bird before the commencement of the playback (pre-playback).
Number of songs during playback (NS_{dp})	Number of songs of the focal bird during the playback.
Number of songs after playback (NS_{ap})	Number of songs of the focal bird after the playback (post-playback).

Closest distance	The closest distance of the focal bird to the playback speaker.

Song analysis

We used linear mixed models to test for differences in song frequency and rate among populations (Cnaan et al., 1997). To control for possible variation within regions explained by ecological gradients, we included elevation as a predictor in the model, and site was included as a random effect to control for any variation explained within site locations. The 25 sites were grouped into three populations as follows: *bilineatus* comprising 14 sites in coastal forest in Tanzania and one in Swaziland; *conciliator* comprising the Udzungwa mountains; *fischeri* comprising seven sites along the coast of Kenya and two in Zanzibar.

Several models were run in R 3.3.0 (R Core Team, 2017) and the best approximating model in explaining variation in song rate and peak frequency was selected using the backward deletion method and compared with the full model using an information-theoretic approach based on Akaike's Information Criterion (AIC).

We compared differences in the dispersion of song frequency and rate among populations, using the coefficient of variation, calculated using the formula:

$$CV = \frac{SD}{Mean} \times 100$$

Where CV = coefficient of variation, and SD = standard deviation

We tested for homogeneity of variances of the measured song variables across populations as a prerequisite to the use of parametric statistical tests based on Levene's test implemented within R 3.3.0 (Table S1). A Multi-Response Permutation Procedure of within- versus among-

group dissimilarities was used to ensure that significant variations observed were not as a result of greater variation in song properties within the populations (vegan, Oksanen et al., 2016). We also used a generalized canonical discriminant analysis on the song properties to estimate the degree of classification efficiency of the populations based on their song characteristics (candisc, Friendly and Fox 2016).

Morphometrics

Specimens from the ornithology collections of the Natural History Museum of Los Angeles County (LACM), British Museum of Natural History (BMNH), and Zoological Museum of the University of Copenhagen (ZMUC) were used to obtain morphometric data. In total, we took morphometric measurements from 71 specimens. Informed by our findings in the field, we assigned subspecies for analysis accordingly: *fischeri* = 19 specimens from Kenya and Zanzibar, *bilineatus* = 41 specimens from Tanzania coast, Mafia Island, Mozambique, Malawi, Zimbabwe and South Africa; and *conciliator* = 11 specimens from the Eastern Arc mountains (Uluguru, Nguru, and Udzungwa mountains). Measurements were taken using digital calipers, and included wing chord, tarsus and tail length, bill length and width, and lower mandible length. The localities where specimens were collected were identified from museum tags, maps, gazetteers, and Google Earth (Google, Inc.), for those specimens where coordinates were not given, and assigned approximate latitude and longitude coordinates and elevation for each locality. Moderate Resolution Imaging Radiometer raster files at 250 m resolution (MODIS/Terra Vegetation Indices 16-Day L3 Global 250m from 2010 were used to extract vegetation continuous field (VCF) and enhanced vegetation index (EVI) data for coordinates of the sampling locations in ArcGIS 10.1 (ESRI, 2012).

Principal Component Analysis (PCA) was used in the analysis of the morphology data, which allowed us to reduce the eight morphological variables (wing, tarsus, tail, bill length, culmen, upper bill depth, bill width and lower mandible) into two principal components to determine the dimensions of variability in body size and bill shape of the study species. The PCA was performed in STATA 10.1 (STATACorp, 2009). The first principal component was used to test for variation in morphology resulting from differences between the sexes using a generalized linear mixed effects model.

Plumage colour measurements

We measured reflectance spectra (200-900 nm) of feathers on the breast, belly, and rump of 31 museum study skins at the BMNH and ZMUC, incorporating 10 *fischeri* (Kenya/Zanzibar), 10 *bilineatus* from Tanzania, three *conciliator* from the Eastern Arc Mountains (Udzungwa), and eight *bilineatus* from Southern Africa, using a JAZ spectrometer (Ocean Optics) with a fiber optic reflectance probe (Ocean Optics R-200) and PX xenon light source. The reflection probe was placed in an RPH-1 Reflection Probe Holder (Ocean Optics), at a 90° angle, and secured at 2 mm from the aperture of the probe holder. Two measurements were taken per plumage patch, per specimen, with the specimen placed flat onto a white background perpendicular to the observer and facing to the left, and then rotated 180° for the second measurement, with the probe holder placed horizontally onto the specimen, so the aperture completely covered the feather patch, thus ensuring ambient light was excluded. Reflectance data for each specimen were obtained following calibration with a white standard (Ocean Optics WS-1) and dark standard (by screwing the lid back onto the fiber optic connector to ensure no light entered), and recorded in SPECTRASuite (Version 1.0, Ocean Optics).

Plumage analysis

Pavo (an R package for the perceptual analysis, visualization and organization of colour data, Maia et al., 2013) implemented within R statistical software (version 3.2.4) was used for the plumage colour analysis. Replicate reflectance spectra were averaged and smoothed with a span of 0.25 for further analysis. Negative value correction on the spectra data were implemented by adding min to all reflectance. The colour distances within and between the populations were calculated by using the function *coldist,* which applies the visual models of Vorobyev et al. (1998) to calculate colour distances with receptor noise based on relative photoreceptor densities. A hue projection plot was produced using the function *projplot.* This is a 2D plot of colour points projected from the tetrahedron to its encapsulating sphere to visualize differences in hue. The Mollweide projection was used in the hue projection plot instead of the Robinson projection, because the Mollweide projection preserves area relationships within latitudes without distortion (Maia et al. 2017). The avian tetracolourspace visual model was computed using the *tcs* function, which calculates coordinates and colourimetric variables that represent reflectance spectra in the avian tetrahedral colour space: *u, s, m, l* (the quantum catch data); *u.r, s.r, m.r, l.r* (relative cone stimulation, for a given hue, as a function of saturation); *x, y, z* (cartesian coordinates for the points in the tetrahedral colour space); *h.theta, h.phi* (angles theta and phi, in radians, determining the hue of the colour); *r.vec* (the r vector indicating saturation, distance from the achromatic center); *r.max* (the maximum r vector achievable for the colour's hue); *r.achieved* (the relative r distance from the achromatic center, in relation to the maximum distance achievable). The function *voloverlap* was used to calculate the overlap between population colour volumes defined by two sets of points in colourspace. The volume from the overlap was then presented relative to: *vsmallest* the volume of the overlap divided by the smallest of that defined by the the two input sets of colour points and *vboth* the ratio of volume of the overlap and the combined volume of both input sets of

colour points. Thus, *vsmallest* = 1 indicates that one of the volumes is entirely contained within the other (Stoddard and Prum 2008; Stoddard and Stevens 2011; Maia et al. 2013). Additional 3 colourimetric variables (hue, brightness, and chroma) of the three plumage patches as reviewed in Montgomerie (2006) were calculated using the *summary* function.

Categorical description analysis of the colourimetric variables within FactoMineR package was used to select variables that best described the species per plumage patch at $P \leq 0.05$. Subsequently, the selected variables were used in Permutational Multivariate Analysis of Variance (with vegan package) using Euclidean Distance Matrices for partitioning distance matrices among sources of variation and fitting linear models (on species as factors) to distance matrices using a permutation test of 10000 iterations. All statistical analyses were run using R Statistical Software versions 3.3.1 (R Core Team, 2017).

Genetic sampling and analysis

Fieldwork was performed in Kenya and Tanzania, including Zanzibar as described above, and in Swaziland in March 2015. Tinkerbirds were captured using targeted mist netting with conspecific playback, given a metal and colour ring combination, and blood samples were obtained from the ulnar superficial vein (wing) and transferred into 2 ml cryovials containing 1 ml Queens Lysis Buffer (Hobson et al. 1997). Samples were stored at -20 °C in the lab, after returning from the field. DNA was extracted using a Qiagen DNeasy blood and tissue kit following manufacturer's protocols (Qiagen, Valencia, CA). PCR was performed to amplify DNA of the mitochondrial Cytochrome *b* gene using primers L14841 (Kocher et al. 1989), and H4a (Harshman 1994), and nuclear intron β-fibrinogen 5 using primers FGB5 and FGB6 (Marini and Hackett 2002) on an Applied Biosystems Thermal Cycler (model 2720) and resulting bands visualised by Gel Electrophoresis on a 1% agarose/TAE gel. Cytochrome *b* and β-fibrinogen intron 5 were sequenced from 64 samples we collected in the field, two samples

from Mozambique, obtained from the Muséum National d'Histoire Naturelle (MNHN), and one sample from Mafia Island, Tanzania, obtained from ZMUC. We chose β-fibrinogen intron 5 because it has been shown to be informative in several avian phylogenetics studies (e.g., Klicka et al. 2014), including in Piciformes (Fuchs and Pons 2015; Dufort 2016). Rates of evolution of nuclear genes may vary from those of mtDNA, and we included a nuclear intron because of their slower evolution rate relative to mtDNA (Prychitko and Moore 1997, 2000; Johnson and Clayton 2000), they are adaptively neutral due to high substitution rates, with frequent occurrence of indels (insertions and deletions), and they have a lower transition/transversion ratio, with lower homoplasy than mtDNA (Prychitko and Moore 2000).

The DNA sequences were aligned using ClustalW implemented in MEGA software version 7 (Kumar et al. 2015). For Cytochrome *b* we added outgroup sequences for *Melanerpes carolinus* and *Lybius dubius* (GenBank U89192 and AY279291), as well as three sequences from two *Pogoniulus bilineatus* and one *P. simplex* from a previous study (GenBank MG211663, 64, 70 respectively) and performed analyses on a 1008 bp fragment. For β-fibrinogen intron 5 we also sequenced a sample of *Tricholaema diadematata* from Kenya, of *Pogoniulus simplex* from Tanzania, and of *P. subsulphureus* from Nigeria, for use as an outgroup, and performed analyses on a 529 bp fragment. Newly generated sequences have been deposited in GenBank (MG437418-79, MG576343-402).

Phylogenetic analysis

Using our aligned sequences, we compared models of evolution using R package phangorn (Schliep 2011). We selected the Hasegawa-Kishino-Yano (HKY) substitution model (Hasegawa et al. 1985) with Invariant distribution for Cytochrome *b* (Hasegawa et al. 1985), one of the highest scoring models based on both AICc and BIC scores that had readily available scripts that could be implemented in RevBayes 1.0.3 (Hohna et al. 2016).

The Maximum Likelihood (ML) trees for Cytochrome *b* and β-fibrinogen 5 were constructed using RAxML BlackBox online tool (Ostberg, Rodriguez 2004, Yau, Taylor 2014) using the Hasegawa-Kishino-Yano (HKY) substitution model (Hasegawa et al. 1985) with Gamma model of rate heterogeneity for the construction of the ML tree for Cytochrome *b* and HKY for β-fibrinogen 5.

We created a stochastic node with a normal distribution (mean = 8, sd = 1, min = 5.38 and max = 11.38) using 5.38 MYA as a minimum age limit for the ancestor of the *Pogoniulus* tinkerbirds (Mlíkovský 2002), to estimate divergence dates in Revbayes 1.0.3 (Hohna et al. 2016) and applied a single substitution model uniformly to all sites. We avoided having the divergence time reference from being fixed and therefore allowed for flexibility (within the lower and upper boundaries of Late Miocene geological time scale) in the calibration of the phylogenetic tree as the divergence may have happened before the proposed 5.38 MYA (Mlíkovský 2002). We applied Birth-Death tree priors with the prior mean centered on the expected number of species under a Yule process and a prior standard deviation of 0.587405. This was to allow us to create a lognormal distribution with 95% prior probability spanning exactly one order of magnitude within which we fixed our prior uncertainty.

We used a relaxed uncorrelated lognormal clock model and an exponential prior for the mean rate of each partition. The sampling probability was set to the ratio of the tips and estimated total number of described bird species (10426) and we ran a burn-in phase of Monte Carlo Markov Chain (MCMC) sampler for 10,000 iterations under two independent replicates using 13 different moves in a random move schedule with 44 moves per iteration and tuning interval of 250. The main phase of the MCMC analysis was run for one million generations sampling every 200 generations under two independent runs and the same random moves as in the burn-in phase. Convergence from the independent runs and ESS values were evaluated in

Tracer 1.6 (Rambaut et al. 2014). The final tree was produced from the generated trees by compiling the maximum posteriori tree using a burn-in of 20%.

Population genetics

We screened our data to determine populations with fixed alleles and removed the uninformative sites from downstream analyses. The strength of our data in discriminating between unique individuals given a random number of sites was determined based on a haplotype accumulation curve. The overall quality of our haplotype data was examined, including a search for missing data and rare alleles.

The analysis of the relationship between individuals, sub-populations, and populations were performed using genetic distance measures by calculating the "distance" between samples based on their genetic profile. Provesti's distance (Prevosti 1975) was used in estimating the genetic distances as it returns the fraction of the number of differences between individuals, sub-populations and populations. These were implemented with the R packages poppr (Kamvar 2014) and mmod (Winter 2012). We used the genetic distance matrix to create a neighbor-joining tree to visualize the relationships in genetic distances at individual, sub-population and population levels. To determine if the major genotypes of the subspecies are closely related and to what degree they contribute to the genotypes of the each other population, we produced a haplotype network (Minimum Spanning Network) for the Cytochrome *b* gene using poppr (Kamvar 2014) and ade4 (Dray and Dufour 2007) R packages. The haplotype network was constructed using 62 sequences (excluding outgroups) of Cytochrome *b* that were obtained from 21 different localities.

AMOVA (Analysis of Molecular Variance) was used to detect population differentiation (Excoffier et al. 1992). The AMOVA was implemented in poppr (Kamvar 2014) and ade4 (Dray and Dufour 2007) R packages based on the Provesti's genotypic distance of the cytb

gene with the major population levels as the specified strata field (Kenya (coast), Tanzania (coast, including south to Swaziland), Zanzibar, and Udzungwa (and Nguru mountains). Our expectation in a typical panmictic population would be to see most of the variance arise from samples within rather than among populations. We would find evidence that we have population structure if most of the variance occurs among populations.

Results

From our fieldwork performed between 2011 and 2014 we found no evidence of *fischeri* occurring in Coastal Tanzania, where instead we found *bilineatus* (Figure 1) These findings were primarily based on songs recorded in each region, where songs in Coastal Kenya and Zanzibar fit the *fischeri* song type, and songs in Tanzania the *bilineatus* song type. All analyses referring to *fischeri*, thus refer to populations from Kenya and Zanzibar only.

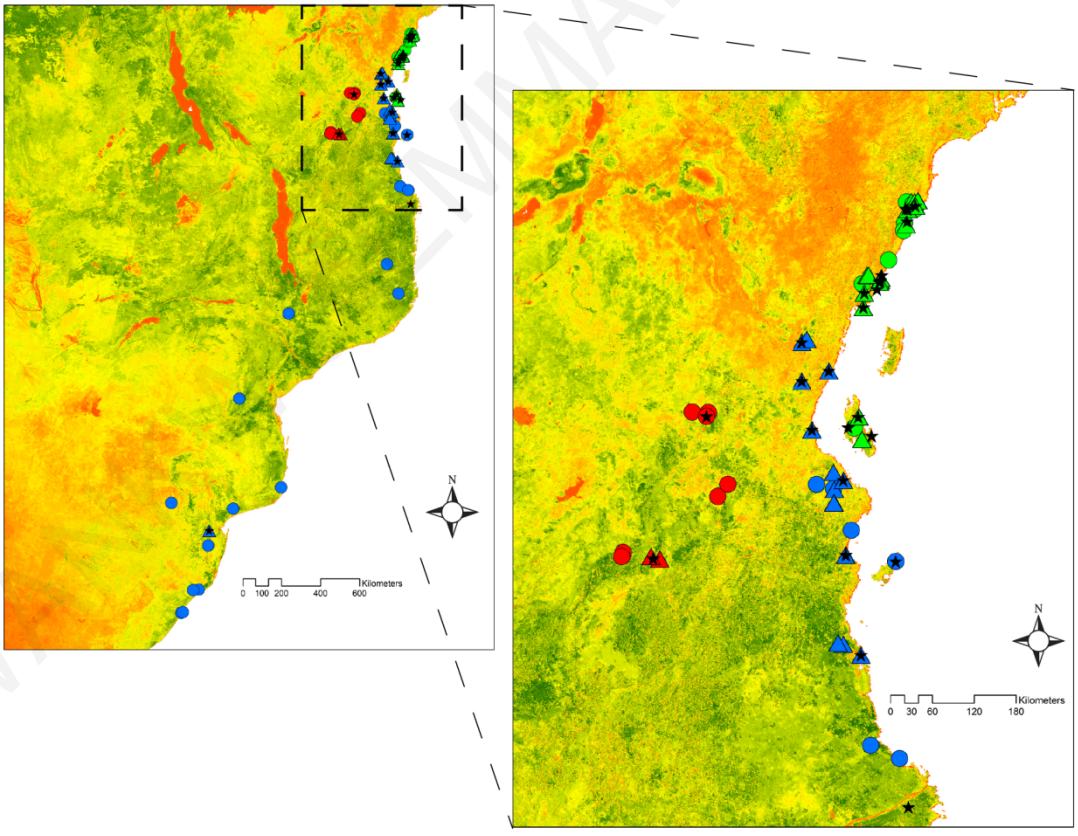

Figure 1. Map of sampling localities showing where recordings (triangles), museum specimens (circles) and genetic material (stars) were obtained. Colours represent the different groups of

fischeri (green), *bilineatus* (blue) and *conciliator* (red), as analyzed in this study. The inset shows the area in East Africa where the three groups come into close proximity. The background image is based on Enhanced Vegetation Index (EVI) data from the MODIS satellite, with levels of EVI ranging from low (red) to high (dark green).

Song Analyses

Peak frequency (PF) did not differ among subspecies ($R^2 = 0.0131$, $F_{2,64} = 1.4367$, $P = 0.245$; Figure 2A): with any differences found between *fischeri* (1102.317 ± 8.712 Hz) *bilineatus* (1094.191 ± 6.523 Hz) and *conciliator* (1088.721 ± 21.304 Hz), not significant. Comparison among the populations showed that the insular *fischeri* population on Zanzibar does not sing at a significantly different frequency (1117 ± 11.845 Hz, $F_{1,35} = 3.025$, $P = 0.0908$) to *fischeri* in Kenya (1097.005 ± 10.265 Hz) and *bilineatus* from Tanzania to Swaziland (1092.449 ± 6.745 Hz). Location ($F_{24,42}= 1.646$, $P = 0.0772$), latitude ($F_{1,63} = 0.0004$, $P = 0.9839$) and longitude ($F_{1,63} = 0.2982$, $P = 0.5869$) had no significant effect on variation in peak frequency.

P. fischeri sang significantly faster songs than *bilineatus* and *conciliator* ($F_{2,64} = 3286.9$, $R^2 = 0.99$, $P < 0.0001$, Figure 2B). Analysing for differences in song pace among the populations from Kenya, Tanzania, and Zanzibar revealed a significant difference ($F_{2,64} = 1711$, $R^2 = 0.9842$, $P < 0001$). Pairwise comparisons revealed significant differences between *bilineatus* from mainland Tanzania and *fischeri* from mainland Kenya ($F_{1,48} = 5080$, $P < 0.00001$), *bilineatus* from mainland Tanzania and *fischeri* from Zanzibar ($F_{1,33} = 2735$, $P < 0.00001$), but no difference between *fischeri* on Zanzibar and Kenya ($F_{1.35} = 0.9686$, $P = 0.3318$; Figure S1). We also found no significant difference in song pace between *conciliator* and *bilineatus* ($F_{1,13} = 0.1572$, $P = 0.6981$). Location ($F_{22,42} = 1.2456$, $P = 0.2642$), latitude ($F_{1,63} = 0.0479$, $P = 0.8275$) and longitude ($F_{1,63} = 0.0021$, $P = 0.964$) had no effect on song pace.

The coefficient of variation was highest in Tanzania for both peak frequency and pace, with pace more variable and frequency less variable in Zanzibar than Kenya (Table 2). The

Multi-Response Permutation Procedure of within- versus among-group dissimilarities showed a greater between group distance than within group distance. Canonical discriminant analysis on peak frequency and song pace clustered *conciliator* with *bilineatus* and retained *fischeri* as distinct (Figure 2C). The discriminant cluster was based on the first dimension which correlates with the song pace ($F_{1,63} = 303.484$, $P < 0.0001$, $R^2 = 99.99$) and no discriminate contribution from the peak frequency was observed.

Table 2: Coefficient of variation in song rate and peak frequency across regions

Regions	Pace	Peak frequency
Tanzania	6.8504	3.4761
Zanzibar	4.9425	2.1222
Kenya	3.4815	2.579

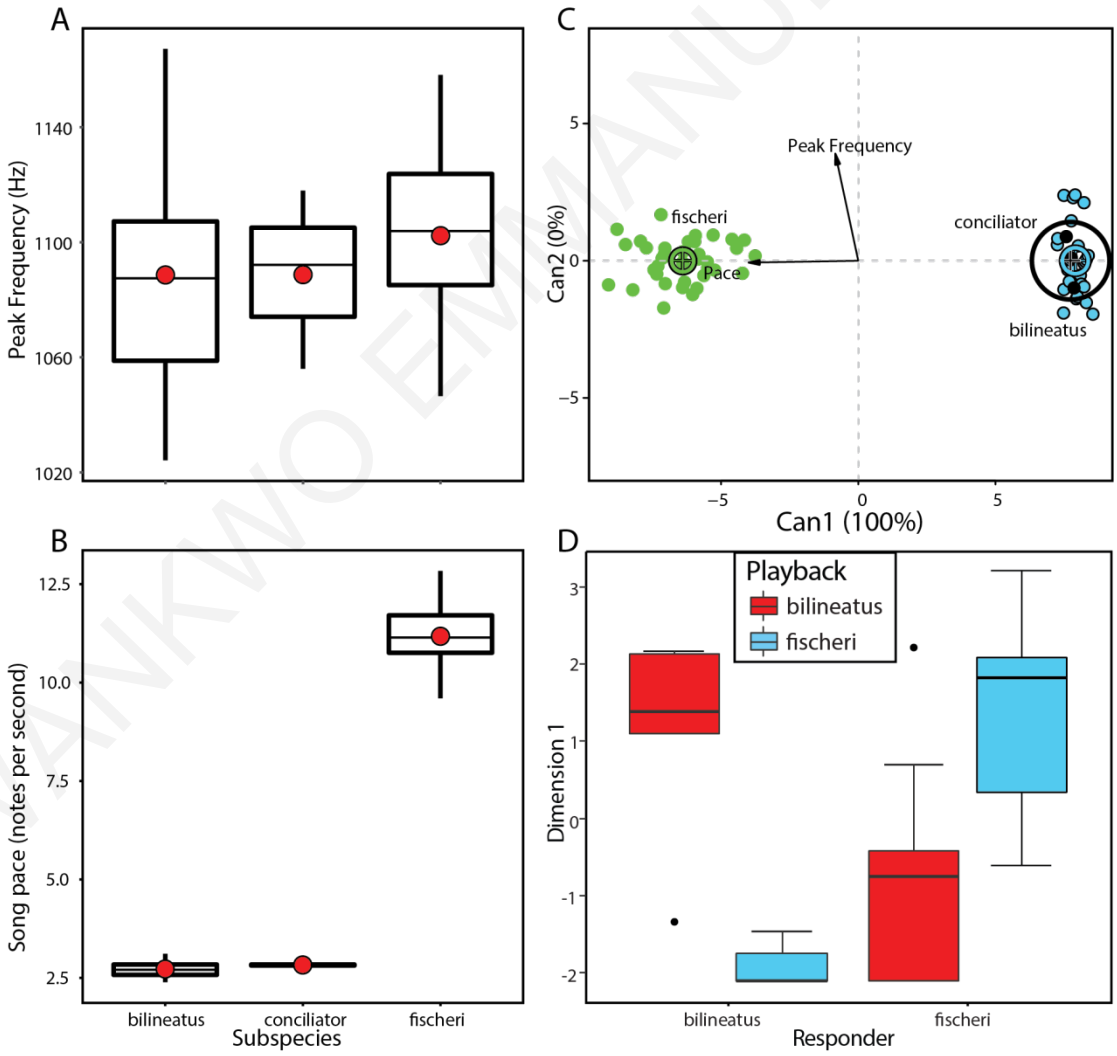

Figure 2. Song traits and responses to playback vary among populations. Boxplots for A) peak frequency and B) pace among populations, reveal that while there is much overlap in song frequency, *fischeri* sings significantly faster than *bilineatus* and *conciliator*, whose songs do not differ in song pace. C) Canonical discriminant analysis demonstrates the extent of variation with *fischeri* completely different from *conciliator* and *bilineatus*, which overlap each other. D) Both *fischeri* and *bilineatus* respond significantly more strongly to their own song than to one another's song, illustrated here with the first principal component dimension.

Playback experiments

The first dimension produced by the factor analysis of mixed data was significantly correlated with total time, time spent within 10m, time spent within 20m, latency, and closest approach distance to the source of the playback stimulus (R^2 = 65%, $P < 0.001$, Table S2). The second dimension was significantly correlated with pre-playback number of songs, post-playback number of songs and number of songs during playback (R^2 = 53%, $P = 0.007$).

The responses of the subspecies during the playback experiment were strongly dependent on the subspecies' song played ($F_{3,28} = 10.535$, $P = 0.001$, Figure 2C). Specifically, *bilineatus* responded significantly more strongly to *bilineatus* song (playback stimulus) ($F_{1,8} = 20.766$, $P = 0.001$) than to *fischeri* song, and *fischeri* responded significantly more strongly to *fischeri* song ($F_{1,20} = 14.319$, $P = 0.001$) than to *bilineatus* song (Figure 2D).

Morphology

PCA was performed with varimax rotation on the morphological data (wing length, tarsus, tail length, bill length, culmen, upper-bill depth) from Tanzania coastal region to Southern Africa including Mozambique, Swaziland, Malawi, Zimbabwe and South Africa (41 specimens), 19 specimens from Kenya mainland and Zanzibar Island and 11 specimens from the Eastern Arc mountain region (Nguru, Uluguru, and Udzungwa). PC1 and PC2 accounted for 43.01 and 18.31 per cent variation respectively (Table S3). PC1 was significantly correlated with wing length, tarsus, tail length, bill length, culmen with *bilineatus* being significantly larger than *fischeri* (R^2 = 38%, $P < 0.001$, Fig. S2, Table S4), and *conciliator* intermediate between the

two. PC2 was significantly correlated with bill width, lower mandible, upper-bill depth with *fischeri* being larger than *conciliator* (R^2 = 18%, $P < 0.001$). There was no significant effect of sex on morphology on either PC1 or PC2. Supplementary variables latitude and EVI had a significant positive correlation and longitude a significant negative correlation with PC1. PC2 was significantly negatively correlated with EVI and elevation. VCF had no significant effect on morphology in relation to any of the principal components.

Plumage

Colour distance

In terms of chromatic and achromatic distances, *fischeri* was most distinct from the other populations based on Just Noticeable Difference levels (JND), where JND > 2, while most similar were *conciliator* from the Eastern Arc Mts. and *bilineatu*s from Southern Africa (Figure S4). Specifically, for the belly patch, chromatic distances were shorter than achromatic distances (approx. 1 to 2.3 vs. 2.2 to 4.5 JND), with largest distances between *fischeri* and *conciliator* followed by *fischeri* and the remaining populations, and smallest between *conciliator* and Southern Africa. In breast plumage, again chromatic distances were shorter than achromatic distances (approx. 1.3 to 2.1 vs. 2.2 to 4.7 JND), with largest distances between *fischeri* and *conciliator* and *bilineatus* from Tanzania and *conciliator*, and shortest distances again between between *conciliator* and Southern Africa. In contrast, in rump plumage, chromatic distances were greater than achromatic distances (approx. 2.2 to 4.3 vs. 1.5 to 3.2 JND), with largest distances between *fischeri* and Southern Africa, and *bilineatus* from Tanzania and Southern Africa, and shortest distances between *conciliator* and Southern Africa and *conciliator* and the remaining populations.

Hue, brightness and chroma

Visualizing differences in hue based on a plot of colour points projected from the tetrahedron to its encapsulating sphere showed that the hue of all plumage patches is between green and red longitudes and specifically in the orange-yellow region (Figure S5). Analysis of variance based on Euclidean distances revealed significant differences in hue, brightness, and chroma of the three plumage patches ($F_{3,104}$ = 3.0736, P = 0.0239, Figure S6). There were significant differences in plumage colouration of the belly patch among populations ($F_{3,27}$ = 3.1649, P = 0.0320). Specifically, the highest hue score was found in *conciliator* and *bilineatus* from Tanzania, followed by *fischeri*, and lowest and most distinct in *bilineatus* from Southern Africa. Brightness and chroma, on the other hand, were highest in fischeri, followed by *bilineatus* from Tanzania and Southern Africa, and lowest in *conciliator*. There were also significant differences in mean brightness, hue and chroma of the breast patch among the populations ($F_{3,27}$ = 10.963, P < 0.0001), however, in contrast to the belly patch, *bilineatus* from Southern Africa had the highest hue score, indicating a greater contrast in hue across the ventral surface, which was more uniform in *fischeri* and *bilineatus* from Tanzania, and with intermediate contrast in *conciliator*. Breast patch brightness and chroma were higher and similar in *fischeri* and *bilineatus* from Tanzania, and lower and similar in *conciliator* and *bilineatus* from Southern Africa. Moreover, there were significant differences in mean brightness, hue and chroma of the rump patch among the populations ($F_{3,27}$ = 3.164, P = 0.03148) Rump hue was higher and similar in *fischeri*, *bilineatus* from Tanzania and *conciliator*, and lower and more distinct in Southern Africa *bilineatus*. Rump brightness was highest in Southern Africa and similar in *fischeri*, lower and similar in *conciliator* and *bilineatus* from Tanzania, and rump chroma was again highest in Southern Africa, and distinctly so, and lower and more similar in the other three populations.

Tetracolour plot and model

Based on the tetracolourspace variables (u, s, l, m, h.theta, h.phi, r.vec, r.max, r.achieved) and using Multivariate Permutational Analysis of variance we found significant differences in the breast ($F_{3,61} = 2.8122$, $P = 0.0314$) and rump ($F_{3,61} = 3.9384$, $P = 0.0119$) plumage patches but not the belly (Figs. 3A, 3B, 3C, Table S6). Applying Canonical discriminant analysis on the tetracolourspace variables, we observed that *conciliator* was closer to *fischeri* than to *bilineatus* from Tanzania in breast and rump colour. Furthermore, across all plumage patches we found *bilineatus* from Southern Africa was distinct from *conciliator*, *bilineatus* and *fischeri* (Figures. 3D, 3E, 3F, Table S6)

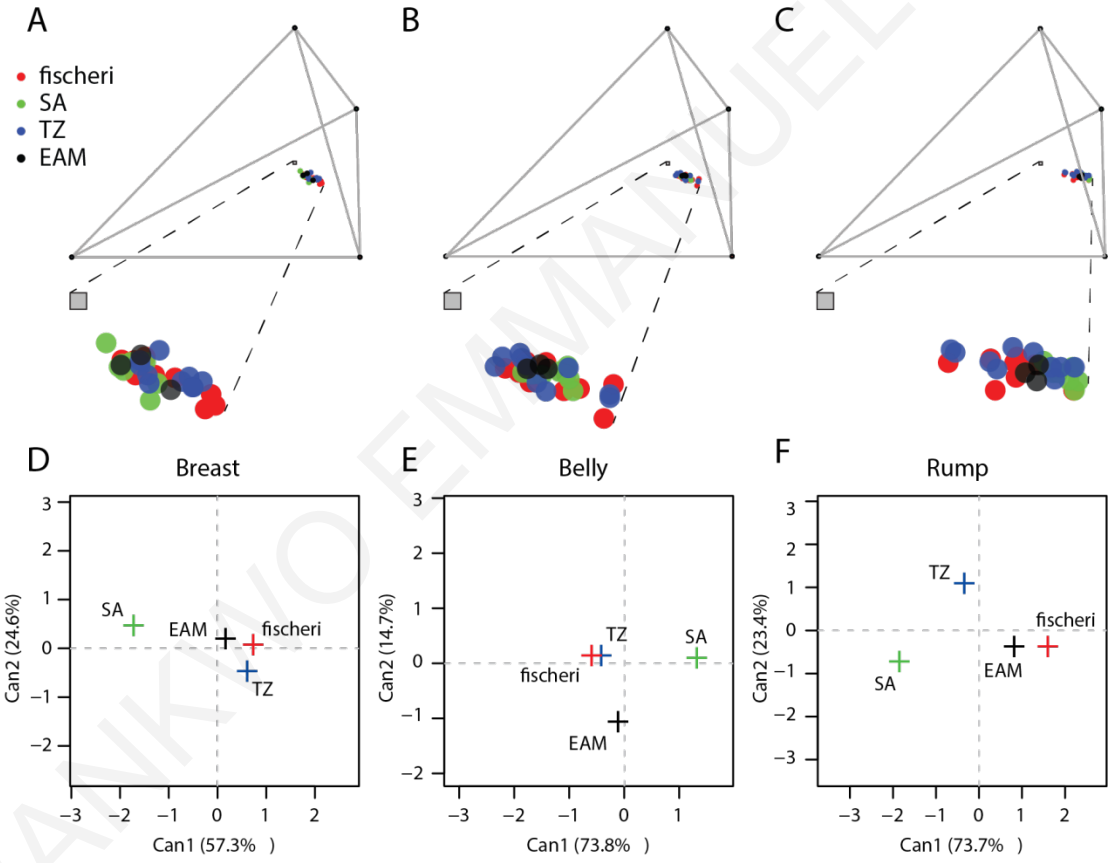

Figure 3. 3D plots of tetrahedral colour space for the three plumage patches, A) breast, B) belly, and C) rump. Insets illustrate the distribution of points for each population in relation to the achromatic origin (grey square). There is much overlap between *fischeri* (red), *bilineatus* from Southern Africa (SA, green), and from Tanzania (TZ, blue), and *conciliator* from the Eastern Arc Mountains (EAM, black). Canonical discriminant analysis illustrates that at the population level (crosses represent population means), *bilineatus* from Southern

Africa is most distant in tetracolour space according to the first two canonical discriminant functions (Can1, Can2) for the plumage patched D) breast, E) belly and F) rump.

Colour volume overlap

In terms of colour volume overlap, *bilineatus* from Southern Africa was the most distinct, with no overlap with conciliator in belly, breast, or rump plumage, no overlap with *bilineatus* from Tanzania in breast (Table S7), and low overlap in rump (18%) and belly (40%), and no overlap with fischeri in rump, and low overlap in breast (6%) plumage. The greatest extent of colour volume overlap was between fischeri and conciliator in rump (93%) and breast (71%), and between *bilineatus* from Tanzania and conciliator (91%) in belly.

Phylogenetic reconstruction

We successfully sequenced 62 fragments of 1008 bp for Cytochrome *b*, and 56 fragments of 529 bp for β-fibrinogen 5. Both Bayesian analysis (Figure 4) and Maximum Likelihood analysis (RAxML; Figure S7) of the Cytochrome *b* gene revealed that *P. b. fischeri* and *P. b. bilineatus* are reciprocally monophyletic and sister groups, with the insular Zanzibar population monophyletic and nested within the *fischeri* clade from mainland Kenya. The *conciliator* group is basal to *bilineatus* and *fischeri*. Divergence of the subspecies is highly supported based on their maximal Bayesian posterior probability values. In contrast, both Bayesian analysis (Figure S8) and Maximum Likelihood analysis (RAxML; Figure S9) of the more slowly evolving β Fibrinogen intron 5 showed no evidence of divergence between the populations. No difference was found even between the *conciliator* group and other subspecies in the nuclear intron, in spite of the greater genetic distances found in mitochondrial DNA.

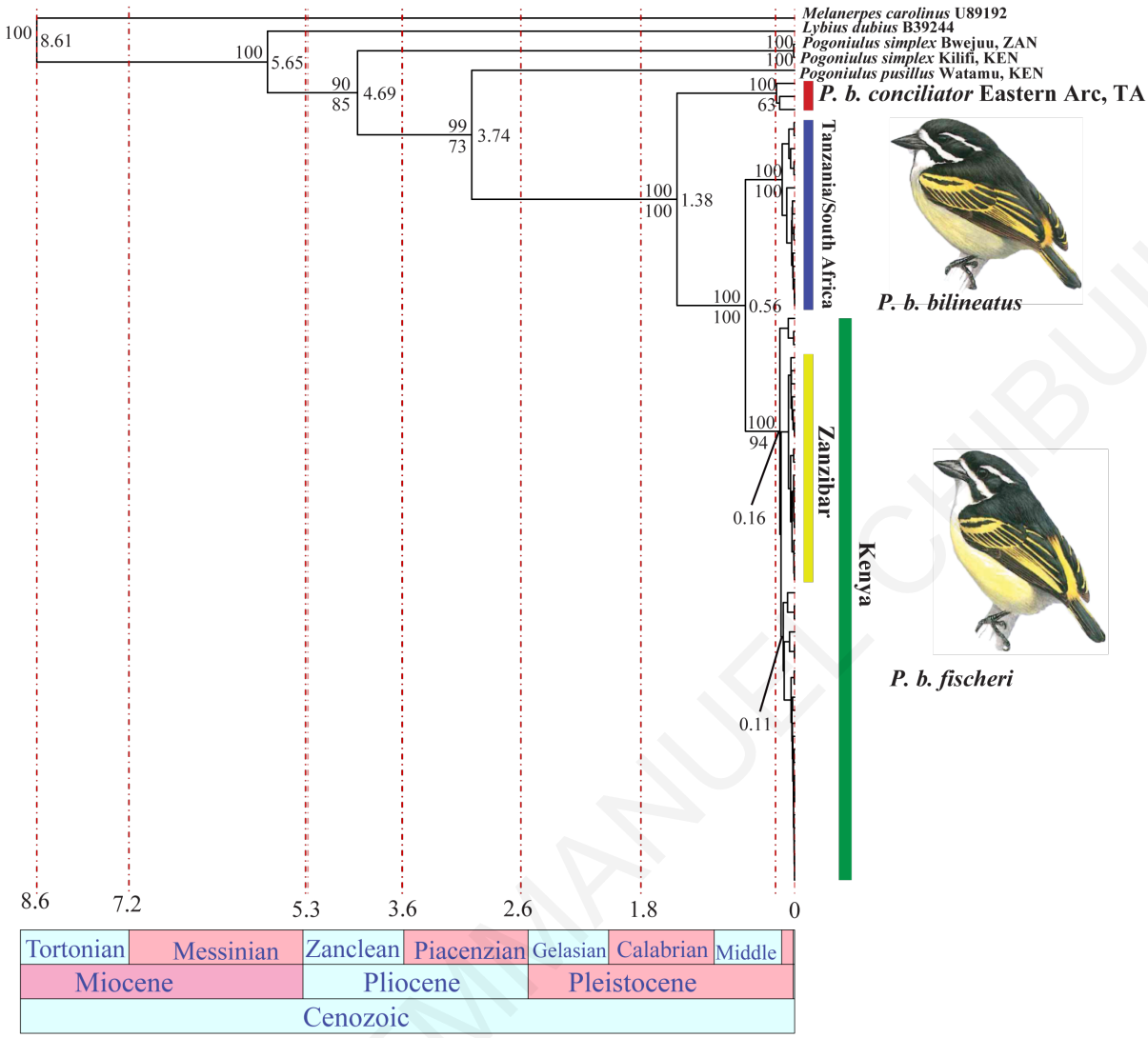

Figure 4. Molecular phylogeny of *P. b. bilineatus, P. b. conciliator* and *P. b. fischeri* based on the Bayesian inference consensus tree of Cytochrome *b*. On the left side of nodes are the posterior probabilities and bootstrap values above and below the branch respectively, with node ages on the right side of the node, calculated using RevBayes 1.0.5. Populations from the Eastern Arc Mountains (*conciliator*) are basal to the rest of the clade, diverging 1.38 mya, while *bilineatus* from Tanzania and South Africa split from the *fischeri* clade 560 kya. The Zanzibar *fischeri* clade split from the Kenya *fischeri* clade 110 kya.

Population Genetics

Out of 91 polymorphic sites from the Cytochrome *b* gene (62 samples) we removed nine uninformative sites and retained 82 single nucleotide polymorphic sites (SNPs) for analysis. The data did plateau at 88 sampled haplotypes necessary to discriminate individuals within populations (Figure S10). The observed number of haplotypes varied between 2 and 3 among individuals.

The individuals showed a structure of clusters into clades that are consistent with their populations (Figures S12, S13). Greater genetic distance was observed between *conciliator* and other *bilineatus* and *fischeri* populations (Figure S12). High bootstrap values provide significant support for the divergence of the subspecies considered in this study (Figure S13, S14).

The minimum spanning network based on genetic distances showed greater diversity within *fischeri* in Kenya and closer relatedness to *fischeri* from Zanzibar (Figure 5). The present network revealed no connection between *bilineatus* and *conciliator* and between *fischeri* in Zanzibar and *bilineatus* in Tanzania. While Zanzibar and Kenya *fischeri* populations are closer related to one another than with *bilineatus* and *conciliator*, genotypic distances within populations are lower than distances among them (Figure 5).

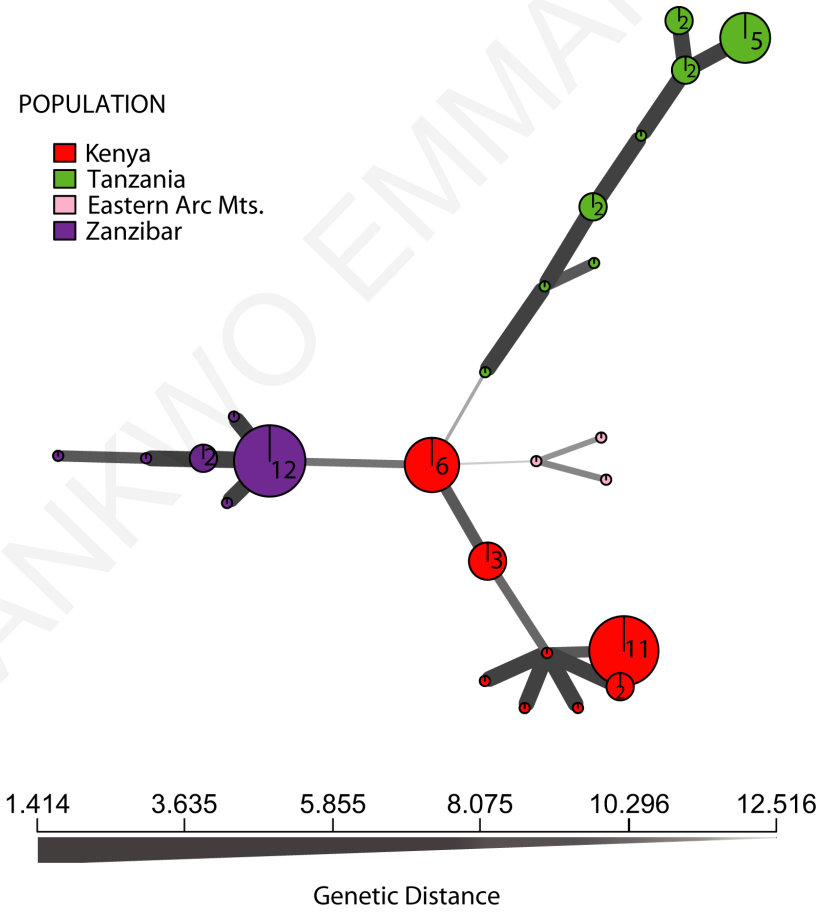

Figure 5. Minimum spanning network using Provesti's genetic distance on 91 polymorphic loci of Cytochrome *b* from 62 individuals. Each node represents a unique multilocus genotype. Node shading (colours) represent population membership, while edge widths and shading represent relatedness (genetic distance). Edge length is arbitrary. The network shows a closer genotypic relationship between Zanzibar (violet) and Kenya (red) *fischeri* population relative to *bilineatus* (green) and *conciliator* (pink) populations.

The variance (σ), the percent of the total variance explained (R^2) and the population differentiation statistics (ϕ) detected between the populations (σ = 13.09, ϕ = 0.909, R^2 = 90.94, P = 0.001) were greater than within the populations (σ = -0.05, ϕ = -0.04, R^2 = -0.38, P = 0.767) and within individuals (σ = 1.36, ϕ = 0.905, R^2 = 0.944, P = 0.001).

Discussion

Taxonomists have over centuries defined species on the basis of differences in morphology between individuals and/or populations. Yet, the extent of differences that was considered worthy of species rather than subspecies status often remained ambiguous, with overlap in the range of variation found within and among related species (Simpson 1951). The description of new species and subspecies within the *Pogoniulus* lineage has followed such a path, including the description of *Pogoniulus makawai*, based on a single specimen collected in Zambia in 1964 (Benson and Irwin 1965), based on, primarily, plumage differences from the local subspecies of *Pogoniulus bilineatus* present at the same locality. Recent phylogenetic studies suggest *P. makawai* is in fact a form of *P. bilineatus*, in spite of the morphological differences found (Kirschel et al. 2018).

Current taxonomy of East African *P. bilineatus* suggests nominate *bilineatus* occurs in Southern Africa and *fischeri* occurs in Eastern Kenya, Tanzania (including Eastern Arc Mountains), and Zanzibar (Short and Horne 2001). Our findings in the present study show that the morphological differences thought to delimit species are explained by patterns such as increasing body size with latitude and plumage differences in breast and belly brightness

consistent with Gloger's rule (Gloger 1833), with populations from higher latitudes (Southern Africa) and elevation (Eastern Arc Mountains) less pigmented than those from more tropical climates.

Molecular phylogenetics reveals the evolutionary history of the clade and contradicts many of the morphological findings. While the nuclear DNA we analysed (β-fibrinogen intron 5) suggests incomplete lineage sorting, faster evolving mitochondrial DNA (Cytochome *b*) shows three monophyletic lineages, with populations from the Eastern Arc Mountains (*conciliator*) as basal, *P. b. bilineatus* extending from Southern Africa northward and including populations along the coast of Tanzania, and *fischeri* occurring in Kenya and Zanzibar, but apparently absent from coastal Tanzania.

What might have led to the biogeographic pattern of a distinct form in *fischeri* occupying Coastal Kenya and Zanzibar, yet *bilineatus* occurring adjacent to Zanzibar in Tanzania? Might this have resulted from a founder event, with dispersal from Tanzania to Zanzibar, followed by genetic change in accordance with peripatric speciation (Mayr 1982), and subsequent dispersal back to the African mainland in Kenya, where *bilineatus* was absent, thus providing the opportunity to establish a population without the presence of a competitor? Our results suggest there is little evidence of peripatric speciation because Zanzibar *fischeri*, though monophyletic, is nested within Kenya *fischeri* (Figure 4, S12). Because dispersal from Kenya to Zanzibar seems unlikely based on geography, we suggest *fischeri* may have been present in Tanzania historically, and certainly during the time of a land bridge connecting the mainland with Zanzibar. There might be several alternative explanations of the observed pattern, such as dispersal from Kenya, dispersal from coastal Tanzania with subsequent extinction of the subspecies, or a vicariant event assuming the subspecies occurred in Tanzania. Nevertheless, at the time being, we cannot select any of these hypotheses as being more parsimonious.

The *fischeri* population from Zanzibar does appear to be diverging genetically and vocally (in song frequency) from Kenya, which we attribute to vicariance, rather than dispersal, following rising Pleistocene sea levels. The absence of tinkerbird species from Pemba island, which is geographically in between Kenya and Zanzibar and has been isolated from the mainland since at least the Pliocene (Kent et al. 1971; Rowson et al. 2010), suggests oceanic dispersal is most unlikely in the genus.

But to what extent does genetic isolation reflect reproductive isolation? We found that song rate differences supported the genetic distinction of *fischeri* from *bilineatus* and confirmed the absence of the former from coastal Tanzania. However, patterns of song variation are discordant with genetic isolation in mtDNA in *conciliator*, which we found overlaps in song characters with *bilineatus*, in spite of its greater genetic distance, with the time of divergence estimated at 1.38 mya. Under the Recognition Species Concept (Paterson 1985), *bilineatus* could be considered a different species to *fischeri* because of the lack of recognition of its song, whereas it would likely be considered the same species as *conciliator* because their songs are the same. Yet, under the Phylogentic Species Concept (Hennig 1966), with *conciliator* basal, it would have to be considered a distinct species if *bilineatus* and *fischeri* were deemed separate species, and hence we have a taxonomic dilemma regarding how to differentiate species. However, we acknowledge the invariability of nuclear markers in resolving adequately the phylogenetic relationship between the subspecies. Acoustic signals play an important role in reproductive isolation (Hoskin et al. 2005; Price 2008; Wilkins et al. 2013), and spectral and temporal variations in acoustic signals have been suggested to affect male response and female preference (Gil and Gahr, 2002; Riebel 2009). Here, rapid divergence has occurred in song in *fischeri*, to the extent that it is unrecognizable to other populations of *bilineatus*, suggesting they would mate assortatively if they coexisted. Meanwhile, other populations evolving in isolation for much longer might interbreed where

songs are more similar, evidence for which has been found in other species of *Pogoniulus* (A. Kirschel unpublished data).

The question remains what may have driven such rapid song divergence in *fischeri* when other subspecies of *Pogoniulus bilineatus* that are genetically more isolated all sing the same song (*bilineatus* and *conciliator* presented here, *P. b. leucolaimus* and *P. b. mfumbiri* studied in Kirschel et al., 2009a)? We would rule out drift, based on the discordant pattern with genetic distance (Wilkins et al. 2013), and acoustic adaptation to transmission properties or the sound environment (e.g. Wiley and Richards 1982; Slabbekoorn and Smith 2002, Slabbekoorn et al. 2002, Kirschel et al. 2009b; Kirschel et al. 2011), because *fischeri* and *bilineatus* with strikingly different songs occur in similar habitat in the coastal forests of East Africa, while other subspecies of *P. bilineatus* occur in diverse habitats from montane forest to ecotone savanna, yet share the same song. Likewise, arbitrary sexual selection (Prum 2012) seems unlikely to have driven this rapid divergence, when there's so little song divergence elsewhere in the genus. One possibility is convergence in song with *Pogoniulus simplex*, with which *fischeri* coexists in its entire range. Such convergence might have occurred through introgressive hybridization, though that seems unlikely based on the extent of genetic distance – *P. simplex* is the most basal outgroup within the genus according to both mitochondrial and nuclear DNA analysed here (Figure 4, Figures S7-9), or convergent character displacement reducing interference competition (e.g., Tobias and Seddon 2009; Grether et al. 2009; Grether et al. 2013). While previous work on the genus found interference competition led to divergent character displacement (Kirschel et al. 2009a), a different interaction based on the extent of ecological competition and relatedness could drive character convergence aiding competitor recognition (Grether et al. 2009).

Conclusion

By integrating genetic analyses with multidimensional phenotypic analyses, we have determined the extent to which the genotype corresponds with the species delimitations of early naturalists and taxonomists, how their delimitations compare with quantitative measurements of morphology and plumage, and how all these characters relate to song, a trait important in reproductive isolation, and one we test recognition of experimentally. While genomic sequencing has transformed the way researchers explore questions in phylogeography and phylogenetics, an integrative approach is still needed to determine the role of variation found in speciation.

References

AGAPOW, P. and BURT, A. 2001. Indices of multilocus linkage disequilibrium. *Molecular Ecology Resources,* **1**: 101–102.

AGARDH, J.G. 1852. *Species Genera et Ordines FLORIDEARUM, seu Descriptiones Succinctae Specierum Generum Et Ordinum Quirus* Floridearum Classis Constituitur. London.

ANDERSSON, M.B. 1994. *Sexual selection*. Princeton University Press, Princeton.

AUDACITY. 2011. Audacity (Version 1.3.3). Available at: http://audacity.sourceforge.net/ (Downloaded: 20 July 2011).

BARROWCLOUGH, G.F., CRACRAFT, J., KLICKA, J. and ZINK, R.M. 2016. How many kinds of birds are there and why does it matter? *PLoS One,* **11**: e0166307.

BENSON, C.W. and IRWIN, M.P.S. 1965. The birds of Cryptosepalum forests, Zambia. *Arnoldia,* **28**: 1–12.

BERGMANN, C. 1847. Ueber die Verhältnisse der Wärmeökonomie der Thiere zu ihrer Grösse. *Gottinger studien*, **3:** 595-708.

BERTELLI, S. and TUBARO, P.L. 2002. Body mass and habitat correlates of song structure in a primitive group of birds. *Biological Journal of Linnean Society* **77**: 423–430.

BOWIE, R.C.K. and Fjeldsa, J. 2005. Genetic and morphological evidence for two species in the Udzungwa forest partridge Xenoperdix udzungwensis. *Journal of East African Naturalist History*. **94**: 191–201.

BOWIE, R.C.K., FJELDSÅ, J., HACKETT, S.J. and CROWE, T.M. 2004. Systematics and Biogeography of Double-Collared Sunbirds from the Eastern Arc Mountains, Tanzania. *Auk,* **121**: 660–681.

BROWN, A.H.D., FELDMAN, M.W. and NEVO, E. 1980. Multilocus structure of natural populations of Hordeum spontaneum. *Genetics* **96**: 523–536.

BURGESS, N.D., BUTYNSKI, T.M., CORDEIRO, N.J., DOGGART, N.H., FJELDSÅ, J., HOWELL, K.M., *et al.* 2007. The biological importance of the Eastern Arc Mountains of Tanzania and Kenya. *Biological Conservation,* **134**: 209–231.

CANDOLIN, U. 2003. The use of multiple cues in mate choice. *Biological Review,* **78**: 575–595.

CHARIF, R.A., STRICKMAN, L.M. and WAACK, A.M. 2010. *Raven Pro 1.4 User's Manual*. The Cornell Lab of Ornithology, Ithaca, NY.

CLAYTON, D.H. 1990. Mate choice in experimentally parasitized rock doves: lousy males lose. *American Zoologist*, **30**: 251-262.

CNAAN, A., LAIRD, N.M. and SLASOR, P. 1997. Tutorial in biostatistics: Using the general linear mixed model to analyse unbalanced repeated measures and longitudinal data. *Statistics in Medicine,* **16**: 2349-2380.

COLLAR, N. J., FISHPOOL, L. D. C., DEL HOYO, J., PILGRIM, J. D., SEDDON, N., SPOTTISWOODE, C. N. and TOBIAS, J. A. 2016. Toward a scoring system for species delimitation: a response to Remsen. *Journal of Field Ornithology,* **87**:104–115.

CRACRAFT, J. 1992. The species of the birds-of-paradise (Paradisaeidae): Applying the phylogenetic species concept to a complex pattern of diversification. *Cladistics,* **8**: 1-43.

DRAY, S. and DUFOUR, A.B. 2007. The ade4 package: implementing the duality diagram for ecologists. *Journal of Statistical Software,* **22**: 1–20.

DUFORT, M. J., An augmented supermatrix phylogeny of the avian family Picidae reveals uncertainty deep in the family tree. *Molecular Phylogenetics and Evolution,* **94**:313-326.

DYNESIUS, M. and JANSSON, R., 2000. Evolutionary consequences of changes in species' geographical distributions driven by Milankovitch climate oscillations. *Proceedings of the National Academic Sciences of the United State of America,* **97**: 9115-9120.

EDWARDS, S.V., KINGAN, S.B., CALKINS, J.D., BALAKRISHNAN, C.N., JENNINGS, W.B., SWANSON, W.J. and SORENSON, M.D. 2005. Speciation in birds: genes, geography, and sexual selection. *Proceedings of the National Academic Sciences of the United State of America,* **102**: 6550-6557.

ESRI. 2012. ArcGIS Desktop: Release 10. Redlands, CA: Environmental Systems Research Institute.

EXCOFFIER, L., SMOUSE, P.E. and QUATTRO, J.M. 1992. Analysis of molecular variance inferred from metric distances among DNA haplotypes: application to human mitochondrial DNA restriction data. *Genetics* **131**: 479–491.

FJELDSÅ, J., BOWIE, R.C.K. and RAHBEK, C. 2012. The Role of Mountain Ranges in the Diversification of Birds. *Annual Review of Ecology, Evolution, and Systematics,* **43**: 249–265.

FRIEDMANN, H. 1929. *Pogoniulus bilineatus conciliator*. *Proceedings of the New England Zoological Club,* **11**: 36.

FRIENDLY, M. and FOX, J., 2016. candisc: Visualizing Generalized Canonical Discriminant and Canonical Correlation Analysis. R package version 0.7-0. https://CRAN.R-project.org/package=candisc

FUCHS, J., and PONS, J.M. 2015. A new classification of the Pied Woodpeckers assemblage (*Dendropicini*, Picidae) based on a comprehensive multi-locus phylogeny. *Molecular Phylogenetics and Evolution,* **88**: 28-37

GAVRILETS, S. 2000. Rapid evolution of reproductive barriers driven by sexual conflict. *Nature* **403**: 886–889.

GIL, D. and GAHR, M. 2002. The honesty of bird song: multiple constraints for multiple traits. *Trends in Ecology and Evolution,* **17**: 133–141.

GLOGER, C. L. 1833. *Das Abändern der Vögel durch Einfluss des Klimas*. A. Schultz and Co., Breslau.

GRETHER, G.F., LOSIN, N., ANDERSON, C.N. and OKAMOTO, K. 2009. The role of interspecific interference competition in character displacement and the evolution of competitor recognition. *Biological Review,* **84**: 617–635.

GRETHER, G.F., ANDERSON, C.N., DRURY, J.P., KIRSCHEL, A.N.G., LOSIN, N., Okamoto, K., *et al.* 2013. The evolutionary consequences of interspecific aggression. *Annals of the New York Academy of Sciences,* **1289**: 48–68.

GRÜNWALD, N.J., GOODWIN, S.B., MILGROOM, M.G. and FRY, W.E. 2003. Analysis of genotypic diversity data for populations of microorganisms. *Phytopathology,* **93**: 738–746.

HARSHMAN, J. 1994. Reweaving the tapestry: What can we learn from Sibley and Ahlquist (1990)? *Auk,* **111**: 377-388.

HASEGAWA, M., KISHINO, H. and YANO, T. 1985. Dating of the human-ape splitting by a molecular clock of mitochondrial DNA. *Journal of Molecular Evolution,* **22**: 160–174.

HENNIG, W. 1966. *Phylogenetic systematics*. University of Illinois Press, Urbana.

HOBSON, K.A., GLOUTNEY, M.L. and GIBBS, H.L. 1997. Preservation of blood and tissue samples for stable-carbon and stable-nitrogen isotope analysis. *Canadian Journal of Zooloogy,* **75**: 1720–1723.

HÖHNA, S., LANDIS, M.J., HEATH, T.A., BOUSSAU, B., LARTILLOT, N., MOORE, B.R., et al. 2016. RevBayes: Bayesian phylogenetic inference using graphical models and an interactive model-specification language. *Systematic Biology,* **65**: 726–736.

HOSKIN, C.J., HIGGIE, M., MCDONALD, K.R. and MORITZ, C. 2005. Reinforcement drives rapid allopatric speciation. *Nature,* **437**: 1353–1356.

JOHNSON, D.P. and CLAYTON, D.H. 2000. A Molecular Phylogeny of the Dove Genus Zenaida: Mitochondrial and Nuclear DNA Sequences. *Condor*, **102**: 864–870.

KAMVAR, Z.N., TABIMA, J.F. and GRÜNWALD, N.J. 2014. *Poppr*: an R package for genetic analysis of populations with clonal, partially clonal, and/or sexual reproduction. *PeerJ*, **2**: e281.

KENT, P. E., HUNT, M.A., and JOHNSTONE, D.W. 1971. *T*he geology and geophysics of coastal Tanzania. *Geophysical Journal International,* **6**: 101.

KIRSCHEL, A. N.G., D. T. BLUMSTEIN, and T. B. SMITH. 2009a. Character displacement of song and morphology in African tinkerbirds. *Proceedings of the National Academic Sciences of the United State of America,* **106**: 8256–8261.

KIRSCHEL, A.N.G., BLUMSTEIN, D.T., COHEN, R.E., BUERMANN, W., SMITH, T.B. and SLABBEKOORN, H. 2009b. Birdsong tuned to the environment: green hylia song varies with elevation, tree cover, and noise. *Behavioural Ecology,* **20**: 1089–1095.

KIRSCHEL, A.N.G., SLABBEKOORN, H., BLUMSTEIN, D.T., COHEN, R.E., De KORT, S.R., BUERMANN, W., *et al*. 2011. Testing alternative hypotheses for evolutionary diversification in an African songbird: rainforest refugia versus ecological gradients. *Evolution,* **65**: 3162–3174.

KLICKA, J., BARKER, F.K., BURNS, K.J., LANYON, S.M., LOVETTE, I.J., CHAVES, J.A., and BRYSON, R.W. 2014. A comprehensive multilocus assessment of sparrow (Aves: Passerellidae) relationships. *Molecular Phylogenetics and Evolution,* **77**: 177-182.

KOCHER, T.D., THOMAS, W.K., MEYER, A., EDWARDS, S. V, PÄÄBO, S., VILLABLANCA, F.X., *et al*. 1989. Dynamics of mitochondrial DNA evolution in animals: amplification and sequencing with conserved primers. *Proceedings of the National Academic Sciences of the United State of America,* **86**: 6196–6200.

KUMAR, S., STECHER, G., and TAMURA, K. 2016. MEGA7: Molecular Evolutionary Genetics Analysis Version 7.0 for Bigger Datasets. *Molecular Biology and Evolution,* **33**:1870-1874.

LAGACHE, L., LEGER, J.B., DAUDIN, J.J., PETIT, R.J. and VACHER, C. 2013. Putting the Biological Species Concept to the Test: Using Mating Networks to Delimit Species. *PLoS One* **8**: e68267.

LÊ, S., JOSSE, J., and HUSSON, F., 2008. FactoMineR : An R Package for Multivariate Analysis. *Journal of Statistical Software*, **25**:253–258.

LEMMON, E.M. and LEMMON, A.R. 2013. High-Throughput Genomic Data in Systematics and Phylogenetics. *Annual Review of Ecology, Evolution and Systematics,* **44**: 99–121.

LINNAEUS, C. 1758. *Systema naturae per regna tria naturae*. Laurentii Salvii, Stockholm.

LUDWIG, J. A., and REYNOLDS, J. F., 1988. *Statistical ecology: a primer in methods and computing*. New York, NY: John Wiley and Sons, Inc.

MAIA, R., ELIASON, C.M., BITTON, P.-P., DOUCET, S.M. AND SHAWKEY, M.D. 2013. pavo: an R package for the analysis, visualization and organization of spectral data. *Methods in Ecology and Evolution,* **4**: 906–913.

MALLET, J. 2005. Hybridization as an invasion of the genome. *Trends in Ecology and Evolution,* **20**: 229-237.

MARINI, M.Â. and HACKETT, S.J. 2002. A multifaceted approach to the characterization of an intergeneric hybrid manakin (Pipridae) from Brazil. *Auk,* **119**: 1114–1120.

MAYR, E., 1947. Ecological factors in speciation. *Evolution* **1**: 263-288.

MAYR, E. 1963. *Animal species and evolution*. Harvard Univ. Press, Cambridge.

MAYR, E., 1982. Speciation and macroevolution. *Evolution* **36:** 1119-1132.

MCGREGOR, P.K., DABELSTEEN, T., SHEPHERD, M. and PEDERSEN, S.B. 1992. The signal value of matched singing in great tits: evidence from interactive playback experiments. *Animal Behaviour,* **43**: 987–998.

MLÍKOVSKÝ, J. 2002. Cenozoic birds of the world. Ninox Press, Praha.

MONTGOMERIE, R. 2006. Analyzing colors. *Bird Color,* **1**: 90–147.

MOORE, W.S., 1995. Inferring phylogenies from mtDNA variation: mitochondrial-gene trees versus nuclear-gene trees. *Evolution,* **49**: 718-726.

MURPHY, R.C. 1938. The need of insular exploration as illustrated by birds. *Science* **88**: 533-539.

NEI, M. 1978. Estimation of average heterozygosity and genetic distance from a small number of individuals. *Genetics,* **89**: 583–590.

OKSANEN, J., BLANCHET, F., KINDT, R., LEGENDRE, P. and O'HARA, R. 2016. Vegan: community ecology package.

PAGÈS, J. 2004. Analyse factorielle de données mixtes. *Rev. Stat. appliquée* **52**: 93–111.

PATERSON, H. E. H. 1985. The recognition concept of species. Pages 21– 29 in Species and speciation (E. S. Vrba, ed.). Transvaal Museum, Pretoria.

PARTAN, S.R. and MARLER, P. 2005. Issues in the Classification of Multimodal Communication Signals. *American Naturalist,* **166**: 231–245.

PIELOU, E. C. 1975. *Ecological diversity*. Wiley, New York.

PODOS, J. 2001. Correlated evolution of morphology and vocal signal structure in Darwin's finches. *Nature,* **409**: 185–188.

PRENDERGAST, M. E., ROUBY, H., PUNNWONG, P., MARCHANT, R., CROWTHER, A., KOURAMPAS, N., *et al*. 2016. Continental island formation and the archaeology of defaunation on Zanzibar, eastern Africa. *PloS one*, **11**: e0149565.

PREVOSTI, A., OCANA, J. and ALONSO, G. 1975. Distances between populations of Drosophila subobscura, based on chromosome arrangement frequencies. *TAG Theoritical and Applied Genetics,* **45**: 231–241.

PRICE, T., 1998. Sexual selection and natural selection in bird speciation. *Philosophical Transactions of the Royal Society of London B: Biological Sciences*, **353**(1366): 251-260.

PRICE T. 2008. *Speciation in Birds*. Roberts and Company, Greenwood Village, CO.

PRUM, R.O. 2012. Aesthetic evolution by mate choice: Darwin's really dangerous idea. *Philosophical Transactions of the Royal Society of London B Biological Sciences,* **367**: 2253–2265.

PRYCHITKO, T.M. and MOORE, W.S. 2000. Comparative evolution of the mitochondrial cytochrome b gene and nuclear beta-fibrinogen intron 7 in woodpeckers. *Molecular Biology and Evolution,* **17**: 1101–1111.

PRYCHITKO, T.M. and MOORE, W.S. 1997. The Utility of DNA Sequences of an Intron from the β-Fibrinogen Gene in Phylogenetic Analysis of Woodpeckers (Aves: Picidae). *Phylogenetics and Evolution,* **8**: 193–204.

R CORE TEAM. 2017. R: A Language and Environment for Statistical Computing. Vienna, Austria. http://www.r-project.org/

RAMBAUT, A., SUCHARD, M., XIE, W. AND DRUMMOND, A. 2014. Tracer v. 1.6. Institute of Evolutionary Biology, University of Edinburgh.

REMSEN Jr, J. V. 2015. HBW and BirdLife International Illustrated Checklist of the Birds of the World Volume 1: Non-passerines Josep del Hoyo and Nigel J. Collar 2014. Lynx Edicions, Barcelona. *Journal of Field Ornithology,* **86**: 182–187.

RIEBEL, K. 2009. Song and female mate choice in zebra finches—a review. *Adv. Stud. Behav*. **40**:197–238.

ROKAS, A., WILLIAMS, B.L., KING, N. and CARROLL, S.B., 2003. Genome-scale approaches to resolving incongruence in molecular phylogenies. *Nature,* **425**: 798-804.

ROWSON, B., WARREN, B.H. and NGEREZA, C.F. 2010. Terrestrial molluscs of Pemba Island, Zanzibar, Tanzania, and its status as an "oceanic" island. *ZooKeys* **70**: 1.

RYAN, M.J. and BRENOWITZ, E.A. 1985. The Role of body size, phylogeny, and ambient noise in the evolution of bird song. *American Naturalist,* **126**: 87–100.

SCHLIEP, K.P. 2011. phangorn: phylogenetic analysis in R. *Bioinformatics* **27**: 592-593.

SEDDON, N. 2005. Ecological adaptation and species recognition drives vocal evolution in Neotropical suboscine birds. *Evolution* **59**: 200–215.

SHANNON, C.E. 2001. A mathematical theory of communication. *ACM SIGMOBILE Mob. Comput. Commun. Rev.* **5**: 3–55.

SHORT, L.L., HORNE, J.F.M. and KIRWAN, G.M. 2002. Yellow-rumped Tinkerbird (*Pogoniulus bilineatus*). In: del Hoyo, J., Elliott, A. and Sargatal, J.(eds.). *Handbook of the Birds of the World Alive*. Vol. 7. Jacamars to woodpeckers. Lynx Edicions, Barcelona, Spain.

SIMPSON, E.H. 1949. Measurement of diversity. *Nature* **163**: 688.

SIMPSON, G. G. 1951. The species concept. *Evolution* **5**: 285-298.

SLABBEKOORN, H., ELLERS, J. and SMITH, T.B. 2002. Birdsong and sound transmission: The benefits of reverberations. *Condor,* **104**: 564–573.

SLABBEKOORN, H. and SMITH, T.B. 2002. Bird song, ecology and speciation. *Philosophical Transactions of the Royal Society of London B: Biological,* **357**: 493–503.

SMITH, J.M., SMITH, N.H., O'Rourke, M. and Spratt, B.G. 1993. How clonal are bacteria? *Proceedings of the National Academic Sciences of the United State of America,* **90**: 4384–4388.

STAMATAKIS, A., HOOVER, P. and ROUGEMONT, J. 2008. A rapid bootstrap algorithm for the RAxML web servers. *Systematic Biology,* **57**: 758-771.

STAMATAKIS, A., 2014. RAxML version 8: a tool for phylogenetic analysis and post-analysis of large phylogenies. *Bioinformatics* **30**: 1312-1313.

STATACORP, L.P. 2009. Stata 10.1. *TX, USA StataCorp LP*.

STEVENSON, T., and FANSHAWE, J. 2002. Birds of East Africa. Princeton University Press, Princeton, New Jersey, US.

STODDARD, M.C. and PRUM, R.O. 2008. Evolution of avian plumage color in a tetrahedral color space: a phylogenetic analysis of new world buntings. *American Naturalist,* **171**: 755–776.

STODDARD, M. C., and STEVENS, M. 2011. Avian vision and the evolution of egg color mimicry in the common cuckoo. *Evolution* **65**: 2004-2013.

STODDART, J.A. and TAYLOR, J.F. 1988. Genotypic diversity: estimation and prediction in samples. *Genetics,* **118**: 705–711.

TOBIAS, J.A. and SEDDON, N. 2009. Signal design and perception in Hypocnemis antbirds: evidence for convergent evolution via social selection. *Evolution,* **63**: 3168–3189.

TOBIAS, J.A., SEDDON, N., SPOTTISWOODE, C.N., PILGRIM, J.D., FISHPOOL, L.D.C. and COLLAR, N.J. 2010b. Quantitative criteria for species delimitation. *Ibis,* **152**: 724–746.

TOEWS, D.P. L. and BRELSFORD, A., 2012. The biogeography of mitochondrial and nuclear discordance in animals. *Molecular Ecology,* **21**: 3907-3930.

UY, J.A.C., MOYLE, R.G., FILARDI, C.E. and CHEVIRON, Z.A., 2009. Difference in plumage colour used in species recognition between incipient species is linked to a single amino acid substitution in the melanocortin-1 receptor. *The American Naturalist,* **174**: 244-254.

VOROBYEV, M., OSORIO, D., BENNETT, A.T.D., MARSHALL, N.J. and CUTHILL, I.C. 1998. Tetrachromacy, oil droplets and bird plumage colours. *Journal of Comparative Physiology A: Neuroethology, Sensory, Neural, and Behavioural Physiology.* **183**: 621–633.

WALLSCHLÄGER, D. 1980. Correlation of song frequency and body weight in passerine birds. *Experientia*, **36**: 412–412.

WILEY, R.H. and RICHARDS, D.G. 1982. Adaptations for acoustic communication in birds: sound transmission and signal detection. *Acoustic Communication in. birds,* **1**: 131–181.

WILKINS, M.R., SEDDON, N. and SAFRAN, R.J. 2013. Evolutionary divergence in acoustic signals: causes and consequences. *Trends in Ecology and Evolution,* **28**: 156–166.

WINGER, B.M. and BATES, J.M. 2015. The tempo of trait divergence in geographic isolation: avian speciation across the Marañon Valley of Peru. *Evolution,* **69**: 772–787.

WINTER, D.J. 2012. MMOD: an R library for the calculation of population differentiation statistics. *Molecular Ecology and Resources,* **12**: 1158–1160.

CHAPTER THREE

Rampant introgressive hybridization in *Pogoniulus* tinkerbirds despite millions of years of divergence

Abstract

Increasing number of hybridisation in birds at the contact zones between related species with incomplete reproductive isolation have been documented. Hybrids are identified based on their intermediate phenotypic characteristics, in addition to molecular techniques using phylogenetic and genetic admixture analysis. We examined interpopulation genetic and phenotypic variation in a pair of African barbets (Lybiidae), from NE South Africa to Swaziland contact zone of yellow-fronted tinkerbird (*Pogoniulus chrysoconus extoni*) and red-fronted tinkerbird (*Pogoniulus pusillus pusillus*). Specifically, we measured the extent of introgressive hybridization at the contact zone of these two tinkerbird species using molecular markers (one mitochondrial gene and a set of microsatellite loci). We found a significant decrease in body size from distant allopatry habitats to near allopatry and converging at the contact zone (sympatry). Differences in plumage was significant between the species in each feather patch, with pronounced differences in crown colour. Genetic variation was explained mostly by distance from the contact zone than based on populations of the species. Genetic admixture analysis recovered pure individuals from the allopatric populations, but admixed individuals from sympatry and near allopatry in both species. More phenotypically *P. p. pusillus* individuals grouped with *chrysoconus* genetically than phenotypically *P. c. extoni* that grouped with *P. p. pusillus* genetically. We show evidence of extensive introgressive hybridisation between *P. p. pusillus* and *P. c. extoni* in the southern Africa contact zone.

Introduction

The distributions of many pairs of related species are parapatric, with several factors potentially keeping them from coexisting with each other. Beyond the existence of geographic barriers such as river valleys (Weir, 2009), factors may include adaptation to the environment on either side of an ecological gradient (Price and Kirkpatrick, 2009), where gene flow from a central population optima swamps adaptation at range boundaries (Kirkpatrick and Barton, 1997; Case et al., 2005), and each species is outcompeted in the other species' range (Price and Kirkpatrick, 2009). Competitive exclusion may also be mediated by behavioural interference (reviewed in Grether et al., 2013; Grether et al., 2017), including reproductive interference (Weir et al., 2011), with many examples of hybrid zones where related species come into contact, (e.g., fish (Crespin et al. 1999); frogs (Littlejohn and Watson, 1985); deer (Senn and Pemberton, 2009); house mice (Payseur et al 2004); newts (Arntzen and Wallis 1991); grasshopper (Hewitt 1989); cricket (Harrison 1986); crows (Meise 1928); buntings (Carling and Brumfield, 2008); woodpeckers (Short, 1965; Johnson and Johnson, 1985), *Ficedula* flycatchers (e.g., Borge et al., 2005); and wood-warblers (Rohwer et al., 2001)).

Where hybridisation is maladaptive, because hybrids suffer from reduced viability or sterility, especially in the heterogametic sex (Haldane, 1922), or because they are poorly adapted to ecological conditions if parental forms are adapted to either side of an ecological gradient (Hatfield and Schluter, 1999), or phenotypically unattractive to either parental form due to intermediate appearance or communication signals (e.g., Svedin et al., 2008), reinforcement may be expected to lead to reproductive character displacement in characters important in assortative mating (Dobzhansky, 1940; Coyne and Orr, 2004). However, where hybrids do not suffer from such reduced fitness, stable hybrid zones can be maintained, and genes of parental species may introgress deep into one another's distribution (Joseph et al, 2008; Baldassarre et al., 2014).

Hybrids can often be identified by intermediate phenotypic patterns between parental species (Wiebe, 2000; Senn and Pemberton, 2009; Toews et al., 2016) though the extent of introgression in the population might not be clear after F1 hybrids have backcrossed with parental forms and resemble parental species (Senn and Pemberton, 2009; Senn et al., 2010), and introgression of phenotypic traits extending well into the genomic background of interacting species (Baldassare et al., 2014; Toews et al., 2016).

In birds, a minimum of 16.4% of species have been documented hybridising with at least one other species in nature (McCarthy, 2006), while specifically in songbirds, individuals meeting at contact zones may also produce mixed song, after copying the song of heterospecific males, which might facilitate hybridisation (Qvarnström et al., 2006), though in other cases song divergence may help maintain parapatry in the face of hybridisation when interacting species are ecological competitors (McEntee et al., 2016). At the same time, hybridisation is widespread in avian families without song learning, such as in ducks (Johnsgard, 1967), quails (Gee, 2003), and woodpeckers (Cicero and Johnson, 1995; Moore, 1995; Wiebe, 2000; Randler, 2002; Fuchs et al., 2013; Michalczuk et al., 2014).

Molecular techniques allow for the identification of hybrids using phylogenetic analyses. Mitochondrial DNA can show evidence of hybridisation when there is a mismatch between the mitochondrial genotype and phenotype, but because it is maternally inherited (Wilson et al., 1985), it may not show evidence of the extent of introgression through recombination. This does not undermine its usefulness in identifying maternal species within the F1 hybrids (McDevitt et al., 2009). Nuclear DNA on the other hand is inherited from both parents and recombines, thus can aid in identifying hybrids of two different species and their backcrosses (Avise and Ball Jr, 1991; Pfennig et al., 2012). The efficiency of nuclear markers in the identification of hybrids has been demonstrated in introns (Nadachowska and Babik, 2009; Pacheco et al., 2002), single nucleotide polymorphisms (Davey et al., 2011; Väli et al.,

2010), and microsatellites (Gay et al., 2009; Väli et al., 2010). A combined set of nuclear and mitochondrial markers in addition to phenotypic traits can provide a clear understanding of the extent of introgression of genotypic and phenotypic characters across a contact zone.

We examined interpopulation genetic and phenotypic variation in a pair of African barbets (Lybiidae), across the contact zone of the yellow-fronted tinkerbird (*Pogoniulus chrysoconus*) and red-fronted tinkerbird (*Pogoniulus pusillus*), with extensive and conspicuous carotenoid-based yellow and red pigmentation on their forecrown feathers, respectively. The two closely related species meet in a narrow contact zone from NE South Africa to Swaziland where a previous study found that songs appear to converge (Monadjem et al. 1994). Yellow-fronted tinkerbird close to the contact zone have been described with intermediate, orange-coloured crowns, suggestive of interbreeding (Ross, 1970). We investigated the possibility that the two species hybridise at the contact zone.

Our aim was to measure the extent of possible introgressive hybridization at the contact zone of these two tinkerbird species using molecular markers (one mitochondrial gene and a set of microsatellite loci). As the extent of hybridization between these two species is not known, it therefore becomes important to identify their hybrids and the extent of introgression.

Materials and Methods

Study species and sites

Pogoniulus chrysoconus and the closely related *P. pusillus* are tinkerbirds found primarily in the savannah region of Africa, though the habitat they occupy varies across each species' range (Short and Horne, 2001). While in East Africa *P. chrysoconus chrysoconus* is distributed in more mesic habitat, and even in montane forest in Ethiopia (*P. c. xanthostictus*), with *P. pusillus affinis* and *P. p. uropygialis* in Acacia woodland, in Southern Africa, the reverse is found, with *P. c. extoni* in drier savannah woodland and *P. p. pusillus* ranging from woodland

to coastal forest. The distribution of each subspecies is listed in Table A2 (Supplement section). In Southern Africa, the two species meet in a narrow contact zone about 20 km wide primarily in northern Swaziland (Monadjem et al., 1994). We performed fieldwork in South Africa and Swaziland from March 2015 to March 2017 at four allopatric sites for *P. chrysoconus* in Mpumalanga, South Africa, five allopatric sites of *P. pusillus* in Swaziland and Kwazulu-Natal, South Africa, and five sympatric sites, four in Swaziland and one in South Africa (Figure 1A, B).

Museum specimens

We received loans of specimens from the ornithology collections of the Natural History Museum of Los Angeles County, the Field Museum of Natural History, the American Museum of Natural History, the British Natural History Museum, the National Museum of Natural History, the Peabody Museum of Yale University, Museum of Natural Science at Louisiana State University (LSUMNS) and the Donald R. Dickey Collection of the University of California Los Angeles to obtain morphometric and colour measurements. In total, we took morphometric measurements from 36 *P. c. extoni* and 28 *P. p. pusillus* museum skins that were collected from sites south of 15°S (Figure 1A). We deemed populations south of 15°S relevant for this study, and far enough to not be affected by interactions at the contact zone in Tanzania further north, which is a similar distance away from populations at 15°S as is the Southern Africa contact zone. We identified the localities where specimens were collected from museum tags and used maps, gazetteers, and Google Earth (Google, Inc.) for those specimens where coordinates were not given and assigned approximate latitude and longitude coordinates and elevation for each locality.

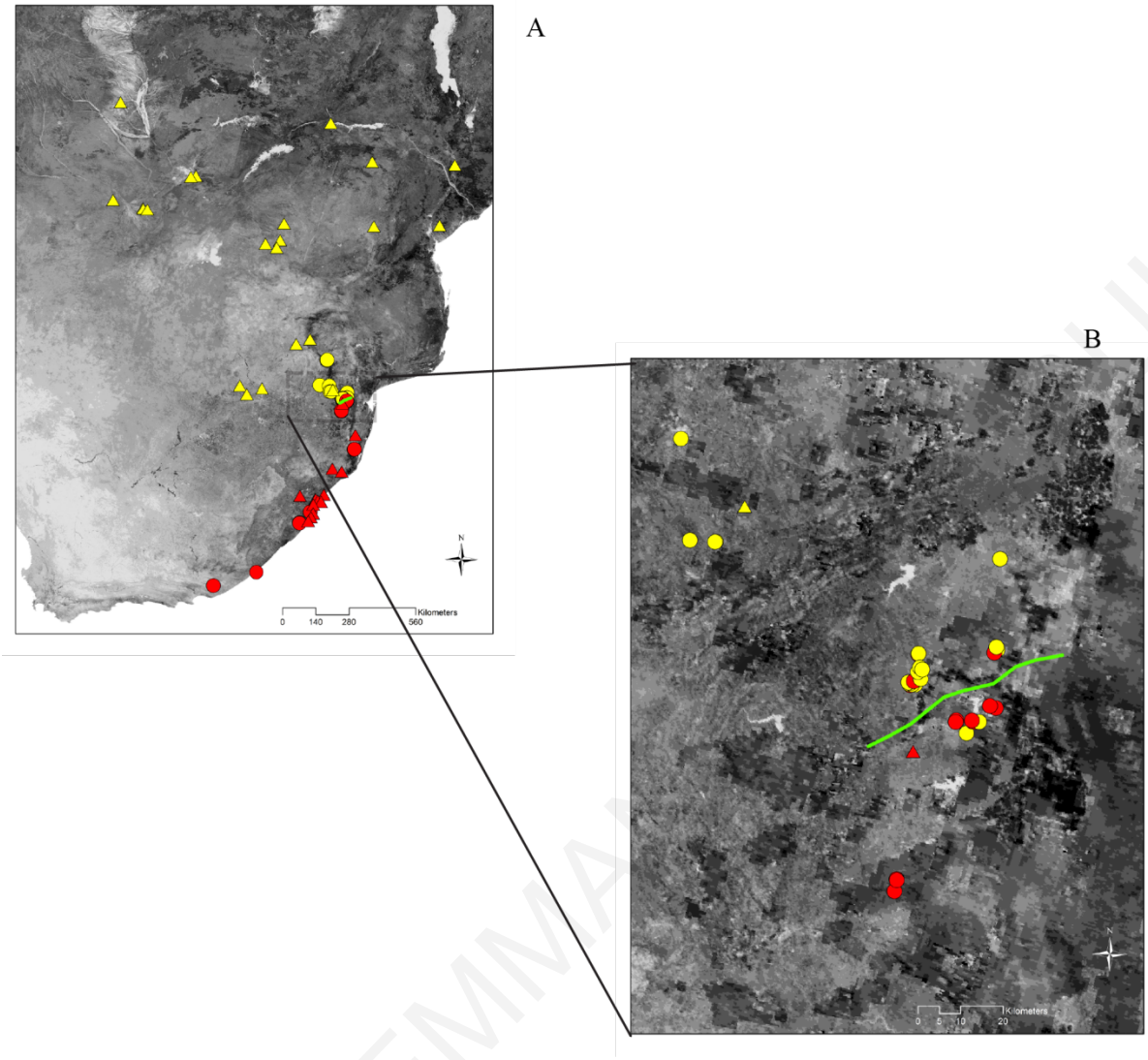

Figure 1. A) Distribution of samples of *P. c. extoni* and *P. p. pusillus* (yellow and red circles, respectively) used in molecular analyses, and museum specimens (yellow and red triangles) used in the plumage analysis. The contact zone is illustrated in green, and the background map is an Enhanced Vegetation Index image from the MODIS satellite with darker shades reflecting more densely vegetated areas. B) Map illustrating the distribution of samples from populations in sympatry and near allopatry. The green contact line is approximately drawn in to divide sympatric sites with a predominance of *chrysoconus* and *pusillus* genotypes all shown within a few km of the line. Near allopatric sites are those where only one of the species was found and were ≥ 20 km from the contact zone or more (but always within 100 km).

Color measurements and analysis

We took reflectance measurements from the 64 study skins, 36 *P. c. extoni* from 1,445 km away in near allopatry in Mpumalanga province of South Africa to almost 1,500 km from the contact zone in Zambia, and 28 *P. p. pusillus* ranging from the zone of sympatry in Swaziland

to over 460 km from the contact zone in Kwazulu-Natal, South Africa. We measured reflectance spectra (300-700 nm) of feathers on the throat, breast, belly, rump, shoulder, and the crown of the head using a diode-array spectrometer (Ocean Optics USB2000) with a fiber optic reflectance probe (Ocean Optics R-400) and xenon strobe light source (Ocean Optics PX-2). Measurements were taken while holding specimens such that the dorsal surface of feathers were placed up to a 1.3 mm diameter aperture in a razor-thin, steel plate. The reflectance probe was oriented at 45 degrees relative to the upper surface of the plate and positioned such that the edges of the aperture matched the acceptance angle of the detector light path and held so that the light source pointed toward the feather rachis (in perpendicular orientation) or the feather base (in parallel orientation). Throat and rump feathers were only scanned in the perpendicular orientation because of the awkwardness in holding the specimen up to the probe for parallel orientation scans. For all feather patches, only the outer side was scanned because the inner side is normally concealed. Each of the regions was scanned on the left, middle and right side, except rump (left and right only), and crown (parallel and perpendicular only), for a total of 25 measurements per bird.

Replicate reflectance spectra were averaged and further processed to yield bird-specific cone excitation estimates (E_j) using typical cone λ_{max} values for Piciformes (Endler and Mielke, 2005). The irradiance spectrum that prevails under open canopy and cloudy conditions (Endler, 1993) was used because tinkerbirds spend much of their time singing from exposed perches whether in woodland or forest habitat. E_j were used to calculate coordinates in tetrahedral color space. We used MANOVA to determine the extent of variation between the two species for each of the six feather patches in tetrahedral x, y, and z color measurements (using the mean value of the different side and orientation of feathers). Statistical analyses were run using STATA version 11 (StataCorp, College Station, TX.).

Morphometrics

Tinkerbirds were captured using targeted mist netting with conspecific playback and given a metal and colour ring combination. We took morphometric measurements from 74 individuals captured in the field: *Pogoniulus pusillus pusillus* = 33 individuals, *Pogoniulus chrysoconus extoni* = 41 individuals. Measurements were taken using digital callipers, and included wing chord, tarsus and tail length, bill length and width, and bill depth. The geographic coordinates of field locations were identified from handheld Garmin GPS devices. To obtain the vegetative characteristics of the surveyed locations, Moderate Resolution Imaging Radiometer raster files at 250 m resolution (MODIS/Terra Vegetation Indices 16-Day L3 Global 250m) from 2010 were used to extract vegetation continuous field (VCF) and enhanced vegetation index (EVI) data for coordinates of the field locations in ArcGIS 10.1 (ESRI, 2012).

Categorical description analysis implemented in FactoMineR software (Sebastien, Julie and Francois 2008) was used to determine the morphological dimensions that best decribed the two species. Principal Component Analysis (PCA) with varimax rotation implemented within Psych version 1.7.8 (Revelle, 2017) R Statistical package was used to reduce the morphology data from eight morphological variables to two principal components to determine the dimensions of variability in body size and bill shape of the study species. The principal component explaining the majority of variation was then used to test for variation in morphology resulting from differences between the species, latitude, longitude and environmental factors (EVI, VCF, Elevation) using a generalized linear mixed effects model implemented in lme4 R statistical package (Douglas et al, 2015).

Genetic sampling and analysis

Blood samples were obtained from the ulnar superficial vein (wing) of field caught tinkerbirds, and transferred into 2 ml cryovials containing 1 ml Queens Lysis Buffer (Hobson

et al. 1997). Samples were stored at -20 °C in the lab, after returning from the field. Six further DNA samples from allopatric populations in South Africa were obtained from museums (two tissue samples of *P. c. extoni* from Mpumalanga courtesy of LSUMNS, and four blood samples of *P. pusillus* from Eastern Cape, received from the Museum of Vertebrate Zoology at University of California Berkeley). Additionally, for the phylogeny we included 15 samples of *P. c. chrysoconus* and *P. p. affinis* from West and East Africa collected for parallel studies (Kirschel et al., 2018, A. Kirschel unpublished data). DNA was extracted using a Qiagen DNeasy blood and tissue kit following manufacturer's protocols (Qiagen, Valencia, CA). PCR was performed to amplify DNA of the mitochondrial Cytochrome *b* gene using primers L14841 (Kocher et al., 1989), and H4a (Harshman, 1994) and ATPase 6/8 gene using primers CO2GQL and C03HMH (Eberhard and Bermingham, 2004) on an Applied Biosystems Thermal Cycler (model 2720) and resulting bands visualised by Gel Electrophoresis on a 1% agarose/TAE gel. The DNA sequences were aligned using Muscle (Edgar 2004) implemented in MEGA software version 7 (Kumar et al., 2016). We added three outgroup sequences for *Tricholaema diadematata* (GenBank: MG230178, MG697232), *Ramphastos toco* (GenBank: AY959852, GQ457946), *Sasia ochracea* (GenBank: NC028019) and performed analyses on combined loci of Cytochrome *b* and ATPase 6/8 genes giving a total of 1859 bp fragment. Estimates of uncorrected pairwise distances were calculated, using the between group mean distance function in MEGA v7 (Kumar et al., 2016).

Using the Cytochrome *b* sequences we calculated within PopArt: (i) the number of sites that differ among individuals as an estimate of number of segregating sites, (ii) the number of sites containing at least two states that occur in at least two sequences each as an estimate of the number of Parsimony-informative sites, (iii) Tajima's D (Tajima, 1999) which estimates the extent of selection among the populations, and (iv) molecular variation among the populations (AMOVA; Excoffier, 1992). The assessment of genetic relatedness between

haplotypes was implemented using PopArt based on Cytochrome *b* gene. We produced a fine-scale picture of relationships between individual samples based on mitochondrial gene (Cytochrome *b*) visualized with minimum-spanning networks generated using PopART (Leigh and Bryant, 2015).

Phylogenetic analysis

Different models of evolution were compared using R package phangorn (Schliep, 2011) based on our aligned sequences. The selection of best-fit model of evolution was based on the model with the lowest Bayesian Information Criterion (BIC) value. The Maximum Likelihood (ML) trees based on 434bp sequences and TPM2+F+G4 model of evolution were constructed using IQ-Tree software version 1.6.2. The sequence alignment used for the ML tree was trimmed down to 434bp fragment because the effort to obtain longer sequences of several samples was not successful.

For Bayesian phylogenetic reconstruction based on the combined loci of two mitochondrial genes, we determined the best partitioning schemes and corresponding nucleotide substitution models for each of the genes using PartitionFinder2 (Lanfear et al., 2016). The data-set blocks were predefined a priori based on the two genes. The corrected Akaike information criterion (AICc) and the 'greedy' algorithm with branch-lengths estimated as unlinked were used to search for the best-fit scheme. Phylogenetic analyses were conducted using Bayesian phylogenetic reconstruction based on the combined loci of two mitochondrial genes with the model partitioning restricted to the genes (ATPase: GTR+I+G; Cyt-*b*: GTR+I+G).

Divergence dates were estimated in RevBayes 1.0.5 (Hohna et al., 2016) by creating a stochastic node using time schedule of 5.38 MYA (mean=35, sd=9, min=5.38, max=65.38) as a minimum age limit for the ancestor of the *Pogoniulus* tinkerbirds based on the Late Miocene

tinkerbirds fossil found at Kohfidisch Austria (Mlíkovský, 2002). The divergence time boundaries were selected to include time of divergence from previous studies (see Paton et al. 2002, Nahum et al. 2003) between the distant species whose sequences were included in the analysis as outgroups (*Ramphastos toco* AY959852, *Sasia ochracea* NC028019 and *Melanerpes carolinus* U89192.1). We used a relaxed uncorrelated lognormal clock model and an exponential prior for the mean rate of each partition. The sampling probability was set to the ratio of the number of *Pogoniulus* species in our data set and estimated total number of described bird species within Lybiidae (52; IUCN, 2017). We ran burn-in phase of Monte Carlo sampler for 10,000 iterations under two independent replicates using 13 different moves in a random move schedule with 44 moves per iteration and tuning interval of 250. The main phase of the MCMC analysis was run for five million generations sampling every 500 generations under two independent runs and the same random moves as in the burn-in phase. Convergence from the independent runs and ESS values were evaluated in Tracer 1.6 (Rambaut et al., 2014). The final tree was produced from the generated trees by compiling a maximum posteriori tree using a burn-in of 20%.

Microsatellite analysis

Fifteen microsatellite loci developed for zebra finch *Taeniopygia guttata*, chicken *Gallus gallus* (Dawson and Horsburgh et al., 2010, Dawson et al., 2013) and barn owls *Tyto alba* (Klein et al., 2017) loci were amplified for 81 samples without multiplexes using M13 fluorescent labelling primers and Kappa PCR master mix. The cycling scheme was as follows: 94 C for 15 s followed by 40 cycles of 94 C for 20 s, 55 C for 90 s, and 72 C for 30 s; the final extension was at 72 C for 10 min. PCR products were electrophoresed on an ABI 3130xl Genetic Analyser with GeneScan 500 LIZ size standard (Applied Biosystems). Allele sizes were determined using GeneMapper software (Applied Biosystems).

Number of alleles, allelic richness, and the observed and expected heterozygosities, tests of departures from Hardy–Weinberg equilibrium, tests of linkage disequilibria and a principal component analysis (PCA) were performed using the poppr (Kamvar, Tabima et al. 2014) adegenet (Jombart 2008) and ade4 (Dray and Dufour, 2007) packages in R 3.4.2 (R Core Team, 2017). Hybridization was tested between species using a Bayesian admixture analysis approach implemented in STRUCTURE v.2.2 (Pritchard et al., 2000; Vaha and Primmer, 2006; Sanz et al., 2009) to obtain individual genetic assignment to either *P. chrysoconus*, *P. pusillus* or their hybrids based on the fifteen microsatellite loci. We allowed for five independent runs for each simulated values of K (K = 1-15). STRUCTURE (McDevitt et al., 2009; Senn and Pemberton, 2009) was run using 5 million iterations, with a burn-in period of 100,000 iterations. The best K value for the population structure analysis was determined based on the Evanno method in STRUCTURE Harvester v0.6.1 (Earl and VonHoldt, 2012) while averaging across iterations using the CLUster Matching and Permutation Program (Jacobsson and Rosenberg, 2007). The output from CLUMPP was visualized using the program DISTRUCT version 1.1 (Rosenberg, 2004). We refrained from assigning any threshold for hybrid identification due to its dependency on the allele frequency differences between species, and thereby avoid the risk of misidentifying 'pure' individuals as hybrids due to ancestral polymorphism (Senn and Pemberton, 2009.).

Population genetics

We screened our microsatellite data to determine populations with fixed alleles and removed the uninformative loci from downstream analyses. The 17 sites from which the samples were obtained were grouped into four populations as follows (Figure 1): *P. p. pusillus* distant allopatry comprising 5 sites in South Africa (15 samples), near allopatry comprising 2 sites in Swaziland (6 samples), and *P. p. pusillus* sympatry comprising 5 sites in Swaziland and South

Africa (17 samples); *P. c. extoni* distant allopatry comprising 1 site in South Africa (5 samples), near allopatry comprising 4 sites in South Africa (10 samples), and *P. c. extoni* sympatry comprising 5 sites as above (28 samples).

The strength of our data in discriminating between unique individuals given a random number of loci was determined based on a genotype accumulation curve. The overall quality of our multilocus genotype loci (MLGs) data was examined, including a search for missing data and rare alleles.

The genotypic diversity indices for each of the major (four) populations were estimated: Number of multilocus genotypes (MLG) observed as an estimate of genotypic richness, number of expected MLG at the smallest sample size ≥ 10 based on rarefaction (eMLG), Standard error based on eMLG (SE), Shannon-Wiener Index of MLG diversity (H, Shannon, 2001), Stoddart and Taylor's Index of MLG diversity (Stoddart and Taylor, 1988), lambda (Simpson's Index; Simpson, 1949), Evenness (E.5; Pielou, 1975), Nei's unbiased gene diversity (H_{exp}; Nei 1978), Index of association ($\boldsymbol{I_A}$ Brown, Brown et al., 1980; Smith et al., 1993), Standardized index of association ($\bar{r}_d$, Agapow and Burt, 2001).

The analysis of the relationship between individuals, sub-populations, and populations were performed using genetic distance measures by calculating the "distance" between samples based on their genetic profile. Provesti's distance (Prevosti et al., 1975) was used in estimating the genetic distances as it returns the fraction of the number of differences between individuals, sub-populations and populations. These were implemented with the R packages poppr (Kamvar et al., 2014) and mmod (Winter, 2012). We used the genetic distance matrix to create a neighbor-joining tree to visualize the relationships in genetic distances at individual, sub-population and population levels. To determine if the major genotypes of the subspecies are closely related and to what degree they contribute to the genotypes of the each other population,

we produced a haplotype network (Minimum Spanning Network) for the microsatellite data using poppr (Kamvar et al., 2014) and ade4 (Dray and Dufour, 2007) R packages.

AMOVA (Analysis of Molecular Variance) was used to detect population differentiation (Excoffier et al., 1992) using the microsatellite data. The AMOVA was implemented in poppr (Kamvar et al., 2014) and ade4 (Dray and Dufour, 2007) R packages based on the Provesti's genotypic distance. The major population level specified in the analysis based on distance from the contact zone include: *pusillus* (allopatry), *pusillus* (sympatry), *chrysoconus* (allopatry), *chrysoconus* (sympatry) while the minor population level was based on the localities where samples were collected for each species. In a typical panmictic population we expected that most of the variance would arise from within populations rather than among populations. Population structure would therefore be evident if most of the variance occurs within populations than between populations.

Genetic and phenotypic cline analysis

The Metropolis-Hastings Markov chain Monte Carlo algorithm implemented within the package hzar in R version 3.0.3 (Derryberry et al., 2014) was used to fit Genetic and phenotypic clines. The genetic cline analyses were fitted to different combinations of the exponential decay curve parameters δ and s (none, right tail only, left tail only, mirrored tails, or both tails separately, for each of mitochondrial DNA (Cytochrome *b* gene) and microsatellite data based on their respective first principal component. Model selection was based on the AIC corrected for small sample size (AICc) and the model with the lowest AICc was selected as the best-fitting model.

Results

Morphology variation

Of the 74 individuals captured and included in the morphology analysis 41 were identified in the field as *P. chrysoconus extoni* and 33 as *P. pusillus pusillus* based on the colour of the fore-crown. The categorical description analysis retained exposed bill length, wing length and tarsus as significant descriptors ($P \leq 0.05$) of variation in the morphology of the two species, including EVI and VCF (Figure 2). There was a decrease in body size (tarsus, wing length and exposed bill length) from distant allopatry habitats to near allopatry and converging at the contact zone (sympatry, Figure 3D). Overall, *P. c. extoni* are larger in body size than *P. p. pusillus* ($F_{17,56}$ = 8.21, $P < 0.001$, $R^2 = 0.7135$), considering significant variation in location, EVI, VCF, latitude and longitude (Table 1). A test of interaction term between body size of the species and distance to contact zone was statistically significant ($F_{2,71} = 12$, $P < 0.001$, $R^2 = 0.6699$).

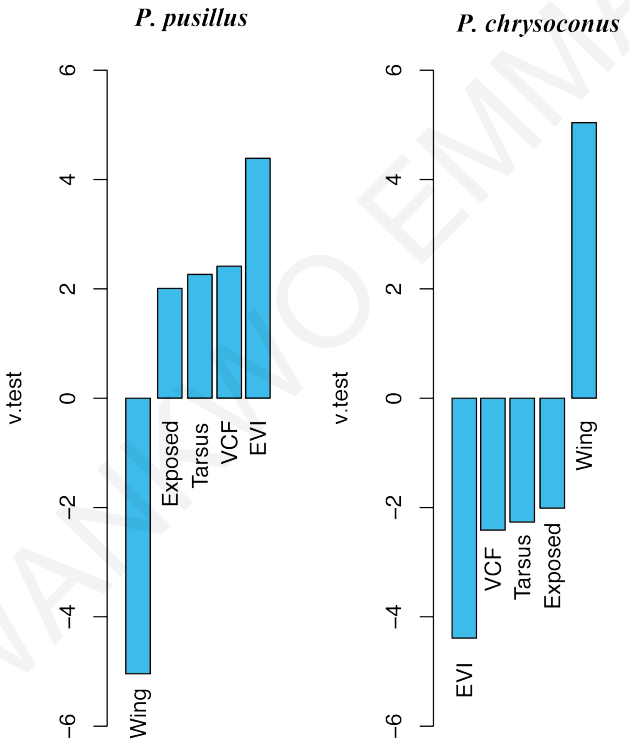

Figure 2. Categorical description analysis indicates the various continuous variables (wing length, exposed, tarsus length, VCF, and EVI) that best describe the morphological differences between the species. *P. c. extoni* (YFT) has longer wing length, but shorter tarsus length and exposed bill compared to *P. p. pusillus* (RFT). Body size varies in relation to VCF and EVI.

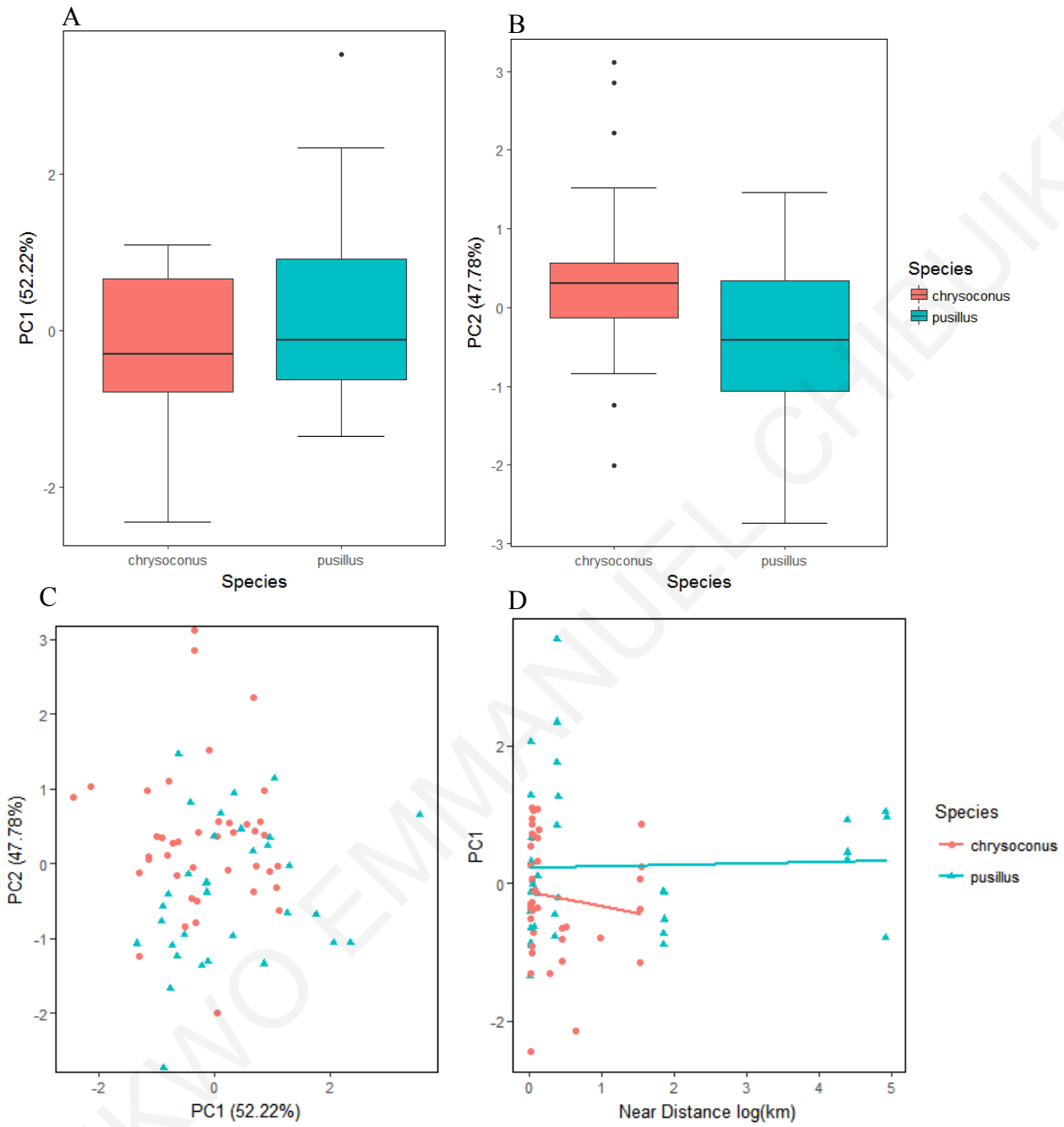

Figure 3. Morphometric analysis showing variation in body size of the species based on Principal component analysis with varimax rotation. (A)The first dimension (PC1) explained 52.22% variation in body size and corresponded with tarsus length and bill dimensions (except for bill depth), with *P. p. pusillus* being larger, (B) while the second dimension explained 47.78% variation in body size which corresponded with wing length, tail length, body mass and bill depth (*P. c. extoni* being larger). (C) In both dimensions there is overlap in body size at the contact zone. (D) *P. c. extoni* body size increased towards the contact zone while *P. p. pusillus* body size did not vary with distance from the contact zone.

Table1. Analysis of Variance in body size (PC1).

	df	F	Pr(>F)
Latitude	1	8.6808	**0.0004**
Longitude	1	14.258	**<0.0001**
AlloSymp	2	4.6907	**0.0014**
VCF	1	3.2655	**0.0445**
Species	1	22.922	**<0.0001**
EVI	1	5.6064	**0.00567**
Location	13	1.7865	**0.00005**

Colour measurements

We found significant differences in plumage between the species in each feather patch using MANOVA (all, $P < 0.001$). Differences in crown colour between the species were especially pronounced ($F = 13.38$, $df = 3$, $P < 0.00001$, Figure 4). Examining distributions of tetrahedral x, y, z (hereafter x, y, and z) against latitude shows a variety of patterns, with convergence and divergence in different measures towards the contact zone. Specifically, in crown colour y and z are distinct throughout, but in x there is considerable overlap and convergence towards the contact zone (Figure A1). In throat, rump, belly and wing covert patches there is some overlap in individual values of x, y, and z, in spite of the significant difference overall between the two species, but most notably, the individual *P. p. pusillus* close to the contact zone has values of x, y, and z in most of these patches close to the line of best fit for *P. c. extoni*, rather than *P. p. pusillus*, at the contact zone (Figure A1, A2).

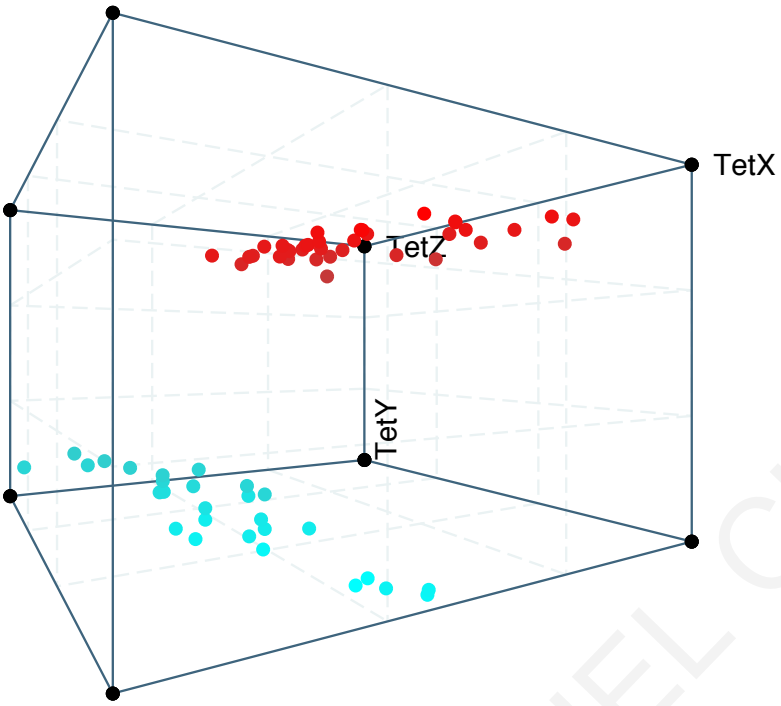

Figure 4. 3D Scatter of tetrahedral x, y, z (multiplied by 1000), illustrating the clear distinction between the forecrown plumage coloration of *P. p. pusillus* (red circles) and *P. c. extoni* (blue circles) in tetrahedral colour space.

Microsatellites

Of the 15 microsatellite loci amplified, 10 were variable and without null alleles. These 10 microsatellite loci were subsequently used for analysis. Eight microsatellite loci were found to be in Hardy-Weinberg equilibrium and 81 alleles were recovered. A Permutational test on the optimum number of markers required to sufficiently distinguish between individuals in the populations plateaued at six loci. Heterozygosity with population structure ($H_{ST,}$ G_{ST}) was highest at three loci (CAM13, CAM 17 and TG02088) and heterozygosity without population structure (H_T, G_{prime_ST}) in six loci (CAM13, CAM 17, TG02088, Bb111TG, CAM18 and TG13009; Table 2). The extent of population differentiation (D) ranging from 0 for a panmictic population to 1 for complete differentiation (Hedrick and Miermans 2011) revealed high differentiation at two loci (CAM13 and TG13009, Table 2). Pairwise genetic differentiation analysis results summarised in Table 3 revealed as expected that *extoni* in sympatry with

pusillus are less differentiated from those in near allopatry compared to those in distant allopatry, with the two allopatric groups least differentiated. Surprisingly, *P. p. pusillus* in sympatry with *P. c. extoni* were less differentiated from *P. p. pusillus* in distant allopatry compared to *P. p. pusillus* in near allopatry. Highest levels of genetic differentiation were, as expected, observed between allopatric *P. c. extoni* and allopatric *P. p. pusillus*. Strikingly, genetic differentiation between the sympatric populations of *P. p. pusillus* and *P. c. extoni* were lower than between *P. p. pusillus* in sympatry and near allopatry and similar to differentiation of *pusillus* in sympatry and distant allopatry. Genotype richness was highest in *extoni* and *P. p. pusillus* in sympatry, followed by *P. p. pusillus* in distant allopatry and least in *P. p. pusillus* in near allopatry based on Shannon-Wiener Index of MLG diversity (H), Stoddart and Taylor's Index of MLG diversity (G), Nei's unbiased gene diversity (Hexp), Number of multilocus genotypes (MLG) observed, and expected MLG (eMLG). The recovered genotypes were evenly distributed within the population based on Pielou's index (E.5) (Table 4).

Table 2. Differentiation indices per locus

	H_S	H_T	G_{ST}	G_{prime_ST}	D
Bb111TG	0.3147	0.6302	0.5005	0.7526	0.48923
CAM13	0.7608	0.9112	0.1650	0.7258	0.6683
CAM17	0.7307	0.8478	0.1381	0.5495	0.4712
CAM18	0.3739	0.6114	0.3883	0.6435	0.4030
HvoB1TTG	0.0947	0.1076	0.1198	0.1396	0.0151
TG06009	0.2482	0.2306	-0.0760	-0.1081	-0.0248
TG03031	0.1795	0.2034	0.1175	0.1511	0.0309
TG13009	0.3764	0.7303	0.4846	0.8120	0.6192
Tgu06	0.1663	0.2389	0.3037	0.3799	0.0925
TG02088	0.6071	0.7211	0.1580	0.4232	0.3082

Table 3. Estimates of the pairwise genetic differentiation (G_{ST}) between different populations of *P. chrysoconus* (Distant Allopatry, Near Allopatry and Sympatric populations) and *P. pusillus* (Distant Allopatry, Near Allopatry and Sympatric populations) based on microsatellite data.

	***P. c. extoni* Distant Allopatry**	***P. c. extoni* Near Allopatry**	***P. c. extoni* Sympatry**	***P. p. pusillus* Sympatry**	***P. p. pusillus* Distant Allopatry**
***P. chrysoconus* Near Allopatry**	0.046				
***P. chrysoconus* Sympatry**	0.1102	0.0655			
***P. pusillus* Sympatry**	0.3828	0.2709	0.1793		
***P. pusillus* Distant Allopatry**	0.6699	0.5201	0.4807	0.1628	
***P. pusillus* Near Allopatry**	0.6722	0.6014	0.432	0.3088	0.3401

Table 4. Genotypic richness and abundance indices

Population	**N**	**MLG**	**eMLG**	**SE**	**H**	**G**	**lambda**	**E.5**	**Hexp**	**Ia**	**rbarD**
*P. chrysoconus*_Distant Allopatry	7	7	7	0.00E+00	1.95	7	0.857	1	0.365	0.303	0.0546
*P. chrysoconus*_Near Allopatry	8	8	8	0.00E+00	2.08	8	0.875	1	0.267	-0.249	-0.0482
*P. chrysoconus*_Sympatry	28	28	10	3.41E-07	3.33	28	0.964	1	0.498	-0.195	-0.0233
*P. pusillus*_Sympatry	17	17	10	2.31E-07	2.83	17	0.941	1	0.56	0.452	0.0559
*P. pusillus*_Near Allopatry	6	6	6	0.00E+00	1.79	6	0.833	1	0.479	0.135	0.0188
*P. pusillus*_Distant Allopatry	15	15	10	2.77E-07	2.71	15	0.933	1	0.367	0.187	0.0301
Total	81	81	10	3.21E-06	4.39	81	0.988	1	0.53	0.217	0.0255

Analysis of Molecular Variance revealed significant variation in genotype at the level of distance from contact zone (sigma2 = 0.9763, $P < 0.0001$) and not based on localitites where the samples were collected (sigma2 = -3.4995, $P = 0.3188$). The Discriminant Principal Component Analysis showed considerable differentiation based on distance from contact zone such that near allopatric *P. p. pusillus* are a lot more differentiated than distant allopatric *P. p. pusillus* and *P. c. extoni* (Figures 5C, 6D).

STRUCTURE analysis recovered distinct individuals from distant allopatric populations, but admixed individuals from sympatry and near allopatry in both species. More phenotypically *pusillus* individuals grouped with *chrysoconus* genetically than phenotypically *chrysoconus* that grouped with *pusillus* genetically based on microsatellite markers (Figure 8), and mitochondrial Cytochrome *b* phylogenetic analysis (Figures 10, 11).

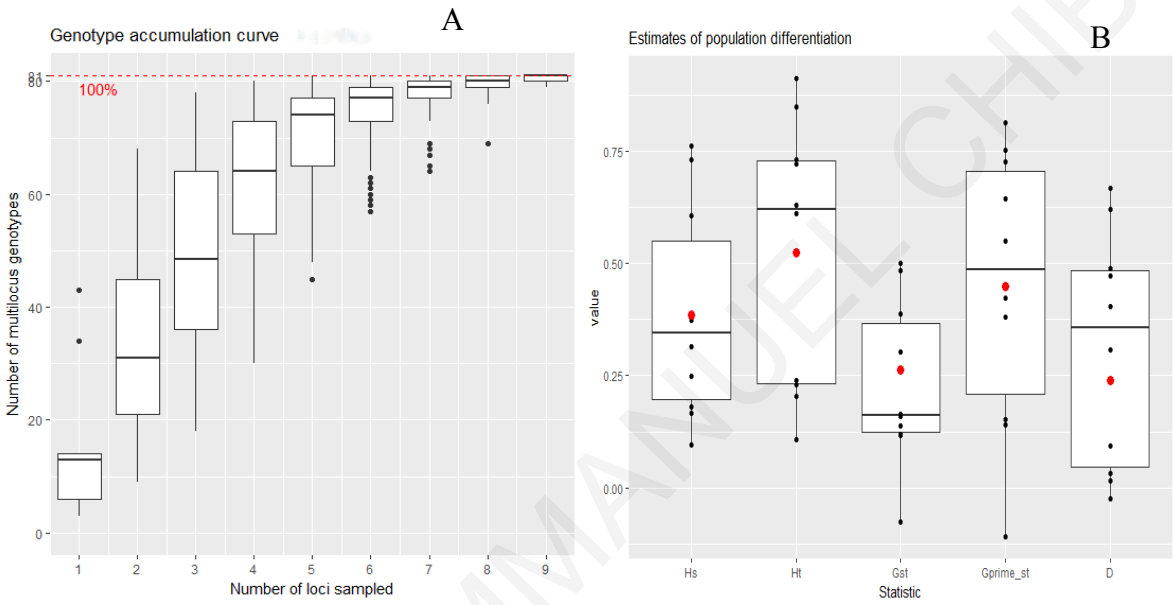

Figure 5. A) Genotype accumulation curve based on a Permutational test on the optimum number of markers required to sufficiently distinguish between individuals in the populations plateaued at six loci. B) Estimates of global indices for population differentiation based on microsatellite data. Heterozygosity with population structure (H_{ST}, G_{ST}) was lower than heterozygosity without population structure (H_T, G_{prime_ST}). The extent of population differentiation (D) ranging from 0 for a panmictic population to 1 for complete differentiation (Hedrick and Miermans 2011) revealed high differentiation at two loci (CAM13 and TG13009, Table 2).

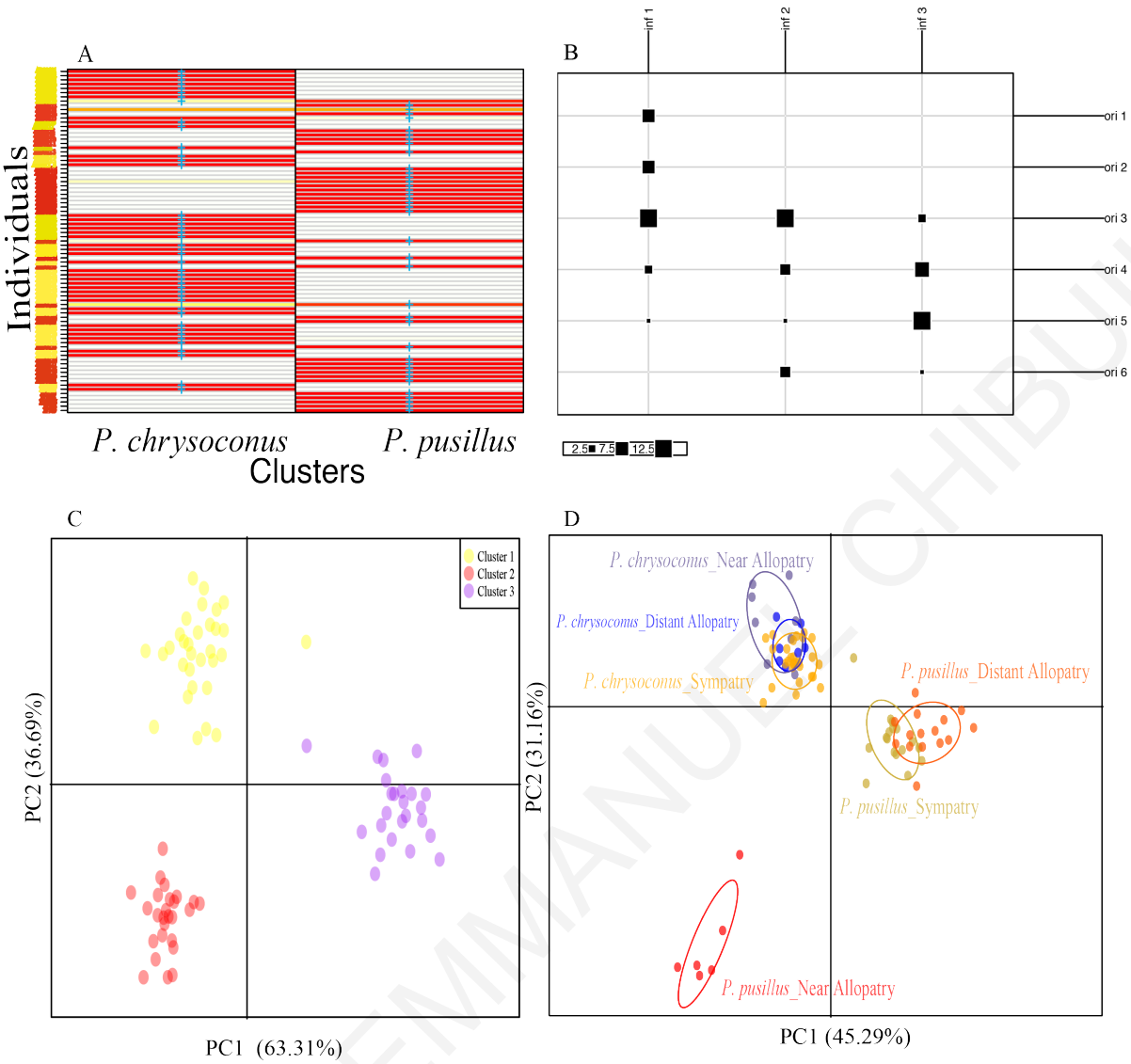

Figure 6. A) Probability clustering of individuals into the two species. Individuals are labelled based on their phenotypes: red *P. p. pusillus* and yellow *P. c. extoni*. The probability values range from 0 (white), 0.5 (yellow) to 1 (red). B) Comparison between the original population (ori) and inferred clusters (inf) from discriminant principal component analysis. ori 1 = distant allopatric *P. c. extoni*, ori 2 = near allopatric *P. c. extoni*, ori 3 = sympatric *P. p. pusillus*, ori 4 = sympatric *P. c. extoni*, ori 5 = distant allopatric *P. p. pusillus*, ori 6 = near allopatric *P. p. pusillus*. The size of the dark squares is proportional to the corresponding number of individuals. C) Inferred genetic clustering based on the best supported cluster recovery with the lowest meaningful BIC value. Clusters 1, 2 and 3 correspond with inferred groups (inf 1, inf 2 and inf 3) described in 6B. D) Principal component analysis illustrating genetic differentiation across samples from distant allopatric, near allopatric, and sympatric samples based on microsatellite data.

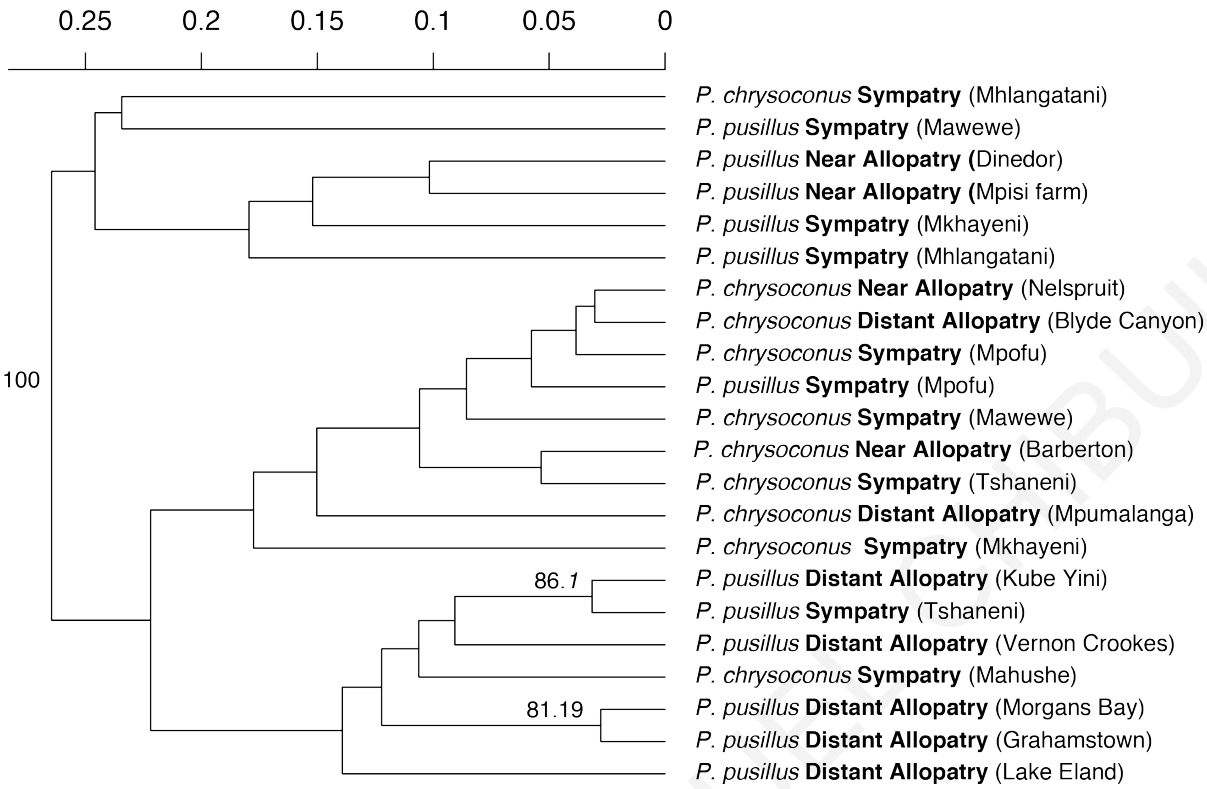

Figure 7. Dendrogram on the genetic distance of the populations using the microsatellite data. Near allopatric *P. p. pusillus* are more closely related to the sympatric *P. c. extoni/ P. p. pusillus* populations than they are to the distant *P. p. pusillus* population.

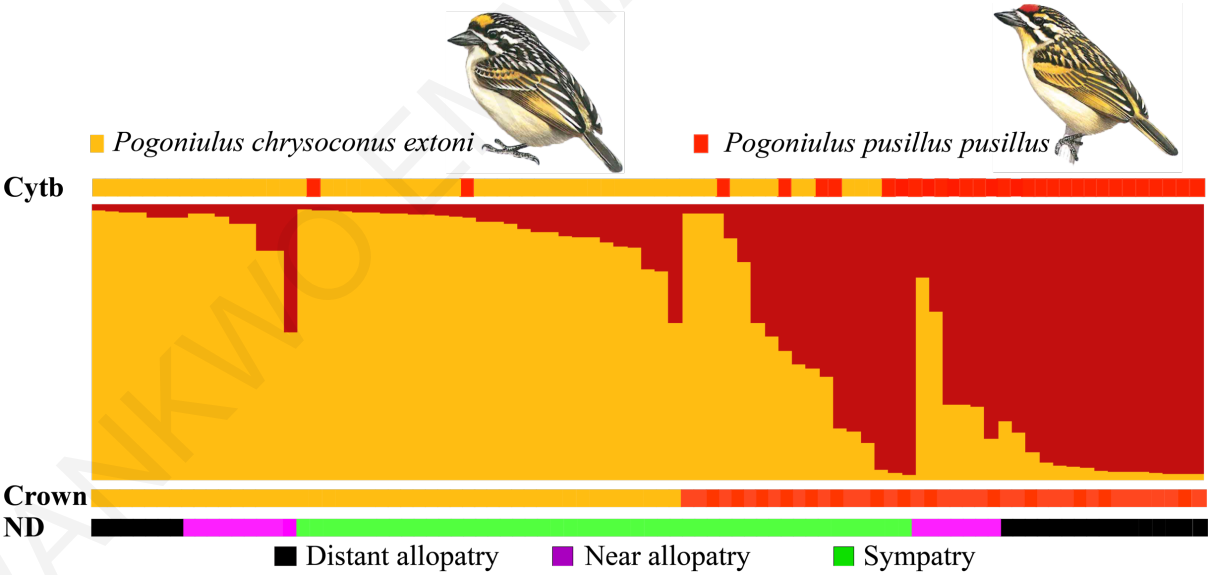

Figure 8. STRUCTURE analysis illustration using the microsatellite data set (n = 81 alleles), with *P. c. extoni* genotypes represented by yellow and *P. p. pusillus* by red. Banners above and below the plot represent the species as identified by mtDNA (Cytb) and phenotypically in the field based on forecrown plumage coloration, respectively. The populations are illustrated to show distance from contact zone (ND). Insets for both species are not drawn to scale.

Phylogenetic reconstruction

Sequences of 434 bp for 81 individuals were successfully obtained for Cytochrome *b* used in Maximum Likelihood analysis (Figure 10). In addition, we also obtained 1027 bp Cytochrome *b* and 832 bp ATPase sequences for 31 individuals used in Bayesian analysis and divergence time estimation. Both Bayesian analysis of two mitochondrial genes (Figure 9) revealed that *P. chrysoconus* is paraphyletic while *P. pusillus* is monophyletic. The *P. c. extoni* group is basal to *P. c. chrysoconus* and *P. pusillus*. Divergence of the subspecies is highly supported based on their maximal Bayesian posterior probability values. The calibrated Bayesian phylogenetic tree based on concatenated 1859 bp sequences revealed a longer time (10.07 mya) since the split of *P. c. extoni* from *P. c. chrysoconus* and *P. p. pusillus*, and 7.89 mya between *P. c. chrysoconus* and *P. p. pusillus*, than between *P. p. pusillus* and *P. p. affinis* 5.0 mya (Figure 9). Uncorrected pairwise sequence divergence between *P. p. pusillus* and *P. c. extoni* was estimated at 8.4%. We recovered 27 segregating sites, nucleotide diversity of pi = 0.0245 and 25 informative sites. A significantly positive Tajima's D statistic (D = 2.1242, *P* = 0.0216) may be an indication of selective pressure or population subdivision. We found greater introgression of *pusillus* mtDNA haplotypes into the genetic background of *chrysoconus* compared to the amount of *chrysoconus* haplotypes found within *pusillus* (Figure 11).

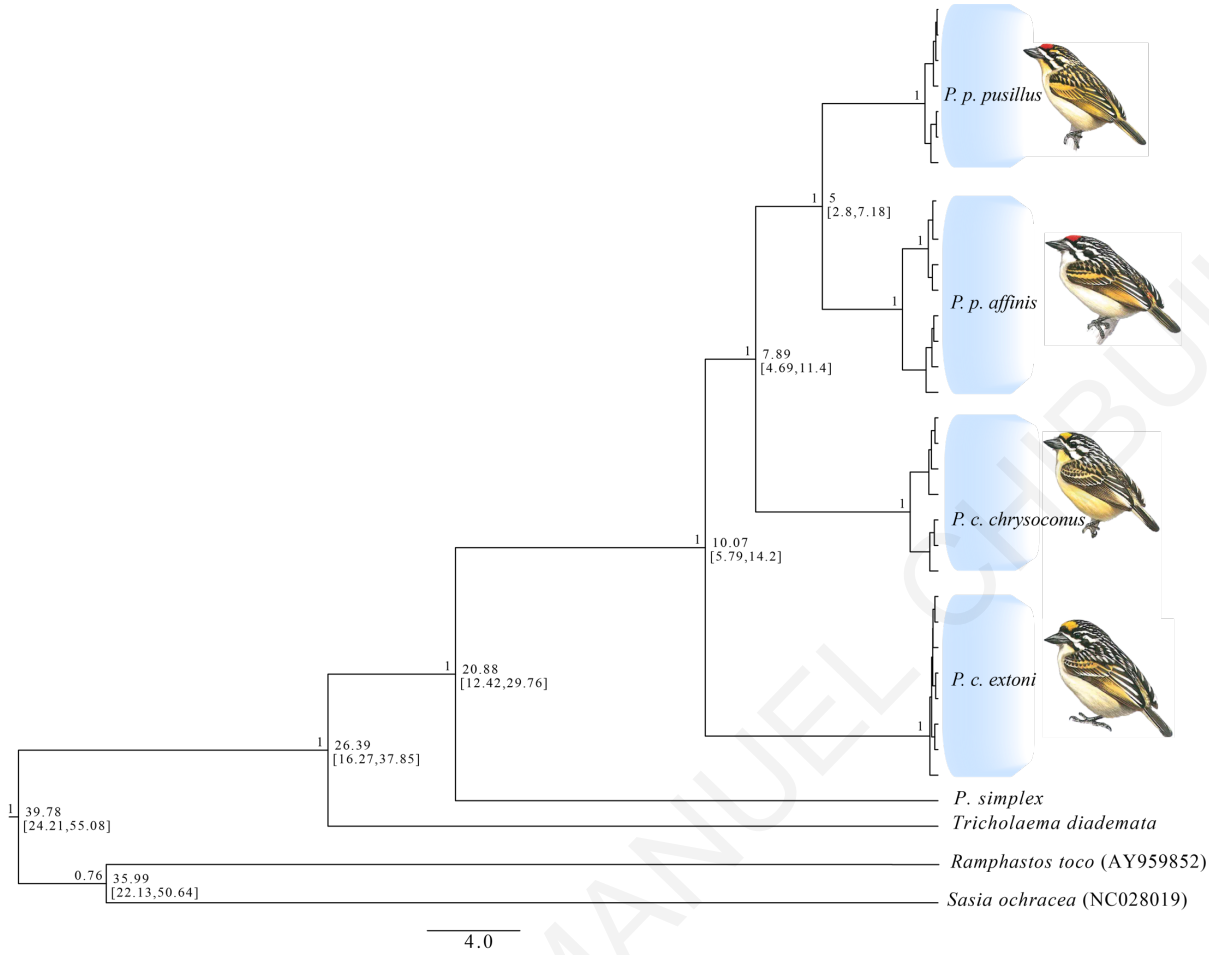

Figure 9. Calibrated phylogenetic tree of *P. pusillus* and *P. chrysoconus* based on the Bayesian Inference consensus tree of Cytochrome *b* and ATPase. Leftward of nodes are the posterior probabilities values indicated above, with node ages (above) and age high posterior density (below) on the right side of the node, estimated using RevBayes 1.0.5. *P. c. extoni* is basal to the rest of the clade, diverging 10.07 [5.79-14.2] mya, while *P. c. chrysoconus* split from the *pusillus* clade 7.89 [4.69-11.4] mya.

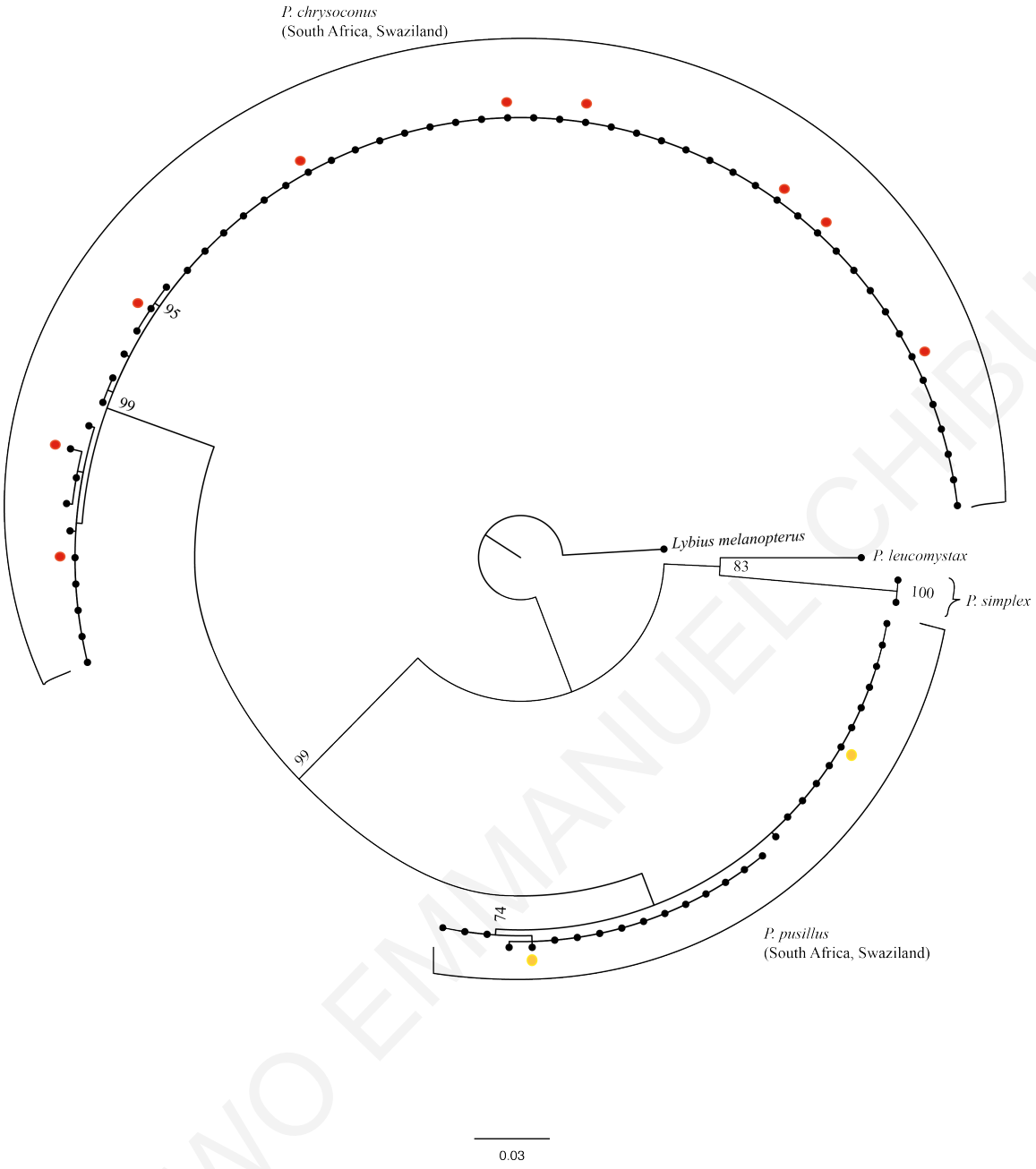

Figure 10. Maximum likelihood phylogenetic tree (IQ tree) based on 434 bp of Cytochrome *b*. The branch labels show bootstrap values. Individuals are labelled based on their phenotype such that red dots are phenotypically *P. pusillus pusillus* with *P. chrysoconus extoni* mtDNA, and yellow dots are phenotypically *P. chrysoconus extoni* with *pusillus* mtDNA

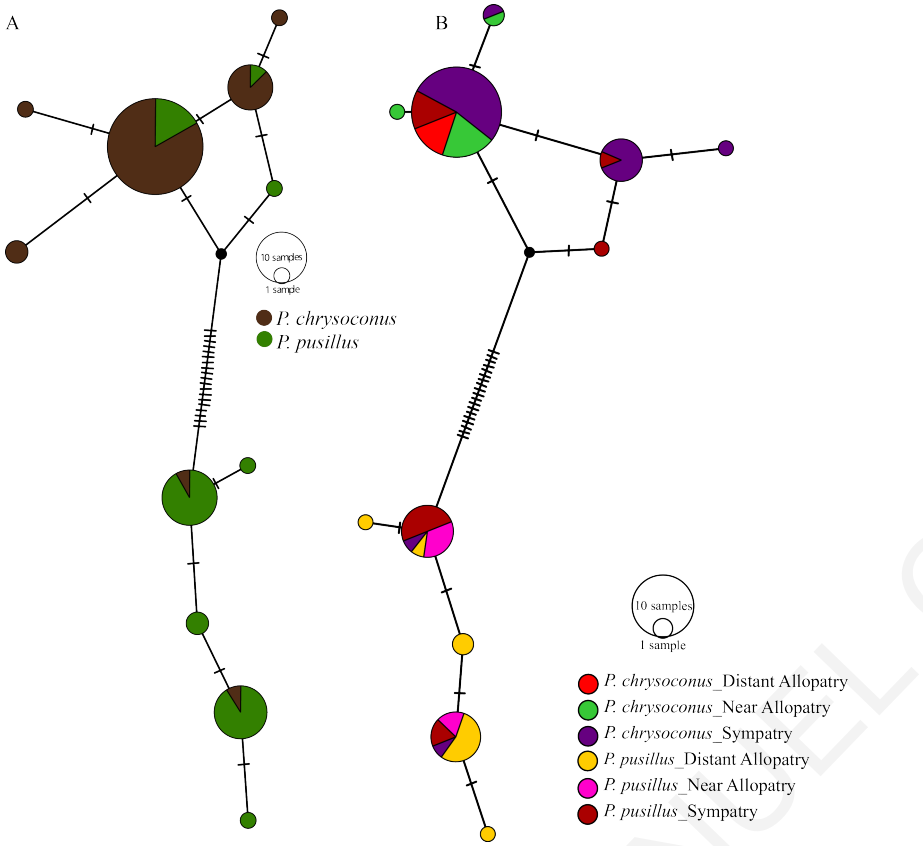

Figure 11. Cytochrome *b* 434 bp haplotype network: (A) between species and (B) among the populations of the species grouped based on their respective distances from the contact zone. There is more structure in the haplotype network of *chrysoconus* than *P. p. pusillus*. More phenotypically *P. p. pusillus* were found with *P. c. extoni* haplotypes than *P. c. extoni* found with *P. p. pusillus* haplotypes.

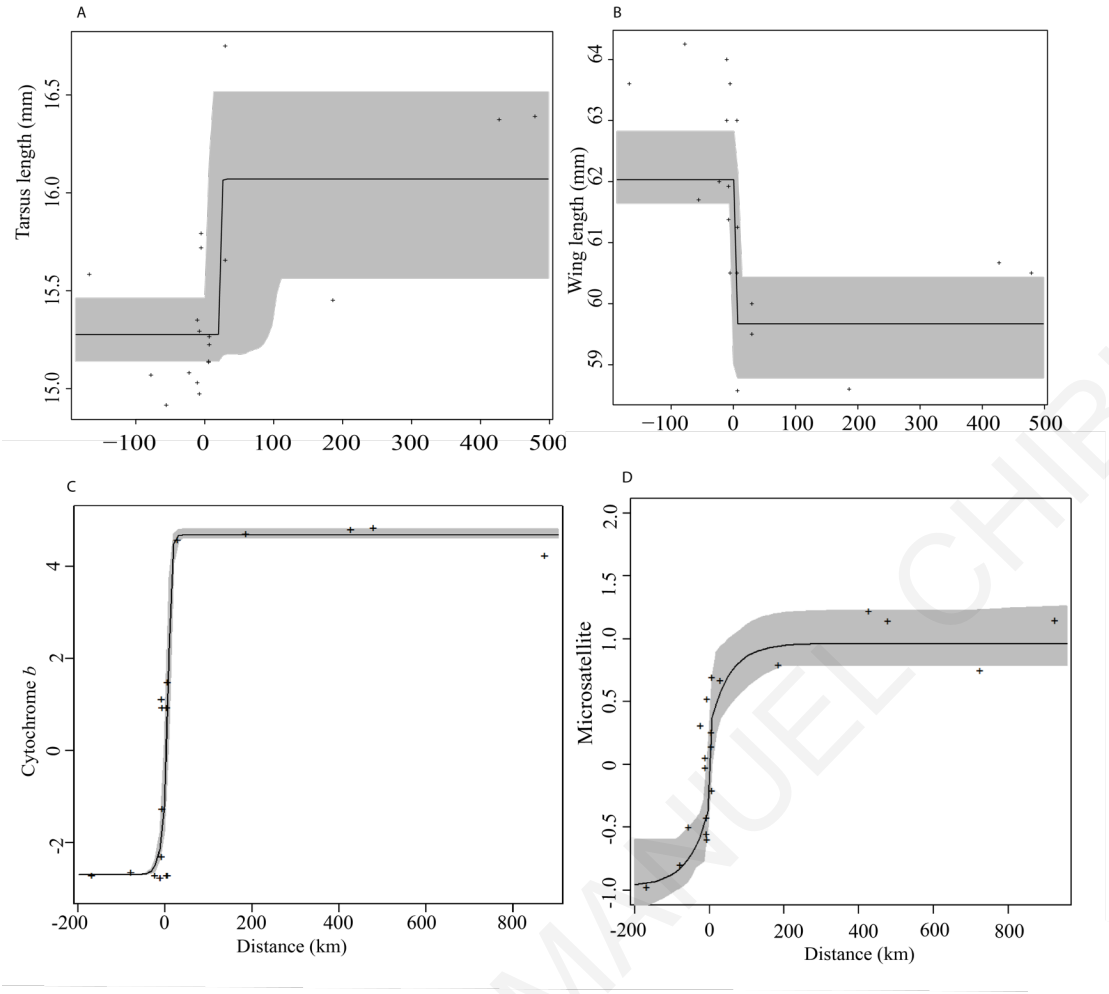

Figure 12. The maximum-likelihood cline and the 95% credible cline region for tarsus length (A), wing length (B), mtDNA gene (C), and microsatellite data (D). Negative distances represent the *P. c. extoni* side and positive the *P. p. pusillus* side of the cline. The distances were measured in km for each population perpendicular to the contact zone at 0 km.

Our cline analysis showed a pattern of wider clines in tarsus length at allopatric, near allopatric and sympatric populations. Cline widths for wing length, cyt *b* and microsatellite markers were narrow at the sympatric population but wide at near and distant allopatric populations (Figure 12).

Discussion

Our analyses reveal rampant introgressive hybridisation in the contact zone between *P. p. pusillus* and *P. c. extoni*, with almost all individuals in the contact zone showing some evidence

of introgression, as do some individuals in near allopatry. This level of introgression is in spite of the extent of divergence between the two species in mtDNA (8.4% pairwise sequence divergence), and significant differences in six plumage patches, though there is evidence that some plumage traits may introgress at the contact zone. There is also substantial overlap in morphological characters at the contact zone, which could be explained by adaptation to local environmental conditions, or by introgression.

In allopatry, we observed limited variation in the morphotype across individuals within *P. c. extoni* and *P. p. pusillus* and each species was distinct in mtDNA. However, in sympatry, the individuals we sampled showed extensive variation in both traits and we found a mixture of the two distinct mtDNA haplotypes. Introgressive hybridisation appeared primarily asymmetric with more phenotypically red-fronted *P. p. pusillus* being identified as *P. c. extoni* based on mtDNA haplotypes and nuclear markers within the contact zone suggesting the predominant occurrence of backcrossing into the *P. c. extoni* lineage. The principal component analysis showed a clear separation of the allopatric populations of *P. c. extoni* and *P. p. pusillus* into two distinct clusters and an intermediate position for some of the investigated sympatric samples from within the contact zone. This indicates that gene flow between the two subspecies has resulted in a higher degree of allele sharing between individuals in sympatry. The pattern of asymmetric introgression of *P. p. pusillus* genes into the genetic background of *P. c. extoni* based on the analyses presented here could either result from a sexual preference for red-fronted males by yellow-fronted females or due to selective pressure against hybrid individuals whose maternal parents are *P. p. pusillus*. STRUCTURE clustering analysis further supports the presense of hybridization between the species by showing the highest likelihood for two distinct populations (allopatric *chrysoconus* and *pusillus*, respectively), while samples from the sympatric zone have a genetic set-up built up by intermixed contributions from the two-parental species.

In most studies on introgression at contact zones, there is clear evidence of mixing of plumage traits that make hybrid identification straightforward (Cicero and Johnson, 1995; Poelstra et al., 2014; Toews et al., 2016; but see Baldassarre et al., 2014), and hybridisation occurs among species with comparatively little divergence in mtDNA (e.g., Lovette et al., 1999; Poelstra et al., 2014; Toews et al., 2016). Here, hybridisation occurs at very high levels despite millions of years of divergence, similar to levels reported in *Passerina* buntings (Klicka et al., 2001; Carling et al., 2010). In the buntings, strong sexual selection appears to have driven dichromatism and elaborate plumage coloration in *P. amoena* and *P. cyanea*, but asymmetric hybridisation at the contact zone leads to extensive introgression from one species into the genome of the other, with clearly identifiable hybrids with intermediate plumage (e.g., Carling and Brumfield, 2008). In the present study, with sexes alike, the primary plumage character used to distinguish between the species, forecrown colour, remained distinct between them, in spite of some evidence of convergence (Ross, 1970) but with no overlap at the contact zone. However, other plumage characters such as throat, rump and belly colour, represented by different shades of pale yellow, could better reflect the level of introgression, and future work could investigate the extent to which some plumage patterns introgress between species while others remain distinct.

Plumage colouration plays a significant role in mate choice and may explain asymmetric patterns of hybridisation in *Passerina* buntings (Carling and Brumfield, 2008) and *Malurus* fairy-wrens (Baldassarre et al., 2014). In our study, there is asymmetric introgression of red-crowned plumage into the *P. c. extoni* genetic background. If this is driven by a preference for red plumage among *P. c. extoni* females, future work could focus on confirming it with identification of the genes responsible for red plumage across the hybrid zone, and if possible, mate choice experiments. Another phenotypic trait mediating interspecific interactions in birds is song. Studies on passerines have found both instances of song mixing

facilitating hybridisation (Qvarnström et al., 2006) and maintaining range boundaries between ecological competitors that hybridise (McEntee et al., 2016), with song a character that has been shown to diverge across ecological gradients in Africa (Slabbekoorn and Smith, 2002; Kirschel et al., 2009a; Kirschel et al., 2011). Previous work on forest tinkerbirds found that songs diverge when related species interact, reducing costly aggressive interactions (Kirschel et al., 2009b), and that songs can diverge rapidly between populations of the same species – an order of magnitude faster than between the pair of species studied here (Nwankwo et al., 2018). But a previous study on song in *P. p. pusillus* and *P. c. extoni* found evidence for convergence in the contact zone (Monadjem et al., 1994), suggesting song differences may be insufficient to maintain the species boundary, and song characters introgress among the species. Further work is needed to determine the importance of song in this system.

The wide cline at allopatric and near allopatric habitats suggests no selection on the specific traits (tarsus length) in the populations of the two species (Figure 12). On the other hand, narrow and steep cline at the sympatric population is an indication of selection of the traits and little or no exchange of alleles that control for these traits (Figures 12). The traits with very narrow clines at the sympatric population are potentially differential traits important in maintaining species boundaries between the lineages. In spite of observed hybridisation in Southern Africa between *P. p. pusillus* and *P. c. extoni*, there is evidence of conserved regions in the genome. Harrison and Larson (2014) suggest these conserved genomic regions unique to the respective species may not be maintained uniformly in space and time, and evidence from ongoing work (Kirschel et al. unpublished data) suggests this might be the case in these tinkerbirds.

Conclusion

The present study provides evidence of discordance in phenotype and genetic characteristics of *P. c. extoni* and *P. p. pusillus* amid a long history of divergence in their primary distinguishing traits of yellow and red forecrowns, respectively. This is based on our analyses of morphology, mtDNA and microsatellite markers. Having increasing numbers of intermediate phenotypic traits coupled with admixed genetic ancestry supports historical and contemporary gene flow at the contact zone of the studied species. Variation in phenotype and genetic traits along the gradient to the contact zone indicates expansion of contact into historically allopatry regions. The intermediate individuals sampled in our study in the light of our analysis represent outcomes of backcrossing and introgression of predominantly *P. p. pusillus* plumage alleles into the *P. c. extoni* genome.

References

ABBOTT, R., ALBACH, D., ANSELL, S., ARNTZEN, J. W., BAIRD, S. J. E., BIERNE, N., BUGGS, R. 2013. Hybridization and speciation. *Journal of Evolutionary Biology*, **26**(2), 229–246.

AGAPOW, P., and BURT, A. 2001. Indices of multilocus linkage disequilibrium. *Molecular Ecology Resources*, **1**(1-2), 101–102.

ARCGIS, E. 2012. 10.1. Redlands, California: ESRI.

ARNOLD, M. L. 2006. *Evolution through genetic exchange*. Oxford University Press.

ARNTZEN, J.W. and WALLIS, G.P., 1991. Restricted gene flow in a moving hybrid zone of the newts Triturus cristatus and T. marmoratus in western France. *Evolution*, **45**(4):.805-826.

AVISE, J. C., and BALL JR, R. M. 1991. Mitochondrial DNA and avian microevolution. *Acta XX Congressus Internationalis Ornithologici,* **1**, 514–524.

BANDELT H, FORSTER, P, and RÖHL A. 1999. Median-joining networks for inferring intraspecific phylogenies. *Molecular Biology Evolution*, **16**(1):37–48.

BALDASSARRE, D.T., WHITE, T.A., KARUBIAN, J. and WEBSTER, M.S., 2014. Genomic and morphological analysis of a semipermeable avian hybrid zone suggests asymmetrical introgression of a sexual signal. *Evolution* **68**: 2644-2657.

BEUCH, S. 2012. Obserwacje mieszańca dzięciołów zielonego Picus viridis i zielonosiwego Picus canus w Bytomiu oraz przegląd literatury dotyczącej hybrydyzacji tych gatunków. *Ptaki S'laska*, **19**, 119–126.

BORGE, T., LINDROOS, K., NADVORNIK, P., SYVÄNEN, A.C. and SÆTRE, G.P., 2005. Amount of introgression in flycatcher hybrid zones reflects regional differences in pre and post-zygotic barriers to gene exchange. *Journal of evolutionary biology*, **18**(6), 1416-1424.

BROWN, A.H.D., FELDMAN, M.W. and NEVO, E., 1980. Multilocus structure of natural populations of Hordeum spontaneum. *Genetics*, **96**(2), pp.523-536.

BUTLIN, R. K. 1987. Species, speciation and reinforcement. *American Naturalist*, **130**: 461-464.

CARLING, M.D. and BRUMFIELD, R.T., 2008. Haldane's rule in an avian system: Using cline theory and divergence population genetics to test for differential introgression of mitochondrial, autosomal, and sex-linked loci across the Passerina Bunting hybrid zone. *Evolution* **62**: 2600-2615

CARLING, M.D., LOVETTE, I. J., and BRUMFIELD, R.T. 2010. Historical divergence and gene flow: coalescent analyses of mitochondrial, autosomal and sex-linked loci in Passerina buntings. *Evolution* **64**: 1762-1772.

CASE, T. J., R. D. HOLT, A. M. MCPEEK, and T. H. KEITT. 2005. The community context of species' borders: ecological and evolutionary perspectives. *Oikos* **108**:28-46.

COCKRUM, E. L. 1952. A check-list and bibliography of hybrid birds in North America north of Mexico. *The Wilson Bulletin*, **64**(3), 140–159.

CICERO, C., and JOHNSON, N. K. 1995. Speciation in Sapsuckers (Sphyrapicus): III. Mitochondrial-DNA sequence divergence at the cytochrome-b locus. *Auk*, **112**: 547-563.

CRESPIN, L., BERREBI, P. and LEBRETON, J.D., 1999. Asymmetrical introgression in a freshwater fish hybrid zone as revealed by a morphological index of hybridization. *Biological Journal of the Linnean Society*, **67**(1), pp.57-72.

DAVEY, J., HOHENLOHE, P., ETTER, P., BOONE, J., CATCHEN, J., and BLAXTER, M. 2011. Genome-wide genetic marker discovery and genotyping using next-generation sequencing. *Nature Reviews Genetics*, **12**(7), 499–510. https://doi.org/10.1038/nrg3012

DAWSON, D.A., BALL, A.D., SPURGIN, L.G., MARTIN-GALVEZ, D., STEWART, I.R., HORSBURGH, G.J., POTTER, J., MOLINA-MORALES, M., BICKNELL, A.W., PRESTON, S.A., EKBLOM, R., SLATE, J. and BURKE, T., 2013. High-utility conserved avian microsatellite markers enable parentage and population studies across a wide range of species. *BMC genomics*, **14**(176) 2164-14176.

DAWSON, D.A., HORSBURGH, G.J., KUPPER, C., STEWART, I.R., BALL, A.D., DURRANT, K.L., HANSSON, B., BACON, I., BIRD, S., KLEIN, A., KRUPA, A.P., LEE, J.W., MARTIN-GALVEZ, D., SIMEONI, M., SMITH, G., SPURGIN, L.G. and BURKE, T., 2010. New methods to identify conserved microsatellite loci and develop primer sets of high cross-species utility - as demonstrated for birds. *Molecular ecology resources*, **10**(3) 475-494.

DERRYBERRY, E.P., DERRYBERRY, G.E., MALEY, J.M. and BRUMFIELD, R.T., 2014. HZAR: hybrid zone analysis using an R software package. *Molecular ecology resources*, **14**(3), pp.652-663.

DOBZHANSKY, T. 1940. Speciation as a stage in evolutionary divergence. *American Naturalist* **74**: 312-321.

DOUGLAS B., MARTIN M., BEN B., STEVE W., 2015. Fitting Linear Mixed-Effects Models using lme4. *Journal of Statistical Software*, **67**(1), 1-48. doi:10.18637/jss.v067.i01.

DRAY, S., and DUFOUR, A.-B. 2007. The *ade4 package: implementing the duality diagram for ecologists. Journal* of Statistical Software, **22**(4) 1–20.

EARL, D.A., 2012. STRUCTURE HARVESTER: a website and program for visualizing STRUCTURE output and implementing the Evanno method. *Conservation genetics resources*, **4**(2), pp.359-361.

EBERHARD, J. R., and BERMINGHAM, E., 2004. Phylogeny and biogeography of the *Amazona ochrocephala* (Aves: Psittacidae) complex. *Auk,* **121**: 318-332.

EDGAR, R.C., 2004. MUSCLE: multiple sequence alignment with high accuracy and high throughput. *Nucleic acids research,* **32**(5), pp. 1792-1797.

EXCOFFIER, L., SMOUSE, P. E., and QUATTRO, J. M. 1992. Analysis of molecular variance inferred from metric distances among DNA haplotypes: application to human mitochondrial DNA restriction data. *Genetics*, **131**(2) 479–491.

FUCHS, J., PONS, J.-M., LIU, L., ERICSON, P. G. P., COULOUX, A., and PASQUET, E. 2013. A multi-locus phylogeny suggests an ancient hybridization event between *Campephilus* and *melanerpine* woodpeckers (Aves: *Picidae*). *Molecular Phylogenetics and Evolution*, **67**(3), 578–588.

GAY, L., NEUBAUER, G., ZAGALSKA-NEUBAUER, M., PONS, J.-M., BELL, D. A., and CROCHET, P.-A., 2009. Speciation with gene flow in the large white-headed gulls: does selection counterbalance introgression? *Heredity*, **102**(2), 133–146. https://doi.org/10.1038/hdy.2008.99

GEE, J.M. 2003. How a hybrid zone is maintained: Behavioral mechanisms of interbreeding between California and Gambel's quail (*Callipepla californica* and *C. gambelii*). *Evolution* **57**: 2407:2415

GORMAN, G. 1997. Hybridisation by Syrian woodpeckers. *British birds*, **90**, 578.

GRANT, P. R., and GRANT, B. R. 1992. Hybridization of Bird Species. *Science*, 256(5054), 193–197. https://doi.org/10.1126/science.256.5054.193

GRAVES, G. R. 2008. Handbook of Avian Hybrids of the World. *The Wilson Journal of Ornithology* (Vol. 120). https://doi.org/10.1676/0043-5643(2008)120[233:HOAHOT]2.0.CO;2

GRAY, A. P. 1958. *Bird hybrids*. Farnham Royal, Bucks, England, Commonwealth Agricultural. Bureaux. 1964. Hybrid. New Dictionary of Birds (AL Thompson, Ed.). New York, McGraw-Hill Book Co, 385–386.

GRAY, D. A. 1996. Carotenoids and sexual dichromatism in North American passerine birds. *The American Naturalist*, **148**(3), 453–480.

GRETHER, G. F., ANDERSON, C. N., DRURY, J. P., KIRSCHEL, A. N. G., LOSIN, N., OKAMOTO, K., and PEIMAN, K. S. 2013. The evolutionary consequences of interspecific aggression. *Annals of the New York Academy of Sciences* **1289**: 48-68.

GRETHER, G.F., PEIMAN, K.S., TOBIAS, J.A. and ROBINSON, B.W., 2017. Causes and consequences of behavioral interference between species. *Trends in ecology and evolution*. xx: 1–13. pmid:28797610.

HALDANE, J.B., 1922. Sex ratio and unisexual sterility in hybrid animals. *Journal of genetics*, **12**(2), pp.101-109.

HARRISON, R.G., 1986. Pattern and process in a narrow hybrid zone. *Heredity*, **56**(3), p.337.

HARRISON, R.G. and LARSON, E.L., 2014. Hybridization, introgression, and the nature of species boundaries. *Journal of Heredity*, **105**(S1), pp.795-809.

HARSHMAN, J., 1994. Reweaving the tapestry: What can we learn from Sibley and Ahlquist (1990)? *The Auk*, pp.377-388.

HATFIELD, T., and SCHLUTER, D. 1999. Ecological speciation in sticklebacks: environment-dependent hybrid fitness. *Evolution* **5**: 866-873.

HEDRICK, P. W. 2013. Adaptive introgression in animals: examples and comparison to new mutation and standing variation as sources of adaptive variation. *Molecular Ecology*, **22**(18), 4606–4618.

HEWITT, G.M., MASON, P. and NICHOLS, R.A., 1989. Sperm precedence and homogamy across a hybrid zone in the alpine grasshopper Podisma pedestris. *Heredity*, **62**(3): 343.

HILL, G. E. 1991. Plumage coloration is a sexually selected indicator of male quality. *Nature*, **350**(6316), 337.

HOBSON, K. A., GLOUTNEY, M. L., and GIBBS, H. L. 1997. Preservation of blood and tissue samples for stable-carbon and stable-nitrogen isotope analysis. *Canadian Journal of Zoology*, **75**(10), 1720–1723.

HÖHNA, S., LANDIS, M.J., HEATH, T.A., BOUSSAU, B., LARTILLOT, N., MOORE, B.R., HUELSENBECK, J.P. and RONQUIST, F., 2016. RevBayes: Bayesian phylogenetic inference using graphical models and an interactive model-specification language. *Systematic Biology,* **65**(4): 726-736.

IUCN, International Union for Conservation of Nature and Natural Resources. 2017. *IUCN red list categories*.

JAKOBSSON, M. and ROSENBERG, N.A., 2007. CLUMPP: a cluster matching and permutation program for dealing with label switching and multimodality in analysis of population structure. *Bioinformatics*, **23**(14), pp.1801-1806.

JOHNSGARD, P.A. 1967. Sympatry changes and hybridization incidence in mallards and black ducks. *The American Midland Naturalist* **77**: 51-63.

JOHNSON, N. K., and JOHNSON, C. B. 1985. Speciation in sapsuckers (Sphyrapicus): II. Sympatry, hybridization, and mate preference in *S. ruber daggetti* and *S. nuchalis*. *The Auk*, 1–15.

JOMBART, T. 2008. adegenet: a R package for the multivariate analysis of genetic markers. *Bioinformatics*, **24**(11), 1403–1405.

JOSEPH, L., DOLMAN, G., DONNELLAN, S., SAINT, K. M., BERG, M. L., BENNETT, A. T. D. 2008. Where and when does a ring start and end? Testing the ring-species hypothesis in a species complex of Australian parrots. *Proceedings of the Royal Society B*: **275**: 2431-2440.

KAMVAR, Z. N., TABIMA, J. F., and GRÜNWALD, N. J., 2014. Poppr: an R package for genetic analysis of populations with clonal, partially clonal, and/or sexual reproduction. *PeerJ*, **2**, e281. https://doi.org/10.7717/peerj.281

KIRKPATRICK, M. and BARTON, N.H., 1997. Evolution of a species' range. *The American Naturalist*, **150**(1), pp.1-23.

KIRSCHEL, A.N., BLUMSTEIN, D.T. and SMITH, T.B., 2009. Character displacement of song and morphology in African tinkerbirds. *Proceedings of the National Academy of Sciences*, **106**(20): 8256-8261.

KLICKA, J., FRY, A. J., ZINK, R. M., THOMPSON, C. W. 2001. A Cytochrome-b perspective on Passerina bunting relationships. *Auk* **118**:611-623.

KLEIN, A., HORSBURGH, G.J., KUEPPER, C., MAJOR, A., LEE, P.L., HOFFMANN, G., MATICS, R. and DAWSON, D.A., 2009. Microsatellite markers characterized in the barn owl (*Tyto alba*) and of high utility in other owls (Strigiformes: AVES). *Molecular ecology resources*, **9**(6), pp.1512-1519.

KOCHER, T. D., THOMAS, W. K., MEYER, A., EDWARDS, S. V, PÄÄBO, S., VILLABLANCA, F. X., and WILSON, A. C., 1989. Dynamics of mitochondrial DNA evolution in animals: amplification and sequencing with conserved primers. *Proceedings of the National Academy of Sciences,* **86**(16), 6196–6200.

KUMAR, S., STECHER, G., and TAMURA, K., 2016. MEGA7: Molecular Evolutionary Genetics Analysis version 7.0 for bigger datasets. *Molecular Biology and Evolution*, **33**(7): 1870–1874.

LANFEAR, R., FRANDSEN, P.B., WRIGHT, A.M., SENFELD, T. and CALCOTT, B., 2016. PartitionFinder 2: new methods for selecting partitioned models of evolution for molecular and morphological phylogenetic analyses. *Molecular Biology and Evolution*, **34**(3), pp.772-773.

LEIGH, J.W. and BRYANT, D., 2015. popart: full-feature software for haplotype network construction. *Methods in Ecology and Evolution*, **6**(9), pp.1110-1116.

LITTLEJOHN, M.J., and WATSON, G. F. *Annual Review of Ecology and Systematics* **16**: 85-112.

LOVETTE, I. J., BERMINGHAM, E., ROHWER, S., and WOOD, C. 1999. Mitochondrial restriction fragment length polymorphism (RFLP) and sequence variation among closely related avian species and the genetic characterization of hybrid Dendroica warblers. *Molecular Ecology* **8**: 1431-1441.

LOZANO, G.A., 1994. Carotenoids, Parasites, and Sexual Selection. *Oikos*, **70**(2), 309-311.

MCCARTHY, E. M. 2006. *Handbook of avian hybrids of the world*. Oxford University Press.

MCCARTHY, E.M., 2006. *Handbook of avian hybrids of the world*. Oxford University Press.

MCDEVITT, A. D., EDWARDS, C. J., O'TOOLE, P., O'SULLIVAN, P., O'REILLY, C., and CARDEN, R. F., 2009. Genetic structure of, and hybridisation between, red (*Cervus elaphus*) and sika (*Cervus nippon*) deer in Ireland. *Mammalian Biology*, **74**(4): 263–273. https://doi.org/10.1016/j.mambio.2009.03.015

MCENTEE, J.P., PEÑALBA, J. V., WEREMA, C., MULUNGU, E., MBILINYI, M., MOYER, D., HANSEN, L., FJELDSÅ, J., AND BOWIE, R.C.K. 2016. Social selection parapatry in Afrotropical sunbirds. *Evolution* **70**: 1307-1321.

MEISE, W., 1928. Die Verbreitung der Aaskrähe (Formenkreis Corvus corone L.). *Journal of Ornithology* **76**: 1-203.

MICHALCZUK, J., MCDEVITT, A. D., MAZGAJSKI, T. D., FIGARSKI, T., ILIEVA, M., BUJOCZEK, M., KAJTOCH, Ł. 2014. Tests of multiple molecular markers for the identification of Great Spotted and Syrian Woodpeckers and their hybrids. *Journal of Ornithology*, **155**(3), 591–600.

MLÍKOVSKY, J., 2002. *Cenozoic birds of the world*. Ninox Press.

MOLLER, A. P., BIARD, C., BLOUNT, J. D., HOUSTON, D. C., NINNI, P., SAINO, N., and SURAI, P. F. 2000. Carotenoid-dependent signals: indicators of foraging efficiency, immunocompetence or detoxification ability? *Poultry and Avian Biology Reviews*, **11**(3), 137–160.

MONADJEM, A., PASSMORE, N. I., 1994. Territorial calls of allopatric and sympatric populations of two species of *Pogoniulus* tinkerbarbet in southern Africa. *Ostrich* **65:** 339-341.

MOORE, W. S. 1995. Inferring phylogenies from mtDNA variation: mitochondrial gene trees versus nuclear gene trees. *Evolution*, **49**(4), 718–726. https://doi.org/10.2307/2410325

NADACHOWSKA, K., and BABIK, W. 2009. Divergence in the face of gene flow: The case of two newts (Amphibia: *Salamandridae*). *Molecular Biology and Evolution*, **26**(4), 829–841. https://doi.org/10.1093/molbev/msp004.

NAHUM, L.A., PEREIRA, S.L., CAMPOS FERNANDES, F.M.D., RUSSO MATIOLI, S. and WAJNTAL, A., 2003. Diversification of Ramphastinae (Aves, Ramphastidae) prior to the Cretaceous/Tertiary boundary as shown by molecular clock of mtDNA sequences. *Genetics and Molecular Biology*, **26**(4), pp.411-418.

NEI, M. 1978. Estimation of average heterozygosity and genetic distance from a small number of individuals. *Genetics*, **89**(3), 583–590.

NWANKWO, E. C., PALLARI, C. T., HADJIOANNOU, L., IOANNOU, A., MULWA, R. K., AND KIRSCHEL, A. N. G. 2018. Rapid song divergence leads to discordance between genetic distance and phenotypic characters important in reproductive isolation. *Ecology and Evolution*, **8**:716–731.

OLSON, V. A., and OWENS, I. P. F. 1998. Costly sexual signals: are carotenoids rare, risky or required? *Trends in Ecology and Evolution*, **13**(12), 510–514.

OTTENBURGHS, J., YDENBERG, R. C., VAN HOOFT, P., VAN WIEREN, S. E., and PRINS, H. H. T. 2015. The Avian Hybrids Project: gathering the scientific literature on avian hybridization. *Ibis*, **157**(4), 892–894.

PACHECO, N. M., CONGDON, B. C., and FRIESEN, V. L. 2002. The utility of nuclear introns for investigating hybridization and genetic introgression: A case study involving Brachyramphus murrelets. *Conservation Genetics*. https://doi.org/10.1023/A:1015209405758

PATON, T., HADDRATH, O. and BAKER, A.J., 2002. Complete mitochondrial DNA genome sequences show that modern birds are not descended from transitional shorebirds. *Proceedings of the Royal Society of London B: Biological Sciences*, **269**(1493), pp.839-846.

PETERSON BK, WEBER JN, KAY EH, FISHER HS, and HOEKSTRA HE (2012) Double Digest RADseq: An Inexpensive Method for De Novo SNP Discovery and Genotyping in Model and Non-Model Species. *PLOS ONE* **7**(5): e37135. https://doi.org/10.1371/journal.pone.0037135

PFENNIG, K. S., ALLENBY, A., MARTIN, R. A., MONROY, A., and JONES, C. D., 2012. A suite of molecular markers for identifying species, detecting introgression and describing population structure in spadefoot toads (*Spea* spp.). *Molecular Ecology Resources*, **12**(5), 909–917. https://doi.org/10.1111/j.1755-0998.2012.03150.x

PIELOU, E.C., 1975. Ecology diversity. *J. Wiley and Sons, New York*.

POELSTRA, J.W., VIJAY, N, BOSSU, C. M., LANTZ, H., RYLL, B., MÜLLER, I., BAGLIONE, V., UNNEBERG, P., WIKELSKI, M., GRABHERR, M. G., and WOLF, J. B. W. 2014. The genomic landscape underlying phenotypic integrity in the face of gene flow in crows. *Science*, **344**: 1410-1414.

PREVOSTI, A., OCANA, J., and ALONSO, G. 1975. Distances between populations of Drosophila subobscura, based on chromosome arrangement frequencies. *TAG Theoretical and Applied Genetics,* **45**(6), 231–241.

PRICE, T.D. and KIRKPATRICK, M., 2009. Evolutionarily stable range limits set by interspecific competition. *Proceedings of the Royal Society of London B: Biological Sciences*, pp.rspb-2008.

PRITCHARD, J.K., STEPHENS, M. and DONNELLY, P., 2000. Inference of population structure using multilocus genotype data. *Genetics,* **155**(2), pp. 945-959.

QVARNSTRÖM, A., HAAVIE, J., SÆTHER, S. A., ERIKSSON, D., and PÄRT, T. 2006. Song similarity predicts hybridization in flycatchers. *Evolution* **19**: 1202-1209.

R CORE TEAM. 2017. R: A Language and Environment for Statistical Computing. R Foundation for Statistical Computing, Vienna, Austria. https://doi.org/http://www.R-project.org/

RANDLER, C. 2002. Avian hybridization, mixed pairing and female choice. *Animal Behaviour*, **63**(1), 103–119. https://doi.org/10.1006/anbe.2001.1884

ROHWER, S., BERMINGHAM, E., and WOOD, C. 2001. Plumage and mitochondrial DNA haplotype variation across a moving hybrid zone. *Evolution* **55**:405-422.

ROSENBERG, N.A., 2004. DISTRUCT: a program for the graphical display of population structure. *Molecular Ecology Resources*, **4**(1), pp.137-138.

ROSS G. J. B., 1970. The specific status and distribution of *Pogoniulus pusillus* (Dumont) and *Pogoniulus chrysoconus* (Temminck) in southern africa. *Ostrich - Journal of African Ornithology* **41**(3):200-204. https://doi.org/10.1080/00306525.1970.9634366

SCHLIEP, K.P., 2011. phangorn: phylogenetic analysis in R. *Bioinformatics (Oxford, England),* **27**(4), pp. 592-593.

SCHUMER, M., ROSENTHAL, G. G., and ANDOLFATTO, P. 2014. How common is homoploid hybrid speciation? *Evolution*, **68**(6), 1553–1560.

SEEHAUSEN, O. 2004. Hybridization and adaptive radiation. *Trends in Ecology and Evolution*, **19**(4), 198–207.

SELANDER, R. K., and GILLER, D. R. 1959. Interspecific relations of woodpeckers in Texas. *Wilson Bulletin*, 71, 107–124.

SENEVIRATNE, S. S., TOEWS, D. P. L., BRELSFORD, A., and IRWIN, D. E. 2012. Concordance of genetic and phenotypic characters across a sapsucker hybrid zone. *Journal of Avian Biology*, **43**(2), 119–130.

SENEVIRATNE, S. S., DAVIDSON, P., MARTIN, K. and IRWIN, D. E., 2016. Low levels of hybridization across two contact zones among three species of woodpeckers. *Journal of Avian Biology*, **47**, 887-898.

SENN, H. V., SWANSON, G. M., GOODMAN, S. J., BARTON, N. H., and PEMBERTON, J. M. 2010. Phenotypic correlates of hybridisation between red and sika deer (genus Cervus). *Journal of Animal Ecology*, **79**(2), 414–425. https://doi.org/10.1111/j.1365-2656.2009.01633.x

SENN, H., V. and PEMBERTON, J., M., 2009. *Hybridisation between red deer (Cervus elaphus) and Japanese sika (C. nippon) on the Kintyre Peninsula, Scotland*. University of Edinburgh, (Degree Dissertation); Barton, Nick.

SHANNON, C. E. 2001. A mathematical theory of communication. ACM SIGMOBILE *Mobile Computing and Communications Review*, 5(1), 3–55.

SHORT, L. L. 1965. Hybridization in the flickers (*Colaptes*) of North America. *Bulletin of the AMNH*; v. **129**, article 4

SHORT, L. L. 1969. Taxonomic aspects of avian hybridization. *The Auk*, **86**(1), 84–105.

SHORT, L. L. and J. F. M. HORNE. 2001. *Toucans, Barbet and Honeyguides*. Oxford University Press, Oxford.

SIMPSON, E. H. 1949. Measurement of diversity. *Nature*, **163**(163), 688.

SMITH, J. M., SMITH, N. H., O'ROURKE, M., and SPRATT, B. G. 1993. How clonal are bacteria? *Proceedings of the National Academy of Sciences*, **90**(10), 4384–4388.

STATACORP, L. P. 2009. Stata 10.1. TX, USA: StataCorp LP.

STODDART, J. A., and TAYLOR, J. F. 1988. Genotypic diversity: estimation and prediction in samples. *Genetics*, **118**(4), 705–711.

SVEDIN, N., WILEY, C., VEEN, T., GUSTAFSSON, L., and QVARNSTRÖM, A. 2008. Natural and sexual selection against hybrid flycatchers. *Proceedings of the Royal Society of London, Series B: Biological Sciences* **275**: 735-744.

TAJIMA F. 1999. Statistical method for testing the neutral mutation hypothesis by DNA polymorphism. *Genetics* **123**:585–595.

TOEWS, D. P. L., TAYLOR, S. A., VALLENDER, R., BRELSFORD, A., BUTCHER, B. G., MESSER, P. W., and LOVETTE, I. J. 2016. Plumage genes and little else distinguish the genomes of hybridising warblers. *Current Biology* **26**: 2313-2318.

VÄHÄ, J.P. and PRIMMER, C.R., 2006. Efficiency of model-based Bayesian methods for detecting hybrid individuals under different hybridization scenarios and with different numbers of loci. *Molecular Ecology*, **15**(1), pp.63-72.

VÄLI, ÜL., DOMBROVSKI, V., TREINYS, R., BERGMANIS, U., DARÓCZI, S. J., DRAVECKY, M., ELLEGREN, H. 2010. Widespread hybridization between the Greater Spotted Eagle *Aquila clanga* and the Lesser Spotted *Eagle Aquila pomarina* (Aves: Accipitriformes) in Europe. *Biological Journal of the Linnean Society*, **100**(3), 725–736. https://doi.org/10.1111/j.1095-8312.2010.01455.x

WEIR, J.T., 2009. Implications of genetic differentiation in neotropical montane forest birds1. *Annals of the Missouri Botanical Garden*, **96**(3), pp.410-433.

WEIR, L.K., GRANT, J.W. and HUTCHINGS, J.A., 2011. The influence of operational sex ratio on the intensity of competition for mates. *The American Naturalist*, **177**(2), pp.167-176.

WIEBE, K. L., 2000. Assortative mating by color in a population of hybrid Northern Flickers. *The Auk*, **117**(2), 525–529.

WILSON, A. C., CANN, R. L., CARR, S. M., GEORGE, M., GYLLENSTEN, U. B., HELM-BYCHOWSKI, K. M., SAGE, and R. D., 1985. Mitochondrial DNA and two perspectives on evolutionary genetics. *Biological Journal of the Linnean Society*, **26**(4), 375–400.

WINTER, D. J. 2012. MMOD: an R library for the calculation of population differentiation statistics. *Molecular Ecology Resources*, **12**(6), 1158–1160.

CHAPTER FOUR

Genomic evidence of song divergence mediating reproductive isolation at contact zones

Abstract

The factors that lead to interbreeding between *Pogoniulus chrysoconus* and *Pogoniulus pusillus* across four independent contact zones were examined and identification of the genomic regions associated with phenotypic traits of plumage colouration in *P. chrysoconus* and *P. pusillus* by analysing RADseq data. Phenotypic characters, specifically song, plumage and morphology, were measured across four contact zones of *P. pusillus* and *P. chrysoconus* tinkerbirds, the extent of introgressive hybridisation across three contact zones between the species using genomic methods was examined and compared with patterns of phenotypic introgression using cline analyses. The major findings from this study include: different patterns of interaction between *Pogoniulus chrysoconus* and *P. pusillus* exist at each of the contact zones, introgressive hybridisation between *Pogoniulus chrysoconus* and *Pogoniulus pusillus* in Southern Africa is mediated by similarity in song and therefore undermine the dependence on visual cues in mate choice in these species, several individuals with intermediate plumage coloration on the forecrown indicate admixture in the alleles that control for plumage coloration between the two populations in Southern Africa contact zone. Little or no evidence of hybridisation was observed at Ethiopia and Kenya contact zone while extensive hybridisation was observed in Southern Africa contact zone than in Tanzania contact zone. Genome wide analysis (GWAS) recovered three genes that specifically control for eye pigmentation (HPS4), visual learning (NDRG4) and detection of light stimulus involved in visual perception (CACNA2D4) and several genes known to control morphological development and specifically for head development. Overall, it is recommended to take into account rapid differentiation is specific traits important in reproductive isolation in delimiting species. This research also contributes to our understanding of the influence of interaction between closely related species on speciation and its impact on our biodiversity by highlighting the factors that explain species distribution, the significance of interplay among phenotypic similarity, genetic relatedness and ecological gradients in maintaining species boundaries.

Introduction

Hybrid zones have been the focus of much recent research on the speciation process (Alcaide et al. 2014, Poelstra et al. 2014, Grossen et al. 2016, Vijay et al. 2016). They have provided the opportunity to examine the role of natural selection in maintaining phenotypic characters among interacting species and identifying corresponding regions of the genome that show extreme divergence against background levels representing random drift (Jones et al. 2012), Toews et al. 2016, Brelsford et al. 2017). Such studies have revealed that a few candidate genes may be sufficient to maintain species limits in spite of gene flow (Stryjewski and Sorenson 2017); alternatively, genome swamping may erode species differences (Toews et al. 2016) and drive the reversal of divergence that had occurred over time in isolation **(**Kleindorfer et al. 2014, Kearns et al. 2018). Despite these advances in the identification of genomic regions associated with phenotypic traits, little is known regarding the extent of phenotypic divergence that is sufficient for reproductive isolation. Studies among sets of interacting species provide opportunities for comparisons of the effect of varying extents of phenotypic and genetic divergence on reproductive isolation (Grossen et al. 2016, Stryjewski and Sorenson 2017). Yet, evidence is lacking regarding which specific levels of phenotypic divergence are sufficient to maintain reproductive isolation, something that a study comparing contrasting interactions of a pair of species that have met repeatedly in secondary contact could potentially reveal.

Communication plays a critical role in interactions among animals and differences in signals among species function in species and mate recognition (Slabbekoorn and Smith 2002, Kirschel et al. 2009a). When closely related species come together in secondary contact, depending on the extent of recognition they might coexist amicably, perhaps facilitated by displacement of signals (Kirschel et al. 2009a), if ecological competitors they may exclude one another from their respective ranges aided by competitor recognition of signals (Grether et al. 2009, 2013), or instead they might not have diverged sufficiently in phenotype, leading to

species recognition failure, and a breakdown of assortative mating. A number of studies have identified pigmentation differences that are associated with maintenance of species limits in spite of gene flow, especially in birds (Poelstra et al. 2014, Grossen et al. 2016, Toews et al. 2016). Yet in other cases, a preference for a heterospecific trait can lead to asymmetric introgression of that trait across a contact zone, as found in pigmentation of lizards (While et al. 2015), as well as birds (Baldassarre et al. 2014). The role of avian acoustic signals in maintaining or eroding species boundaries has received less attention (but see flycatchers: Qvarnstrom et al. 2006, crickets: Mullen 2007, Izzo and Gray 2004, mammals: Klump and Shalter 1984, fish: Myrberg 1981, Myrberg et al 1986, reptiles: Angulo and Reichie 2008, Bass and Chagnaud 2012, Ptacek 2000), presumably because the majority of studies on birds have focused on passerines, where cultural learning may occur across species boundaries, with much evidence of mixed singing in contact zones (Haavie et al. 2004, Shipilina et al. 2017). Cultural learning may confound efforts to identify the role of genomic introgression on song characters. While a growing body of work has examined the effects of interactions among species in both acoustic and visual signals and their recognition (reviewed in Grether et al. 2009), these have involved pairs of species presumed to be reproductively isolated (e.g. Kirschel et al. 2009a, Tobias and Seddon 2009, Kirschel et al. in review), or where reproductive character displacement may drive reproductive isolation between hybridising species (Wheatcroft and Qvarnstrom 2017), but no study has examined a range in phenotypic divergence among separate contact zones that may mediate an extent of introgressive hybridisation ranging from random mating to reproductive isolation.

There is a long history of association of adaptations in species that increase their fitness along environmental gradients, and much work has documented such phenotypic adaptations in spite of gene flow (e.g. Smith et al. 1997), with regions of the genome associated with adaptation to different habitats (Steiner et al. 2007, Jones et al. 2012, Zhen et al. 2017. Such

adaptation to environmental gradients is dependent on the extent of gene flow and the strength of selection, which are influenced by the steepness of environmental gradients. If species on either side of a steep gradient are better adapted to the conditions in their own ranges, gene flow from range centres may swamp adaptation at range boundaries (Kirkpatrick and Barton 1997), and hybrids with intermediate traits might be unfit for either parental environment (Barton and Hewitt 1985, Case and Taper 2000), with reinforcement against maladaptive hybridisation predicted to evolve (Butlin 1987). Thus, when investigating hypotheses of the role the extent of phenotypic variation plays on maintaining reproductive isolation, the steepness of environmental gradients should also be accounted for.

Next-generation sequencing (NGS) technology has made it possible to study heritable polymorphisms across populations of both model and nonmodel species by generating thousands or even millions of genetic markers. This has allowed for several genome-wide association studies in several organisms including wild birds. Having such tools as NGS has contributed tremendously within a short period to studies in ecology and evolution (Allendorf et al 2010). Several ecological studies using NGS have relied on sequenced SNPs obtained using restriction enzymes (Derjusheva et al. 2004, Fidler 2007, Griffin et al 2008, Bers et al. 2010, Kraus et al. 2011, Jonker et al. 2012). Restriction site-associated DNA sequencing (RADseq) is one method that generates a high density of genomic markers that has transformed the study of relationships among individuals and between populations. Other advantages include the ability to apply techniques across many species without species-specific primers allowing studies at the genomic level to be carried out without an available reference genome of the focal species (Davey et al. 2010, Peterson et al 2012, Andrews et al 2016). This has permitted genomic studies of nonmodel species (Catchen et al 2013a, b, Hohenlohe et al 2013, Senn et al. 2013), and high numbers of SNPs recovered through RADseq allow for population

structure and genetic diversity studies with relatively fewer individuals (Felsenstein 2006, Green et al. 2010, Rheindt et al. 2013).

The importance of multi-locus recombination of ancestral genetic variation in generating phenotypic novelty and diversity has been demonstrated based on genome-wide association study (GWAS, Stryjewski and Sorenson 2017). GWASs attempt to identify associations between single-nucleotide polymorphisms (SNPs) and quantifiable phenotypic traits. Similar analyses have been extensively used in identifying the genomic regions that control for pigmentation and colour patterns among birds (Toews 2017, Cuthill et al. 2017, Brelsford et al. 2017), as well as other vertebrates (Nachman et al 2003), invertebrates (Bastide et al 2013), and plants (Arabidopsis Genome Initiative 2000, Kahawara 2013). Finding introgressive hybridisation between species of *Pogoniulus* tinkerbirds across the contact zone where hybrid individuals have intermediate forecrown plumage colouration makes it important to identify the genomic regions associated with red versus yellow plumage colouration between the two species.

Here we investigate the factors that lead to interbreeding between two species of *Pogoniulus* tinkerbird that meet in a series of independent contact zones, with variation in the extent of their interactions. We measure the extent of genotypic and phenotypic introgression among each contact zone, and identify genomic regions associated with phenotypic traits of plumage colouration by analysing RADseq data. *Pogoniulus* tinkerbirds are an ideal study system for research involving the role of song in species interactions, because they emit very simple songs that do not involve cultural song learning and can be measured quantitatively in two linear dimensions: frequency and pace (Kirschel et al. 2009a). Red-fronted (*P. pusillus*) and yellow-fronted (*P. chrysoconus*) tinkerbird share similar ecology, song, and morphology, but differ in plumage most strikingly in whether they sport a red or yellow forecrown. Their distributions abut in East Africa, with different subspecies coming together in Ethiopia,

Western Kenya and Northeastern Uganda, and across much of Tanzania, and disjunctly in Southern Africa. These separate contact zones between different subspecies of the two species allow for multiple comparisons of the causes and consequences of hybridisation.

The objective of this study was to compare and contrast phenotypic variation and its effect on species interactions across the different contact zones. We aimed to measure variation in song, plumage and morphology, across up to four contact zones and to identify the extent of introgressive hybridisation across three of the contact zones between the two species using genomic methods and to compare these with patterns of phenotypic introgression using cline analyses. We also aimed to identify the regions of the genome associated with red versus yellow plumage coloration in tinkerbirds.

Methods

Fieldwork was performed in Kenya and Uganda between June 2011 and March 2014, in Tanzania between October 2012 and October 2013, in Nigeria in October 2016, in Ethiopia in February 2016 and in South Africa and Swaziland between March 2015 and March 2017. Field sites were selected to allow sampling from populations of each species in distant allopatry, near allopatry (within 100 km) and at contact zones where both species, identified based on forecrown colour, were found in sympatry. Hereafter we refer to each contact zone by the country or region where the two species were found in sympatry (i.e. Ethiopia, Kenya, Tanzania and Southern Africa).

Field recordings and song analyses

Songs of yellow-fronted and red-fronted tinkerbird are simple in phonology and remarkably similar. They consist of a single pulse repeated about twice a second at a constant frequency (Figure 1). Songs were recording using a Marantz PMD661 digital solid-state recorder with

Sennheiser MKH 8020/50/70 microphones onto SD cards as 16 bit .WAV files at a sampling frequency of 48 kHz. This involved moving along trails and tracks at study sites and listening for tinkerbird songs or eliciting them with song playback initially used to identify tinkerbird presence. Raven 1.5 software was used to analyse song features (Charif et al. 2010). Fifteen notes and note intervals were measured per recording and mean values calculated. The following parameters were measured: Peak frequency (Hz), note duration (s), internote interval (gap). The rate of each song was estimated based on the average internote interval duration in seconds between consecutive pulses in a song. We analysed recordings of 35 individuals across the Ethiopia contact zone (*P. chrysoconus xanthostictus* = 18, *P. pusillus uropygialis* = 17), 64 across the Kenya contact zone (*P. chrysoconus chrysoconus* = 30, *P. pusillus affinis* = 34), 64 across the Tanzania contact zone (*P. chrysoconus extoni* = 46, *P. pusillus affinis* = 18) and 98 across the Southern Africa contact zone (*P. chrysoconus extoni* = 41, *P. pusillus pusillus* = 57).

Because phenotypic traits might vary because of adaptation to local environmental conditions (Kirschel et al. 2009b, 2011), we controlled for the effects of the environment by incorporating data from remote sensing in statistical analyses. Moderate Resolution Imaging Radiometer (MODIS) raster files at 250 m resolution (MODIS/Terra Vegetation Indices 16-Day L3 Global 250m from 2010) were used to extract vegetation continuous field (VCF) and enhanced vegetation index (EVI) data for coordinates of the sampling locations in ArcGIS 10.1 (ESRI 2012). Several models were run in R 3.3.0 (R Core Team, 2017) to statistically test the variation in song features among populations of the species in relation to environmental factors (elevation), habitat vegetation characteristics (the Enhanced Vegetation Index (EVI), the Vegetation Continuous Field (VCF), latitude and longitude. The best approximating model in explaining variation in song rate and peak frequency was selected using the backward deletion method and compared with the full model using an information-theoretic approach based on Akaike's Information Criterion (AIC).

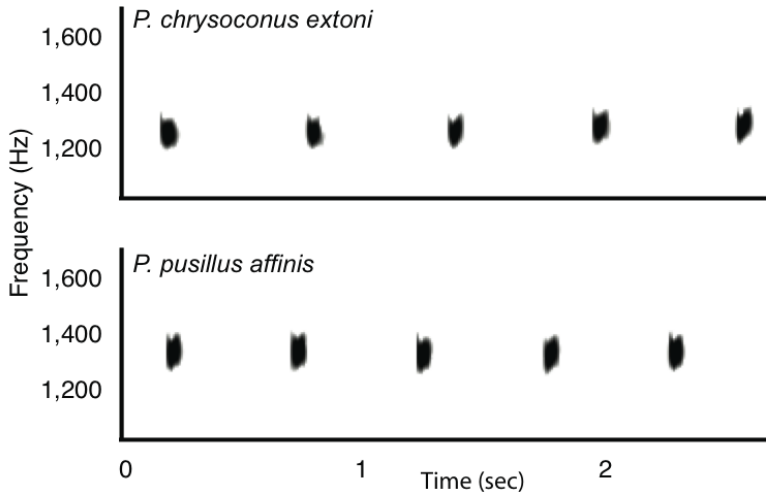

Figure 1. Spectrograms of songs of *P. chrysoconus extoni* (yellow-fronted tinkerbird, recorded in Namibia) and *P. pusillus affinis* (red-fronted tinkerbird, recorded in Kenya) obtained from the Macaulay library at the Cornell Lab of Ornithology. The spectrograms show how similar songs of the two species are from different geographic regions in allopatry.

GIS

We used ArcGIS 10.1 (ESRI 2012) to map localities where samples were collected, and songs recorded across contact zones. To visualise the pattern of variation in song among contact zones, we used the Inverse Distance Weighting (IDW) function to map salient song features across the landscape. We set the parameters in ARCGIS to use two local points in the interpolation of each cell value to minimise the effect of surrounding points on calculating cell values, bearing in mind the proximity of individuals of the two species at contact zones. We opted for the power setting of 3, to again allow for surrounding points to have a lower influence on each cell value than the default setting of 2 (and within the ARCGIS recommended range of 0.5 - 3). We chose the natural breaks (jenks) option to delineate the song features into categories.

Playback experiments

We performed a total of 108 playback experiments of yellow-fronted tinkerbird song to red-fronted tinkerbird and vice versa across three contact zones (Kenya = 38, Tanzania = 32 and Southern Africa = 38). The simple phonology of tinkerbird songs allows for the straightforward production of synthetic stimuli for use in experiments to unambiguously test differences in two acoustic characters, pace and frequency. Playback stimuli were thus produced synthetically in Audacity 2.1.0 (Audacity Team 2012) in accordance with methods used previously in other studies on *Pogoniulus* tinkerbirds (Kirschel et al. 2009a, Nwankwo et al. 2018). Briefly, we used mean values measured from recordings of song from several individuals of each species in each region, thus avoiding pseudoreplication on specific individuals' songs (McGregor et al. 1992). The playback stimuli consisted of a one-minute silence pre-playback, two minutes playback of the first song stimulus and one minute of silence post-playback. The focal bird's singing behaviour was recorded during the pre-playback silence and then during stimulus playback and in the post-playback silence to allow for testing of the effect of playback on song behaviour. A further four minutes of silence was observed before initiating the second experiment of the pair. Playback experiments were scored according to measures including latency to approach, closest approach distance to loudspeaker, time spent within 10m and 20m from loudspeaker and number of songs before and after playback stimulus began. The six variables were reduced to a single variable by Factor Analysis of Mixed Data (FactoMineR, Pages, 2004; Lê et al., 2008). This method calculated principal components accounting for both continuous and categorical variables. The first principal component was used to test for significant variation in responses to playbacks using a generalized linear model in R 3.3.4 (R Core Team 2017).

Field collection of samples and morphological data

We used mist nets and conspecific playback to capture and ring individual tinkerbirds across three contact zones (Kenya, Tanzania, and Southern Africa). Tinkerbirds are canopy birds and typically can only be attracted to nets with song playback once their presence has been established. This involved placement of 12 m x 2.5 m mist nets in strategic locations. Blood samples were obtained for genomic analysis, while specifically from the Southern Africa contact zone three to five forecrown feather samples were collected for reflectance spectrometry in the lab. Blood samples (approx. 50 µl) were obtained using venepuncture of the brachial vein in accordance with established protocols (e.g. Kirschel et al. 2009a).

Museum specimens

We received loans of specimens from the ornithology collections of the Natural History Museum of Los Angeles County, the Field Museum of Natural History, the American Museum of Natural History, the British Natural History Museum, the National Museum of Natural History, the Peabody Museum of Yale University, the Museum of Natural Science of Louisiana State University and the Donald R. Dickey Collection of the University of California Los Angeles to obtain morphometric and colour measurements. In total, we took morphometric measurements from 115 *P. chrysoconus* and 127 *P. pusillus* museum skins that were collected from sites across the four contact zones. We measured wing chord, tarsus and tail length, bill length and width, and lower mandible length using digital calipers. We identified the localities where specimens were collected from museum tags and used maps, gazetteers, and Google Earth (Google, Inc.), for those specimens where coordinates were not given, and assigned approximate latitude and longitude coordinates and elevation for each locality. Principal Component Analysis (PCA) with varimax rotation implemented within Psych version 1.7.8

(Revelle 2017) R Statistical package was used to reduce the morphology data from eight morphological variables to two principal components to determine the dimensions of variability in body size and bill shape of the study species. The principal component explaining the majority of variation was then used to test for variation in morphology resulting from differences between the species, sexes, locations, latitude, longitude and the environmental factors obtained from remote sensing using a generalized linear mixed effects model.

Plumage colouration and pattern analysis

The primary focus of the colour comparison is on the forecrown patch of the two species, which is the character on which their common names are based. It is the most striking plumage difference between the two species, though some other plumage patterns may also vary between the species among specific contact zones. We measured reflectance spectra (300-700 nm) of feathers on the forecrown using a JAZ spectrometer (Ocean Optics) with a fibre optic reflectance probe (Ocean Optics R-200) and PX xenon light source. The reflection probe was placed in an RPH-1 Reflection Probe Holder (Ocean Optics), at a 90° angle, and secured at 2 mm from the aperture of the probe holder. Two measurements were taken per plumage patch, per specimen, with the specimen placed flat onto a white background perpendicular to the observer and facing to the left, and then rotated 180° for the second measurement, with the probe holder placed horizontally onto the specimen, so the aperture completely covered the feather patch, thus ensuring ambient light was excluded. Reflectance data for each specimen were obtained following calibration with a white standard (Ocean Optics WS-1) and dark standard (by screwing the lid back onto the fibre optic connector to ensure no light entered), and recorded in SPECTRASuite (Version 1.0, Ocean Optics).

Specific quantitative variables that were measured within a 300 - 700 nm wavelength from plumage patches include colour distance between individuals from different populations,

segment classification of the individual plumage patch, hue differences and the avian tetracolourspace visual model (Endler et al. 2005, Stoddard and Prum 2008).

Plumage colour analysis was performed using the R 3.3.3 statistical software (R Core Team 2017) to implement Pavo (an R package for the perceptual analysis, visualization and organization of colour data, Maia et al. 2013). Visual inspection of replicate reflectance spectra was performed, and replicate measurements were averaged and smoothed using the 'procspec' function within Pavo prior to analysis. The colour distances within and between the populations were calculated by using the function 'coldist', which applies the visual models of Vorobyev et al. (1998) to calculate colour distances with receptor noise based on relative photoreceptor densities. The function 'segclass' was used to calculate segment classification measures as defined in Endler (1990). A 2D plot of colour points projected from the tetrahedron to its encapsulating sphere to visualise differences in hue was produced using the function 'projplot'. We used the Mollweide projection in the hue projection plot as it preserves area relationships within latitudes without distortion. The avian tetracolourspace visual model was computed using the 'tcs' function to calculate the coordinates and colourimetric variables that represent reflectance spectra in avian tetrahedral colour space: u, s, m, l (the quantum catch data); x, y, z (cartesian coordinates for the points in tetrahedral colour space).

Categorical description analysis of colourimetric variables within the FactoMineR package (Lê et al. 2008) was used to select variables that best described the species per plumage patch at $P \leq 0.05$. Subsequently, the selected variables were used in Permutational Multivariate Analysis of Variance (with the 'vegan' package, Dixon 2003) using Euclidean Distance Matrices for partitioning 'distance matrices' among sources of variation and fitting linear models (on species as factors) to the matrices using a permutation test of 10,000 iterations.

Molecular analysis

We obtained a total of 167 samples from the field in Nigeria (*P. c. chrysoconus* = 4), Kenya and Uganda (*P. c. chrysoconus* = 6, *P. p. affinis* = 28), Tanzania (*P. c. extoni* = 28, *P. p. affinis* = 23), Swaziland (*P. c. extoni* = 23, *P. p. pusillus* = 23) and South Africa (*P. c. extoni* = 19, *P. p. pusillus* = 13). We also obtained three tissue samples of *P. c. chrysoconus* from Malawi and one from Ghana, and four blood samples of *P. p. pusillus* from South Africa, provided by the Field Museum of Natural History, LSUMNS and Museum of Vertebrate Zoology of the University of California Berkeley respectively.

Double-digest RAD Sequencing

DNA was extracted using a Qiagen DNeasy blood and tissue kit following manufacturer's protocols (Qiagen, Valencia, CA). Extracted DNA from samples was quantified using a NanoDrop (Thermo Scientific 2000c) and a Qubit 2.0 fluorometer with the DNA HS assay kit (Life Technologies) for double-digest Restriction site associated DNA sequencing (RADseq). We also checked for DNA quality based on migration on agarose gel, which allowed for the selection of samples with appropriate DNA concentration (> 20 ng/μL) and molecular weight (> 10000 bp).

The ddRAD sequencing was carried out by the Brelsford laboratory at the University of California, Riverside. Double-digest RAD sequencing libraries were prepared following the protocol described by Brelsford et al. (2016). Briefly, genomic DNA was digested with restriction enzymes *SbfI* and *MseI*, individually barcoded adapters were ligated to the resulting DNA fragments, and a bead cleanup was performed to remove excess adapters. Each sample was amplified in four replicate PCR reactions. The PCR product was run an agarose gel and fragements between 400 and 500bp were selected. Prior to sequencing, PCR products were pooled and carried out a bead cleanup on the resulting pool. The 174 samples reported here

were sequenced in two separate libraries, along with samples from a different project (A. Kirschel unpublished data). Each library was sequenced on one Illumina HiSeq 4000 lane at the Vincent J. Coates Genomics Sequencing Laboratory at University of California Berkeley, with 100 bp paired-end reads.

A matrix of genotypes from the raw sequence reads were obtained using Stacks version 1.40 (Catchen et al. 2013b). Reads were demultiplexed using process_radtags. He then ran the denovo_map.pl pipeline separately for reads 1 and 2, using parameter values -n 3 and --bound_high 0.05, with default values for all other parameters. The resulting SNPs were exported to VCF format, and VCFs for read 1 and read 2 were merged into a single file. Finally, he filtered the SNPs using VCFtools (Danecek et al. 2011), retaining genotypes supported by at least 4 reads, and loci with less than 20% missing data and minor allele count of at least 4.

Genomewide association study on phenotypic traits

I conducted genomewide association study (GWAS) on the RADseq data and two phenotypic traits: calculations of chroma and hue based on spectral reflectance of forecrown feathers and a binary classification of forecrown plumage colour (yellow = 0 and red = 1) based on observations in the field hereafter referred to as "binary pheno". The binary pheno study was performed in order to incorporate samples from all individuals for which genomic data was obtained, including from those contact zones from which crown feathers were not collected. It also provided a check on the reliability of spectral measurements. All markers were screened using PLINK 1.9 (Chang et al 2015) based on minimum scale of missing genotypes = 0.9, read depth = 4, call rate = 1, and minor allele frequency (MAF) = 0.03 resulting in 29,675 SNPs selected to conduct the GWAS. The filtering was considered necessary because of Radseq data batches with lower than desired quality still pass the pre-release data quality checks despite the stringent quality controls (Laurie et al 2010).

The Fixed and random model Circulating Probability Unification (FarmCPU; Liu et al., 2016) and GAPIT (Lipka et al., 2012) implemented within R 3.4.3 was used to conduct GWAS to determine the genetic bases for the variation in forecrown plumage of *P. chrysoconus* and *P. pusillus*. FarmCPU is a model selection algorithm designed to take into account the confounding problem between covariates and test markers by using both a Fixed Effect Model and a Random Effect Model and provides additional function for iteration of the models, which is not commonly implemented in other algorithms. The covariates used in the GWAS were based on the first three principal components calculated using GAPIT (Lipka et al., 2012).

The function "*FarmCPU.P.Threshold*" within FarmCPU was used to determine the *p*-value threshold based on 10,000 permutations used in the GWAS analysis. The quantile–quantile (Q–Q) plot was used for assessing the fit of the model to account for population structure implemented by plotting the negative logarithms of the *p*-value from the GWAS model against their expected value under a null hypothesis of no association with the trait.

The rad_tags of the significantly associated SNPs were used in the BLAST online program (http://blast.ncbi.nlm.nih.gov) on the genomic background of *Picoides pubescens, Serinus canaria, Taeniopygia guttata* and *Gallus gallus* to identify candidate genes that contribute to the regulation of forecrown plumage colouration in the two species. The ontology of the detected candidate genes was extracted from avian gene annotation on The UniProt Knowledgebase (UniProtKB) which is the central hub for the collection of functional information on proteins, with accurate, consistent and rich annotation (http://www.uniprot.org/uniprot).

Genetic population structure analysis

To quantify the extent of hybridisation the RADseq filtered data set (29,675 loci) was used in Bayesian population structure analyses in STRUCTURE v2.3.3 (Pritchard et al. 2000).

The parameters used in the STRUCTURE analysis to identify the number of sub-populations present (K) were a burn-in period of 100,000 Markov Chain Monte Carlo iterations and 300,000 run length and an admixture model following Hardy-Weinberg equilibrium and correlated allele frequencies. We performed four independent runs for each simulated value of K (K = 1–15). The best K value for the population structure analysis was determined using StructureSelector (Li and Liu 2018) while averaging among iterations across each K values using the program Clumpak (Kopelman et al. 2015).

The R package HZAR (Derryberry et al. 2014) was used to perform cline analysis to test for differences in introgression of genes and salient song features across the contact zone.

Population genetics

Principal component analysis on the filtered RADseq data (29,675 loci) was performed to show the overall clustering of genetic variation in 174 individuals across three contact zones from which molecular data were obtained (Kenya, Tanzania and Southern Africa). Pruned set of the Radseq data which are in approximate linkage equilibrium with each other was used for the PCA analysis to avoid the strong influence of SNP clusters in principal component analysis and relatedness analysis (Laurie et al. 2010). To quantitatively measure the extent of genetic similarity among individuals across contact zones an Identity by State (IBS) analysis was implemented in SNPRelate (Zheng et al., 2012) statistical package in R 3.4.0 (R Core Team 2017). This estimates the percentage of alleles shared among individuals across all loci, which was visualized in a heatmap. To determine the genetic relationship of the sampled individual based on the amount of genetic material (alleles) they share, without prior specification of species or population, we performed a permutational clustering analysis using a Z threshold of 15 and outlier threshold of 5 on the IBS coefficients. The result of this analysis was visualised in a dendrogram to show the relatedness of individuals. To determine the extent of genetic

differentiation across the populations of each species from allopatry to sympatry we performed a Pairwise Genetic Differentiation Analysis (Hedrick's G'_{ST}, Hedrick 2005) implemented within the mmod R statistical package (Winter, 2012).

Results

Song analysis

Song recordings obtained across the four contact zones in Ethiopia, Kenya, Tanzania and Southern Africa between *P. pusillus* and *P. chrysoconus* showed significant variation in song pace between the species ($F_{1,277} = 397.232$, $P < 0.0001$) and among the contact zones ($F_{1,278} = 19.921$, $P < 0.0001$). Song inter-note also showed strong postive correlation with latitude ($F_{1,276} = 8.3725$, $P = 0.0041$) but negative correlation with elevation ($F_{1,281} = 106.1165$, $P < 0.0001$) across contact zones. The song of *P. pusillus* was significantly faster than *P. chrysoconus* across contact zones ($t = 19.958$, $P < 0.0001$), yet the pattern varied among the contact zones with steep transitions in song pace between the two species in Ethiopia and Kenya, with more gradual clines evident in Tanzania and Southern Africa (Figure 2). We found strong negative correlation in Southern Africa ($F_{1,55} = 30.632$, $P < 0.0001$) and Tanzania ($F_{1,20} = 4.436$, $P = 0.048$), strong postive correlation in Ethiopia ($F_{1,15} = 6.6464$, $P = 0.021$) between distance to contact zone and inter-note interval duration in *pusillus*, but not in Kenya ($F_{1,46} = 0.0097$, $P = 0.9218$). While in *chrysoconus* we found strong postive correlation in Tanzania ($F_{1,44} = 8.892$, $P = 0.0046$) between distance to contact zone and inter-note interval duration in *pusillus*, but not in Ethiopia ($F_{1,15} = 0.0018$, $P = 0.9665$), Kenya ($F_{1,32} = 0.3305$, $P = 0.5694$) and Southern Africa ($F_{1,39} = 0.09$, $P = 0.7658$).

In Ethiopia, we found divergence in song towards the contact zone based on internote interval duration (Figure 3A) and no overlap at Kenya contact zone (Figure 3A). Relatively, there is extensive convergence in song internote interval in Tanzania (Figure 3A), over a wide

contact zone. In Southern Africa, there is the most extensive range overlap at a narrow contact zone and song convergence from allopatry to sympatry for both species (Figure 3A). No clear pattern of convergence or divergence was found across the four contact zones in peak frequency (Figure 3B) and note duration (Figure 4D).

There was much overlap in EVI of the two species in all four contact zones irrespective of distance to contact zone (Figure 4A), while in VCF there was again much overlap, except in Ethiopia where yellow-fronted tinkerbird had a preference for more forested habitat (Figure 4C). Ecological gradients across the contact zone were overall much steeper in Ethiopia than across the other contact zones (Figure 4A, B, C).

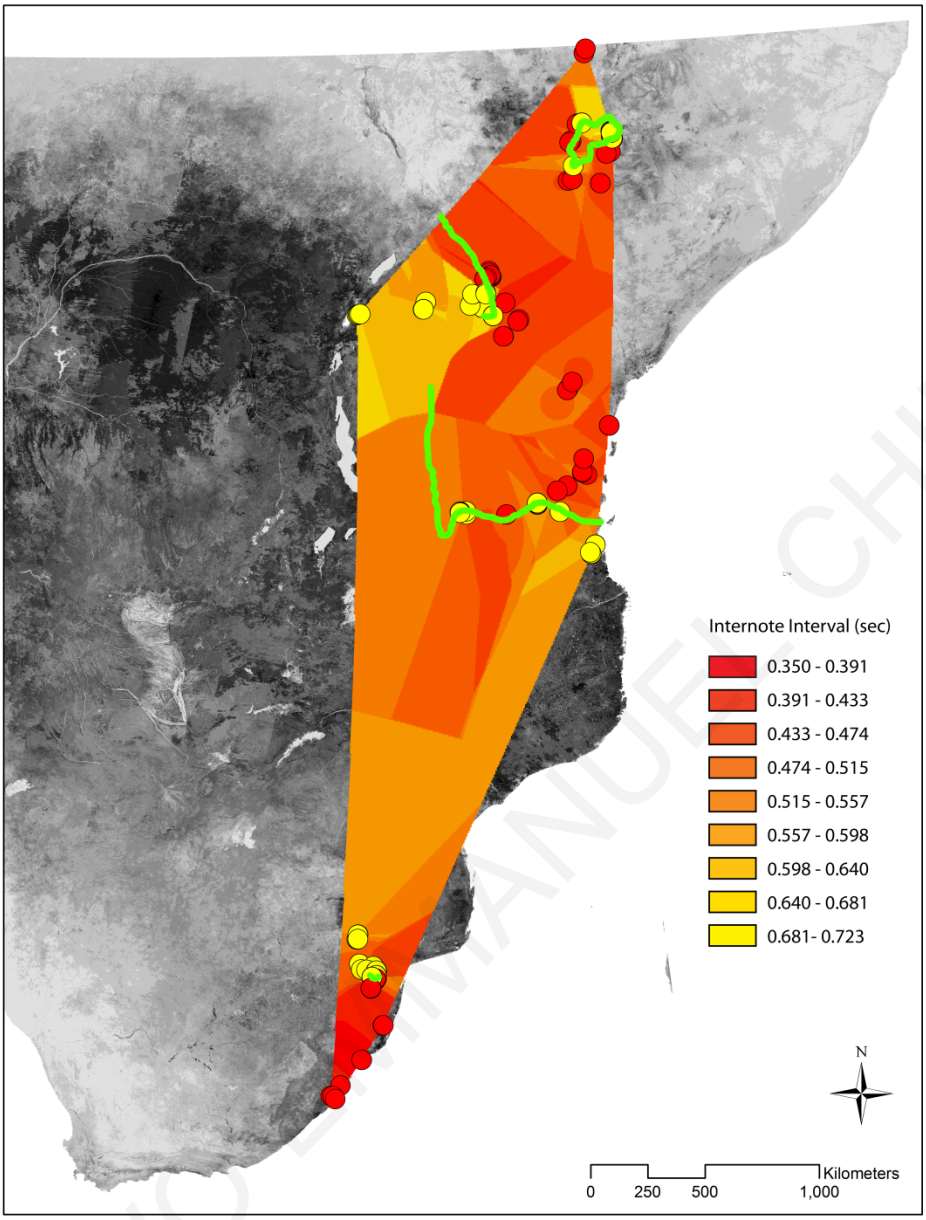

Figure 2. Inverse Distance Weighting (IDW) used to map song internote interval from previously collected recordings across each contact zone. The cline in song rate is precipitous in Ethiopia and Kenya, represented by sudden transitions from slow pace (yellow) to fast pace (red) across the contact zone. By contrast, song pace varies gradually (shades of orange) across contact zones in Tanzania and Southern Africa. Recording localities of red-fronted and yellow-fronted tinkerbird represented by red and yellow circles respectively, with approximate locations of contact zones represented by green lines.

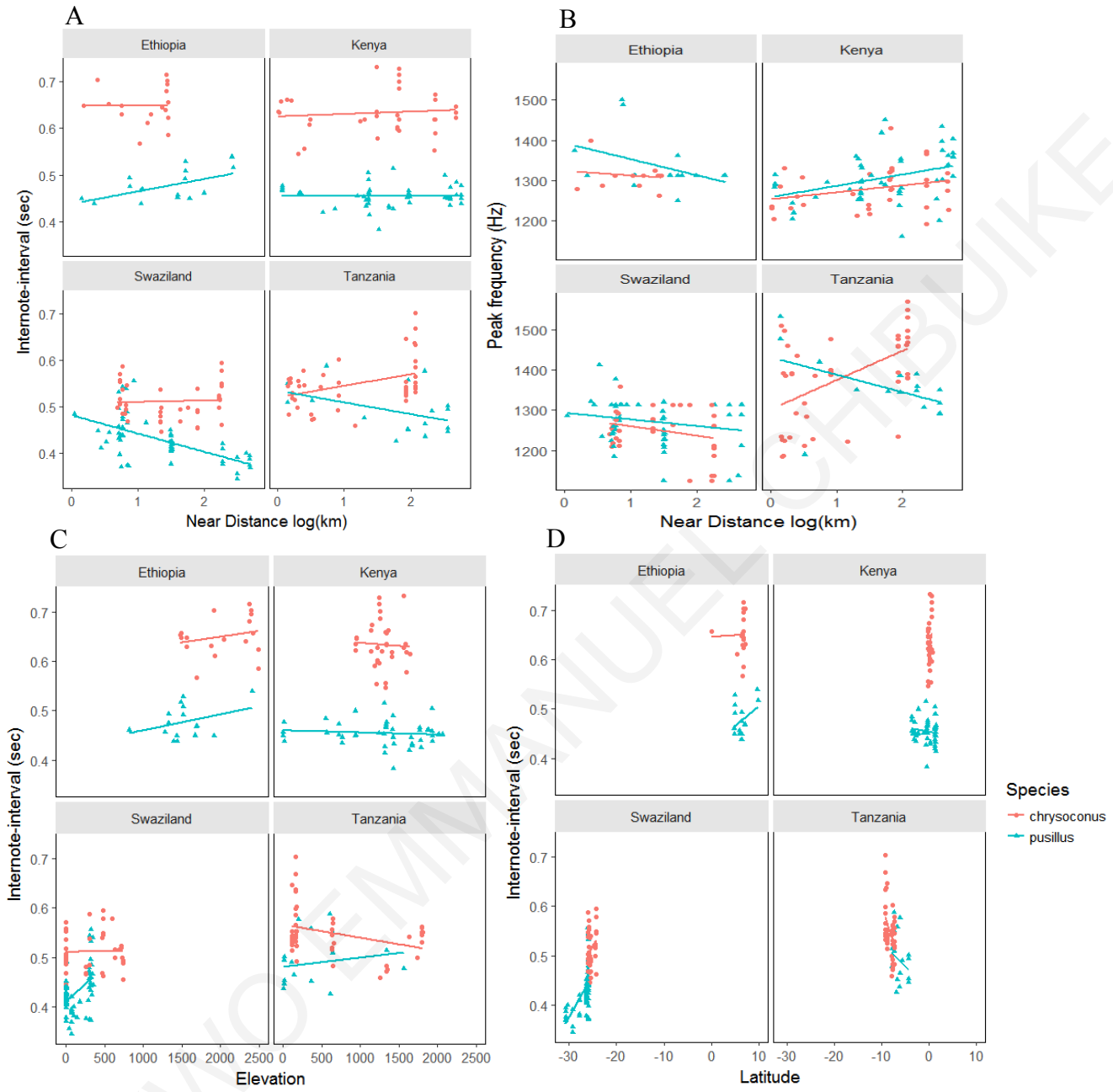

Figure 3. Variation in song traits between species across the contact zones and along ecological gradients. (A) Song trait (internote interval duration) converged towards sympatry in Southern Africa and Tanzania but diverged in Ethiopia towards the contact zone and showed no variation from allopatry to sympatry in Kenya. (B) Peak frequency showed no clear pattern from allopatry to sympatry across contact zones. (C) There is extensive overlap in EVI in relation to song inter-note interval duration in Kenya, Tanzania and Swaziland but not in Ethiopia. (D) Song pace among Southern Africa *P. p. pusillus* individuals were faster at a higher latitude than lower latitude, but the reverse is the case in Tanzania contact zone among *P. p. affinis* individuals. Song inter-note interval duration overlapped extensively between species along latitude in Ethiopia and Kenya.

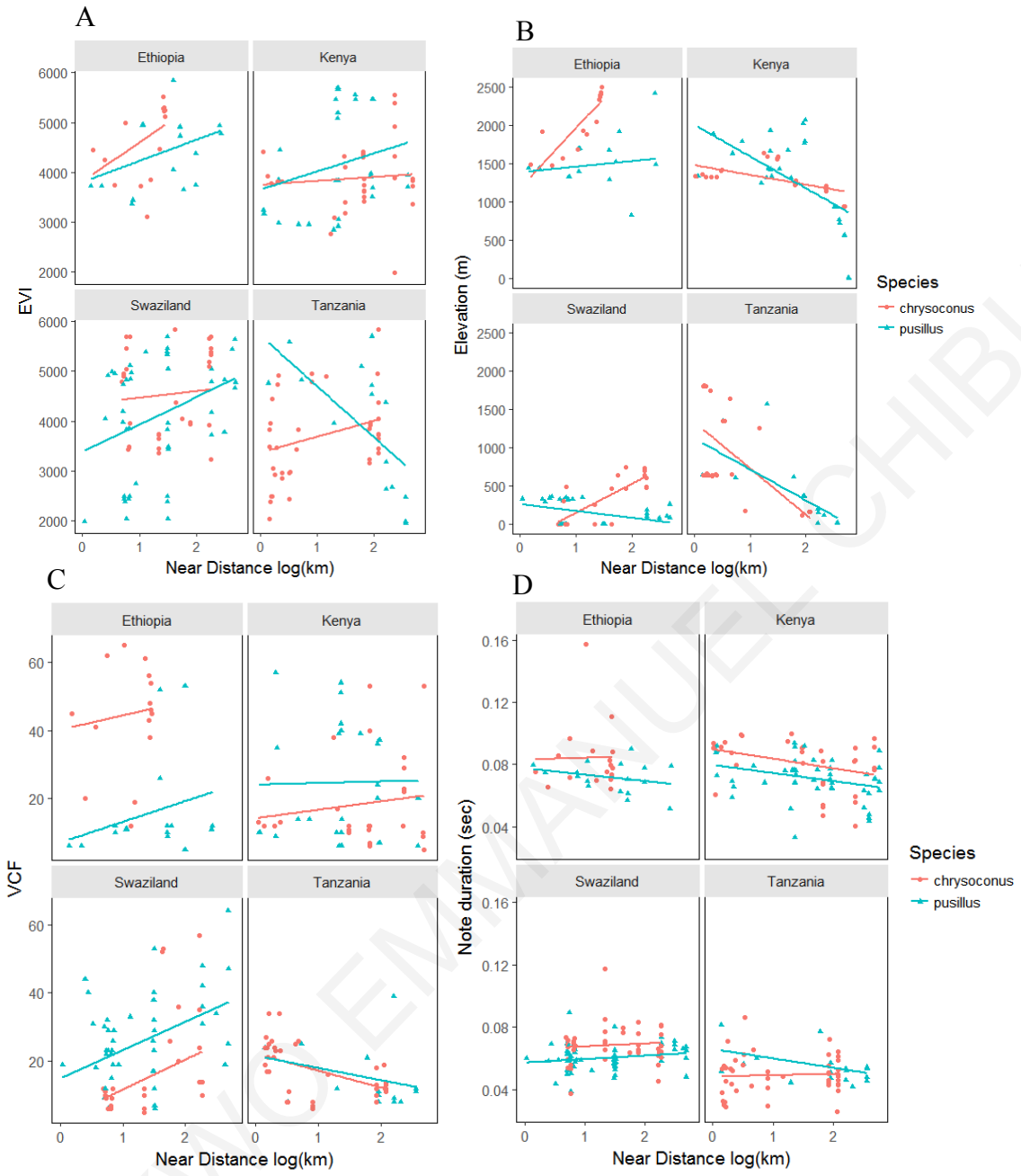

Figure 4. Ecological gradients across the contact zone were overall much steeper in Ethiopia than across the other contact zones. (A) EVI overlapped in the two species in all four contact zones irrespective of distance to contact zone. (C) VCF showed much overlap, except in Ethiopia where yellow-fronted tinkerbird had a preference for more forested habitat.

Playback experiments

Principal Component Analysis on the measured responses to conspecific and heterospecific playbacks across the contact zones showed some differential patterns (Figure 4). Overall birds responded significantly more strongly to conspecific song than to heterospecific song in Kenya

(df = 1, χ^2 = 6.052, *P* = 0.0139), but not in Tanzania (df = 1, χ^2 = 2.0674e-05, *P* = 0.9964) and Southern Africa (df = 1, χ^2 = 0.60167, *P* = 0.4379). More specifically, in terms of latency to respond to playback, focal individuals showed a tendency to respond quicker to conspecific song than to heterospecific song in Kenya (df = 1, χ^2 = 3.5494, *P* = 0.0595) but not in Southern Africa (df = 1, χ^2 = 0.9767, *P* = 0.323), nor in Tanzania (df = 1, χ^2 = 0.0863, *P* = 0.7689), while they approached significantly closer to the loudspeaker in response to conspecific song than to heterospecific song in Kenya (df = 1, χ^2 = 5.5485, *P* = 0.0185), but not in Southern Africa (df = 1, χ^2 = 0.1340, *P* = 0.7142), nor in Tanzania (df = 1, χ^2 = 0.1342, *P* = 0.7141). Furthermore, individuals spent significantly more time within 10m from the playback source in response to conspecific song than to heterospecific song in Kenya (df = 1, χ^2 = 6.2755, *P* = 0.0122), but not in Southern Africa (df = 1, χ^2 = 0.1376, *P* = 0.7107), and Tanzania (df = 1, χ^2 = 0.0013, *P* = 0.9702). Focal individuals did not differ in the time spent within 10-20m in response to conspecific song and heterospecific song in Tanzania (df = 1, χ^2 = 9.3246e-05, *P* = 0.9923), Southern Africa (df = 1, χ^2 = 0.1628, *P* = 0.6866), nor Kenya (df = 1, χ^2 = 1.2934, *P* = 0.2554).

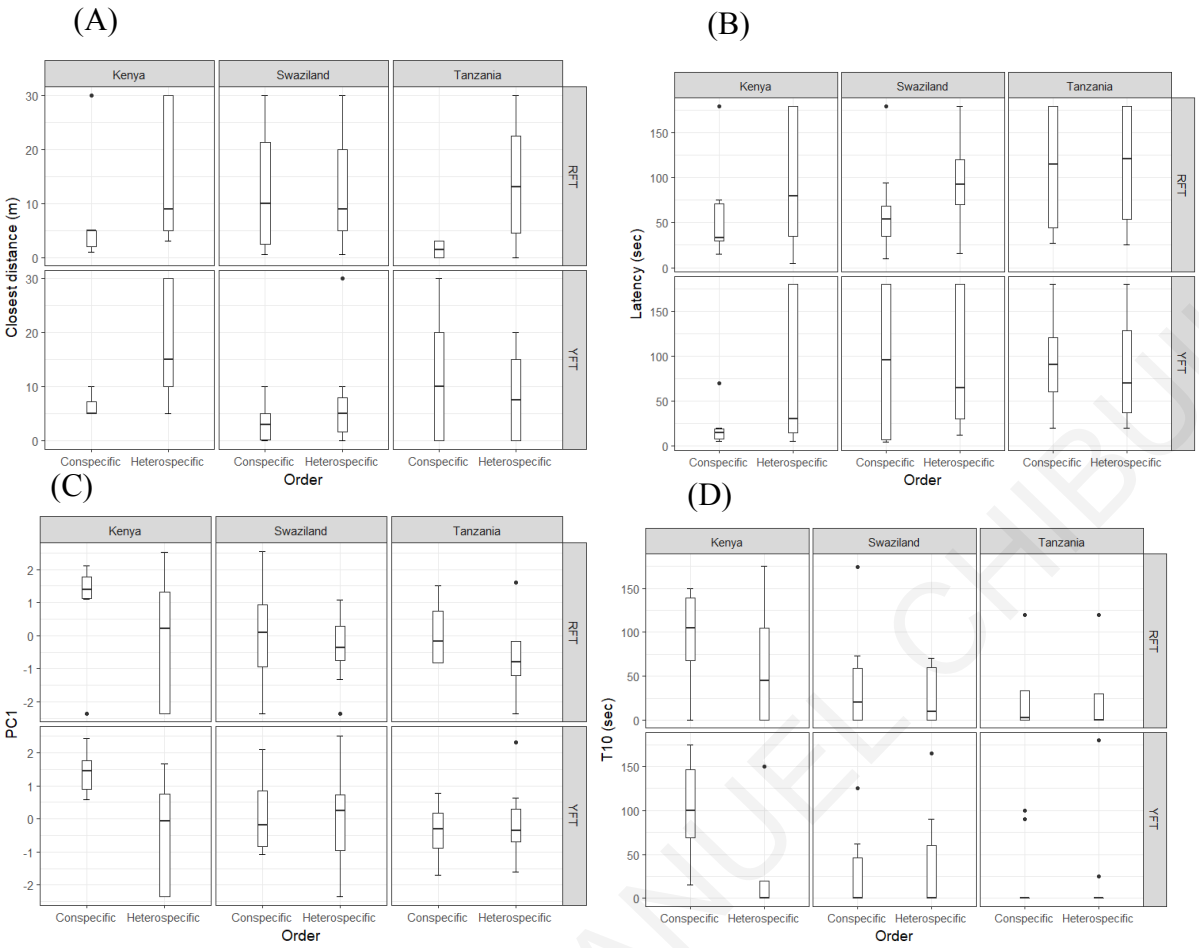

Figure 4. Differential responses to song playbacks across contact zone.

Morphology Analysis

Principal component analysis on morphometrics (tarsus, tail length, bill length, bill depth, bill width, exposed, and lower mandible) revealed significant difference in body size between *P. chrysoconus* and *P. pusillus* ($F_{1,235}$ = 89.1337, $P < 0.0001$) across each contact zones ($F_{3,236}$ = 26.8050, $P < 0.0001$, Figure 5A). We also found significant variation in body size (PC1) in relation to longitude ($F_{1,239}$ = 15.4523, $P = 0.0001$), but not with EVI ($F_{1,234}$ = 1.9737, $P = 0.1614$), latitude ($F_{1,239}$ = 2.7190, $P = 0.1005$) and distance from ($F_{1,223}$ = 3.1615, $P = 0.0768$) contact zone across contact zones. PC1 explained 59% of the varitation with body size and was positively associated with wing length, bill length, exposed, upper bill depth, bill width, and lower mandible, while PC2 (40.44% variation in body size explained) was postively associated with tarsus length, tail length, patch depth and patch width (see Table A1 in Appendix section). Based on PC1, in Ethiopia ($F_{1,95}$ = 71.874, $P < 0.0001$), Kenya ($F_{1,46}$ = 119.05, $P < 0.0001$),

and Tanzania ($F_{1,38}$ = 16.881, P = 0.0002) *chrysoconus* were significantly larger in body size relative to *pusillus* except in Southern Africa ($F_{1,55}$ = 0.7242, P = 0.3985). Based on PC2, in Ethiopia ($F_{1,95}$ = 11.207, P = 0.0011) and Tanzania ($F_{1,38}$ = 6.7262, P = 0.0134) *chrysoconus* were significantly larger in body size relative to *pusillus* except in Kenya ($F_{1,46}$ = 3.8394, P = 0.056), Southern Africa ($F_{1,55}$ = 92.289, P <0.0001).

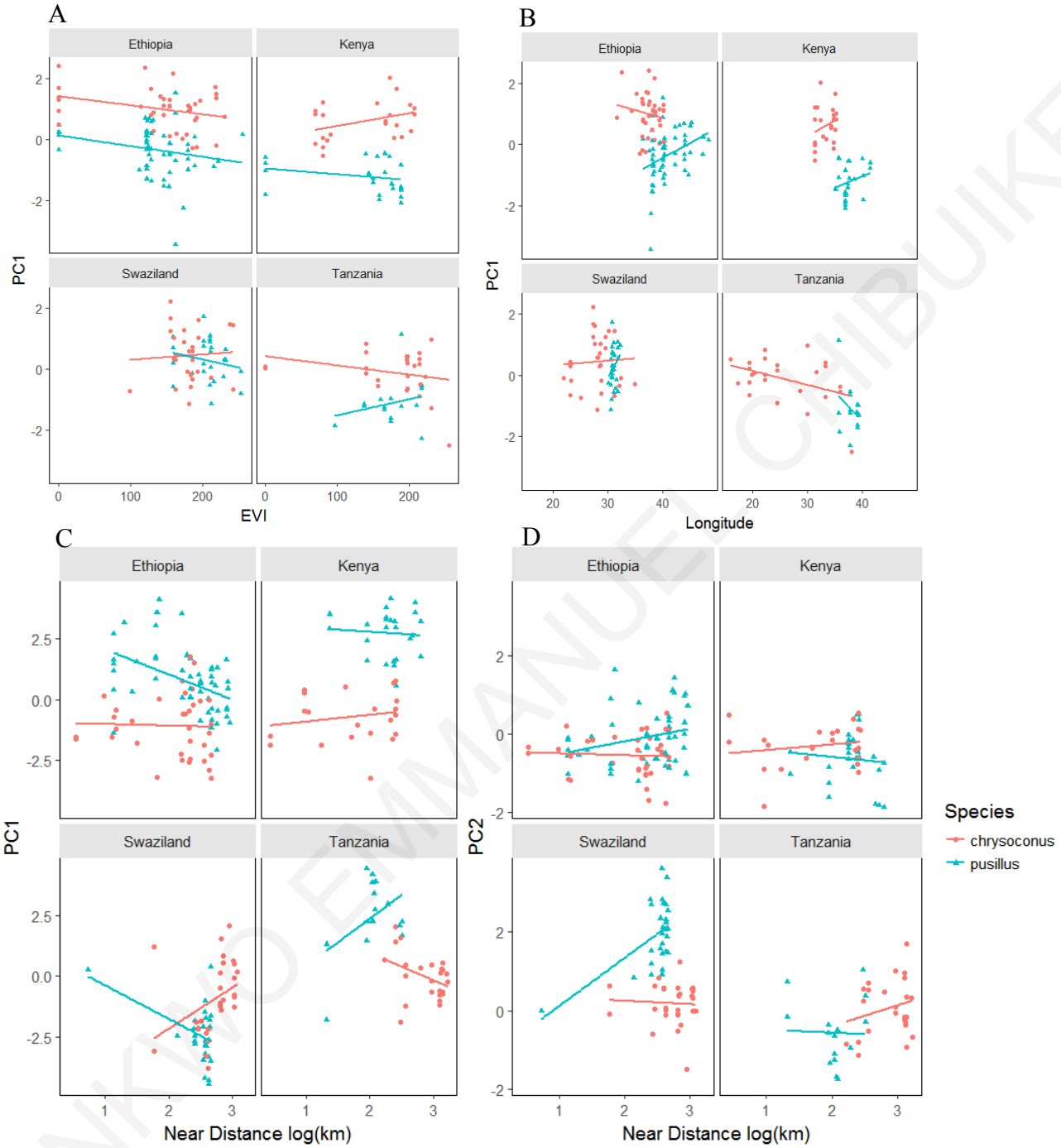

Figure 5. Variation in body size based on PC1 and PC2 along ecological gradients across four contact zones.

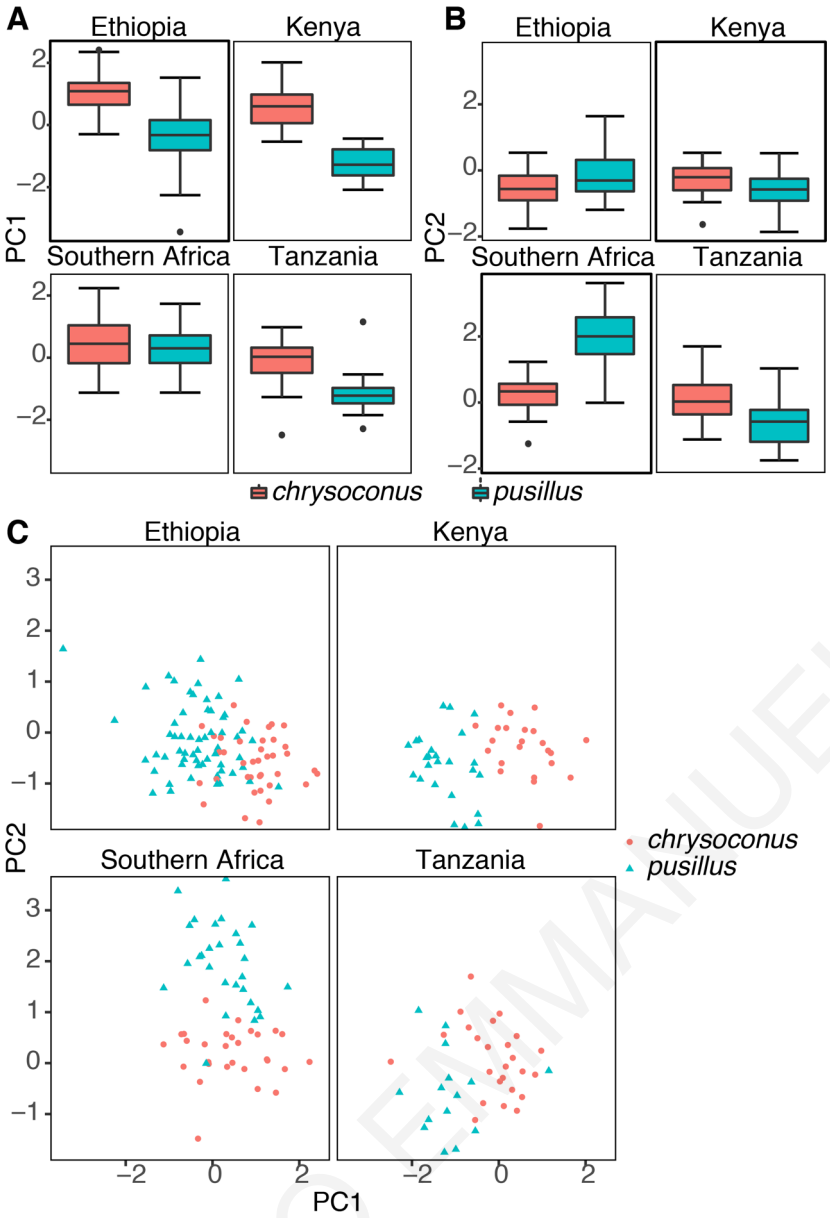

Figure 6. Variation in body size based on PC1 and PC2 between the species, across four contact zones.

Plumage

Colour distance and segment classification of forecrown colour

Overall comparison across the populations of *P. p. pusillus* and *P. c. extoni* in Southern Africa based on chromatic distances revealed that the populations are significantly different ($F_{9, 1643}$ = 48.519, R^2 = 0.2099, P = 0.0001, Figure 7). Allopatric *P. p. pusillus* was most distinct from *P. c. extoni* populations both in allopatry and sympatry based on Just Noticeable Difference levels (JND), where JND > 2, while sympatric *P. p. pusillus* were more like allopatric *P. p. pusillus*

than allopatric and sympatric *P. c. extoni*. Very low within species colour distance was found in the allopatric *P. c. extoni* population (JND < 2). Significant variation in the chromatic distance (JND > 7) was found within the allopatric *P. p. pusillus* population. Sympatric *P. c. extoni* were more like allopatric *P. c. extoni* than sympatric *P. p. pusillus* and there was higher dissimilarity based on chromatic distance (JND > 2) within sympatric *P. p. pusillus* than with the sympatric *P. c. extoni* population (Figure7A). Scoring the colour points between the short and long wavelength spectrum based on segment classification measures as defined in Endler (1990) revealed that the colour points fall within the red-orange-yellow regions of the spectrum width. A significant difference was found in the different position of the populations within the colour spectrum ($F_{3,54}$ = 17.541, R^2 = 0.49354, P = 0.0001, Figure 7B) and the variation in colour within population category (0.1610) was lower than between population category (0.2542) (Figure 7A).

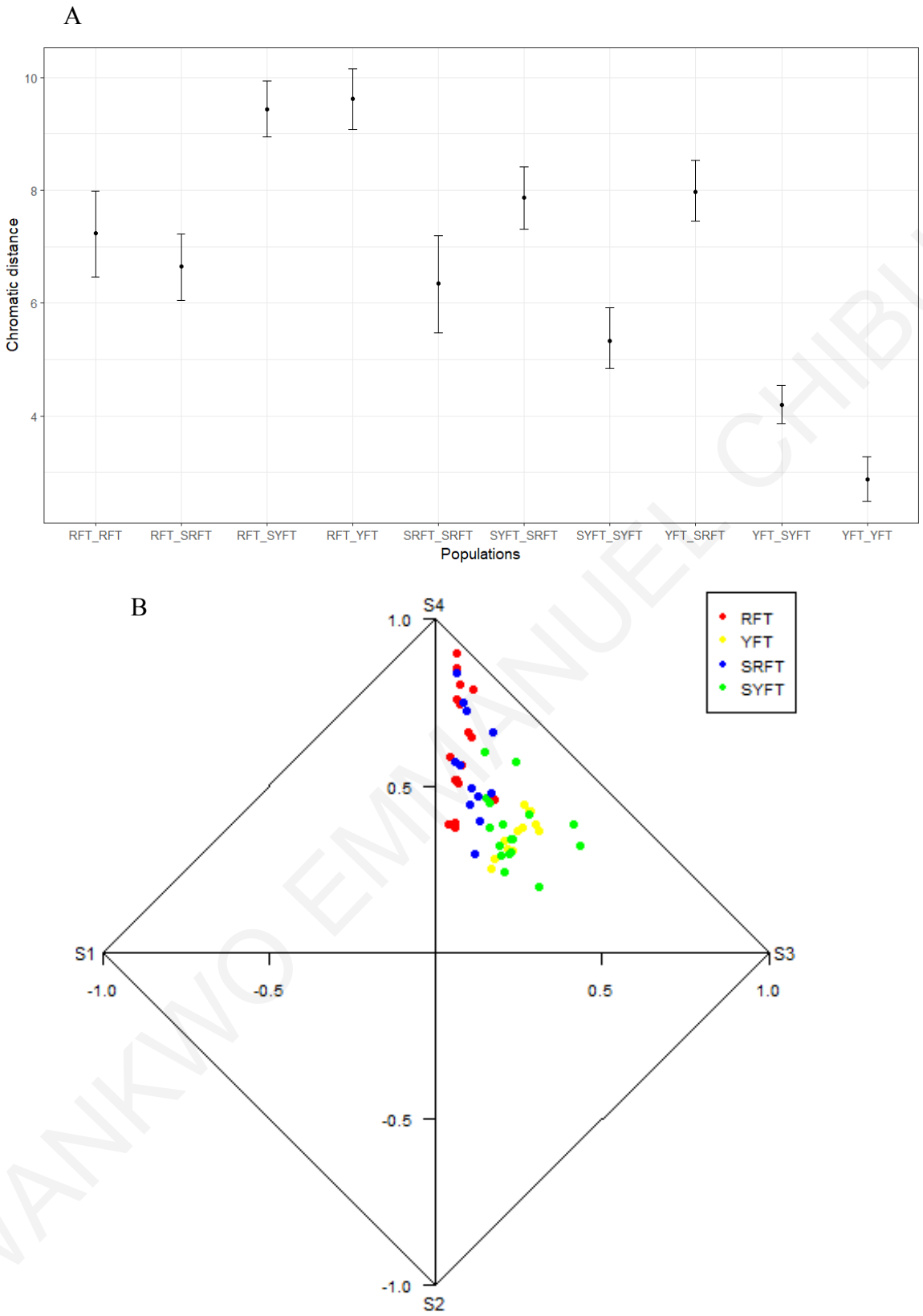

Figure 7. (A) Chromatic distance within and between the species' populations. (B) Segment classification plot for the allopatric and sympatric populations. Allopatric *P. p. pusillus* (RFT) in red, sympatric *P. p. pusillus* (SRFT) in blue, allopatric *P. c. extoni* (YFT) in yellow and sympatric *P. c. extoni* (SYFT) in green.

Hue, brightness and chroma

Visualizing differences in hue based on a plot of colour points projected from the tetrahedron to its encapsulating sphere showed that the hue of crown plumage patch is between green and red longitudes and specifically in the red-yellow region (Figure 9C, D). Analysis of variance based on Euclidean distances revealed significant differences in hue, brightness, and chroma of the crown plumage patch among the populations of the two species ($F_{3,54}$ = 13.924, R^2 = 0.44, P = 0.0001, Figure 8). Specifically, the highest hue score was found in allopatric *P. c. extoni* and sympatric *P. c. extoni*, followed by sympatric *P. p. pusillus*, and lowest in allopatric *P. p. pusillus* ($F_{3,54}$ = 52.85, R^2 = 0.7318, P < 0.0001). Chroma, on the other hand, was highest in allopatric *P. p. pusillus*, followed by sympatric *P. p. pusillus*, and lowest in allopatric *chrysoconus* ($F_{3,54}$ = 7.436, R^2 = 0.253, P = 0.0002). There were also significant differences in mean brightness of the crown patch among the populations ($F_{3,54}$ = 8.126, R^2 = 0.2728, P = 0.0001). Crown brightness was highest in allopatric and sympatric *P. c. extoni*, lower and similar in allopatric and sympatric *P. p. pusillus*.

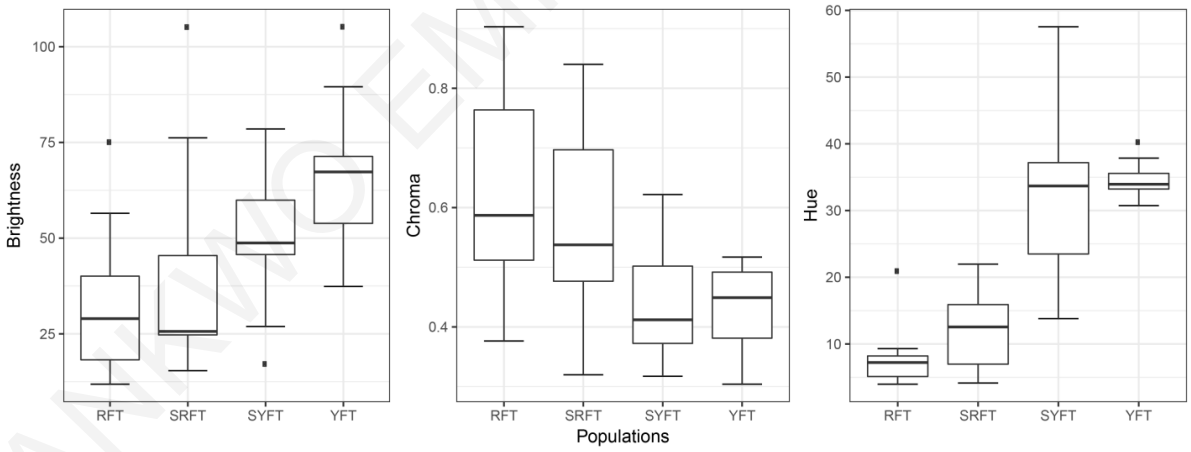

Figure 8. Boxplots illustrating forecrown brightness, chroma and hue in allopatric and sympatric populations of the two species. Allopatric *P. p. pusillus* (RFT), sympatric *P. p. pusillus* (SRFT), allopatric *P. c. extoni* (YFT) and sympatric *P. c. extoni* (SYFT).

Tetracolour plot and model

Based on the tetracolourspace variables (s, l, m) and using Multivariate Permutational Analysis of variance we found significant differences in the crown of the species across the populations ($F_{3,54} = 55.32$, $R^2 = 74$, $P < 0.0001$) (Figures 9C, 9D). Specifically, allopatric *pusillus* showed highest reflectance within the long wavelength but least in short and medium wavelengths. The reflectance of the sympatric populations for both species were similar within the short wavelength but not in the long and medium wavelengths. Allopatric *chrysoconus* showed the highest reflectance within the medium wavelength but least in the short wavelength. Canonical discriminant analysis on the tetracolourspace variables, showed that sympatric and allopatric populations of the respective species were closer to each other (Figure 9). The misclassified individuals within the error region were mainly from the sympatric population for both species (Figure 10).

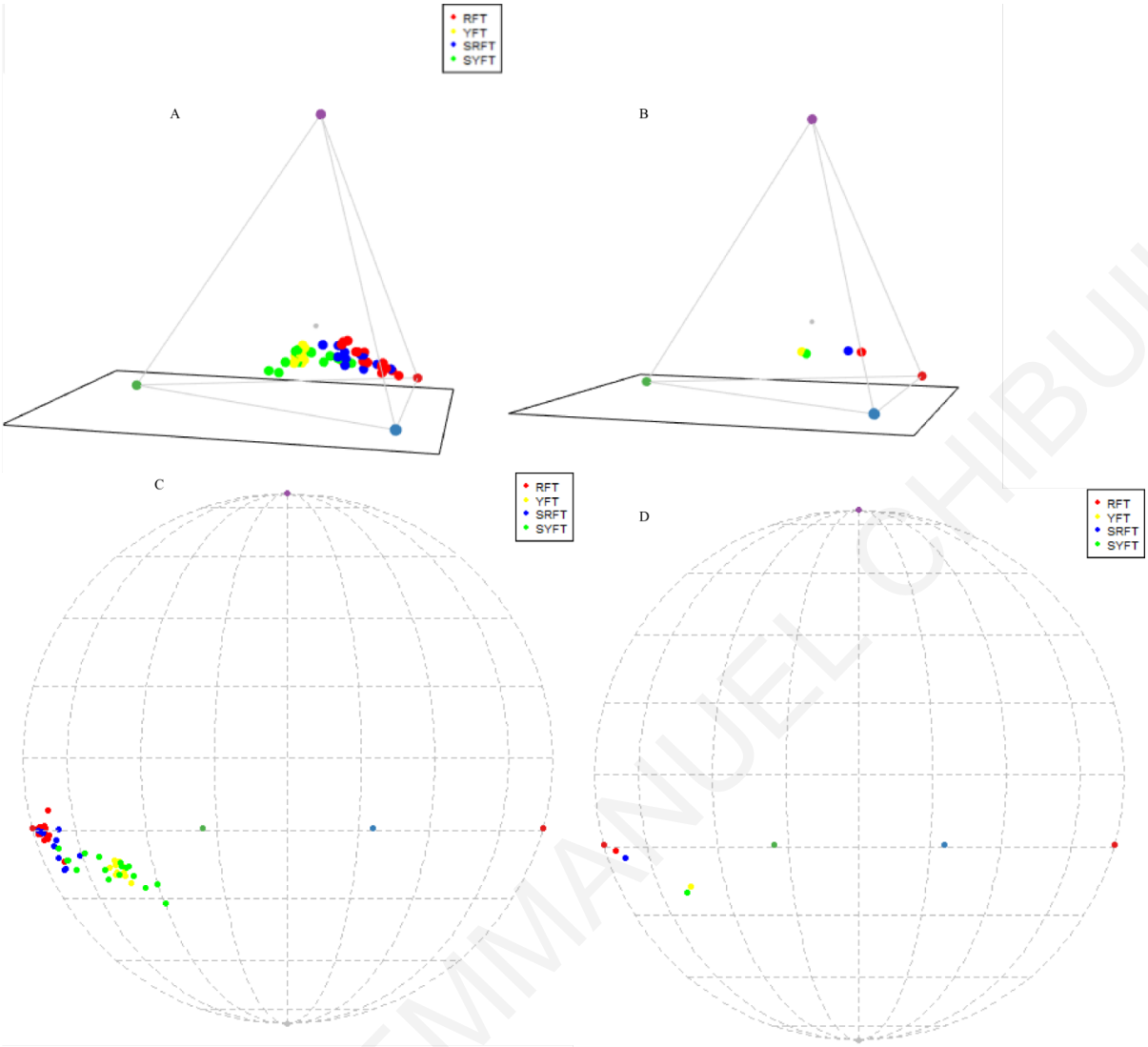

Figure 9. Tetracolourspace plot at A) individuals level and B) average for population. Hue projection plot encapsulated within a sphere at C) individuals level and D) average for population.

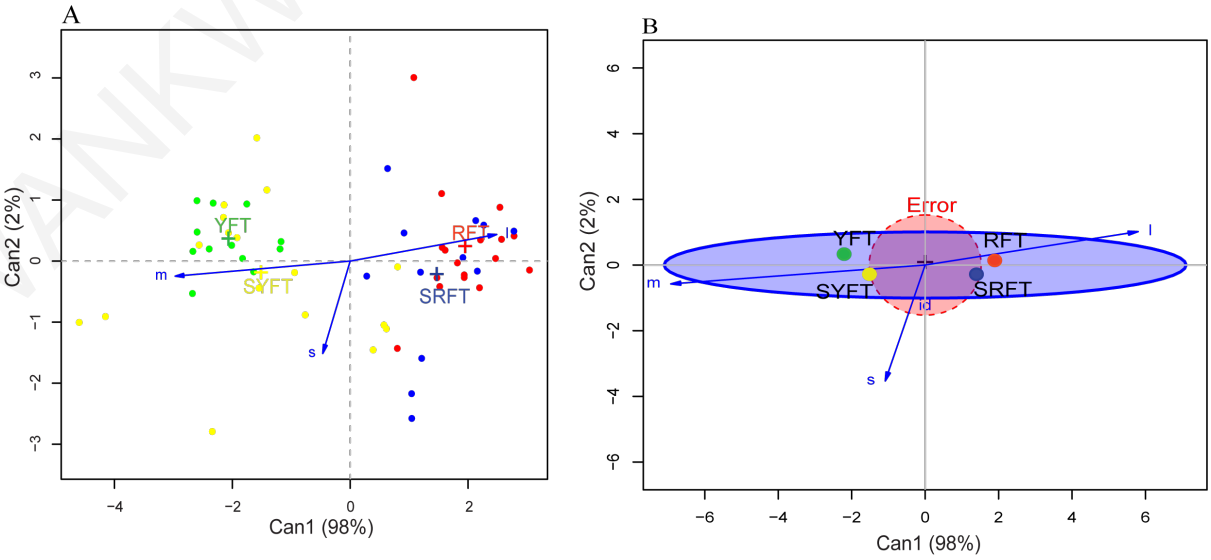

Figure 10. Canonical discriminant analysis plot based on the colour points estimated from the tetracolourspace model for the populations: allopatric *P. p. pusillus* (RFT, red dots), sympatric *P. p. pusillus* (SRFT, blue), allopatric *P. c. extoni* (YFT, green dots) and sympatric *P. c. extoni* (SYFT, yellow dots).

Colour volume overlap

Colour volume overlap analysis showed no overlap between allopatric populations of *P. c. extoni* and *P. p. pusillus*, and sympatric populations of *P. c. extoni* vs *P. p. pusillus* (Table 1). The greatest extent of colour volume overlap was between allopatric and sympatric *P. c. extoni* (86%) with less overlap between allopatric and sympatric populations of *P. p. pusillus* (47%).

Table 1. Colour volume overlap between the sympatric and allopatric populations of the species

Population1	Population2	Volume1	Volume2	Overlap	Vsmallest	Vboth
RFT	YFT	0.00036	0.000038	0	0	0
RFT	SRFT	0.00036	0.00037	0.00017	0.47	0.30
RFT	SYFT	0.00036	0.00091	0	0	0
SRFT	SYFT	0.00037	0.00091	0	0	0
YFT	SYFT	0.000038	0.00091	0.000033	0.86	0.036
YFT	SRFT	0.000038	0.00037	0	0	0

Molecular Analysis

We recovered 127,000 SNP markers for 174 individuals across 3 contact zones (Southern Africa, Kenya and Tanzania) using Stacks 1.3 (Catchen et al, 2013). The three contact zones where samples were collected include Southern Africa (77 samples), Kenya (40) and Tanzania (57). Based on the Evanno method in STRUCTURE Harvester v0.6.1 (Earl & VonHoldt, 2012) K = 4 value was the best for the population structure analysis. STRUCTURE analysis (Figure 11) and principal components analysis, four main groups were recovered with extensive hybridization evident at the Southern Africa contact zone between *P. c. extoni* and *P. p. pusillus* (Figure 14D), consistent with findings using microsatellite markers (Chapter 3). Potential F1 hybrid individuals identified based on the PCA and Q value of 0.5-0.6 from STUCTURE

analysis within the Swaziland contact zone include K69365, AR93118, AR93112, AR93159, AR93157, AR93122, AR93168 and AR93115 (Figure 11)

Principal component and kinship analyses based on the filtered 29,675 set of SNP markers (see methods section) showed the overall clustering of genetic variation in 174 individuals. Principal component analysis recovered three main groups with high level of hybridisation in Swaziland and less hybridisation in Tanzania contact zone. Intermediate individuals were found mostly in the Southern Africa contact zone and Tanzania but not in Kenya contact zone. PC1 explained 6.3 percent variation among the subspecies and separated *P. chrysoconus extoni* (blue circles) and *P. p. affinis* (blue triangles) from Tanzania contact zone. PC2 explained 5.4 percent genetic variation among the subspecies and separated *P. chrysoconus chrysoconus* (red circles) and *P. p. affinis* (red triangles) from the Kenya contact zone. *P. c. extoni* (green circles) and *P. p. pusillus* (green triangles) from Southern Africa showed close relationship to each other. *P. c extoni* from Tanzania and Southern Africa both grouped with each other. *P. p. affinis* from Tanzania and Kenya contact zones also grouped together.

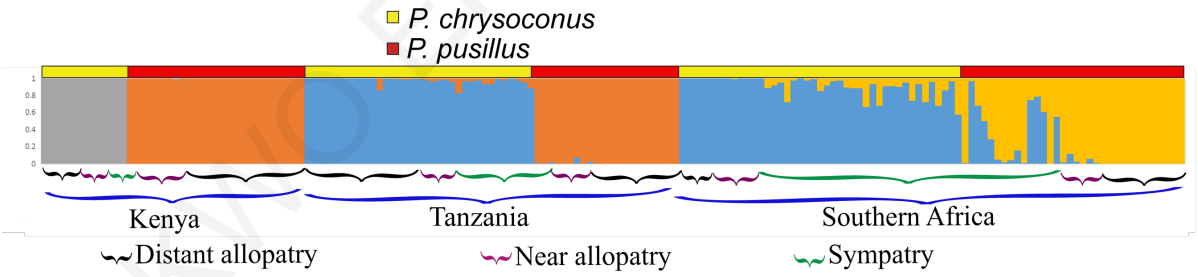

Figure 11. Structure plot illustrating the extent of introgressive hybridisation based on ddRadseq data. Different genetic groups for the subspecies are represented *extoni* (blue), *affinis* (orange), *chrysoconus* (grey) and *pusillus* (yellow).

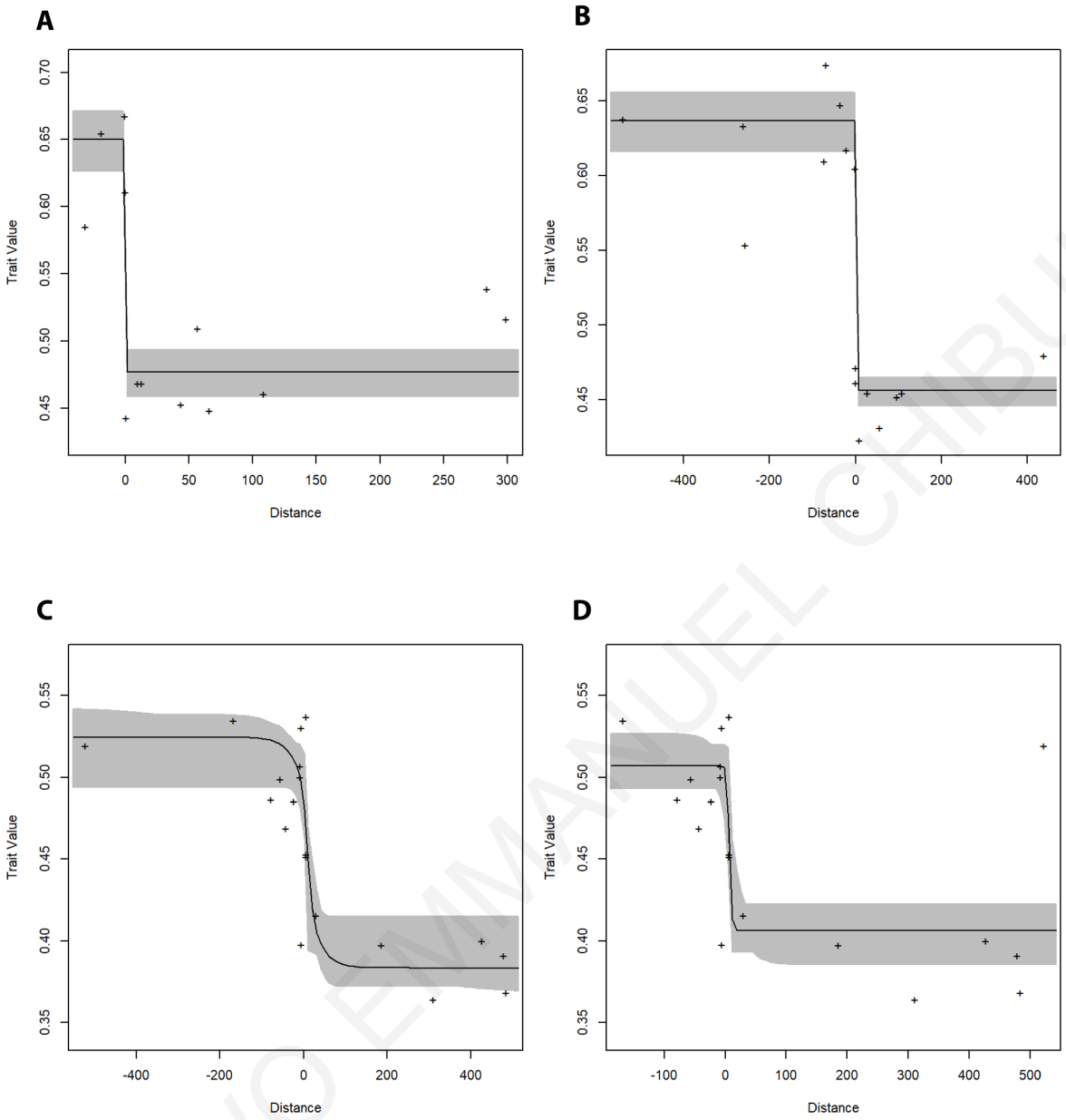

Figure 12. Cline analysis showing differences in the song trait introgression between the species across the different contact zones: Ethiopia (A), Kenya (B), Southern Africa (C) and Tanzania (D). *P. chrysoconus* distribution along the transect shown as negative distances and *P. pusillus* as positive distances.

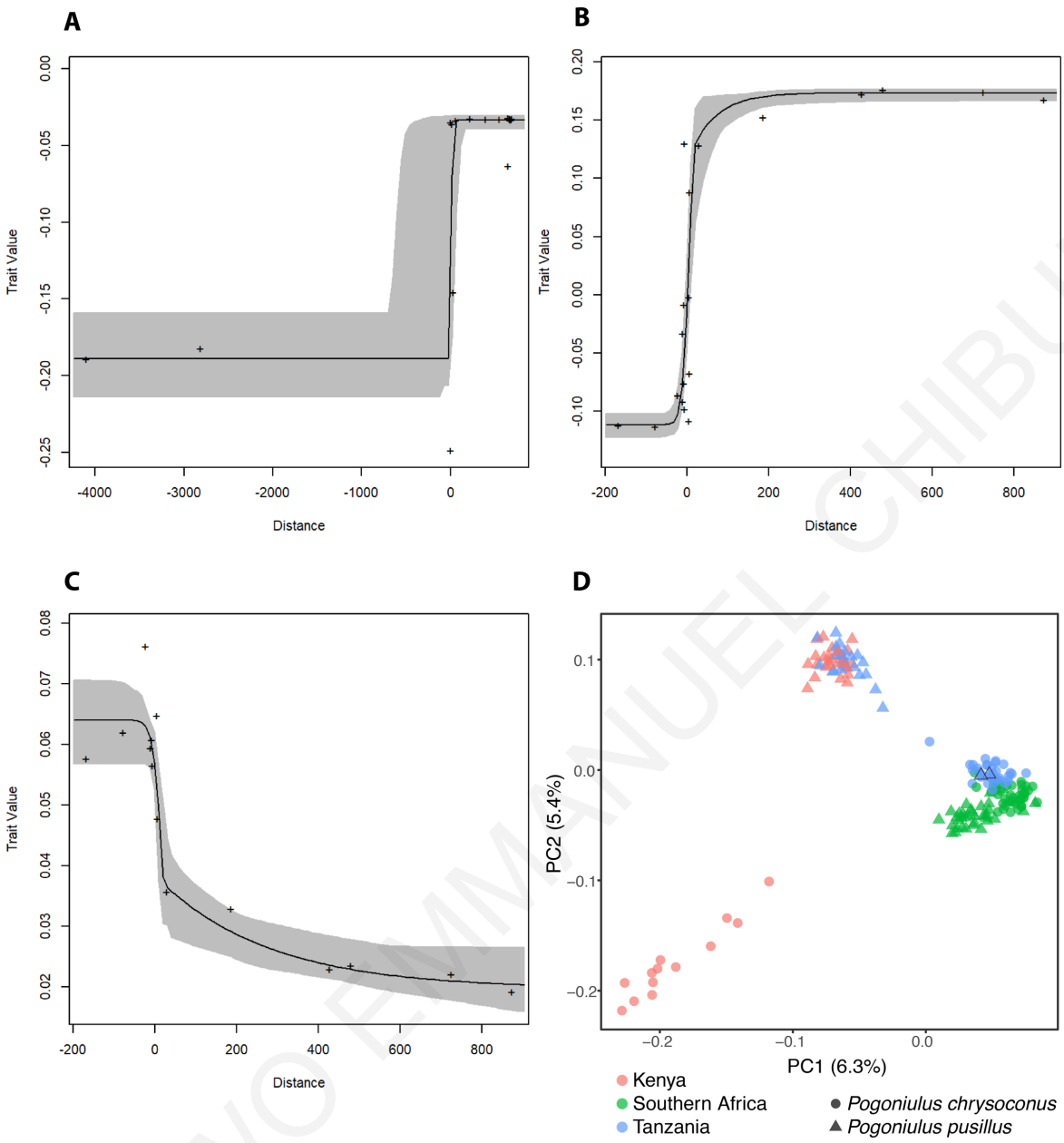

Figure 13. Genetic cline analyses show differences in genetic traits between the species across the different contact zones: Kenya (A), Southern Africa (B) and Tanzania (C). *P. chrysoconus* distribution along the transect shown as negative distances and *P. pusillus* as positive distances. (D) Principal component analysis recovered three main groups with high level of hybridisation in Swaziland and less hybridisation in Tanzania contact zone. Intermediate individuals were found in the Southern Africa contact zone, in Tanzania and Kenya contact zones. PC1 explained 6.3 percent variation among the subspecies and separated *P. chrysoconus extoni* (blue circles) and *P. p. affinis* (blue triangles) from Tanzania contact zone. PC2 explained 5.4 percent genetic variation among the subspecies and separated *P. chrysoconus chrysoconus* (red circles) and *P. p. affinis* (red triangles) from the Kenya contact zone. *P. c. extoni* (green circles) and *P. p. pusillus* (green triangles) from Southern Africa showed close relationship to each other. *P. c extoni* from Tanzania and Southern Africa both grouped with each other. *P. p. affinis* from Tanzania and Kenya contact zones also grouped together.

Identity by State and Pairwise Genetic Differentiation Analysis

A measure of genetic similarity based on Identity by State analysis in SNPRelate, which estimates the percentage of alleles across all loci that are shared among individuals was visualized in a heatmap (Figure 14). This revealed that *P. c. chrysoconus* from Kenya shared 98% of their alleles with *P. c. chrysoconus* from West Africa (Nigeria and Ghana) and *P. c. extoni* Southern Africa contact zone, and approximately 65% with *P. c. extoni* in Tanzania. *P. p. affinis* from Kenya share fewer alleles among their own population (63%) than they do with *P. p. pusillus* from Southern Africa and *P. p. affinis* from Tanzania (88%). *P. p. affinis* and *P. c. chrysoconus* within Kenya contact zone are 65% identical based on the number of alleles they have in common. *P. c. extoni* individuals within Southern Africa contact zone population were 68-82% similar to each other. A few *P. p. pusillus* individuals within Southern Africa contact zone shared up to 96% alleles with each other and with *P. p. affinis* individuals from Tanzania and Kenya contact zones.

A permutational clustering of the individuals based on their identity by state z scores using a clustering threshold of 15 and outlier threshold of 5 recovered 6 main groups (Figure 15). West Africa and Kenya *P. c. chrysoconus* populations were basal in the dendrogram while Tanzania and Southern Africa *P. c. extoni* were nested within *P. pusillus*. *P. chrysoconus* individuals from Malawi grouped with *P. c. chrysoconus* individuals from Tanzania but both were nested within *P. c. extoni* from Southern Africa. One *P. p. affinis* (J31351) from Tanzania grouped with Southern Africa *P. c. extoni* while 8 *P. p. pusillus* from Southern Africa grouped with *P. chrysoconus*. The 8

P. p. pusillus from Southern Africa that grouped with *P. c. extoni* were all from the hybrid zone and were recovered in the PCA as intermediate individuals (Figure 13D).

A pairwise differentiation index for each region based on distance from the contact zone revealed dramatic differences among contact zones (Table 2) Specifically, while distances between the two species were high both among allopatric and sympatric populations in Kenya, in Tanzania and Southern Africa the pairwise difference between the species decreased markedly from distant allopatry to sympatry. Indeed, in Tanzania, pairwise differences between *P. p. affinis* in sympatry and all *P. c. extoni* populations were lower than among nearby populations of *P. p. affinis* in sympatry and allopatry.

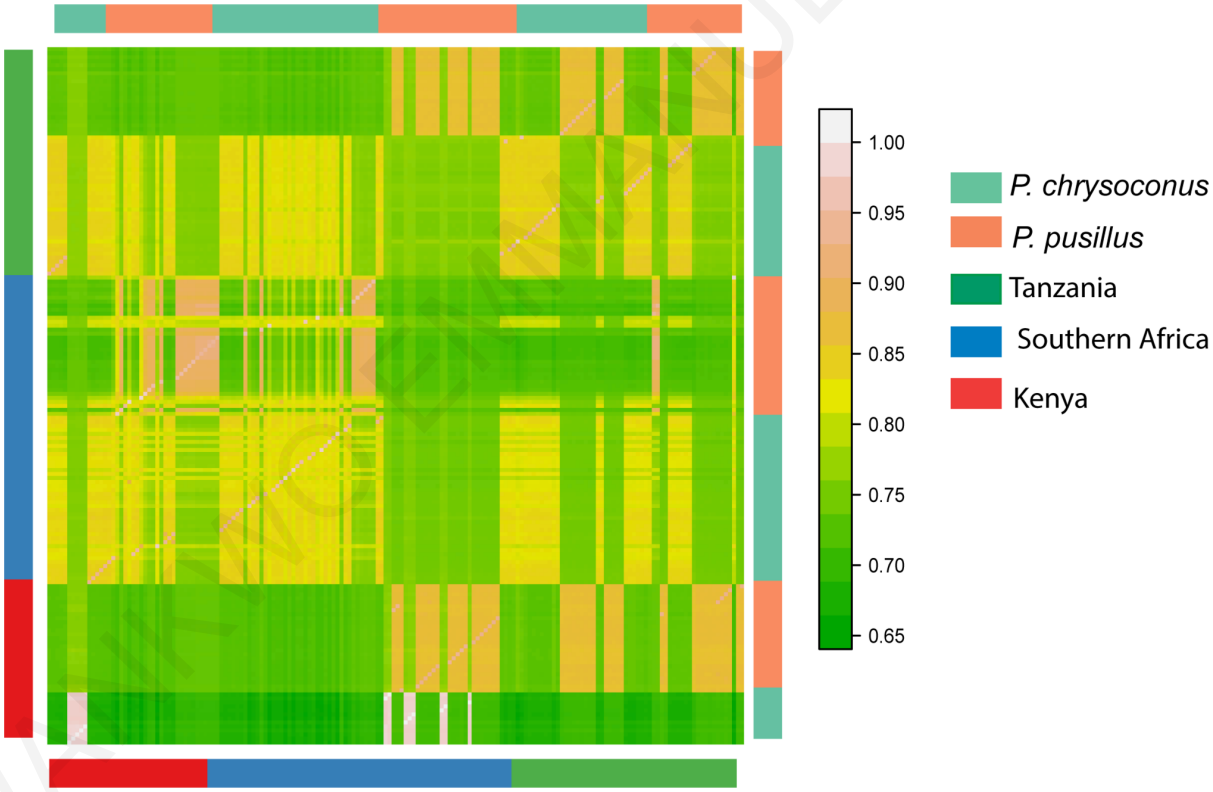

Figure 14. Heatmap of the kinship matrix with genetic relatedness among the individuals across the contact zones calculated from 29,675 SNPs.

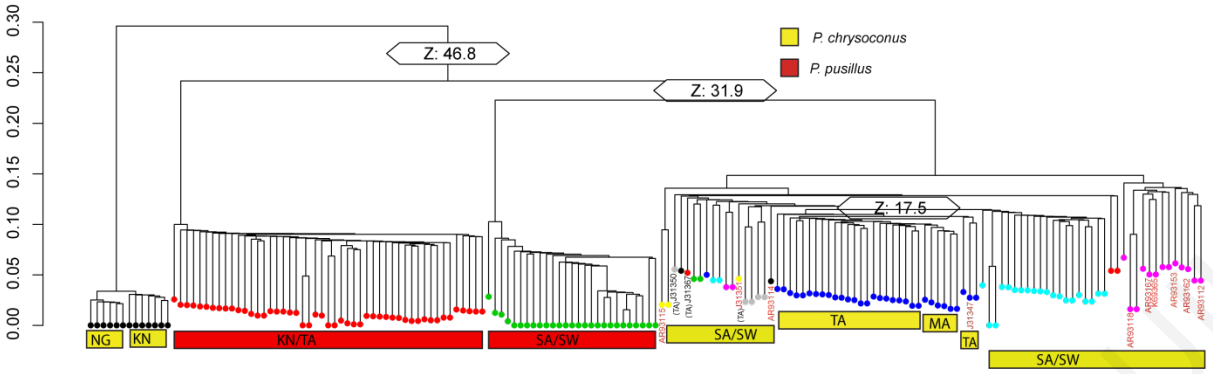

Figure 15. A dendrogram of the relatedness of individuals based on permutational clustering with Z threshold = 15 and outlier threshold = 5 on Identity by State (IBS) coefficients. NG = Nigeria, KN = Kenya, TA = Tanzania, SA = South Africa, SW = Swaziland, MA = Malawi. Red rectangles indicate *P. pusillus* phenotypes while yellow rectangles indicate *P. chrysoconus* phenotypes based on forecrown plumage coloration. Individuals labelled with red circles within the *chrysoconus* clade were phenotypically *pusillus* as identified based on forecrown plumage colouration in the field. Individuals labelled in black were phenotypically yellow on their forecrown. There is greater structure within the *chrysoconus* clade from Southern Africa with individuals labelled cyan and pink. Individuals labelled (with ring numbers given in red) are presumed F1 hybrids clustering with *chrysoconus* but phenotypically have red forecrowns.

GWAS Analysis

Genomewide analysis with the plumage data for binary classification of the crown plumage, chroma and hue reflectance data showed significant association with 15 SNPs (Table 3). One SNP (ID 4257) with an association *P*-value of 8.04E-45 was significantly associated with both the binary classification of the crown plumage patch and hue reflectance data. The alleles recovered for the SNP ID 4257 were C and T, which were CC homozygous for *P. c. extoni* allopatric individuals and TT homozygous for *P. p. pusillus* allopatric individuals without any form of heterozygosity in the individual of both species from the distant allopatric populations. We found more heterozygous individuals towards sympatry, with one individual of *P. p. pusillus* in near allopatry a CT heterozygote and approximately equal numbers of heterozygous individuals of both species in sympatry (nine of each). No *P. c. extoni* was found among our samples that had TT genotype and no *P. p. pusillus* was found with CC genotype in Southern Africa. The quantile-quantile (QQ) plot showed greater deviation from the observed *P*-values for visual binary crown plumage classification relative to hue and chroma (Figure 16d-f).

Substantial deviation of the observed and expected *P*-values for a few SNPs in the QQ plot supports the fit of the GWAS model to the data analysed. PC1 used as a covariate in the GWAS accounted for 99%, 95% and 49% variation of the binary phenotype classification, hue and chroma respectively (Table 6), which was higher than the variation explained by the remaining PCs (PC2 and PC3).

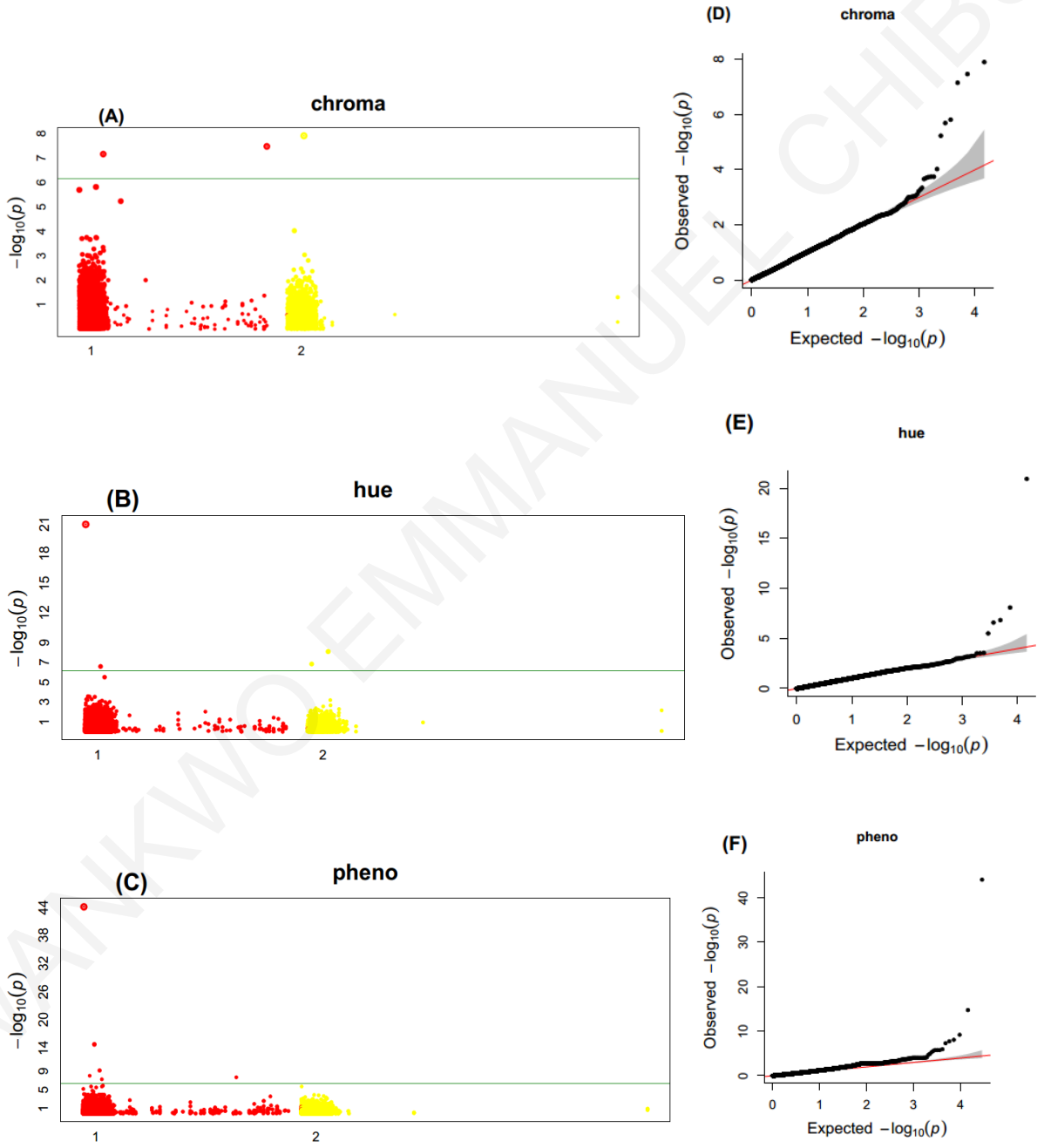

Figure 16. Manhattan plots (A, B, C) showing the significance of association [log10(p)] between each single nucleotide polymorphism (SNP) and plumage phenotypes and QQ plots

(D, E, F) plots based on the GWAS model. SNPs above the threshold horizontal line are significant as indicated in Table 3. The horizontal axis values are arbitrary values assigned by Stacks.

Table 2. Pairwise differentiation index (G'_{ST}) between populations towards the contact zone for each region. P. c. DA = *P. chrysoconus* Distant Allopatry, P. c NA = *P. chrysoconus* Near Allopatry and P. c. SY = *P. chrysoconus* Sympatry populations; P. p. DA = *P. pusillus* Distant Allopatry, P. p NA = *P. pusillus* Near Allopatry and P. p. SY = *P. pusillus* Sympatry populations. Pairwise differences between the two species differ dramatically across contact zones.

Southern Africa Contact zone					
	P. c. DA	**P. c. NA**	**P. c. SY**	**P. p. SY**	**P. p. DA**
P. c. NA	0.0275				
P. c. SY	0.0393	0.025			
P. p. SY	0.3683	0.3554	0.2453		
P. p. DA	0.7196	0.7017	0.606	0.2157	
P. p. NA	0.6266	0.6096	0.5027	0.0943	0.1006
Tanzania Contact zone					
	P. c. DA	**P. c. NA**	**P. c. SY**	**P. p. SY**	**P. p. DA**
P. c. NA	0.0253				
P. c. SY	0.0082	0.0214			
P. p. SY	0.1285	0.1036	0.1029		
P. p. DA	0.5777	0.574	0.5515	0.2928	
P. p. NA	0.5552	0.549	0.5276	0.2637	0.0156
Kenya Contact zone					
	P. c. DA	**P. c. NA**	**P. c. SY**	**P. p. SY**	**P. p. DA**
P. c. NA	0.2064				
P. c. SY	0.2052	0.0466			
P. p. SY	0.8648	0.8546	0.8556		
P. p. DA	0.8319	0.8233	0.8254	0.0985	
P. p. NA	0.8165	0.8068	0.8094	0.0611	0.0241

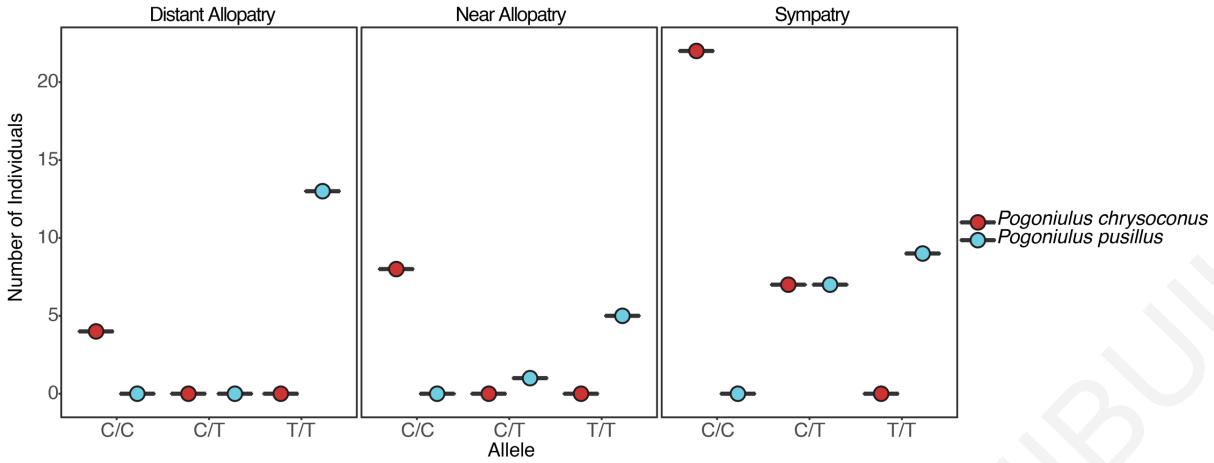

Figure 17. Distribution of alleles significantly associated with the phenotypes across for SNP 4257 identified both with binary phenotype and hue reflectance data for only individuals within the Southern Africa contact zone.

Plumage association candidate genes

Using the Radtags of the SNPs significantly associated with the plumage colouration of the forecrown *P. c. extoni and P. p. pusillus* 31 candidate protein coding genes were identified based on a search for genetic similarity on the genomic background of *Picoides pubescens*, *Serinus canaria*, *Taeniopygia guttata* and *Gallus gallus* (Table 4).

Of the 31 candidate genes, three were specifically implicated in eye pigmentation (HPS4), visual learning (NDRG4) and detection of light stimulus involved in visual perception (CACNA2D4). Nine genes are known to be involved in body morphological development (MyO18B, SSH1, CORO1C, IL11RA, NDRGA, WWOX, MAP2K5, GAP43, NRARP), while IL11RA gene was specifically implicated in head development. Four genes (SEZ6L, CORO1C, LRTM2, MAP2K5) that were associated with forecrown plumage coloration are known to be involved in protein kinase activities; WWOX and NRARP are known to be involved in RNA polymerase II transcription. Two genes (CACNA2D4 and GRM3) were known to be actively involved in regulation of calcium channel activity while five genes (CACNA2D4, ASPHD2, SLC25A48, EXD3, LOC100231635) involved in transmembrane transport were also detected

to be associated with our plumage coloration reflectance data. Specific ontology of the detected genes based on their annotation from UNIPROKT (see method section) are shown in Table 5.

Table 3. SNPs significantly associated with binary phenotype classification based on appearance in the field and plumage reflectance data (hue and chroma) from the crown plumage patch. The highlighted SNP (ID: 4257) was significantly associated with both binary phenotype and hue and was the only SNP detected both in GAPIT and FarmCPU.

Traits	SNP ID	Chromosome	Position	P.value	effect	Ref Allele	Alt Allele
Binary pheno	3673	1	2071900	8.14E-09	0.2239	C	T
Binary pheno	**4257**	1	235289	8.04E-45	-0.4881	C	T
Binary pheno	9686	1	3523057	1.67E-15	0.2960	A	C
Binary pheno	16684	1	5161234	6.05E-10	-0.2773	C	G
Binary pheno	19312	1	5870468	4.70E-08	-0.1514	G	A
Binary pheno	20445	1	6208163	1.09E-06	0.0942	G	A
Binary pheno	24352	1	47938218	1.77E-08	-0.4200	G	A
Chroma	17979	1	5514938	1.54E-06	-379.4855	G	A
Chroma	23362	1	7896563	6.98E-08	310.8804	C	T
Chroma	24415	1	61547750	3.38E-08	417.8380	A	G
Chroma	26011	2	5522872	1.24E-08	420.8810	C	A
Hue	**4257**	1	235289	1.09E-21	0.2569	C	T
Hue	15130	1	4778671	2.51E-07	-0.0536	G	A
Hue	26435	2	6298169	7.86E-09	-0.0871	G	A
Hue	28163	2	1243458	1.42E-07	0.0521	G	A

Table 4. Candidate genes associated with forecrown plumage coloration based on nucleotide similarity BLAST on the genomic background of *Picoides pubescens*, *Serinus canaria*, *Taeniopygia guttata* and *Gallus gallus.*

Trait	SNP ID	Position	Ref Allele	Alt Allele	Gene name	Relative position	Protein name	Organism	Location	Chromosome	E value	Identity (%)	Accession number
Binary pheno	3673	255,676-255,708	C	T	UACA	overlap	Uveal autoantigen with coiled-coil domains and ankyrin repeats	*Picoides pubescens*	38,238-64,035	Unplaced Scaffold	8E-05	94%	NW_009664774.1
					TLE3	left flank	transducin like enhancer of split 3		264,633-302,829	Unplaced Scaffold			NW_009664774.1
Binary pheno	4257	71,175,140 - 71,175,173	C	T	CACNA2D4	right flank	voltage-dependent calcium channel subunit alpha-2/delta-4	*Taeniopygia guttata*	71,116,200-71,243,775	A1	0.012	91	NC_0011463.1
					LRTM2	right flank	leucine-rich repeat and transmembrane domain-containing protein 2		71,197,416-71,217,044	A1	0.012	91	NC_0011463.1
Binary pheno	9686	47,768-47,850	A	C	LOC104298771	overlap	hydrocephalus-inducing protein homolog	*Picoides pubescens*	9,272-58,952	Unplaced scaffold	1E-15	84	NW_009663190.1
Binary pheno	16684	8,069,226-8,069,324	C	G	GRM3	overlap	glutamate metabotropic receptor 3	*Picoides pubescens*	8,024,914-8,073,639	Unplaced scaffold	1E-33	92	NW_009663614.1
		38,163,822-38,163,911			GRM3	overlap	glutamate metabotropic receptor 3	*Serinus canaria*	38100065-38202660	Unplaced scaffold	1E-10	78	NW_007931128.1
Binary pheno	19312	76,096-76,196	G	A	LOC104299908	left flank	dual specificity testis-specific protein kinase 2-like	*Picoides pubescens*	53,077-67,600	Unplaced scaffold	9E-24	85	NW_009663529.1

		2,952,196-2,952,223			POU6F2	overlap	POU class 6 homeobox 2	*Picoides pubescens*	2,914,494-3,172,713	Unplaced scaffold	0.041	93	NW_009664987.1
Binary pheno	20445	7,152,946-7,153,046	G	A	SEZ6L	right flank	seizure related 6 homolog like	*Gallus gallus*	7,156,283-7,183,241	15	6E-07	74	NC_006102.4
					ASPHD2	right flank	aspartate beta-hydroxylase domain containing 2	*Gallus gallus*	7,185,460-7,191,933	15			NC_006102.4
					HPS4	right flank	biogenesis of lysosomal organelles complex 3 subunit 2	*Gallus gallus*	7193051-7204799	15			NC_006102.4
Binary pheno	24352	7,152,950-7,153,046	G	A	SEZ6L	right flank	seizure related 6 homolog like	*Gallus gallus*	7,156,283-7,183,241	15	2E-06	74	NC_006102.4
					MYO18B	left flank	myosin XVIIIB	*Gallus gallus*	7,098,287-7,142,554	15			NC_006102.4
Chroma	17979	962,253-962,334	G	A	SLC25A48	left flank	solute carrier family 25 member 48	*Picoides pubescens*	947,243-957,854	Unplaced scaffold	3E-16	84	NW_009661407.1
					IL9	right flank	interleukin 9	*Picoides pubescens*	965,934-968,678	Unplaced scaffold			NW_009661407.1
		9,310,958-9,311,038			LOC100231635	overlap	solute carrier family 25 member 48-like; Mitochondrial carrier protein	*Taeniopygia_guttata*	9,300,825-9,318,214	13	2E-06	75	NC_011477.1
Chroma	23362	4,337,416-4,337,437	C	T	SSH1	overlap	Slingshot protein phosphatase 1	*Taeniopygia guttata*	4,316,230-4,348,419	15	0.16	100	NC_011479.1
					DAO	right flank	D-amino acid oxidase	*Taeniopygia guttata*	4357575-4363055	15			NC_011479.1
					CORO1C	left flank	Coronin	*Taeniopygia guttata*	4260857-4282375	15			NC_011479.1

					SVOP		SV2 related protein	*Taeniopygia guttata*	4366281-4391516	15			NC_011479.1
Chroma	24415	1,103,882-1,103,924	A	G	IL11RA	right flank	Interleukin 11 receptor subunit alpha	*Picoides pubescens*	1,131,090-1,136,119	Unplaced scaffold	0.51	85	NW_009666237.1
					CNTFR	left flank	Ciliary neurotrophic factor receptor	*Picoides pubescens*	972,344-1,072,736	Unplaced scaffold			NW_009666237.1
					N307_05835	right flank	Interleukin-11 receptor subunit alpha	*Picoides pubescens*	1,131,090-1,136,008	Unplaced scaffold			NW_009666237.1
Chroma	26011	4,042,274-4,042,303	C	A	NDRG4	overlap	NDRG family member 4	*Taeniopygia guttata*	4,034,652-4,043,534	11	0.003	93	NC_011475.1
					WWOX	left flank	WW domain containing oxidoreductase	*Taeniopygia guttata*	3,537,445-4,030,153	11			NC_011475.1
					GINS3 (PSF3)	right flank	DNA replication complex GINS protein PSF3 (GINS complex subunit 3)	*Taeniopygia guttata*	4,063,867-4,068,277	11			NC_011475.1
Hue	4257	235289	C	T	CACNA2D4	right flank	voltage-dependent calcium channel subunit alpha-2/delta-4	*Taeniopygia guttata*	71,116,200-71,243,775	A1	0.012	91	NC_0011463.1
					LRTM2	right flank	leucine-rich repeat and transmembrane domain-containing protein 2		71,197,416-71,217,044	A1	0.012	91	NC_0011463.1
Hue	15130	19,042,031-19,042,056	G	A	MAP2K5	overlap	mitogen-activated protein kinase kinase 5	*Gallus gallus*	18,970,555-19,082,529	10	0.55	92	NC_006097.4

Hue	26435	3376982 to 3377074	G	A	LSAMP (IGLON3, LAMP)	overlap	Limbic system-associated membrane protein	*Picoides pubescens*	3,031,742-3,423,730	Unplaced scaffold	4E-21	85	NW_009661767.1
					GAP43	left flank	Growth associated protein 43	*Picoides pubescens*	2,922,565-2,991,932				NW_009661767.1
Hue	28163	214498 to 214586	G	A	EXD3	overlap	exonuclease 3'-5' domain containing 3	*Picoides pubescens*	38,994-312,081	Unplaced scaffold	9E-17	84	NW_009665384.1
					NRARP		NOTCH regulated ankyrin repeat protein	*Picoides pubescens*	34,995-35,267	Unplaced scaffold			NW_009665384.1
					AMBP		Alpha-1-microglobulin/bikunin precursor	*Picoides pubescens*	11,126-14,407	Unplaced scaffold			NW_009665384.1

Table 5. The cellular location, protein names and ontology of genes detected by association mapping in GAPIT/FARMCPU to be associated with the forecrown plumage characteristics of *P. chrysoconus* and *P. pusillus*.

Trait	SNP ID	Position	Gene name	Relative position	Protein name	Ontology
Binary pheno	3673	255,676-255,708	UACA	overlap	Uveal autoantigen	cytosol; extracellular exosome; nucleus; apoptotic signaling pathway; regulation of NIK/NF-kappaB signaling
			TLE3	left flank	transducin like enhancer of	nucleoplasm; nucleus; animal organ morphogenesis; beta-catenin-TCF complex assembly; regulation of transcription, DNA-templated; signal
Binary pheno	4257	71,175,140-71,175,173	CACNA2D4	right flank	voltage-dependent	calcium ion transmembrane transport; cardiac conduction; detection of light stimulus involved in visual perception; regulation of ion transmembrane
			LRTM2	right flank	leucine-rich repeat and	cytoplasm; integral component of membrane; protein kinase inhibitor activity; cytokine-mediated signaling pathway; negative regulation of JAK-
Binary pheno	9686	47,768-47,850	LOC10429877	overlap	hydrocephalus-inducing	axonemal central pair projection; axonemal central apparatus assembly; cilium movement; epithelial cell development; trachea development;
Binary pheno	16684	8,069,226-8,069,324	GRM3	overlap	glutamate metabotropic	axon; dendritic spine; integral component of membrane; postsynaptic density; postsynaptic membrane; presynaptic membrane; calcium channel
		38,163,822-38,163,911	GRM3	overlap	glutamate metabotropic	axon; dendritic spine; integral component of membrane; postsynaptic density; postsynaptic membrane; presynaptic membrane; calcium channel
Binary pheno	19312	76,096-76,196	LOC10429990	left flank	dual specificity testis-specific	ATP binding; metal ion binding; protein kinase activity
		2,952,196-2,952,223	POU6F2	overlap	POU class 6 homeobox 2	nucleus; DNA binding; DNA binding transcription factor activity; central nervous system development; ganglion mother cell fate determination;
Binary pheno	20445	7,152,946-7,153,046	SEZ6L	right flank	seizure related 6 homolog like	endoplasmic reticulum membrane; integral component of membrane; neuronal cell body; adult locomotory behavior; cerebellar Purkinje cell layer
			ASPHD2	right flank	aspartate beta-hydroxylase	integral component of membrane; membrane; dioxygenase activity; metal ion binding; peptidyl-amino acid modification
			HPS4	right flank	biogenesis of lysosomal	BLOC-3 complex; cytoplasm; cytosol; lysosome; melanosome; membrane; platelet dense granule; guanyl-nucleotide exchange factor activity; protein
Binary pheno	24352	7,152,950-7,153,046	SEZ6L	right flank	seizure related 6 homolog like	endoplasmic reticulum membrane; integral component of membrane; neuronal cell body; adult locomotory behavior; cerebellar Purkinje cell layer
			MYO18B	left flank	myosin XVIIIB	filamentous actin; myosin complex; Z disc; actin binding; ATP binding; motor activity; cardiac muscle fiber development; vasculogenesis
Chroma	17979	962,253-962,334	SLC25A48	left flank	solute carrier family 25	integral component of membrane; mitochondrion; transmembrane transport
			IL9	right flank	interleukin 9	Interleukin 7/9 family IL-7 is a cytokine that acts as a growth factor for early lymphoid cells of both B- and T-cell lineages. IL-9 is a multi-functional cytokine
		9,310,958-9,311,038	LOC10023163	overlap	solute carrier family 25	integral component of membrane; transmembrane transport
Chroma	23362	4,337,416-4,337,437	SSH1	overlap	Slingshot protein	cytoplasm; plasma membrane; actin binding; protein tyrosine phosphatase activity; protein tyrosine/serine/threonine phosphatase activity; actin
			DAO	right flank	D-amino acid oxidase	FAD dependent oxidoreductase; cytosol; mitochondrial outer membrane; peroxisomal membrane; D-amino-acid oxidase activity; FAD binding; protein
			CORO1C	left flank	Coronin	actin cytoskeleton; flotillin complex; lamellipodium; lateral plasma membrane; vesicle; actin filament binding; Rac GTPase binding; actin
			SVOP		SV2 related protein	
Chroma	24415	1,103,882 - 1,103,924	IL11RA	right flank	Interleukin 11 receptor	integral component of membrane; cytokine receptor activity; cytokine-mediated signaling pathway; developmental process; head development
			CNTFR	left flank	Ciliary neurotrophic	apical plasma membrane; ciliary neurotrophic factor receptor complex; CNTFR-CLCF1 complex; ciliary neurotrophic factor receptor activity; cytokine
			N307_05835	right flank	Interleukin-11 receptor	integral component of membrane; cytokine receptor activity
Chroma	26011	4,042,274-4,042,303	NDRG4	overlap	NDRG family member 4	basolateral plasma membrane; cell projection membrane; cytoplasm; cell migration involved in heart development; negative regulation of platelet-
			WWOX	left flank	WW domain containing	cytosol; Golgi apparatus; microvillus; mitochondrion; plasma membrane; RNA polymerase II transcription factor complex; enzyme binding; RNA polymerase
			GINS3 (PSF3)	right flank	DNA replication complex GINS	nucleoplasm; DNA strand elongation involved in DNA replication; Unwinding of DNA.
Hue	4257	235289	CACNA2D4	right flank	voltage-dependent	calcium ion transmembrane transport; cardiac conduction; detection of light stimulus involved in visual perception; regulation of ion transmembrane
			LRTM2	right flank	leucine-rich repeat and	cytoplasm; integral component of membrane; protein kinase inhibitor activity; cytokine-mediated signaling pathway; negative regulation of JAK-
Hue	15130	19,042,031-19,042,056	MAP2K5	overlap	mitogen-activated	cytoplasm; cytosol; nucleus; spindle; ATP binding; metal ion binding; protein kinase activity; protein serine/threonine kinase activity; protein tyrosine
Hue	26435	3376982 to 3377074	LSAMP (IGLON	overlap	Limbic system-associated	anchored component of membrane; cytosol; extracellular region; plasma membrane; C-terminal protein lipidation; cell adhesion; locomotory
			GAP43	left flank	Growth associated	axon; axon terminus; cytoplasm; dendrite; filopodium membrane; membrane; neuronal cell body; postsynaptic density; axon choice point
Hue	28163	214498 to 214586	EXD3	overlap	exonuclease 3'-5' domain	cytoplasm; nucleus; RNA nuclear export complex; nuclear export signal receptor activity; Ran GTPase binding; RNA binding; intracellular protein
			NRARP		NOTCH regulated	blood vessel endothelial cell proliferation involved in sprouting angiogenesis; branching involved in blood vessel morphogenesis; negative regulation of
			AMBP		Alpha-1-microglobulin/	blood microparticle; cell surface; extracellular exosome; extracellular matrix; extracellular region; extracellular space; intracellular membrane-bounded

Table 6. Percentage variation explained by the Principal components on the ddRadseq data from GWAS analysis in GAPIT. The first dimension explained most of the variation relative to PC2 and PC3.

	PC1 (%)	PC2 (%)	PC3 (%)
Binary pheno	99	9	15
Chroma	49	34	4
Hue	95	3	1

Discussion

The present study provides evidence of differential patterns of interaction between *Pogoniulus chrysoconus* and *P. pusillus* across four contact zones centred in Ethiopia, Kenya, Tanzania and Southern Africa where the species' ranges abut. We found extensive introgressive hybridisation between the two species in Southern Africa (cf. Chapter 3) as well as limited introgression from Tanzania. By contrast, there is little or no hybridisation evident in Kenya, and based on distinctly different songs, we consider hybridisation in Ethiopia unlikely. Patterns of differential introgression are supported by convergence in body size and song traits from allopatric populations towards sympatric populations in Southern Africa and Tanzania.

Species specific song is most distinguishable based on song speed, with *P. pusillus* singing faster songs than *P. chrysoconus*. Song functions in long distance communication (Naguib and Wiley, 2001), and because of the habits and singing behavior of tinkerbirds, we expect song plays a far more important role in territory defence and mate attraction than visual cues. Their songs can be projected over 100 m, eliciting intrasexual and potentially intersexual responses at such distances, whereas visual cues are only likely to function at an order of magnitude lower distances in birds of that size. An encounter between individuals is thus likely to be elicited initially by song production, acoustic ranging (Naguib 1996), and then approach by the receiver before any visual cues might function in species recognition and mate choice. Based on our song analysis, songs of the two species converged towards the contact zone in

Southern Africa and Tanzania while they remained distinct in Ethiopia and Kenya. We suggest that greater song similarity between the two species in Southern Africa and Tanzania explains the observed higher degree of hybridization there relative to other contact zones, and playback experiments provide further support for this hypothesis. Specifically, no differences between responses to conspecific and heterospecific songs by individuals of both species in Southern Africa and Tanzania suggest a breakdown in species recognition at those contact zones, while in Kenya they responded significantly more strongly to conspecific than to heterospecific song. Song could thus be the primary factor mediating the extent of introgressive hybridisation across contact zones (Qvarnström et al. 2006).

Morphometric analyses revealed a pattern of convergence towards the contact zone in PC1 in Tanzania and Swaziland, but not in Kenya and Tanzania. PC1 was correlated with mostly bill shape measurements and wing chord, a pattern potentially reflecting adaptation to the environment, but might also reflect gene flow between populations. Yet, we found no effect of the environment overall on PC1, suggesting instead that gene flow where present explains the pattern of convergence in these traits. PC2, which was positively correlated with tarsus and tail length, as well as forecrown patch size, overlapped substantially between species within regions, differing more among contact zones, likely reflecting patterns of adaptation to the environment consistent with Bergmann's rule, with body size increasing with latitude and elevation. In Southern Africa in particular, a pattern of convergence in PC2 towards the contact zone is evident, suggestive of gene flow. We found no significant difference in body size between the sexes in either species, suggesting stabilizing selection on body size in relation to sex.

Our analyses of song and morphology suggest introgressive hybridisation in Southern Africa and Tanzania leads to convergence in phenotypic traits. Divergence in song might reflect reproductive character displacement in Ethiopia with a steep ecological gradient across the

species boundary there suggesting reproductive isolation may have evolved through reinforcement if hybrids suffered from reduced fitness (Liou and Price 1994, Nosil et al 2003, Mallet, 2007, Sæther et al 2007). By contrast, contact zones with flatter ecological gradients, such as in Southern Africa, coupled with greater similarity in song, might support ongoing hybridisation. Yet in Kenya, songs remain distinct despite the flatter ecological gradient, and distinct clusters of *P. pusillus affinis* and *P. chrysoconus chrysoconus* across Kenya shown in the STRUCTURE analysis (Figure 11) suggests absence of hybridisation. Indeed, narrow song clines in Ethiopia and Kenya and wider clines in Tanzania and Southern Africa likely better reflect differences in introgressive hybridisation among contact zones, though we cannot rule out a possible role of ecological gradients, at least in Ethiopia. The overall pattern in Southern Africa shows substantial gene flow between *P. c. extoni* and *P. p. pusillus*. While introgressive hybridisation between the two species in Southern Africa is extensive based on genomic analyses performed here and microsatellite analyses (Chapter 3), in Tanzania pairwise distances (G'_{ST}) suggest their genomes have become homogenised to the extent *P. p. affinis* in sympatry is closer to *P. c. extoni* in sympatry than to *P. p. affinis* in allopatry. Closer inspection of the data reveals that this finding likely reflects the fact that two of three *P. pusillus affinis* sampled from the contact zone had in essence *P. c. extoni* genomes, suggesting historic introgression of red forecrown plumage genes. More samples from the contact zone would be needed to determine whether introgressive hybridisation is as extensive as in Southern Africa, where *P. p. pusillus* shares more alleles across the genome with *P. c. extoni* than with conspecific *P. p. affinis*. Gene flow between *P. p. pusillus* and *P. c. extoni* has been so extensive over time that introgression of alleles has homogenised their genomes (Stuglik and Babik 2016), despite genetic distance based on mtDNA suggesting divergence between red and yellow-fronted tinkerbirds occurred 7.89 mya (95% HPD 5.79 – 14.2 mya) (Chapter 3).

Our plumage tetracolorspace analysis revealed a lack of overlap between the colour space of allopatric *pusillus* and *chrysoconus* in Southern Africa, with sympatric populations of both species occupying intermediate colour space. Our field identification of the species based on forecrown plumage coloration, even of hybrids, agreed with the distribution of individual colour points within avian tetracolorspace, supported by a lack of overlap in the colour volume of the sympatric populations of *chrysoconus* and *pusillus* (Table 1). Yet, while discriminant analysis based on colour scores on long, medium and short wavelengths of forecrown plumage patches revealed that allopatric populations are distinct, sympatric populations are on the border of the error region suggesting some admixture in plumage coloration (Figure 10). The evolutionary implication of the recovered plumage pattern is that of gene flow and introgression of genes that control for forecrown colour between *chrysoconus* and *pusillus* in Southern Africa. There is substantial variation in the red forecrown colour of allopatric *pusillus* leading to their wider distribution in colour space relative to the yellow coloration of allopatric *chrysoconus* (Figures 7, 9). While in sympatry, hue reliably distinguishes sympatric populations of *chrysoconus* and *pusillus* (Figure 8), higher variation in hue is observed within sympatric populations than in allopatric populations, a further indication of introgression of plumage colouration genes, with individuals heterozygous in those genes potentially expressing intermediate phenotypes (Uy et al. 2016). The considerably higher number of phenotypically *P. pusillus* with a predominantly *P. chrysoconus* genomic background than vice versa, from Tanzania and Southern Africa, might reflect a preference for red forecrowns, with the red plumage genes introgressing asymmetrically into *P. chrysoconus* populations. Asymmetric introgression of red colouration has been reported in other birds, including *Malurus* fairy-wrens (Baldassarre et al. 2014), suggesting it could play a role in mate choice in birds, and future studies could tease apart the relative preferences of female yellow- and red-fronted tinkerbirds for males with either trait.

Of the 31 identified candidate genes associated with plumage coloration of both species based on GWAS (Figure 16, 17), we recovered three genes that specifically control for eye pigmentation (HPS4), visual learning (NDRG4) and detection of light stimulus involved in visual perception (CACNA2D4) and several genes known to control morphological development and specifically for head development. We recovered SNP ID 4257 using both FarmCPU and GAPIT as highly significantly associated with forecrown plumage colouration in Southern Africa, and this SNP mapped onto CACNA2D4, emphasising the potential role of this gene in plumage colouration. We did not recover any of the genes within the domain of CYP (Cytochrome P450) loci reported by previous studies on red and yellow colouration in birds (Lopes et al., 2016; Mundy et al., 2016; Twyman et al., 2018). This may be attributed to possible differential gene to phenotype pathways in Piciformes, or more specifically in the family Lybiidae or genus *Pogoniulus* to what has been identified in Passeriformes in the family Fringillidae in *Serinus canaria* (common canary), and Estrildidae, in *Taeniopygia guttata* (zebra finch) or in Galliformes in *Gallus gallus* (red junglefowl). Twyman et al., 2018 were able to recover a fulllength (1431bp) sequence of CYP2J19 gene from one Piciformes species, *Picoides pubescens* (downy woodpecker). However, only a few of the 70 species they sampled had red coloration, and red coloration due to ketocarotenoids have only been confirmed in zebra finch and American flamingo (Twyman et al., 2018). Our study does not completely rule out the possibility of genes from the CYP domain controlling red coloration in *Pogoniulus* tinkerbirds. Instead our results suggest a likely different gene complex capable of controlling for pigmentation and visual learning between *P. chrysoconus* and *P. pusillus*.

Conclusion

We found that interactions between red-fronted and yellow-fronted tinkerbird varied among four contact zones in East and Southern Africa. Substantial gene flow occurs between *P. c*

extoni and *P. p. pusillus* within their contact zone in Southern Africa, which takes the form of asymmetric introgression of *P. p. pusillus* into the genetic background of *P. c. extoni*, and convergence found in morphology, plumage, and song is consistent with the homogenizing effect of introgression. By contrast, at the two northernmost contact zones in Kenya and Ethiopia, there was no evidence of introgressive hybridization, with songs remaining distinct. Indeed, they appear to have diverged enough to maintain reproductive isolation and a stable species boundary. Overall, our results contribute to the understanding of factors that explain species distributions and highlight the role of species interactions in the speciation process.

References

ABBOTT, R., ALBACH, D., ANSELL, S., ARNTZEN, J.W., BAIRD, S. J. E., BIERNE, N, BOUGHMAN, J., BRELSFORD, A., BUERKLE, C. A., BUGGS, R., BUTLIN, R. K., DIECKMANN, U., et al. 2013. Hybridization and speciation. *Journal of Evolutionary Biology* **26**: 229-26.

ALCAIDE, M., SCORDATO, E.S., PRICE, T.D. and IRWIN, D.E., 2014. Genomic divergence in a ring species complex. *Nature*, **511**(7507), p.83.

ALLENDORF, F. W., HOHENLOHE, P. A. and LUIKART, G. 2010. Genomics and the future of conservation genetics. *Nature Reviews Genetics*. 11(10), 697-709.

ANDREWS, K.R., GOOD, J.M., MILLER, M.R., LUIKART, G. and HOHENLOHE, P.A., 2016. Harnessing the power of RADseq for ecological and evolutionary genomics. *Nature Reviews Genetics*, **17**(2), p.81.

ANGULO, A. and REICHLE, S., 2008. Acoustic signals, species diagnosis, and species concepts: the case of a new cryptic species of Leptodactylus (Amphibia, Anura, Leptodactylidae) from the Chapare region, Bolivia. *Zoological Journal of the Linnean Society*, **152**(1), pp.59-77.

AUDACITY TEAM. 2012. *Audacity Version 2.0.2.*, Audacity Team. Retrieved from http://audacityteam.org

BALDASSARRE, D. T., WHITE, T. A., KARUBIAN, J., and WEBSTER, M. S., 2014. Genomic and morphological analysis of a semipermeable avian hybrid zone suggests asymmetric introgression of a sexual signal. *Evolution* **68**: 2644-2657.

BASS, A.H. and CHAGNAUD, B.P., 2012. Shared developmental and evolutionary origins for neural basis of vocal–acoustic and pectoral–gestural signaling. *Proceedings of the National Academy of Sciences*, **109**(Supplement 1), pp.10677-10684.

BARTON, N. H., HEWITT, G. M. 1985. Analysis of hybrid zones. *Annual Review of Ecology and Systematics* **16**: 113-148.

BERS, N.E.V., OERS, K.V., KERSTENS, H.H., DIBBITS, B.W., CROOIJMANS, R.P., VISSER, M.E. AND GROENEN, M.A., 2010. Genome-wide SNP detection in the great tit *Parus major* using high throughput sequencing. *Molecular Ecology*, 19(s1), pp.89-99.

BIRDLIFE INTERNATIONAL, 2018. Species factsheet: *Pogoniulus pusillus*. Downloaded from http://www.birdlife.org on 22/03/2018.

BRELSFORD, A., DUFRESNES, C. and PERRIN, N., 2016. High-density sex-specific linkage maps of a European tree frog (*Hyla arborea*) identify the sex chromosome without information on offspring sex. *Heredity*, **116**(2), p.177.

BRELSFORD, A., MILA, B., and IRWIN, D. 2011. Hybrid origin of Audubon's warbler. *Molecular Ecology,* **20**: 2380-2389.

BRELSFORD, A., TOEWS, D.P. and IRWIN, D.E., 2017. Admixture mapping in a hybrid zone reveals loci associated with avian feather coloration. *Proc. R. Soc. B*, **284**(1866), p.20171106.

BUTLIN, R. K. 1987. Species, speciation and reinforcement. *American Naturalist*, **130**: 461-464.

CASE, T.J. and TAPER, M.L., 2000. Interspecific competition, environmental gradients, gene flow, and the coevolution of species' borders. *The American Naturalist*, **155**(5), pp.583-605.

CATCHEN, J.M., AMORES, A., HOHENLOHE, P., CRESKO, W. and POSTLETHWAIT, J.H., 2011. Stacks: building and genotyping loci de novo from short-read sequences. *G3: Genes, Genomes, Genetics*, **1**:171–182.

CATCHEN, J., S. BASSHAM, T. WILSON, M. CURREY, C. O'BRIEN, Q. YEATES, AND W. A. CRESKO 2013a. The population structure and recent colonization history of Oregon threespine stickleback determined using restriction-site associated DNA-sequencing. *Molecular Ecology* **22**:2864-2883.

CATCHEN, J., HOHENLOHE, P.A., BASSHAM, S., AMORES, A., and CRESKO, W.A. 2013b. Stacks: an analysis tool set for population genomics. *Molecular Ecology*, **22**:3124–3140.

CHANG, C.C., CHOW, C.C., TELLIER, L.C., VATTIKUTI, S., PURCELL, S.M. and LEE, J.J., 2015. Second-generation PLINK: rising to the challenge of larger and richer datasets. *Gigascience*, **4**(1), p.7.

DACOSTA, J. M., and SORENSON, M. D. 2016. ddRAD-seq phylogenetics based on nucleotide, indel, and presence-absence polymorphisms: Analyses of two avian genera with contrasting histories. *Molecular Phylogenetics and Evolution*, **94**: 122-135.

DANECEK, P., AUTON, A., ABECASIS, G., ALBERS, C.A., BANKS, E., DEPRISTO, M.A., HANDSAKER, R.E., LUNTER, G., MARTH, G.T., SHERRY, S.T. and MCVEAN, G. 2011. The variant call format and VCFtools. *Bioinformatics*, **27**:2156–2158.

DANLEY, P.D., MARKERT, J.A., ARNEGARD, M.E. and KOCHER, T.D., 2000. Divergence with gene flow in the rock-dwelling cichlids of Lake Malawi. *Evolution*, **54**(5), pp.1725-1737.

DAVEY, J.W. and BLAXTER, M.L., 2010. RADSeq: next-generation population genetics. *Briefings in functional genomics*, **9**(5-6), pp.416-423.

DELMORE, K. E., TOEWS, D. P. L., GERMAIN, R. R., OWENS, G. L., IRWIN, D. E. 2016. The genetics of seasonal migration and plumage colour. *Current Biology* **26**: 2167-2173.

DERJUSHEVA S, KURGANOVA A, HABERMANN F, GAGINSKAYA E., 2004. High chromosome conservation detected by comparative chromosome painting in chicken, pigeon and passerine birds. *Chromosome Research*, **12**, 715-723.

DERRYBERRY, E.P., DERRYBERRY, G.E., MALEY, J.M. and BRUMFIELD, R.T. 2014. HZAR: hybrid zone analysis using an R software package. *Molecular Ecology Resources*, **14**:652-663.

DIXON, P., 2003. VEGAN, a package of R functions for community ecology. *Journal of Vegetation Science*, **14**: 927-930.

ENDELMAN J., 2011 Ridge regression and other kernels for genomic selection in the R package rrBLUP. *Plant Genome* **4**: 250–255.

ENDLER, J.A., 1990. On the measurement and classification of colour in studies of animal colour patterns. *Biological Journal of the Linnean Society*, **41**: 315-352.

ENDLER, J.A., WESTCOTT, D.A., MADDEN, J.R. and ROBSON, T., 2005. Animal visual systems and the evolution of color patterns: sensory processing illuminates signal evolution. *Evolution*, *59*(8), pp.1795-1818.

ESRI (2012) ArcGIS Desktop: Release 10.1 (Environmental Systems Research Institute, Redlands, CA)

FELSENSTEIN, J. 2006. Accuracy of coalescent likelihood estimates: do we need more sites, more sequences, or more loci? *Molecular Biology and Evolution* 23:691-700.

FIDLER AE, VAN OERS K, DRENT PJ, KUHN S, MUELLER JC, and KEMPENAERS B. 2007. Drd4 gene polymorphisms are associated with personality variation in a

passerine bird. *Proceedings of the Royal Society of London. Series B: Biological Sciences*, **274**, 1685-1691.

FRIDOLFSSON, A. K., and ELEGREN, H. 1999. A simple and universal method for moelcular sexing on non-ratite birds. *Journal of Avian Biology*, **30**: 116-121.

GILL, F. B. 1980. Historical aspects of hybridization between blue-winged and golden-winged warblers. *The Auk*, **97**: 1-18.

GREEN, R.E., KRAUSE, J., BRIGGS, A.W., MARICIC, T., STENZEL, U., KIRCHER, M., PATTERSON, N., LI, H., ZHAI, W., FRITZ, M.H.Y. and HANSEN, N.F., 2010. A draft sequence of the Neandertal genome. *Science*, **328**(5979), pp.710-722.

GRETHER, G.F., ANDERSON, C.N., DRURY, J.P., KIRSCHEL, A.N., LOSIN, N., OKAMOTO, K. and PEIMAN, K.S., 2013. The evolutionary consequences of interspecific aggression. *Annals of the New York Academy of Sciences*, **1289**(1), pp.48-68.

GRETHER, G.F., LOSIN, N., ANDERSON, C.N. and OKAMOTO, K. 2009. The role of interspecific interference competition in character displacement and the evolution of competitor recognition. *Biological Review,* **84**: 617–635.

GRIFFIN, D.K., ROBERTSON, L.B., TEMPEST, H.G., VIGNAL, A., FILLON, V., CROOIJMANS, R.P., GROENEN, M.A., DERYUSHEVA, S., GAGINSKAYA, E., CARRÈ, W. and WADDINGTON, D., 2008. Whole genome comparative studies between chicken and turkey and their implications for avian genome evolution. *BMC genomics*, **9**(1), p.168.

GROSSEN, C., SENEVIRATNE, S. S., CROLL, D., and IRWIN, D. E. 2016. Strong reproductive isolation and narrow genomic tracts of differentiation among three woodpecker species in secondary contact. *Molecular Ecology*, **25**: 4247-4266.

HAAVIE, J., BORGE, T., BURES, S., GARAMSZEGI, L.Z., LAMPE, H.M., MORENO, J., QVARNSTRÖM, A., TÖRÖK, J. and SÆTRE, G.P., 2004. Flycatcher song in allopatry and sympatry–convergence, divergence and reinforcement. *Journal of evolutionary biology*, **17**(2), pp.227-237.

HALDANE, J. B. S. (1922). "Sex ratio and unisexual sterility in hybrid animals". *Journal of Genetics*, **12**: 101–109.

HENDRICK, P. W., 2005. A Standardized genetic differentiation measure. *Evolution* **59**: 1633-1638.

HOHENLOHE, P., M. D. DAY, S. J. AMISH, M. R. MILLER, N. KAMPS-HUGHES, M. C. BOYER, C. C. MUHLFELD et al. 2013. Genomic patterns of introgression in rainbow and westslope cutthroat trout illuminated by overlapping paired-end RAD sequencing. *Molecular Ecology* 22:3002-3013.

IZZO, A.S. and GRAY, D.A., 2004. Cricket song in sympatry: species specificity of song without reproductive character displacement in Gryllus rubens. *Annals of the Entomological Society of America*, **97**(4), pp.831-837.

JEFFRIES, D.L., COPP, G.H., LAWSON HANDLEY, L., OLSÉN, K.H., SAYER, C.D. and HÄNFLING, B., 2016. Comparing RADseq and microsatellites to infer complex hylogeographic patterns, an empirical perspective in the Crucian carp, Carassius carassius, L. *Molecular ecology*, **25**(13), pp.2997-3018.

JONES, F.C., CHAN, Y.F., SCHMUTZ, J., GRIMWOOD, J., BRADY, S.D., SOUTHWICK, A.M., ABSHER, D.M., MYERS, R.M., REIMCHEN, T.E., DEAGLE, B.E. and SCHLUTER, D., 2012. A genome-wide SNP genotyping array reveals patterns of global and repeated species-pair divergence in sticklebacks. *Current biology*, **22**(1), pp.83-90.

JONKER, R.M., ZHANG, Q., VAN HOOFT, P., LOONEN, M.J., VAN DER JEUGD, H.P., CROOIJMANS, R.P., GROENEN, M.A., PRINS, H.H. and KRAUS, R.H., 2012. The development of a genome wide SNP set for the Barnacle goose *Branta leucopsis*. *PLoS One*, **7**(7), p.e38412.

KEARNS, A.M., RESTANI, M., SZABO, I., SCHRØDER-NIELSEN, A., KIM, J.A., RICHARDSON, H.M., MARZLUFF, J.M., FLEISCHER, R.C., JOHNSEN, A. and OMLAND, K.E., 2018. Genomic evidence of speciation reversal in ravens. *Nature communications*, **9**(1), p.906.

KIRKPATRICK, M. and BARTON, N.H., 1997. Evolution of a species' range. *The American Naturalist*, **150**(1), pp.1-23.

KIRSCHEL, A. N. G., BLUMSTEIN, D. T., and SMITH, T. B. 2009a. Character displacement of song and morphology in African tinkerbirds. *Proceedings of the National Academy of Sciences of the United States of America*, **106**: 8256-8261.

KIRSCHEL, A. N. G., BLUMSTEIN, D. T., COHEN, R. E., BUERMANN, W., SMITH, T. B., and SLABBEKOORN, H. 2009b. Birdsong tuned to the environment: green hylia song varies with elevation, tree cover, and noise. *Behavioral Ecology*, **20**:1089-1095.

KIRSCHEL, A. N. G., SLABBEKOORN, H., BLUMSTEIN, D. T., COHEN, R. E., DE KORT, S. R., BUERMANN, W., and SMITH, T. B. 2011. Testing alternative hypotheses for evolutionary diversification in an African songbird: Rainforest refugia versus ecological gradients. *Evolution*, **65**: 3162-3174.

KLEINDORFER, S., O'CONNOR, J. A., DUDIANEC, R. Y., MYERS, S. A., ROBERTSON, J., and SULLOWAY, F. J. 2014. Species collapse via hybridization in Darwin's tree finches. *The American Naturalist*, **183**: 325-341.

KLUMP, G.M. and SHALTER, M.D., 1984. Acoustic behaviour of birds and mammals in the predator context; I. Factors affecting the structure of alarm signals. II. The functional significance and evolution of alarm signals. *Ethology*, **66**(3), pp.189-226.

KOPELMAN, N.M., MAYZEL, J., JAKOBSSON, M., ROSENBERG, N.A. AND MAYROSE, I., 2015. Clumpak: a program for identifying clustering modes and packaging population structure inferences across K. *Molecular ecology resources*, **15**(5), pp.1179-1191.

KRAUS, R.H., KERSTENS, H.H., VAN HOOFT, P., CROOIJMANS, R.P., VAN DER POEL, J.J., ELMBERG, J., VIGNAL, A., HUANG, Y., LI, N., PRINS, H.H. and GROENEN, M.A., 2011. Genome wide SNP discovery, analysis and evaluation in mallard (*Anas platyrhynchos*). *BMC genomics*, **12**(1), p.150.

LANG, J. M. and BENBOW, M. E. 2013. Species Interactions and Competition. *Nature Education Knowledge* **4**(4):8.

LAURIE, C.C., DOHENY, K.F., MIREL, D.B., PUGH, E.W., BIERUT, L.J., BHANGALE, T., BOEHM, F., CAPORASO, N.E., CORNELIS, M.C., EDENBERG, H.J. and GABRIEL, S.B., 2010. Quality control and quality assurance in genotypic data for genome-wide association studies. *Genetic epidemiology*, **34**(6):591-602.

LÊ, S., JOSSE, J. and HUSSON, F., 2008. FactoMineR: an R package for multivariate analysis. *Journal of statistical software*, **25(**1):1-18.

LEPAIS, O., PETIT, R. J., GUICHOUX, E., LAVABRE, J.E., ALBERTO, F., KREMER, A., and GERBER, S. 2009. Species relative abundance and direction of introgression in oaks. *Molecular Ecology*, **18**: 2228-2242.

LEVIN, D. A. 2002. Hybridization and extinction. *American Scientist*, **90**: 254-261.

LI Y. L., and LIU J. X., 2018. StructureSelector: A web-based software to select and visualize the optimal number of clusters using multiple methods. *Molecular Ecology Resources*, **18**:176–177.

LIPKA A. E., TIAN, F., and WANG, Q. et al., 2012. GAPIT: genome associ- ation and prediction integrated tool. *Bioinformatics*, **28**, 2397– 2399.

LIU X., HUANG M., FAN B., BUCKLER E. S., and ZHANG Z., 2016. Iterative Usage of Fixed and Random Effect Models for Powerful and Efficient Genome-Wide Association Studies. *PLoS Genetics*. **12**: e1005767.

LIOU, L.W. and PRICE, T.D., 1994. Speciation by reinforcement of premating isolation. *Evolution*, **48**(5), pp.1451-1459.

LOPES, R.J, JOHNSON, J. D., TOOMEY, M. B., FERREIRA, M.S., ARAUJO, P.M. MELO-FERREIRA, J., ANDERSSEN, L., HILL, G. E., CORBO, J. C., and CARNEIRO, M. 2016. Genetic basis for red colouration in birds. 2016. *Current Biology*, **26**: 1427-1434.

LOWRY, D. B. HOBAN, S., KELLEY, J. L., LOTTERHOS, K. E., REED, L. R., ANTOLIN, M. F., and STORFER, A. 2016. Breaking RAD: an evaluation of the utility of restriction site-associated DNA sequencing for genome scans of adaptation. *Molecular Ecology Resources*, **17**: 142-152.

LUDWIG, J.A. and REYNOLDS, J.F. 1988. *Statistical ecology: a primer in methods and computing*. John Wiley and Sons.

MAGI, A., BENELLI, M., GOZZINI, A., GIROLAMI, F., TORRICELLI, F. and BRANDI, M.L. 2010. Bioinformatics for Next Generation Sequencing Data. *Genes*, **1**:294-307.

MAIA, R., ELIASON, C.M., BITTON, P.P., DOUCET, S.M. and SHAWKEY, M.D., 2013. pavo: an R package for the analysis, visualization and organization of spectral data. *Methods in Ecology and Evolution*, **4**: 906-913.

MALLET, J., 2007. Hybrid speciation. *Nature*, **446**(7133), p.279.

MCGREGOR, P.K., DABELSTEEN, T., SHEPHERD, M. and PEDERSEN, S.B., 1992. The signal value of matched singing in great tits: evidence from interactive playback experiments. *Animal Behaviour*, **43**(6), pp.987-998.

MCKINNEY, G. J., LARSON, W. A., SEEB, L. W., and SEEB, J. E. 2017. RADseq provides unprecedented insights into molecular ecology and evolutionary genetics: comment on Breaking RAD by Lowry et al. 2016. *Molecular Ecology Resources*, doi: 10.1111/1755-0998.12649

MUNDY, N.I., STAPLEY, J., BENNISON, C., TUCKER, R., TWYMAN, H., KIM K.-W., BURKE, T., BIRKHEAD, T.R. ANDERSSON, S., and SLATE, J. 2016. Red carotenoid colouration in the zebra finch is controlled by a cytochrome P450 gene cluster. *Current Biology*, **26**: 1435-1440.

MULLEN, S.P., MENDELSON, T.C., SCHAL, C. and SHAW, K.L., 2007. Rapid evolution of cuticular hydrocarbons in a species radiation of acoustically diverse Hawaiian crickets (Gryllidae: Trigonidiinae: Laupala). *Evolution*, **61**(1), pp.223-231.

MYRBERG, A.A., 1981. Sound communication and interception in fishes. In Hearing and sound communication in fishes (pp. 395-426). Springer, New York, NY.

MYRBERG Jr, A.A., MOHLER, M. and CATALA, J.D., 1986. Sound production by males of a coral reef fish (Pomacentrus partitus): its significance to females. *Animal Behaviour*, **34**(3), pp.913-923.

NAGUIB, M., 1996. Auditory distance estimation in song birds: implications, methodologies and perspectives. *Behavioural Processes*, **38**(2), pp.163-168.

NAGUIB, M. and WILEY, R.H., 2001. Estimating the distance to a source of sound: mechanisms and adaptations for long-range communication. *Animal behaviour*, **62**(5), pp.825-837.

NOSIL, P., CRESPI, B.J. and SANDOVAL, C.P., 2003. Reproductive isolation driven by the combined effects of ecological adaptation and reinforcement. *Proceedings of the Royal Society of London B: Biological Sciences*, **270**(1527), pp.1911-1918.

NWANKWO, E. C., PALLARI, C. T., HADJIOANNOU, L., IOANNOU, A., MULWA, R. K., AND KIRSCHEL, A. N. G. 2018. Rapid song divergence leads to discordance between genetic distance and phenotypic characters important in reproductive isolation. *Ecology and Evolution*, **8**:716–731.

PAGÈS, J. 2004. Analyse factorielle de données mixtes. *Rev. Stat. appliquée* **52**: 93–111.

PAYSEUR, B.A., KRENZ, J.G. and NACHMAN, M.W., 2004. Differential patterns of introgression across the X chromosome in a hybrid zone between two species of house mice. *Evolution*, **58**(9), pp.2064-2078.

PENTERIANI, V. and DEL MAR DELGADO, M., 2017. Living in the dark does not mean a blind life: bird and mammal visual communication in dim light. *Philosophical Transactions of Royal Society B*, **372**(1717), p.20160064.

PÉREZ, P. and DE LOS CAMPOS, G., 2014. Genome-wide regression and prediction with the BGLR statistical package. *Genetics*, pp.genetics-114.

PETERSON, B.K., WEBER, J.N., KAY, E.H., FISHER, H.S. and HOEKSTRA, H.E., 2012. Double digest RADseq: an inexpensive method for de novo SNP discovery and genotyping in model and non-model species. *PloS one*, **7**(5), p.e37135.

POELSTRA, J.W., VIJAY, N, BOSSU, C. M., LANTZ, H., RYLL, B., MÜLLER, I., BAGLIONE, V., UNNEBERG, P., WIKELSKI, M., GRABHERR, M. G., and WOLF, J. B. W. 2014. The genomic landscape underlying phenotypic integrity in the face of gene flow in crows. *Science*, **344**: 1410-1414.

PRITCHARD, J.K., STEPHENS, M. and DONNELLY, P. 2000. Inference of population structure using multilocus genotype data. *Genetics*, **155**: 945-959.

PTACEK, M.B., 2000. The role of mating preferences in shaping interspecific divergence in mating signals in vertebrates. *Behavioural Processes*, **51**(1-3):111-134.

PURCELL, S., NEALE, B., TODD-BROWN, K., THOMAS, L., FERREIRA, M.A., BENDER, D., MALLER, J., SKLAR, P., DE BAKKER, P.I., DALY, M.J. and SHAM, P.C., 2007. PLINK: a tool set for whole-genome association and population-based linkage analyses. *The American Journal of Human Genetics*, **81**(3), pp.559-575.

QVARNSTRÖM, A., HAAVIE, J., SAETHER, S.A., ERIKSSON, D. and PÄRT, T., 2006. Song similarity predicts hybridization in flycatchers. *Journal of evolutionary biology*, **19**(4), pp.1202-1209.

R CORE TEAM. 2017. R: A Language and Environment for Statistical Computing. R Foundation for Statistical Computing, Vienna, Austria. https://doi.org/http://www.R-project.org/

REVELLE, W.R., 2017. psych: Procedures for personality and psychological research (R package version 1.7.8).

RHEINDT, F.E., FUJITA, M.K., WILTON, P.R. and EDWARDS, S.V., 2013. Introgression and phenotypic assimilation in Zimmerius flycatchers (Tyrannidae): population genetic and phylogenetic inferences from genome-wide SNPs. *Systematic Biology*, **63**(2), pp.134-152.

SARDELL, J. M., and UY, J. A. C. 2016. Hybridization following recent secondary contact results in asymmetric genotypic and phenotypic introgression between island species of Myzomela honeyeaters. *Evolution*, **70**: 257-269.

SÆTHER, S.A., SÆTRE, G.P., BORGE, T., WILEY, C., SVEDIN, N., ANDERSSON, G., VEEN, T., HAAVIE, J., SERVEDIO, M.R., BUREŠ, S. and KRÁL, M., 2007. Sex chromosome-linked species recognition and evolution of reproductive isolation in flycatchers. *Science*, **318**(5847), pp.95-97.

SENN, H., OGDEN, R.O.B., CEZARD, T., GHARBI, K., IQBAL, Z., JOHNSON, E., KAMPS-HUGHES, N., ROSELL, F. and MCEWING, R., 2013. Reference-free SNP discovery for the Eurasian beaver from restriction site–associated DNA paired-end data. *Molecular Ecology*, **22**(11), pp.3141-3150.

SHIPHAM, A., SCHMIDT, D. J., JOSEPH, L., and HUGHES, J, M. 2015. Phylogenetic analysis of the Australian rosella parrots (Platycercus) reveals discordance among molecules and plumage. *Molecular Phylogenetics and Evolution*, **91**: 150-159.

SHIPHAM, A., SCHMIDT, D. J., JOSEPH, L., AND HUGHES, J, M. 2017. A genomic approach reinforces a hypothesis of mitochondrial capture in eastern Australian rosellas. *The Auk*, **134**: 181-192.

SHIPILINA, D., SERBYN, M., IVANITSKII, V., MAROVA, I. and BACKSTRÖM, N., 2017. Patterns of genetic, phenotypic, and acoustic variation across a chiffchaff (*Phylloscopus collybita abietinus/tristis*) hybrid zone. *Ecology and evolution*, **7**(7), pp.2169-2180.

SLABBEKOORN, H. and SMITH, T.B. 2002. Bird song, ecology and speciation. *Philosophical Transactions of the Royal Society of London B: Biological,* **357**: 493–503.

SMITH, B. T., HARVEY, M. G., FAIRCLOTH, B. C., GLENN, T. C., AND BRUMFIELD, R. T. 2014. Target capture and massively parallel sequencing of ultraconserved elements for comparative studies at shallow evolutionary time scales. *Systematic Biology*, **63**: 83-95.

SMITH, T.B., WAYNE, R.K., GIRMAN, D.J. and BRUFORD, M.W., 1997. A role for ecotones in generating rainforest biodiversity. *Science*, **276**(5320), pp.1855-1857.

STEINER, C.C., WEBER, J.N. and HOEKSTRA, H.E., 2007. Adaptive variation in beach mice produced by two interacting pigmentation genes. *PLoS biology*, **5**(9), p.e219.

STODDARD, M.C. and PRUM, R.O., 2008. Evolution of avian plumage color in a tetrahedral color space: a phylogenetic analysis of new world buntings. *The American Naturalist*, **171**(6), pp.755-776.

STUGLIK, M.T. and BABIK, W., 2016. Genomic heterogeneity of historical gene flow between two species of newts inferred from transcriptome data. *Ecology and evolution*, **6**(13), pp.4513-4525.

SZYMURA, J.M. AND BARTON, N. H. 1986. Genetic analysis of a hybrid zone between the fire-bellied toads, *Bombina bombina* and *B. variegata*, near Cracow in Southern Poland. *Evolution*, **40**: 1141-1159.

TANG, Y., LIU, X., WANG, J., LI, M., WANG, Q., TIAN, F., SU, Z., PAN, Y., LIU, D., LIPKA, A.E. and BUCKLER, E.S., 2016. GAPIT version 2: an enhanced integrated tool for genomic association and prediction. *The plant genome*, **9**(2).

TOBIAS, J.A. and SEDDON, N. 2009. Signal design and perception in Hypocnemis antbirds: evidence for convergent evolution via social selection. *Evolution,* **63**: 3168–3189.

TOEWS, D. P. L., TAYLOR, S. A., VALLENDER, R., BRELSFORD, A., BUTCHER, B. G., MESSER, P. W., and LOVETTE, I. J. 2016. Plumage genes and little else distinguish the genomes of hybridising warblers. *Current Biology*, **26**: 2313-2318.

TOEWS, D. P. L., HOFFMEISTER, N. R., and TAYLOR, S. A. 2017.The evolution and genetics of carotenoid processing in animals. *Trends in Genetics*, **33**: 171-182.

TWYFORD, A. D., and ENNOS, R. A. 2012. Next-generation hybridization and introgression. *Heredity*, **108**: 179-189.

TWYMAN, H., ANDERSSON, S. and MUNDY, N.I., 2018. Evolution of CYP2J19, a gene involved in colour vision and red coloration in birds: positive selection in the face of conservation and pleiotropy. *BMC evolutionary biology*, **18**(1), p.22.

UY JAC, COOPER EA, CUTIE S, CONCANNON MR, POELSTRA JW, MOYLE RG, and FILARDI, C. E., 2016. Mutations in different pigmentation genes are associated with parallel melanism in island flycatchers. Proceedings of Royal Soceity B 283, 20160731. (doi:10.1007/s00265-013-1492-y)

VALLIN, N., RICE, A. M., BAILEY, R. I., HUSBY, A., and QVARNSTRÖM, A. 2012. Positive feedback between ecological and reproductive character displacement in a young avian hybrid zone. *Evolution*, **66**: 1167-1179.

VIJAY, N., BOSSU, C.M., POELSTRA, J.W., WEISSENSTEINER, M.H., SUH, A., KRYUKOV, A.P. and WOLF, J.B., 2016. Evolution of heterogeneous genome differentiation across multiple contact zones in a crow species complex. *Nature communications*, **7**, p.13195.

VOROBYEV, M., OSORIO, D., BENNETT, A.T., MARSHALL, N.J. and CUTHILL, I.C., 1998. Tetrachromacy, oil droplets and bird plumage colours. *Journal of Comparative Physiology A*, **183**:621-633.

WALSH, J., SHRIVER, W. G., OLSEN, B. J, and KOVACH, A. I. 2016. Differential introgression and the maintenance of species boundaries in an advanced generation avian hybrid zone. *BMC Evolutionary Biology*, **16**: 65

WHEATCROFT, D. and QVARNSTRÖM, A., 2017. Reproductive character displacement of female, but not male song discrimination in an avian hybrid zone. *Evolution*, 71:1776-1786.

WHILE, G. M., MICHAELIDES, S., HEATHCOTE, R. J. P., MACGREGOR, H. E. A., ZAJAC, N., BENINDE, J., and CARAZO, P. et al. 2015. Sexual selection drives asymmetric introgression in wall lizards. *Ecology Letters*, **18**: 1366-1375.

WINTER, D. J. 2012. MMOD: an R library for the calculation of population differentiation statistics. *Molecular Ecology Resources*, **12**(6), 1158–1160.

ZHEN, Y., HARRIGAN, R.J., RUEGG, K.C., ANDERSON, E.C., NG, T.C., LAO, S., LOHMUELLER, K.E. and SMITH, T.B., 2017. Genomic divergence across ecological gradients in the Central African rainforest songbird (*Andropadus virens*). *Molecular ecology*, **26**:4966–4977

ZHENG, X., LEVINE, D., SHEN, J., GOGARTEN, S. M., LAURIE, C., and WEIR, B. S., 2012. A high- performance computing toolset for relatedness and prin- cipal component analysis ofSNP data. *Bioinformatics*, **28**, 3326–3328.

ZHOU, X. and STEPHENS, M. 2012. Genome-wide efficient mixed-model analysis for association studies. *Nature Genetics*, **44**:821-824.

CHAPTER FIVE

CONCLUSIONS

Species delimitation among the feathered creatures in recent times has been largely based on on molecular phylogenetics where efforts are being made to use as many markers as possible to enhance support for the recovered topology, or alternatively on phenotypic differences, including morphology, plumage and songs. But these methods take no account of the event of rapid differentiation in specific traits important in reproductive isolation.

In the first section of my project, we examined the variation in phenotype, including morphology, plumage and song and genotypic variation, specifically in mitochondrial and nuclear genes among populations of yellow-rumped tinkerbird *Pogoniulus bilineatus* in East Africa. Based on the data and analysis presented in Chapter 2 of my thesis, we provided evidence for discordance between genetic distance and phenotypic traits driven by rapid song divergence between *P. b. fischeri* from Kenya and Zanzibar and *P. b. bilineatus* from Tanzania. *P. b. bilineatus* and *P. b. fischeri* failing to recognize one another's songs implies assortative mating in secondary contact. There is the possibility of interbreeding between *P. b. bilineatus* and *P. b. conciliator* from the Eastern Arc Mountains due to song similarity irrespective of the fact that they are genetically more distant from each other compared to the genetic distance between *P. b. bilineatus* and *P. b. fischeri*. Having found considerable divergence in song, supported by variation in morphology and plumage and reciprocal monophyly, it will be a credit to our biodiversity and conservation efforts to reclassify the subspecies into separate species.

In the following chapter I examined an interaction between two species of tinkerbirds that do come into secondary contact and have been diverging an order of magnitude longer than *P. b. bilineatus* and *P. b. fischeri* have, yet there is evidence of extensive hybridisation.

Two natural possibilities in the event of hybridisation between closely related species could either be that hybridisation is maladaptive or the hybrids do not suffer from reduced fitness. Hybridisation would be maladaptive if the hybrids suffer from reduced viability, they are sterile, or they are poorly adapted to the prevailing ecological conditions of their habitats, mostly if the adaptation of the parental forms is restricted to the either side of an ecological gradient (Hatfield and Schluter 1999). A further scenario whereby hybridisation could result in reduced fitness is if hybrids are selected against through sexual selection due to their intermediate appearance or differences in communication signals from parental forms. On the other hand, the absence of a reduction in fitness among hybrids would lead to the persistence of the hybrid zone, which would allow for genetic introgression between the interacting species. This may be the case where the habitats of the hybrids provide ecological conditions favourable to the hybrids and the intermediate appearance of the hybrids does not constitute a barrier to gene flow with parental forms. We examined interpopulation genetic and phenotypic variation across the contact zone of Yellow-fronted tinkerbird (*Pogoniulus chrysoconus*) and Red-fronted tinkerbird (*Pogoniulus pusillus*) to test the extent of introgressive hybridization between the species based on one mitochondrial gene (Cytochrome *b*) and 10 microsatellite markers. We found evidence of a mismatch between phenotypic and genetic characteristics of *P. c. extoni* and *P. p. pusillus* despite a long history of divergence in their primary distinguishing traits of yellow and red forecrowns respectively. There is evidence of asymmetrical introgression of *P. p. pusillus* plumage into the genome of *P. c. extoni* and indication of expansion of the contact zone into the historical allopatric region. The results from the second section of my thesis contributes to our understanding of the extents of phenotypic and genetic divergence that might be insufficient to maintain reproductive isolation.

There is increasing interest in the use of hybrid zones to study speciation processes, mostly as they provide a natural laboratory to examine the role of selection in maintaining

phenotypic characters among interacting species with efforts to identify the genomic regions that maintain species boundaries. In the third section of my research, we examined the factors that mediate interbreeding between *Pogoniulus chrysoconus* and *Pogoniulus pusillus* across four independent contact zones and identified genomic regions associated with phenotypic traits of plumage colouration by analysing RADseq data. This section of my research involved the following: measuring phenotypic characters, specifically song, plumage and morphology, across four contact zones of *P. pusillus* and *P. chrysoconus* tinkerbirds, identifying the extent of introgressive hybridisation across three contact zones between the two species using genomic methods and comparing with patterns of phenotypic introgression using cline analyses, and identifying the regions of the genome associated with red versus yellow plumage coloration in tinkerbirds. Among the contact zones considered in this study, different patterns of interaction between *Pogoniulus chrysoconus* and *P. pusillus* exist at each of the contact zones. Similarity in song drives introgressive hybridisation between *Pogoniulus c. extoni* and *Pogoniulus p. pusillus* in Southern Africa and therefore undermines the dependence on visual cues in mate choice in these species. The introgressive hybridisation between the species is also reflected in the finding that several individuals had intermediate plumage coloration on the forecrown, suggesting admixture in the alleles that control for plumage coloration between the two populations in Southern Africa. Several candidate genes were associated with red versus yellow plumage coloration in tinkerbirds.

Overall, the data and analyses presented in this research contribute to our understanding of the criteria important in species delimitation, with recommendation to take into account rapid differentiation in specific traits important in reproductive isolation. Also, it provided additional insight on the influence of interactions between closely related species on speciation and ultimately on biodiversity by highlighting the factors that maintain species distributions,

and specifically the significance of the interplay between phenotypic similarity, genetic relatedness and ecological gradients in maintaining species boundaries.

APPENDIX TO CHAPTER TWO

Table S1: Levene's test of homogeneity of variances across the populations' song characteristics.

Song variables	Population	Mean±Variance	df	F	*P*
Song rate	*bilineatus*	0.434±1.044e-03	2	2.839	0.0658
	fischeri	1.047±1.465e-05			
	conciliator	0.451±9.162e-04			
Peak frequency	*bilineatus*	1088.609±1738.661	2	2.555	0.0855
	fischeri	1102.318±613.603			
	conciliator	1088.722±968.472			

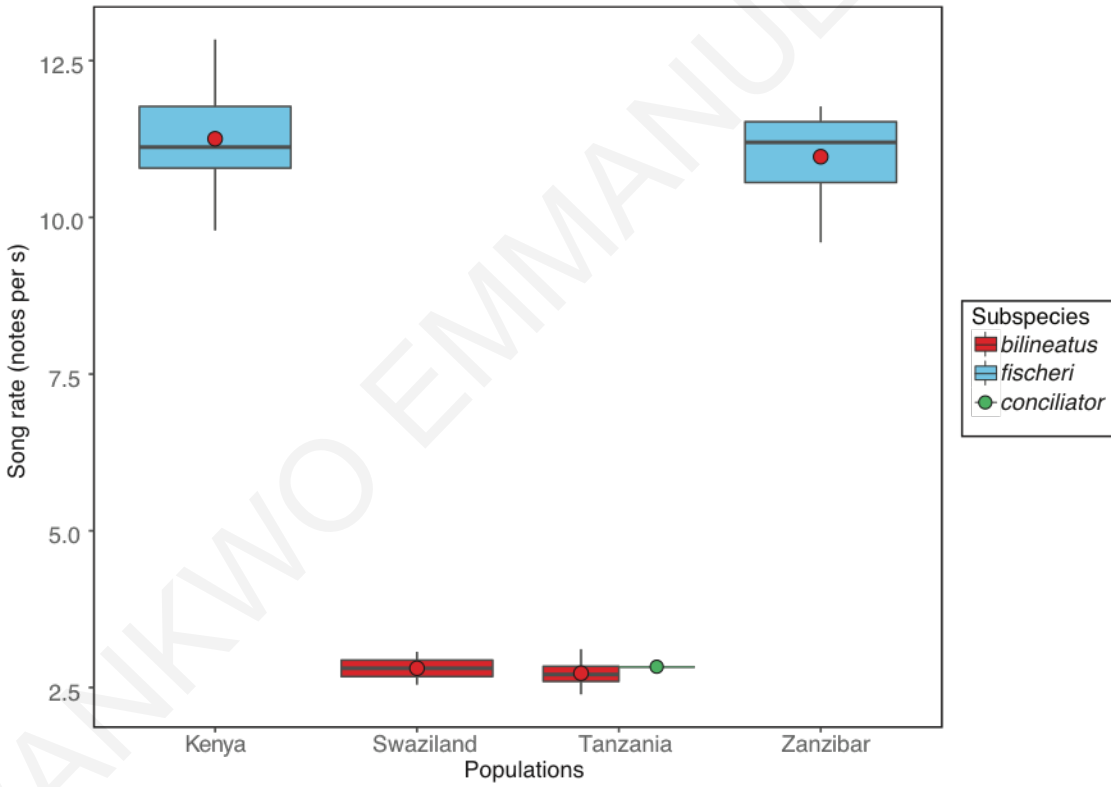

Figure S1. Song rate by population, showing *fischeri* from Kenya and Zanzibar do not differ in song rate from each other, though sing significantly faster than the other three populations. Southern Africa *bilineatus* (from Swaziland) sing at the same rate as *bilineatus* from Tanzania and *conciliator* from the Eastern Arc Mountains.

Table S2

Principal components extraction on playback measurements. 2 PCs had eigenvalues > 1

Component	Eigenvalue	Difference	Proportion	Cumulative
Comp1	3.70403	2.50249	0.463	0.463
Comp2	1.20154	0.27892	0.1502	0.6132
Comp3	0.922617	0.167815	0.1153	0.7285
Comp4	0.754802	0.191255	0.0944	0.8229
Comp5	0.563547	0.193013	0.0704	0.8933
Comp6	0.370534	0.123263	0.0463	0.9396
Comp7	0.247271	0.0116114	0.0309	0.9705
Comp8	0.235659	.	0.0295	1

Table S3. Varimax rotation of extracted components based on body size variables.

Component	Variance	Difference	Proportion	Cumulative
Comp1	3.44059	1.97561	0.4301	0.4301
Comp2	1.46498	.	0.1831	0.6132

Table S4. Rotated Principal Component Matrix using Varimax rotation on morphology variables.

Variable	Comp1	Comp2	Unexplained
wing	0.4858	-0.0975	0.2469
tarsus	0.4594	-0.2389	0.359
tail	0.4719	-0.0078	0 .2393
bill_length	0.4019	0.1002	0.3676
culmen	0.256	0.172	0.6635
upper_bill	-0.123	0.7063	0.3505
bill_width	0.1151	0.4925	0.512
lower_mandible	0.2735	0.3902	0.3557

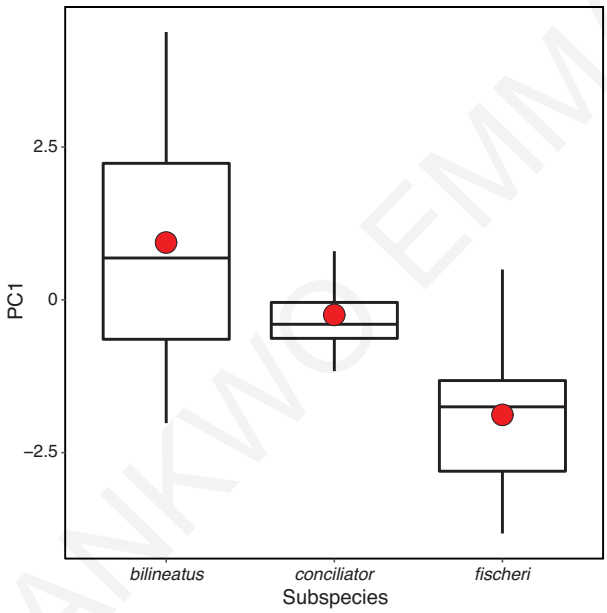

Figure S2: Differences in body size between *bilineatus*, *conciliator* and *fischeri* based on the first principal component from the PCA.

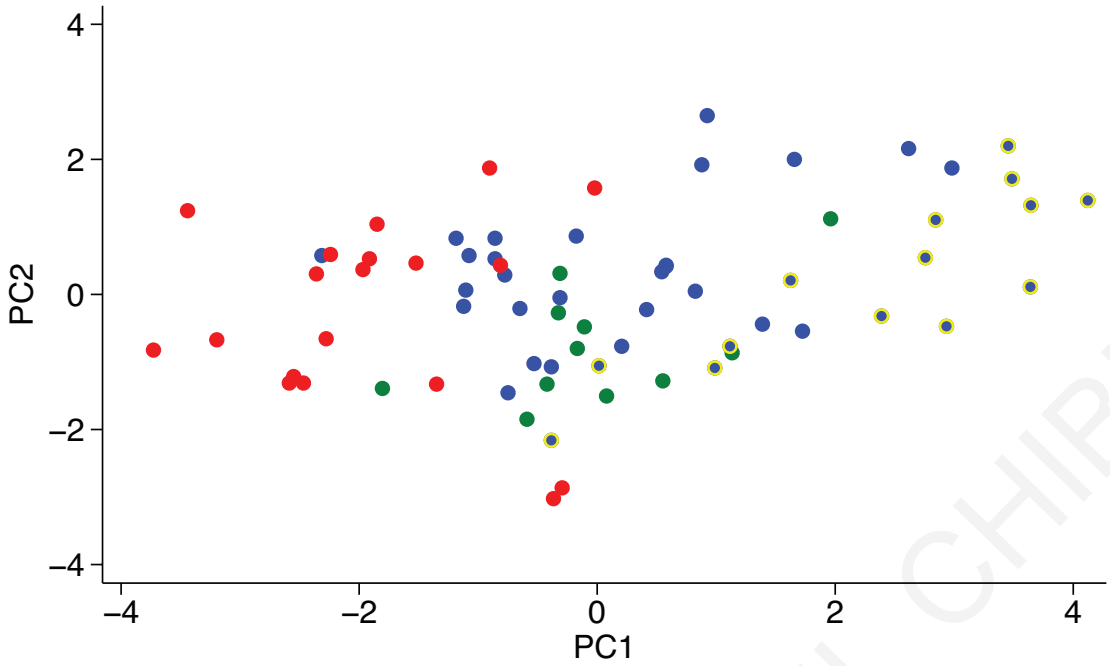

Figure S3. Scatter plot of morphology based on the first two principal components. PC1 was correlated with wing, tarsus, tail and bill length, and PC2 with bill width, upper bill depth and lower mandible length. While there is overlap in PC2 and PC1, in the latter, *fischeri* (red circles) appears smaller overall than *bilineatus*, (blue circles) *and conciliator* (green circles), though less so with the latter after accounting for those individuals at higher latitudes (< -11.0, blue circles with yellow outline.

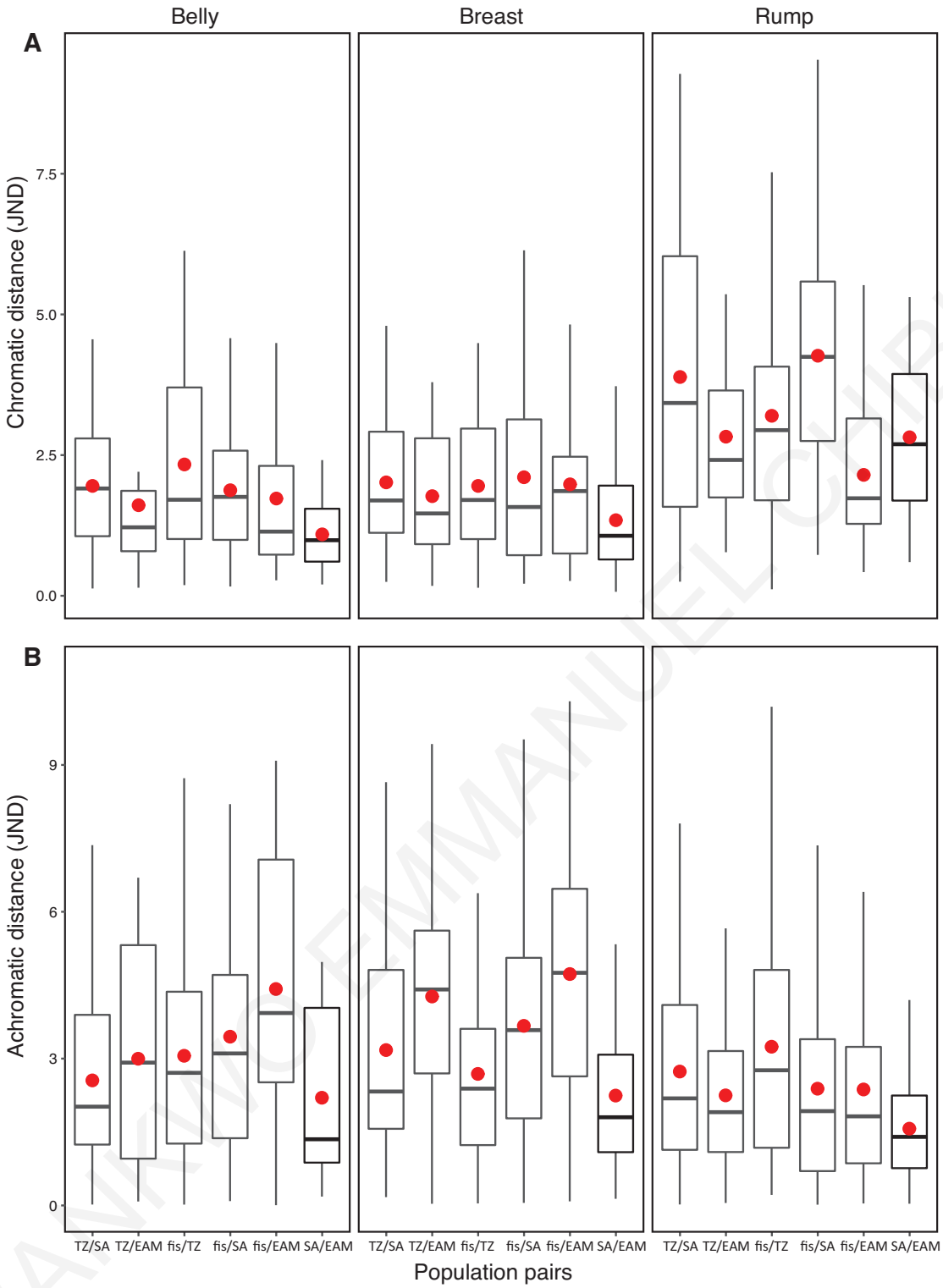

Figure S4. A) Chromatic and B) achromatic distance of the plumage patches of *P. bilineatus* and *P. fischeri*. Boxes represent interquartile range, black lines the median, and red dots the mean values TZ = *bilineatus* from Tanzania, EAM = Eastern Arc Mountains (*conciliator*), SA = *bilineatus* from Southern Africa, *fis* = *fischeri*.

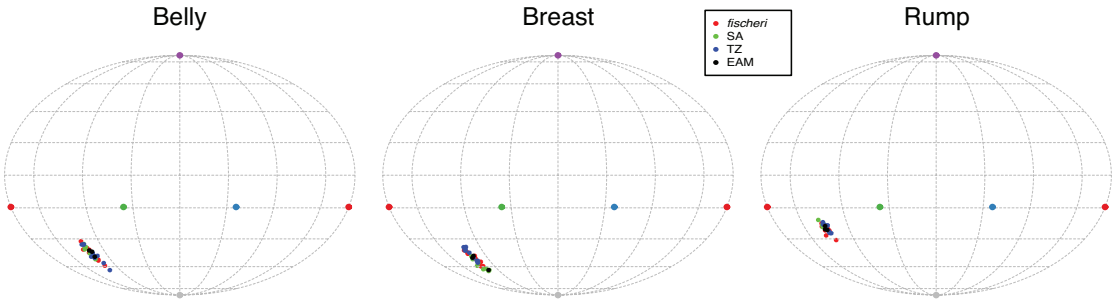

Figure S5. Hue projection plot of colour points from the plumage patches.

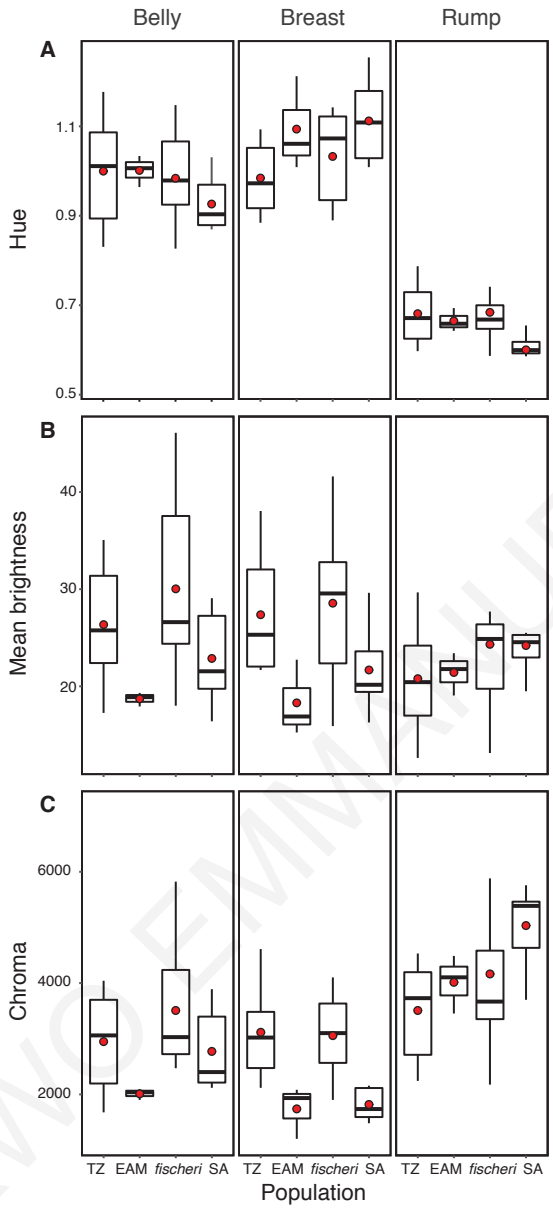

Figure S6: Boxplots illustrating hue, mean brightness and chroma of belly, breast, and rump patches for four populations. Boxes represent interquartile range, black lines the median, and red dots the mean values. TZ = *bilineatus* from Tanzania, EAM = Eastern Arc Mountains (*conciliator*), SA = *bilineatus* from Southern Africa.

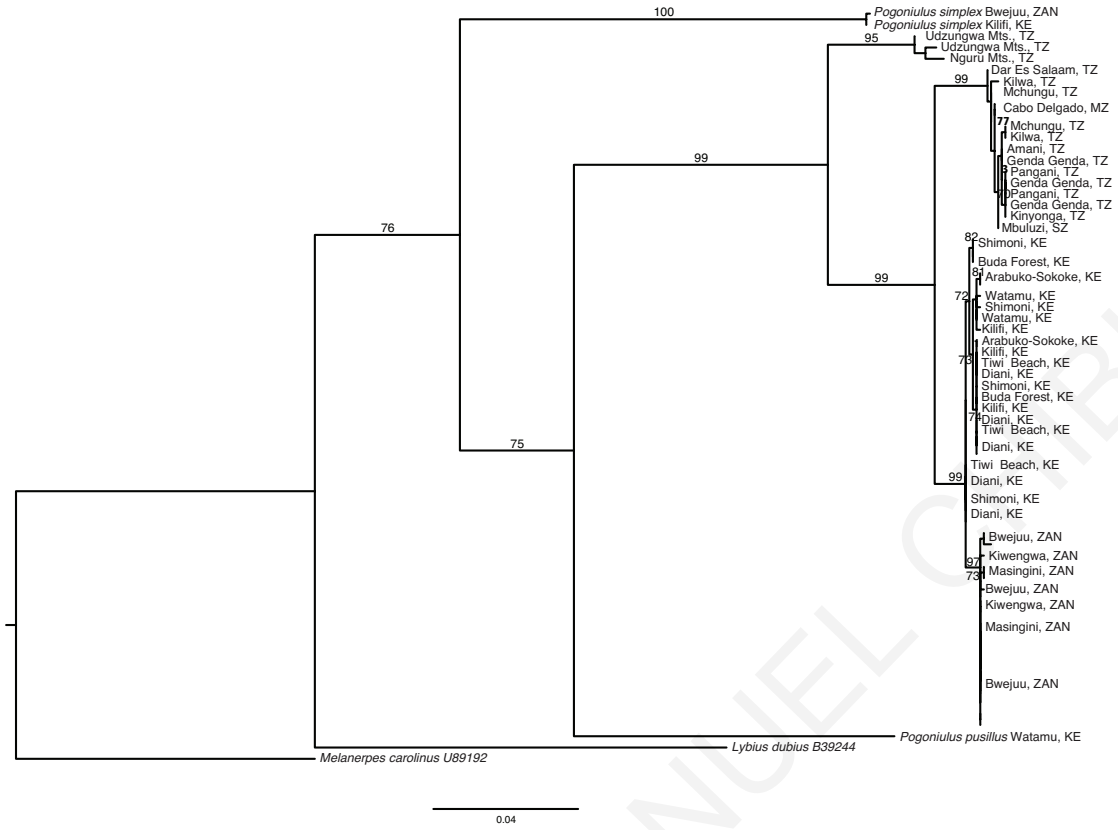

Figure S7. Maximum likelihood tree (RAxML) of Cytochrome *b*. The branch labels show bootstrap values over 70.

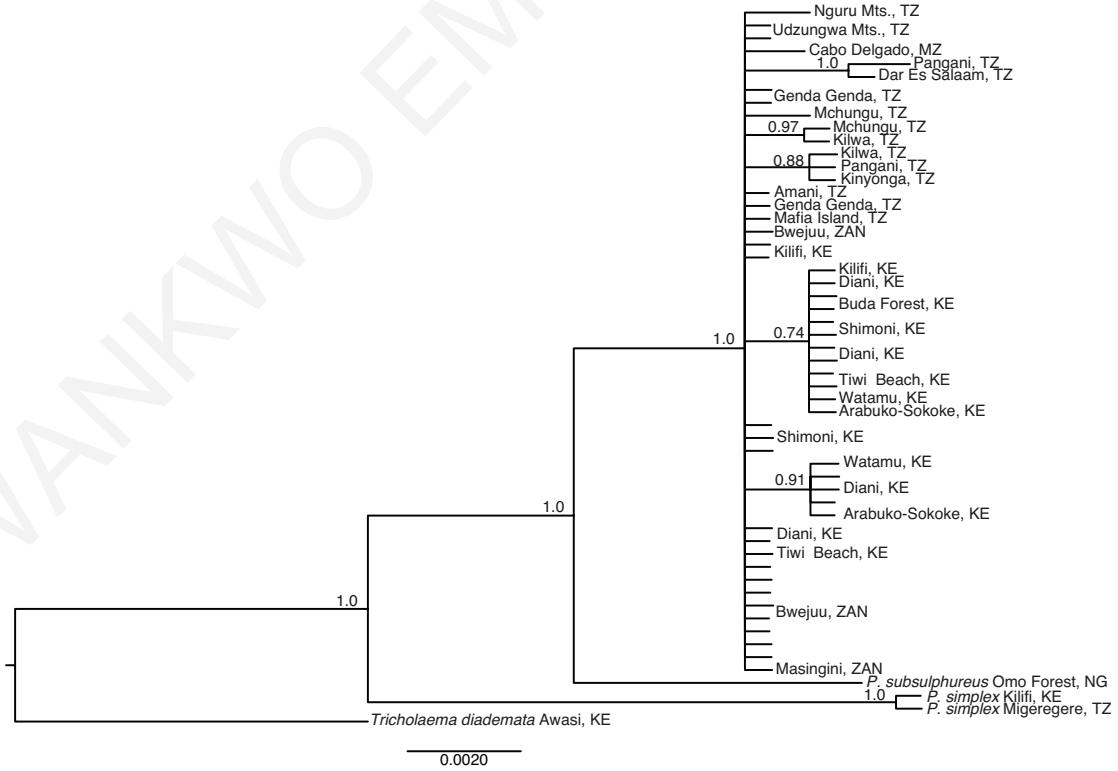

Figure S8. Bayesian inference consensus tree of β fibrinogen intron 5 (node values represent Posterior values over 0.7).

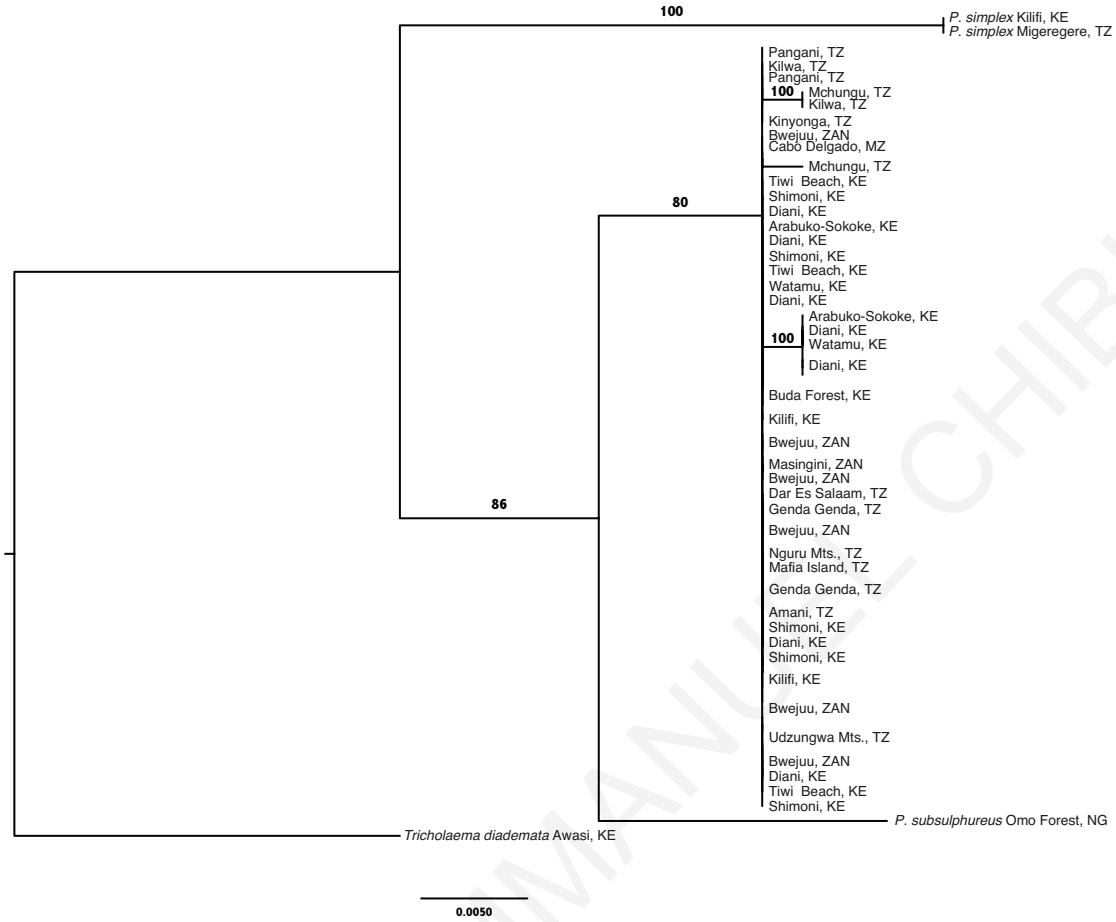

Figure S9. Maximum likelihood tree (RAxML) of β fibrinogen intron 5. The branch labels show bootstrap values over 70.

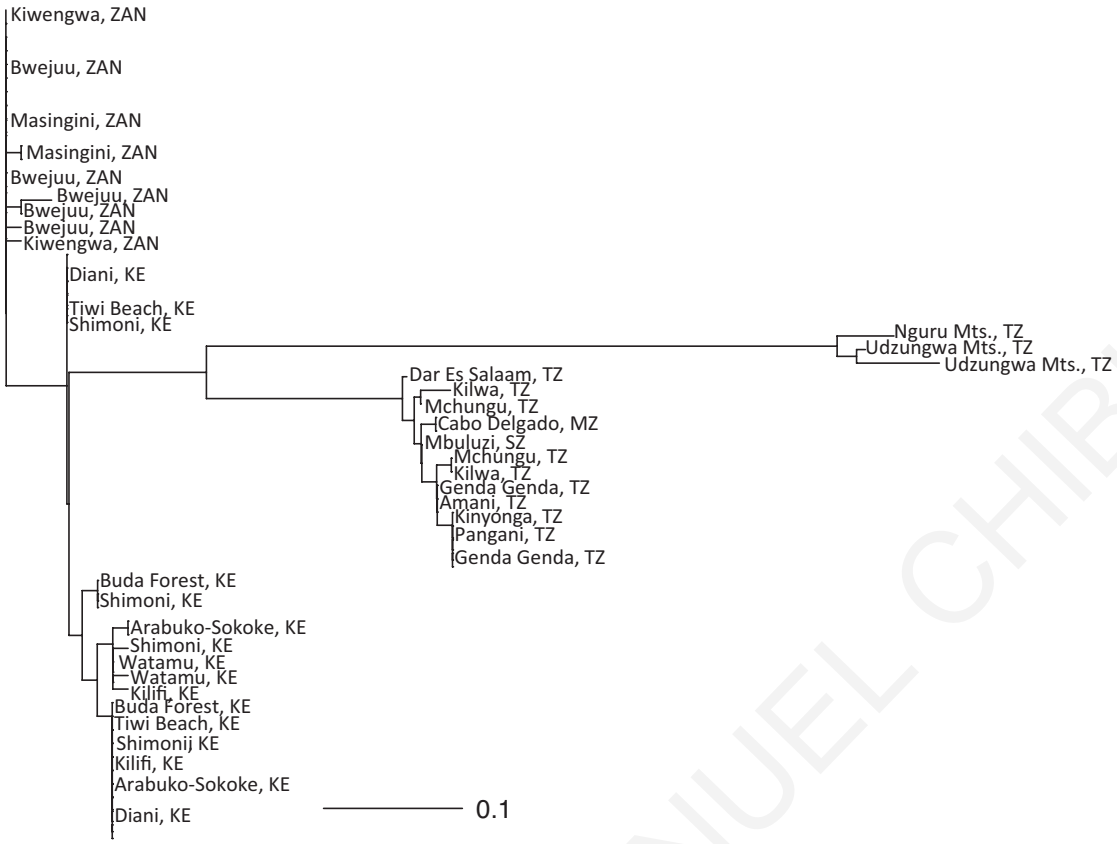

Figure S12. Dendrogram based on genetic distance among individuals. UPGMA tree produced from Provesti's distance with 10000 bootstrap replicates (node values representing bootstrap values greater than 50% are shown). Edge length is in proportion to the genetic distances.

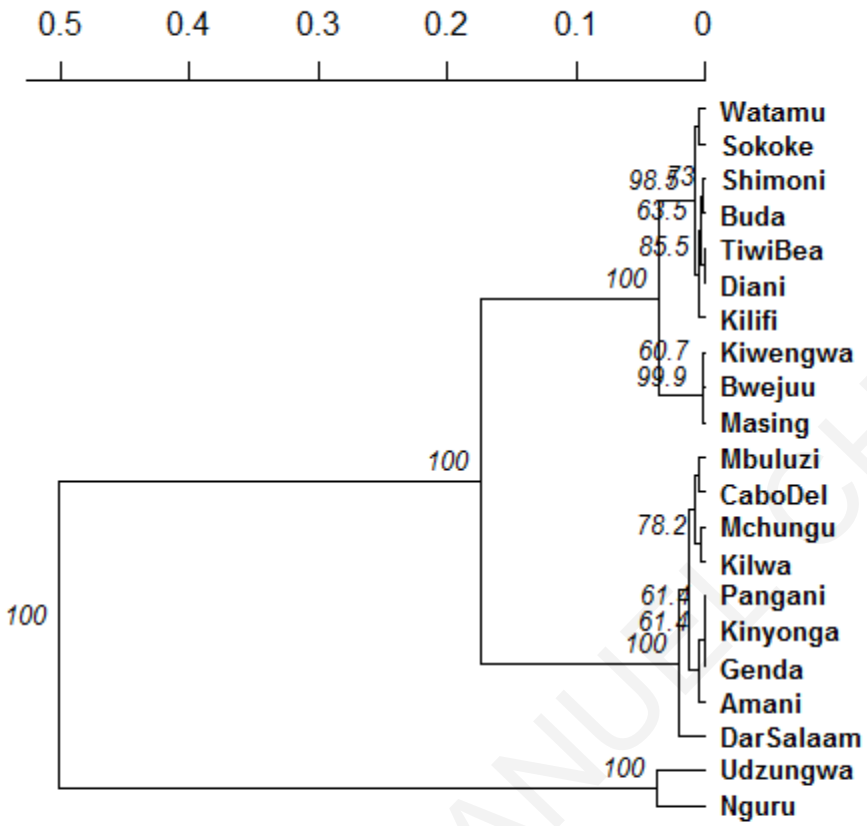

Figure S13. Dendrogram based on genetic distance among the species sampling locations. UPGMA tree produced from Provesti's distance with 10000 bootstrap replicates (node values representing bootstrap values greater than 50% are shown).

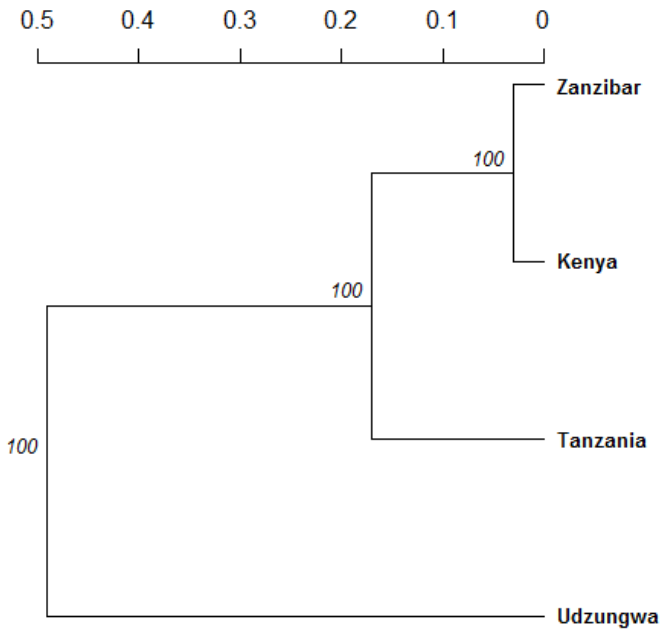

Figure S14. Dendrogram based on genetic distance among the subspecies populations. UPGMA tree produced from Provesti's distance with 10000 bootstrap replicates (node values representing bootstrap values greater than 50% are shown).

Table S6: Coordinates and colorimetric variables that represent reflectance spectra of the populations' belly, breast and rump patches in the avian tetrahedral color space (mean±sd).

Patch	Subspecies	Violet wavelength	Short wavelength	medium wavelength	Long wavelength	h.theta	h.phi	r.achieved
Belly	*bilineatus*	0.13±0.03	0.19±0.03	0.33±0.02	0.33±0.03	0.53±0.05	-0.89±0.11	0.47±0.12
	conciliator	0.13±0.004	0.19±0.01	0.33±0.01	0.32±0.01	0.54±0.02	-0.86±0.04	0.44±0.17
	fischeri	0.12±0.02	0.19±0.03	0.34±0.02	0.34±0.03	0.52±0.04	-0.88±0.09	0.51±0.11
	SA	0.12±0.01	0.18±0.01	0.34±0.01	0.34±0.01	0.49±0.02	-0.83±0.06	0.49±0.04
Breast	*bilineatus*	0.13±0.02	0.19±0.01	0.33±0.01	0.33±0.02	0.52±0.02	-0.88±0.07	0.47±0.08
	conciliator	0.14±0.02	0.21±0.01	0.32±0.01	0.31±0.02	0.55±0.04	-0.97±0.10	0.41±0.1
	fischeri	0.12±0.03	0.20±0.02	0.33±0.02	0.33±0.03	0.53±0.05	-0.93±0.08	0.48±0.12
	SA	0.15±0.02	0.22±0.01	0.30±0.01	0.31±0.01	0.51±0.06	-1.03±0.07	0.38±0.08
Rump	*bilineatus*	0.11±0.02	0.09±0.03	0.37±0.02	0.41±0.03	0.43±0.02	-0.57±0.04	0.62±0.14
	conciliator	0.10±0.01	0.08±0.01	0.38±0.001	0.42±0.01	0.41±0.02	-0.57±0.02	0.66±0.03
	fischeri	0.11±0.01	0.10±0.02	0.37±0.01	0.41±0.02	0.40±0.04	-0.59±0.05	0.60±0.08
	SA	0.09±0.01	0.05±0.01	0.39±0.01	0.45±0.01	0.38±0.02	-0.53±0.02	0.76±0.04

Table S7: Colour volume overlap between the subspecies

Body part	Species1	Species2	Volume1	Volume2	Overlap	Percentage
Belly	*bilineatus*	*fischeri*	9.47e-06	1.47e-05	6.30e-06	66%
	bilineatus	*conciliator*	9.47e-06	6.73e-07	6.10e-07	91%
	bilineatus	SA	9.47e-06	8.01e-07	3.23e-07	40%
	fischeri	*conciliator*	1.47e-05	6.73e-07	2.91e-07	43%
	fischeri	SA	1.47e-05	8.01e-07	5.25e-07	65%
	conciliator	SA	6.73e-07	8.01e-07	0	0%
Breast	*bilineatus*	*fischeri*	4.34e-06	7.18e-06	2.02e-06	47%
	bilineatus	*conciliator*	4.34e-06	8.21e-07	2.84e-07	35%
	bilineatus	SA	4.34e-06	1.90e-06	0	0%
	fischeri	*conciliator*	7.18e-06	8.21e-07	5.85e-07	71%
	fischeri	SA	7.18e-06	1.90e-06	3.34e-07	18%
	conciliator	SA	8.21e-07	1.90e-06	0	0%
Rump	*bilineatus*	*fischeri*	1.71e-05	2.69e-05	3.91e-06	23%
	bilineatus	*conciliator*	1.71e-05	1.11e-06	3.92e-07	35%
	bilineatus	SA	1.71e-05	3.60e-06	2.08e-07	6%
	fischeri	*conciliator*	2.69e-05	1.11e-06	1.03e-06	93%
	fischeri	SA	2.69e-05	3.60e-06	0	0
	conciliator	SA	1.11e-06	3.60e-06	0	0

APPENDIX TO CHAPTER THREE

Table A1. Factor Loadings on morphology variables with varimax rotated PC1 and PC2.

Variables	PC1	PC2
Mass	-0.0774	0.307
Wing	-0.0375	0.8329
Tarsus	0.6037	0.1535
Tail	-0.0257	0.7585
Culmen	0.5102	-0.2039
Exposed	0.828	-0.0132
Depth	0.7562	0.0419
Width	0.2902	0.6134
	PC1	PC2
SS loadings	1.9745	1.8067
Proportion Var	0.2468	0.2258
Cumulative Var	0.2468	0.4727
Proportion Explained	0.5222	0.4778
Cumulative Proportion	0.5222	1

Table A2. Distrubution and subspecies of *P. chrysoconus* and *P. pusillus*.

Species	Subspecies	Distribution
P. pusillus	*uropygialis* (Heuglin, 1862)	Eritrea and N and C Ethiopia to N Somalia
	affinis (Reichenow, 1879)	SE South Sudan, S Ethiopia and S Somalia, S to SE Tanzania
	pusillus (Dumont de Sainte Croix, 1816)	S Mozambique, S to E South Africa (to S Eastern Cape)
P. chrysoconus	*chrysoconus* (Temminck, 1832)	SW Mauritania and Senegal E to NW Ethiopia, S to N edge of forest in C Cameroon, N and NE DRCongo, Burundi and NW Tanzania
	xanthostictus (Blundell and Lovat, 1899)	highlands of C and S Ethiopia
	extoni (E. L. Layard, 1871)	Angola, SE Congo and S DRCongo, E to S Tanzania, S to NC Namibia, N Botswana, NE South Africa and S Mozambique

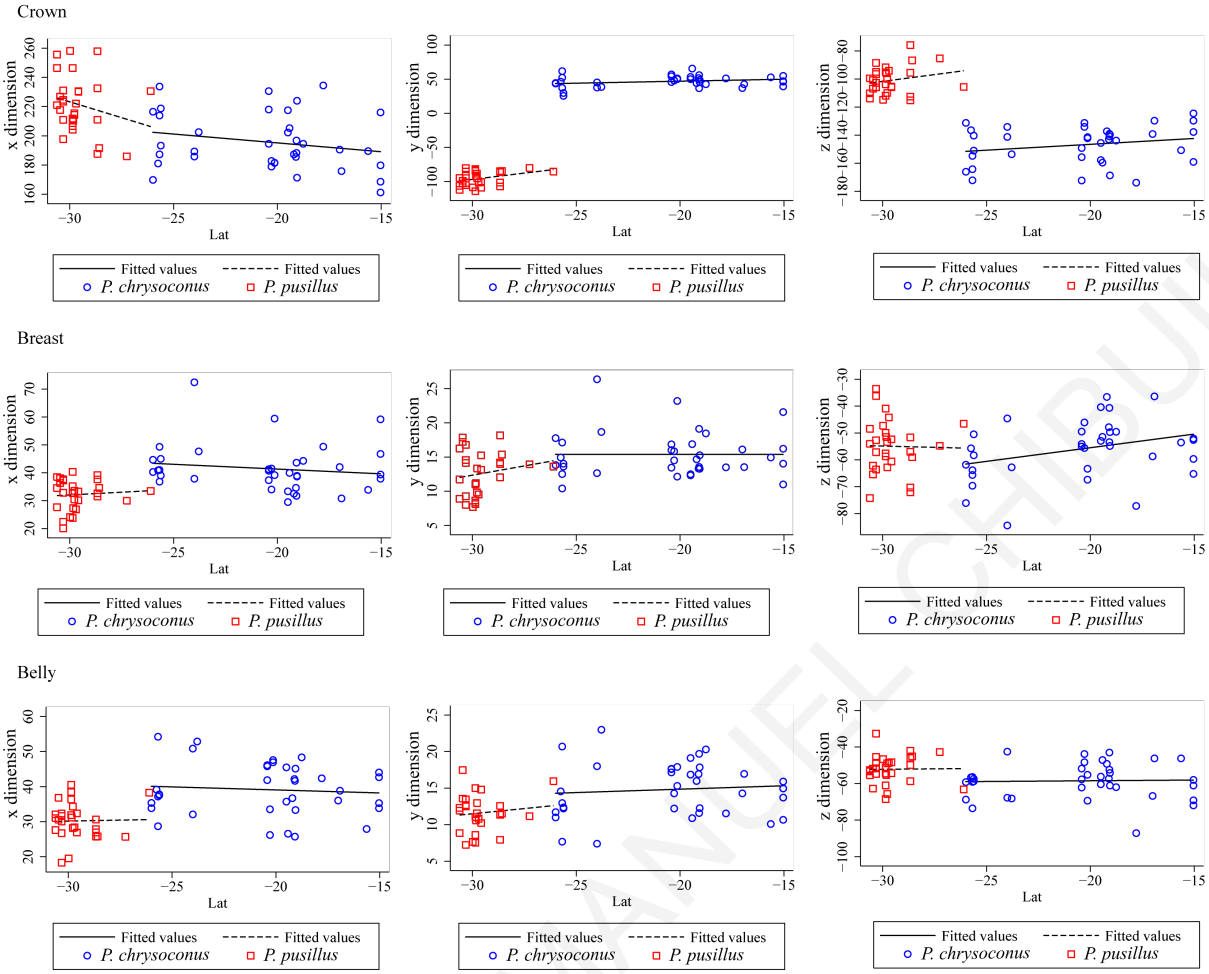

Figure A1. Distributions of tetrahedral x, y, z colour cordinates for crown, breast and belly plumage patches against latitude shows a variety of patterns, with convergence and divergence in different measures towards the contact zone.

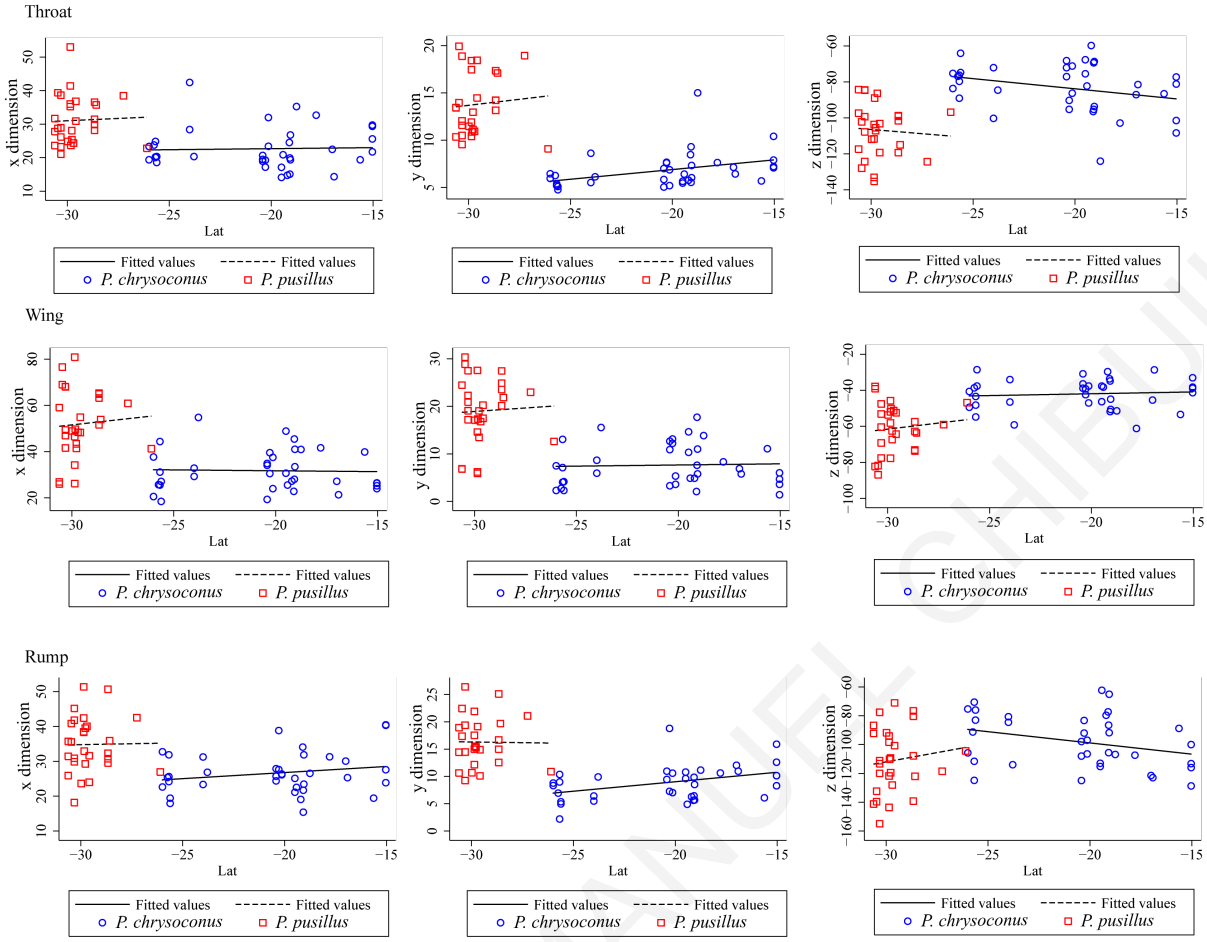

Figure A2. Distributions of tetrahedral x, y, z colour cordinates for throat, wing and rump plumage patches against latitude shows a variety of patterns, with convergence and divergence in different measures towards the contact zone.

APPENDIX TO CHAPTER FOUR

Table A2. Factor Loadings on morphology variables with varimax rotated PC1 and PC2.

	PC1	PC2
Wing	0.6048	0.4371
Tarsus	0.4275	0.6999
Tail	0.4081	0.7115
Bill length	0.7663	0.0263
exposed	0.8518	0.1785
Upper bill length	0.2806	0.2098
Bill width	0.6244	-0.0121
lowermandible	0.8022	0.1655
patch_depth	-0.3568	0.6057
patch_width	0.0028	0.7488

	PC1	PC2
SS loadings	3.2673	2.2187
Proportion Var	0.3267	0.2219
Cumulative Var	0.3267	0.5486
Proportion Explained	0.5956	0.4044
Cumulative Proportion	0.5956	1

Table A3. Summary of samples used in this study and analyses conducted with the samples.

Taxon	Locality	mtDNA	nDNA	Biometrics/ Reflectance	Microsat/ RADseq	Catalogue/ Ring number	Source
P. b. fischeri	Mtwara, Mikindani, Tanzania			Reflectance		74.169	ZMUC
P. b. fischeri	Mtwara, Mikindani, Tanzania			Reflectance		74.171	ZMUC
P. b. fischeri	Mtwara, Mikindani, Tanzania			Reflectance		74.172	ZMUC
P. b. fischeri	Mtwara, Mikindani, Tanzania			Reflectance		74.173	ZMUC
P. b. fischeri	Mtwara, Mikindani, Tanzania			Reflectance		74.174	ZMUC
P. b. fischeri	Mtwara, Mikindani, Tanzania			Reflectance		74.178	ZMUC
P. b. fischeri	Mtwara, Mikindani, Tanzania			Reflectance		74.179	ZMUC
P. b. fischeri	Mtwara, Mikindani, Tanzania			Reflectance		74.197	ZMUC
P. b. fischeri	Mtwara, Mikindani, Tanzania			Reflectance		74.198	ZMUC
P. p. pusillus	Natal, Hillcrest, nr. Durban			Biometrics		7546	Peabody
P. p. pusillus	Natal, Pinetown nr. Durban			Biometrics		7547	Peabody
P. p. uropygialis	Somalia, Hullier			Biometrics		7772	FMNH
P. p. uropygialis	Somalia, Hullier			Biometrics		7773	FMNH
P. p. pusillus	South Africa, Natal, Durban			Biometrics		8619	FMNH
P. c. extoni	South Africa, Transvaal, Pretoria			Biometrics		8620	FMNH

P. p. affinis	Kenya (British E Africa) Tsavo		Biometrics	11008	Peabody
P. scolopaceus	CSRS	MH364239(Cytb), MH364255(ATP6/8)	Biometrics	20237	FMNH
P. p. uropygialis	Somalia, Hargeisa		Biometrics	23378	Peabody
P. p. affinis	Kenya, 8 mi S Isiolo		Biometrics	25711	LSU
P. p. affinis	Kenya, 22 mi N Garsen		Biometrics	25712	LSU
P. p. affinis	Kenya, 22 mi N Garsen		Biometrics	25713	LSU
P. p. affinis	Kenya, W. Suk, Kongelai		Biometrics	25715	LSU
P. p. affinis	Kenya, W. Suk, Kongelai		Biometrics	25716	LSU
P. p. pusillus	S. Africa, Natal, Umbuzi MS, 16km NE of Port Shepstone		Biometrics	37335	UCLA
P. p. pusillus	S. Africa, Natal, Umbuzi MS, 16km NE of Port Shepstone		Biometrics	37336	UCLA
P. c. extoni	Zimbabwe, Matopos SR, Silosi Dip Tank		Biometrics	47640	Peabody
P. c. extoni	Zimbabwe, Matopos, Bedja dip		Biometrics	47641	Peabody
P. c. extoni	Angola, Carolo 15 km SW		Biometrics	50619	Peabody
P. c. extoni	Angola, Carolo 15 km SW		Biometrics	50621	Peabody
P. c. extoni	Angola, Carolo 15 km SW		Biometrics	50622	Peabody
P. c. extoni	Angola, Carolo 15 km SW		Biometrics	50623	Peabody
P. c. extoni	Angola, Carolo 40 km E		Biometrics	50624	Peabody

P. c. extoni	Angola, Rio Luachimo, 50 km W (or N?) of Dala, Distr. Lunde	Biometrics	50625	Peabody
P. c. extoni	Angola, 40 km NE of Silva Porto (=Bie)	Biometrics	50626	Peabody
P. c. extoni	Angola, Duque de Bragaura (42 km N of)	Biometrics	50627	Peabody
P. b. fischeri	Kenya, Coast Province, Kilifi	Reflectance	55068	LACM
P. b. fischeri	Kenya, Coast Province, Kilifi	Reflectance	55069	LACM
P. b. fischeri	Kenya, Coast Province, Kilifi	Reflectance	55070	LACM
P. b. fischeri	Kenya, Coast Province, Kilifi	Reflectance	55071	LACM
P. c. chrysoconus	W. Kenya, Bungoma, Elgon, Nyanza	Biometrics	55072	LACM
P. c. chrysoconus	W.Kenya, Kisumu	Biometrics	55073	LACM
P. c. chrysoconus	W. Kenya, Kisumu	Biometrics	55074	LACM
P. c. extoni	Uganda, Butiaba	Biometrics	55075	LACM
P. p. affinis	Kenya, Bura, Tana River	Biometrics	55076	LACM
P. p. pusillus	Natal, Park Rynie, S. Coast	Biometrics	58541	Peabody
P. c. extoni	Tanzania, Songea dist, Namabengo	Biometrics	58724	LACM
P. c. extoni	Namalinago, Sangia Dist.	Biometrics	58725	LACM
P. c. extoni	Tanzania, Nachingwea dist, Kilimarondo	Biometrics	58726	LACM
P. b. fischeri	Tanzania, Coast Region, Kisaware Dist, Soga	Reflectance	58730	LACM

P. b. fischeri	Tanzania, Coast Region, Kisaware Dist, Soga	Reflectance	58731	LACM
P. p. affinis	Kenya, Samburu dist, Karissia Hills	Biometrics	60816	LACM
P. p. affinis	Kenya, Samburu dist, Karissia Hills	Biometrics	60817	LACM
P. p. affinis	Kenya, Samburu dist, Karissia Hills	Biometrics	60819	LACM
P. p. affinis	Kenya, Samburu dist, Karissia Hills	Biometrics	60820	LACM
P. p. affinis	Kenya, Samburu dist, Karissia Hills	Biometrics	60821	LACM
P. p. affinis	Kenya, Samburu dist, Karissia Hills	Biometrics	60822	LACM
P. c. chrysoconus	W. Kenya, 30mi E of Tororo	Biometrics	61067	LACM
P. b. bilineatus	Rhodesia, Haroni-Rusitu R Junction	Reflectance	63592	LACM
P. p. pusillus	S. Africa, Natal, Hillcrest, Shongweni	Biometrics	63595	LACM
P. p. pusillus	South Africa, Natal, Durban	Biometrics	63596	LACM
P. p. pusillus	South Africa, Natal, Durban	Biometrics	63597	LACM
P. b. fischeri	Kenya, Coast Province, Kilifi District, Sokoke Forest	Reflectance	68617	LACM
P. p. pusillus	Natal, Elandskop	Biometrics	69037	Peabody
P. p. affinis	Kenya, Mt. Nyiru, Sanburu	Biometrics	69688	LACM

	Dist, West Base			
P. p. affinis	Kenya, Samburu dist, Mt. Ngiru	Biometrics	69689	LACM
P. b. fischeri	Lindi, SE Tanzania	Reflectance	72228	ZMUC
P. b. fischeri	Lindi, SE Tanzania	Reflectance	72229	ZMUC
P. b. fischeri	Lindi, SE Tanzania	Reflectance	72240	ZMUC
P. b. fischeri	Lindi, SE Tanzania	Reflectance	72241	ZMUC
P. p. pusillus	Natal, Tongaat, N. Coast, South Africa	Biometrics	72381	Peabody
P. p. pusillus	Natal, Park Rynie, S. Coast, South Africa	Biometrics	72617	Peabody
P. p. pusillus	Natal, Park Rynie, S. Coast, South Africa	Biometrics	72618	Peabody
P. p. pusillus	Natal, Park Rynie, S. Coast, South Africa	Biometrics	72619	Peabody
P. p. affinis	Kenya, Lotongot area, Turkana dist.	Biometrics	75287	LACM
P. p. affinis	Kenya, Turkana dist, Lotangot area	Biometrics	75288	LACM
P. p. affinis	Kenya, Lotongot area, Turkana dist.	Biometrics	75289	LACM
P. p. affinis	Kenya, Machakos dist, Nbuami area, Kalam	Biometrics	77154	LACM
P. p. affinis	Kenya, Machakos, Kavguni	Biometrics	77357	LACM
P. p. pusillus	Natal, Ifafa, S. Coast	Biometrics	77863	Peabody

P. p. pusillus	Natal, Ifafa, S. Coast	Biometrics	77864	Peabody
P. p. pusillus	Natal, Tongaat, N. Coast	Biometrics	77866	Peabody
P. p. affinis	Kenya, Marsabit Dist, Mt. Kulal, above Gatab	Biometrics	78556	LACM
P. b. bilineatus	South Africa, Natal, Durban District, Reunion Rocks	Reflectance	78914	LACM
P. b. bilineatus	Mozambique, Gaza Dist., Macia, Sul do Save, Coastal Forest	Reflectance	78915	LACM
P. b. bilineatus	Mozambique, Inhambane, Coastal Forest	Reflectance	78916	LACM
P. p. affinis	Kenya, 5 mi NW of Isiolo NFD	Biometrics	79929	Peabody
P. b. fischeri	Kenya, Coast Prov, Kwale Dist, Kichaka Shimba	Reflectance	81213	LACM
P. b. fischeri	Kenya, Coast Prov, Kwale Dist, Shimba Hills	Reflectance	81355	LACM
P. b. fischeri	Kenya, Coast Prov, Kwale Dist, Shimba Hills	Reflectance	81431	LACM
P. b. fischeri	Kenya, Coast Province, Kilifi District, Arabuko	Reflectance	81767	LACM
P. c. extoni	Botswana, Monochela River; Xugana area	Biometrics	82502	LSU
P. c. extoni	Botswana, Monochela River; Xugana area	Biometrics	82503	LSU

P. c. extoni	Botswana, Four Rivers Camp; 60 mi. W Khwai Lodge	Biometrics	82504	LSU
P. p. uropygialis	Ethiopia, Webi River, near Cadjo	Biometrics	82727	FMNH
P. p. uropygialis	Ethiopia, Amhara, Gonder, Abala	Biometrics	82728	FMNH
P. c. xanthostictus	Ethiopia, Amhara, Gonder, Shimie	Biometrics	82729	FMNH
P. c. xanthostictus	Ethiopia, Gojam, Dembecha, 5 mi E	Biometrics	82730	FMNH
P. c. xanthostictus	Ethiopia, near Alata	Biometrics	82731	FMNH
P. p. affinis	Kenya, Lamu dist, Boni Forest, Bodhei	Biometrics	83917	LACM
P. p. affinis	Kenya, Lomu Dist, Boni Forest, Bodhei	Biometrics	83918	LACM
P. p. affinis	Tanzania, Dar Es Salaam 9 mi N	Biometrics	88662	Peabody
P. p. affinis	Tanzania, Dar Es Salaam 15 mi W	Biometrics	88663	Peabody
P. p. affinis	Tanzania, Dar Es Salaam 5 mi N	Biometrics	88664	Peabody
P. p. affinis	Tanzania, Dar Es Salaam	Biometrics	88665	Peabody
P. p. affinis	Tanzania, Morogoro, 15 mi N	Biometrics	88666	Peabody
P. p. affinis	Tanzania, Morogoro, 15 mi N	Biometrics	88667	Peabody
P. p. affinis	Tanzania, Lake Marigara (Western side)	Biometrics	88668	Peabody
P. p. affinis	Tanzania, Iringa	Biometrics	88670	Peabody
P. p. affinis	Tanzania, Dar Es Salaam 15 mi W	Biometrics	88671	Peabody

P. p. affinis	Tanzania, Dar Es Salaam 15 mi W			Biometrics	88672	Peabody
P. p. affinis	Tanzania, Morogoro, 18 mi N			Biometrics	88673	Peabody
P. p. affinis	Tanzania, Same			Biometrics	88674	Peabody
P. p. affinis	Tanzania, Iringa			Biometrics	88675	Peabody
P. p. affinis	Tanzania, Same			Biometrics	88676	Peabody
P. p. affinis	Kenya, Machakos dist, Muumandu			Biometrics	90889	LACM
P. b. bilineatus	Mafia Island		MG576361(BFIB)	Biometrics	91504	FMNH
P. c. chrysoconus	Tchibati	MH364231(Cytb), MH364262(ATP6/8)		Biometrics	95887	FMNH
P. c. xanthostictus	Sudan, Torit, Equatorial Province			Biometrics	103413	FMNH
P. c. xanthostictus	Sudan, Juba			Biometrics	103516	FMNH
P. c. chrysoconus	Kenya, Kisumu			Biometrics	113306	FMNH
P. c. extoni	Uganda, Lake Albert, Kibero			Biometrics	113307	FMNH
P. c. extoni	Uganda, Lake Albert, Butiaba			Biometrics	113308	FMNH
P. c. extoni	Uganda, Lake Albert, Butiaba			Biometrics	113309	FMNH
P. c. extoni	Uganda, Lake Albert, Butiaba			Biometrics	113310	FMNH
P. c. extoni	Uganda, Lake Albert, Butiaba			Biometrics	113311	FMNH
P. c. extoni	Uganda, Fatiko, Acholi			Biometrics	113312	FMNH
P. leucomystax	Mt Shengen	MH364245(Cytb), MH364252(ATP6/8)		Biometrics	114294	FMNH
P. leucomystax	Mramba	MH364244(Cytb), MH364253(ATP6/8)		Biometrics	114557	FMNH
P. b. conciliator	Iringa, Tanzania		MH364335(Myo)	Biometrics	115048	FMNH
P. p. affinis	Marsabit, Kenya	MH364241(Cytb)	MH364336(Myo)	Biometrics	132482	FMNH

P. b. conciliator	Nguru South Forest Reserve	MH364254(ATP6/8)	MH364306(Myo)	Biometrics	132768	FMNH
P. b. conciliator	Nguru Mts,Tanzania		MH364337(Myo)	Biometrics	132771	FMNH
P. leucomystax	Mdandu Forest	MH364243(Cytb)	MH364338(Myo)	Biometrics	134161	FMNH
P. p. uropygialis	Somalia, Erigavo, Daloh		MH364316(Myo)	Biometrics	134327	LSU
P. p. uropygialis	Somalia, 40m E Hargeisa		MH364352(Myo)	Biometrics	134328	LSU
P. p. uropygialis	Somalia, 12 mi. N Erigavo		MH364339(Myo)	Biometrics	134329	LSU
P. p. uropygialis	Somalia, 25 mi. N Erigavo		MH364340(Myo)	Biometrics	134330	LSU
P. b. mfumbiri	Kasiha Forest, Mahale Mountains National Park		MH364317(Myo)	Biometrics	135162	FMNH
P. b. bilineatus	Nguru South Forest Reserve, Tanzania	MG437419(Cytb)	MG576345(BFIB), MH364318(Myo)	Biometrics	136182	FMNH
P. c. extoni	Tanzania, Rukwa region		MH364319(Myo)	Biometrics	138925	LSU
P. b. mfumbiri	Kalambo River Forest Reserve		MH364320(Myo)	Biometrics	140629	FMNH
P. b. mfumbiri	Mbizi Forest Reserve		MH364310(Myo)	Biometrics	140883	FMNH
P. scolopaceus	DRC	MH364242(Cytb)	MH364311(Myo)	Biometrics	143433	FMNH
P. p. affinis	Mt. Kulal, Kenya	MH364240(Cytb)	MH364305(Myo)	Biometrics	146923	FMNH
P. c. extoni	South Africa, Mpumalanga, Boblands Farm		MH364312(Myo)	Biometrics	165339	LSU
P. c. extoni	South Africa, Mpumalanga, Boblands Farm		MH364313(Myo)	Biometrics	165340	LSU
P. c. chrysoconus	Kenya, Nyarondo, Kaimosi, N. Kavirondo		MH364314(Myo)	Biometrics	195066	Field
P. c. xanthostictus	Ethiopia, Sidamo, Alghe		MH364315(Myo)	Biometrics	195067	Field
P. c. extoni	Zambia, Ndola		MH364341(Myo)	Biometrics	205283	Field
P. c. extoni	Zambia, Lundazi		MH364321(Myo)	Biometrics	205284	Field

P. c. extoni	Zambia, Mwinilunga		MH364322(Myo)	Biometrics	205285	Field
P. c. extoni	Zambia, Lundazi, Mwase		MH364342(Myo)	Biometrics	205286	Field
P. c. extoni	Zambia, Lundazi		MH364346(Myo)	Biometrics	205288	Field
P. atroflavus	Tai_ent	MH364238(Cytb), MH364256(ATP6/8)	MH364343(Myo)	Biometrics	210056	FMNH
P. scolopaceus	Tai_ent	MH364237(Cytb), MH364257(ATP6/8)	MH364347(Myo)	Biometrics	210086	FMNH
P. c. extoni	Uganda, Bugondo, Teso		MH364344(Myo)	Biometrics	214708	FMNH
P. c. extoni	Zambia, Mwinilunga		MH364345(Myo)	Biometrics	219698	Field
P. c. extoni	Zambia, Mwinilunga		MH364307(Myo)	Biometrics	219701	Field
P. coryphaeus	Angola	MH364235(Cytb)	MH364323(Myo)	Biometrics	224408	Field
P. p. uropygialis	Abyssinia, Sadi Malka, Ethiopia		MH364324(Myo)	Biometrics	244342	AMNH
P. p. uropygialis	Abyssinia, Sadi Malka, Ethiopia		MH364325(Myo)	Biometrics	244343	NMNH
P. p. uropygialis	Abyssinia, Sadi Malka, Ethiopia		MH364326(Myo)	Biometrics	244344	NMNH
P. p. uropygialis	Ethiopia, Iron Bridge, Hawash River		MH364309(Myo)	Biometrics	244345	NMNH
P. p. uropygialis	Abyssinia, Sagon River, Ethiopia		MH364327(Myo)	Biometrics	244350	NMNH
P. p. uropygialis	Abyssinia, El Ade, Ethiopia		MH364328(Myo)	Biometrics	244351	NMNH
P. c. xanthostictus	Arussi Plateau, Ethiopia		MH364348(Myo)	Biometrics	244353	NMNH
P. c. xanthostictus	Ethiopia, near Loku, Sidamo		MH364329(Myo)	Biometrics	244354	NMNH
P. c. extoni	Zambia, Sikongo, Barotseland		MH364330(Myo)	Biometrics	263013	FMNH
P. c. extoni	Zambia, S. Lueti River,Angola Border, Barotseland		MH364349(Myo)	Biometrics	263014	FMNH

P. c. extoni	Zambia, S. Lueti River, WNLA Camp, Barotseland		MH364350(Myo)	Biometrics		263015	FMNH
P. c. extoni	Zambia, Sikongo, Barotseland		MH364331(Myo)	Biometrics		263016	FMNH
P. c. extoni	Botswana, Nqamiland, 20 mi W of Sepopa		MH364351(Myo)	Biometrics		263017	FMNH
P. c. extoni	Zimbabwe, Mnewa, Maramba Reserve		MH364353(Myo)	Biometrics		268989	FMNH
P. c. extoni	Zimbabwe, Sabi River, Maranka Reserve		MH364332(Myo)	Biometrics		268990	FMNH
P. c. extoni	Mozambique, Sofala, Dondo Forest, 25 mi NE Dondo		MH364333(Myo)	Biometrics		282799	FMNH
P. p. pusillus	N. Swaziland, Balegane, near, Komati River		MH364334(Myo)	Biometrics		285275	FMNH
P. p. uropygialis	SE Ethiopia, Sadi Malka			Biometrics		289189	AMNH
P. c. extoni	Belgian Congo, Lubenga, (Marungu)			Biometrics		289387	AMNH
P. c. extoni	Belgian Congo, Lubenga			Biometrics		289388	AMNH
P. p. uropygialis	Kassala, Telaweit, on Gash river			Biometrics		293482	FMNH
P. p. pusillus	S. Africa, Natal, Umbuzi MS, 16km NE of Port Shepstone (or is it Umzumbi Mts and 16 miles)			Biometrics		313950	NMNH
P. coryphaeus	Rwenzori	MH364234(Cytb), MH364258(ATP6/8)		Biometrics		355267	FMNH
P. coryphaeus	Rwenzori	MH364233(Cytb), MH364259(ATP6/8)	MH364319(Myo)	Biometrics		355270	FMNH
P. c. extoni	Malawi		MH364345(Myo)	Biometrics	Radseq	440452	FMNH

P. c. extoni	Malawi	MH364232(Cytb), MH364260(ATP6/8)	MH364307(Myo)	Biometrics	Radseq	440453	FMNH
P. c. extoni	Malawi		MH364323(Myo)	Biometrics	Radseq	440454	FMNH
P. c. extoni	Malawi		MH364324(Myo)	Biometrics	Radseq	440455	FMNH
P. c. extoni	Malawi		MH364325(Myo)	Biometrics	Radseq	440456	FMNH
P. p. pusillus	S. Africa, Melmoth, Zululand		MH364326(Myo)	Biometrics		518837	NMNH
P. c. extoni	Rhodesia, Mangwe dist, Matopos Hills, South Marula Station		MH364309(Myo)	Biometrics		520116	NMNH
P. c. extoni	Rhodesia, Mangwe dist, Matopos Hills, South Marula Station		MH364327(Myo)	Biometrics		520117	NMNH
P. c. extoni	Rhodesia, Dist. Lonely Mine		MH364328(Myo)	Biometrics		520122	NMNH
P. c. extoni	Rhodesia, Dist. Lonely Mine		MH364348(Myo)	Biometrics		520123	NMNH
P. p. uropygialis	Ethiopia, Balaghes Valley, Tihon Marlam		MH364329(Myo)	Biometrics		522460	NMNH
P. c. xanthostictus	Ethiopia, Kaffa, Afallo (Ghera)		MH364330(Myo)	Biometrics		522461	NMNH
P. c. extoni	Botswana, Xugana, 19'05'S 23'06'E		MH364349(Myo)	Biometrics		527353	NMNH
P. c. extoni	Botswana, Xugana, 19'05'S 23'06'E		MH364350(Myo)	Biometrics		527354	NMNH
P. p. pusillus	S. Africa, Heatonville, Zululand		MH364331(Myo)	Biometrics		545203	NMNH
P. p. pusillus	S. Africa, Park Rynie, S. Coast		MH364351(Myo)	Biometrics		545204	NMNH
P. p. pusillus	S. Africa, Heatonville, Zululand		MH364353(Myo)	Biometrics		545205	NMNH
P. p. pusillus	S. Africa, Heatonville, Zululand		MH364332(Myo)	Biometrics		545206	NMNH

P. p. pusillus	S. Africa, Heatonville, Zululand	MH364333(Myo)	Biometrics	545207	NMNH
P. p. pusillus	S. Africa, N. Zululand, Makatini Flats	MH364334(Myo)	Biometrics	546059	NMNH
P. p. pusillus	S. Africa, Natal, Umbumbulu		Biometrics	546060	NMNH
P. p. pusillus	S. Africa, Durban, Natal		Biometrics	546061	NMNH
P. p. uropygialis	Ethiopia, Bulcha, Sidamo Province		Biometrics	552843	NMNH
P. p. uropygialis	Ethiopia, Bulcha, Sidamo Province		Biometrics	552846	NMNH
P. p. uropygialis	Ethiopia, Bulcha, Sidamo Province		Biometrics	552847	NMNH
P. p. uropygialis	Ethiopia, Bulcha, Sidamo Province		Biometrics	552848	NMNH
P. p. uropygialis	Ethiopia, Bulcha, Sidamo Province		Biometrics	552849	NMNH
P. c. xanthostictus	Ethiopia, Didessa, Wollega Province		Biometrics	552850	NMNH
P. c. xanthostictus	Ethiopia, Gambela, Illubabor province		Biometrics	552851	NMNH
P. p. uropygialis	Ethiopia, Bulcha, Sidamo Province		Biometrics	569499	NMNH
P. c. xanthostictus	Ethiopia, Gojjam Prov. Lake Tana, Debre Mariam Is.		Biometrics	569501	NMNH
P. c. xanthostictus	Ethiopia, Gojjam Prov. Lake Tana, Debre Mariam Is.		Biometrics	569502	NMNH
P. c. xanthostictus	Ethiopia, Gojjam Prov. Lake Tana, Debre Mariam Is.		Biometrics	569503	NMNH
P. c. xanthostictus	Ethiopia, Bulcha, Sidamo Province		Biometrics	569504	NMNH

P. p. affinis	NE Tanzania, Bagamoyo	Biometrics	646230	AMNH
P. p. uropygialis	SE Ethiopia, Galla Countries, Ladjo River(Zaphiro)	Biometrics	646251	AMNH
P. p. uropygialis	SE Ethiopia, Galla Countries, la R. Herer(Zaphiro)	Biometrics	646252	AMNH
P. p. uropygialis	SE Ethiopia, Galla Countries, Isasseur Nir (Kassam River)	Biometrics	646253	AMNH
P. p. uropygialis	SE Ethiopia, Galla countries, Armaressa	Biometrics	646255	AMNH
P. p. uropygialis	SE Ethiopia, Galla Countries, Balassire	Biometrics	646257	AMNH
P. p. uropygialis	SE Ethiopia, Galla Countries, Balassire	Biometrics	646258	AMNH
P. p. uropygialis	SE Ethiopia, Galla Countries, Balassire	Biometrics	646259	AMNH
P. p. uropygialis	SE Ethiopia, Galla countries, Bissidimo	Biometrics	646260	AMNH
P. p. uropygialis	SE Ethiopia, Galla countries, Hurgira (Harawa)	Biometrics	646261	AMNH
P. p. uropygialis	SE Ethiopia, Sadi Malka (Galla countries)	Biometrics	646262	AMNH
P. p. uropygialis	S. Abyssinia, Auvadi, Arussi	Biometrics	646264	AMNH
P. p. uropygialis	Hawash, Soddo	Biometrics	646266	AMNH
P. p. uropygialis	S. Abyssinia, Riviere Hauche	Biometrics	646268	AMNH
P. p. uropygialis	S. Abyssinia, Riviere Hoache	Biometrics	646269	AMNH

P. p. uropygialis	S. Abyssinia, Godja Mariam (M Trofimoff)	Biometrics	646270	AMNH
P. p. uropygialis	S. Abyssinia, Dobbana, Morenguo (Maraco)	Biometrics	646271	AMNH
P. p. uropygialis	S. Abyssinia, Dobbana, Morenguo (Maraco)	Biometrics	646272	AMNH
P. p. uropygialis	S. Abyssinia, Maraco	Biometrics	646273	AMNH
P. p. uropygialis	Karan Haliesch, Keren, Eritrea	Biometrics	646274	AMNH
P. p. uropygialis	Ali Beret, (Habeschi)	Biometrics	646276	AMNH
P. p. uropygialis	Somalia, Hargeisa	Biometrics	646277	AMNH
P. p. uropygialis	Somalia, Hargeisa	Biometrics	646279	AMNH
P. p. uropygialis	Somalia, Hargeisa	Biometrics	646280	AMNH
P. p. uropygialis	Somalia, Sheikh	Biometrics	646281	AMNH
P. p. uropygialis	Somalia, Mush Haled, Warsaugh	Biometrics	646282	AMNH
P. p. uropygialis	Somalia, Dabolak	Biometrics	646283	AMNH
P. p. uropygialis	Somalia, Durass (Sir Geoffrey Archer)	Biometrics	646284	AMNH
P. p. uropygialis	Somalia, Durass	Biometrics	646285	AMNH
P. c. chrysoconus	Uganda, Unyoro, Masindi	Biometrics	646291	AMNH
P. c. chrysoconus	Uganda, Fatiko, upper white nile	Biometrics	646292	AMNH
P. c. chrysoconus	Uganda, nr Mbale	Biometrics	646293	AMNH
P. c. chrysoconus	Uganda, Businga Forest, nr. Elgon(van someren)	Biometrics	646294	AMNH

P. c. chrysoconus	Uganda, Kama	Biometrics	646295	AMNH
P. c. xanthostictus	S. Ethiopia, Anderatseha, Kaffa	Biometrics	646303	AMNH
P. c. xanthostictus	Anderatscha, Kaffa	Biometrics	646304	AMNH
P. c. xanthostictus	S. Ethiopia, Anderatseha, Kaffa	Biometrics	646305	AMNH
P. c. xanthostictus	S Ethiopia, Setscha - Schubba, W. Kaffa	Biometrics	646306	AMNH
P. c. xanthostictus	S. Ethiopia, Budda, Gimirra	Biometrics	646307	AMNH
P. c. xanthostictus	alata, Gembitscho, Sidamo	Biometrics	646308	AMNH
P. c. xanthostictus	S. Ethiopia, Habela (Alata), Sidamo	Biometrics	646309	AMNH
P. c. xanthostictus	S. Abyssinia, Auvadi, Arussi	Biometrics	646310	AMNH
P. c. xanthostictus	S. Abyssinia, Kulisa, Arussi	Biometrics	646311	AMNH
P. c. xanthostictus	Riviere Hoache	Biometrics	646312	AMNH
P. c. xanthostictus	S. Abyssinia, Tersaleffo, Schoa	Biometrics	646313	AMNH
P. c. xanthostictus	Tersalefo, Schoa	Biometrics	646314	AMNH
P. c. xanthostictus	S. Abyssinia, Tersaleffo, Schoa	Biometrics	646315	AMNH
P. c. extoni	S. Africa, Oliphants, Nak, Magaliesberg	Biometrics	646316	AMNH
P. c. extoni	Limpopo, S. Africa	Biometrics	646318	AMNH
P. c. chrysoconus	Mahagi Port, Lake Albert	Biometrics	764216	AMNH
P. c. chrysoconus	Kenya, NW Kericho	Biometrics	814827	AMNH

P. c. chrysoconus	Kenya, NW Kericho			Biometrics	814828	AMNH
P. c. chrysoconus	Kenya, Kapsorok, Sondo Rd			Biometrics	814829	AMNH
P. c. extoni	S. Rhodesia, Bulawayo			Biometrics	824925	AMNH
P. c. extoni	S. Rhodesia, Bulawayo			Biometrics	824926	AMNH
P. atroflavus	Ndiki	MH364230(Cytb), MH364263(ATP6/8)	MH364320(Myo)	Biometrics	970024	CTR
P. subsulphureus	Ndokmen Nord	MH364248(Cytb), MH364249(ATP6/8)	MH364310(Myo)	Biometrics	07N50200	Field
P. b. leucolaimus	Nkolbisson Ce.			Biometrics	07N50218	Field
P. b. leucolaimus	Wakwa	MH364247(Cytb), MH364250(ATP6/8)	MH364311(Myo)	Biometrics	07N50222	Field
P. b. leucolaimus	Wakwa	MH364246(Cytb)	MH364305(Myo)	Biometrics	07N50223	Field
P. b. mfumbiri	Uganda		MH364312(Myo)	Biometrics	07N50236	Field
P. b. mfumbiri	Uganda		MH364313(Myo)	Biometrics	07N50243	Field
P. b. mfumbiri	Kibale			Biometrics	07N50254	Field
P. subsulphureus	Royal Mile		MH364314(Myo)	Biometrics	07N50263	Field
P. b. mfumbiri	MtCameroon	MH364251(ATP6/8)	MH364315(Myo)	Biometrics	07N50283	Field
P. b. bilineatus	Ndundulu forest, Udzungwa mts, Tanzania			Reflectance	100394	ZMUC
P. b. bilineatus	Ndundulu forest, Udzungwa mts, Tanzania			Reflectance	100395	ZMUC
P. b. bilineatus	Ndundulu forest, Udzungwa mts, Tanzania			Reflectance	100396	ZMUC
P. b. bilineatus	Ukami Forest, Udzungwa mts, Tanzania			Reflectance	100397	ZMUC

P. b. bilineatus	Ndundulu forest, Udzungwa mts, Tanzania	Reflectance	100398	ZMUC
P. b. fischeri	Nguru South Forest Reserve, Tanzania	Reflectance	100399	ZMUC
P. c. xanthostictus	Abyssinia, Chellia	Biometrics	1900.1.3.114	Tring
P. c. extoni	NE Transvaal, Woodbush, Zouifausberg	Biometrics	1905.12.29.463	Tring
P. b. bilineatus	Ngoye Forest, Zululand	Reflectance	1905.12.29.464	Tring
P. c. xanthostictus	S. Abyssinia, Kindjo, Jimma	Biometrics	1912.10.15.388	Tring
P. c. xanthostictus	S. Abyssinia, Charada Forest, Kaffa.	Biometrics	1912.10.15.391	Tring
P. c. xanthostictus	S. Abyssinia, Mt. Mergeta, near Addis Alam	Biometrics	1912.10.15.395	Tring
P. c. xanthostictus	S. Abyssinia, Charada Forest, Kaffa.	Biometrics	1912.10.15.396	Tring
P. c. xanthostictus	Abyssinia, Gibbeh valley	Biometrics	1923.8.7.4910	Tring
P. c. xanthostictus	Abyssinia, Jimma	Biometrics	1923.8.7.4911	Tring
P. b. fischeri	Zanzibar	Reflectance	1926.8.9.56	Tring
P. c. xanthostictus	Abyssinia, Zingini River, Big Abbai - Abai River	Biometrics	1929.11.5.121	Tring
P. b. fischeri	Zanzibar	Reflectance	1929.6.27.33	Tring
P. b. fischeri	Zanzibar	Reflectance	1929.6.27.35	Tring
P. b. fischeri	Zanzibar	Reflectance	1929.6.27.36	Tring
P. c. extoni	Botswana, Kabulabula, Chobe R.	Biometrics	1932.5.5.325	Tring

P. b. bilineatus	Cholo Mt, S. Nyasaland (Malawi)	Reflectance	1933.3.1.396	Tring
P. b. fischeri	Near Netia, Mozambique Prov., Port. E. Africa	Reflectance	1933.3.1.397	Tring
P. b. fischeri	Sierra Mirrote, Mozambique Prov., Port. E. Africa	Reflectance	1933.3.1.398	Tring
P. b. bilineatus	Brighton Beach, Near Jacobs, Near Durban, Natal	Reflectance	1933.7.14.174	Tring
P. b. fischeri	Mafia Island, Tanganyika Terr.	Reflectance	1939.1.28.91	Tring
P. b. fischeri	Ndagoni, Mafia Island	Reflectance	1939.1.28.92	Tring
P. b. fischeri	Kange (bush) Mafia Island	Reflectance	1939.1.28.93	Tring
P. b. fischeri	Kilindono, Mafia Island	Reflectance	1939.1.28.94	Tring
P. b. fischeri	Mafia Island, bush, Tanganyika Territory	Reflectance	1939.1.28.95	Tring
P. b. bilineatus	Mangangu forest, Nguru Mts.	Reflectance	1939.1.28.96	Tring
P. b. bilineatus	Mangangu forest, Nguru Mts.	Reflectance	1939.1.28.97	Tring
P. b. bilineatus	Kinole Forest, N. Uluguru Mts.	Reflectance	1939.1.28.98	Tring
P. b. fischeri	Kisiju on coast, 40m south of Dar Es Salaam, Tanzania	Reflectance	1939.6.19.162	Tring
P. b. fischeri	Pugu Forest, west of Dar Es Salaam	Reflectance	1939.6.19.164	Tring
P. b. fischeri	Buthat, Pugu, west of Dar es salaam	Reflectance	1939.6.19.165	Tring
P. b. fischeri	Mkokotoni, Zanzibar	Reflectance	1939.7.19.15	Tring
P. b. fischeri	Chwaka, Zanzibar	Reflectance	1939.7.19.16	Tring

P. c. xanthostictus	Abyssinia, Uondo			Biometrics	1942.12.1.29	Tring
P. p. uropygialis	S. Abyssinia, 40 mi W of Yavello			Biometrics	1946.5.1244	Tring
P. p. uropygialis	S. Abyssinia, nr. Yavello			Biometrics	1946.5.1245	Tring
P. p. uropygialis	S. Abyssinia, Yavello			Biometrics	1946.5.1247	Tring
P. p. uropygialis	S. Abyssinia, Yavello			Biometrics	1946.5.1248	Tring
P. p. uropygialis	S. Abyssinia, Yavello			Biometrics	1946.5.1249	Tring
P. p. uropygialis	S. Abyssinia, 10 mi NE of Burgi			Biometrics	1946.5.1250	Tring
P. p. uropygialis	S. Abyssinia, 20 mi S of Mega			Biometrics	1946.5.1251	Tring
P. c. xanthostictus	S. Abyssinia, Alghe			Biometrics	1946.5.1255	Tring
P. b. bilineatus	Cholo Mt, S. Nyasaland (Malawi)			Reflectance	1946.5.323	Tring
P. b. fischeri	Fufuma well, near Chwaka, Zanzibar			Reflectance	1946.76.14	Tring
P. b. bilineatus	Border of Mozambique and NE Zululand			Reflectance	1956.35.14	Tring
P. b. fischeri	Zanzibar			Reflectance	1963.43.16	Tring
P. b. fischeri	Mida Creek, S of Malindi, Coastal Kenya			Reflectance	1971.16.25	Tring
P. scolopaceus	Kibale	MH364236(Cytb)	MH364341(Myo)	Biometrics	29-15018	Field
P. b. fischeri	Uluguru Mts, Morogoro Dist., Tanzania			Reflectance	74.168	ZMUC
P. b. fischeri	Soga, Kisarawe dist. Tanzania			Reflectance	74.170	ZMUC
P. b. fischeri	Soga, Kisarawe dist. Tanzania			Reflectance	74.176	ZMUC
P. b. fischeri	Soga, Kisarawe			Reflectance	74.177	ZMUC

	dist Tanzania						
P. b. fischeri	Nguru mts, Morogoro, Tanzania			Reflectance		74.180	ZMUC
P. c. extoni	Magallesberger gen? (Magaliesburg), Transvaal			Biometrics		85.9.1.139	Tring
P. b. bilineatus	Mifunti river, NE Transvaal, South Africa			Reflectance		87.2.26.2	Tring
P. c. extoni	Limpopo, Hutton Exchange			Biometrics		88.11.25.426	Tring
P. c. extoni	Rustenburg			Biometrics		89.6.20.79	Tring
P. c. extoni	Rustenburg			Biometrics		89.6.20.81	Tring
P. scolopaceus	Bioko	MH364261(ATP6/8)				960089	FMNH
P. c. extoni	Rustenburg			Biometrics		90.10.16.36	Tring
P. b. bilineatus	Etchowe (Eshowe) Zululand			Reflectance		96.4.17.55	Tring
P. b. bilineatus	Etchowe (Eshowe) Zululand			Reflectance		96.4.17.56	Tring
P. b. sharpei	Ghana	MH364229(Cytb), MH364264(ATP6/8)		Biometrics		A19907	Field
P. b. sharpei	Ghana	MH364228(Cytb), MH364265(ATP6/8)	MH364321(Myo)	Biometrics		A19910	Field
P. b. sharpei	Ghana	MH364227(Cytb), MH364266(ATP6/8)	MH364322(Myo)	Biometrics		A19912	Field
P. c. chrysoconus	Jos	MH364226(Cytb), MH364267(ATP6/8)	MH364342(Myo)	Biometrics	Radseq	AP88977	Field
P. b. leucolaimus	Jos	MH364225(Cytb), MH364268(ATP6/8)		Biometrics		AP88978	Field
P. c. chrysoconus	Jos			Biometrics	Radseq	AP88979	Field
P. b. mfumbiri	Nigeria	MH364224(Cytb)	MH364346(Myo)	Biometrics		AP88980	Field
P. c. chrysoconus	Jos			Biometrics	Radseq	AP88981	Field

P. c. chrysoconus	Jos	MH364223(Cytb), MH364269(ATP6/8)		Biometrics	Radseq	AP88983	Field
P. c. chrysoconus	Jos			Biometrics	Radseq	AP88984	Field
P. subsulphureus	Omo, Nigeria		MG576399(BFIB)	Biometrics		AP88988	Field
P. scolopaceus	Nigeria	MH364222(Cytb)	MH364343(Myo)	Biometrics		AP88992	Field
P. b. leucolaimus	Nigeria	MH364221(Cytb)	MH364347(Myo)	Biometrics		AP88994	Field
P. c. extoni	Blyde River Canyon, South Africa	MH364117(Cytb)		both	both	AR93101	Field
P. c. extoni	Blyde River Canyon, South Africa	MH364118(Cytb)		both	both	AR93102	Field
P. c. extoni	Blyde River Canyon, South Africa	MH364119(Cytb)	MH364344(Myo)	both	Microsat	AR93103	Field
P. c. extoni	Blyde River Canyon, South Africa	MH364120(Cytb)		both	both	AR93104	Field
P. c. extoni	Blyde River Canyon, South Africa	MH364121(Cytb)		both	both	AR93105	Field
P. c. extoni	Nelspruit, South Africa	MH364122(Cytb)		both	both	AR93107	Field
P. c. extoni	Nelspruit, South Africa	MH364123(Cytb)		both	both	AR93109	Field
P. c. extoni	Mahushe Shongwe, South Africa	MH364124(Cytb)		both	both	AR93110	Field
P. p. pusillus	Tshaneni, Swaziland	MH364125(Cytb)		both	both	AR93112	Field
P. p. pusillus	Tshaneni, Swaziland	MH364126(Cytb)		both	both	AR93113	Field
P. p. pusillus	Mpofu, Swaziland	MH364127(Cytb)		both	both	AR93114	Field
P. p. pusillus	Mpofu, Swaziland	MH364128(Cytb)		both	both	AR93115	Field
P. c. extoni	Mpofu, Swaziland	MH364129(Cytb)		both	both	AR93116	Field
P. c. extoni	Tshaneni, Swaziland	MH364130(Cytb)		both	both	AR93117	Field
P. p. pusillus	Tshaneni, Swaziland	MH364131(Cytb)		both	both	AR93118	Field

P. p. pusillus	Tshaneni, Swaziland	MH364132(Cytb)		Biometrics	both	AR93119	Field
P. p. pusillus	Tshaneni, Swaziland	MH364133(Cytb)		both	both	AR93120	Field
P. p. pusillus	Tshaneni, Swaziland	MH364134(Cytb)		both	both	AR93121	Field
P. c. extoni	Tshaneni, Swaziland	MH364135(Cytb)		both	both	AR93122	Field
P. p. pusillus	Tshaneni, Swaziland	MH364136(Cytb)		both	both	AR93123	Field
P. c. extoni	Mpofu, Swaziland	MH364137(Cytb)		both	both	AR93124	Field
P. c. extoni	Mpofu, Swaziland	MH364138(Cytb)		both	both	AR93125	Field
P. c. extoni	Mpofu, Swaziland	MH364139(Cytb)		both	both	AR93126	Field
P. p. pusillus	Kube Yini, South Africa	MH364140(Cytb)		both	both	AR93128	Field
P. p. pusillus	Kube Yini, South Africa	MH364141(Cytb)		both	both	AR93129	Field
P. p. pusillus	Kube Yini, South Africa	MH364142(Cytb)		both	both	AR93130	Field
P. p. pusillus	Kube Yini, South Africa	MH364143(Cytb)		both	both	AR93131	Field
P. p. pusillus	Kube Yini, South Africa	MH364219(Cytb)		both	both	AR93132	Field
P. p. pusillus	Vernon Crookes, South Africa	MH364144(Cytb)		both	both	AR93133	Field
P. p. pusillus	Vernon Crookes, South Africa	MH364218(Cytb)	MH364345(Myo)	both	both	AR93134	Field
P. p. pusillus	Vernon Crookes, South Africa	MH364145(Cytb)		both	both	AR93135	Field
P. b. bilineatus	Mpofu, Swaziland	MH364270(ATP6/8)	MH364307(Myo)	Biometrics		AR93136	Field
P. p. pusillus	Lake Eland, South Africa	MH364217(Cytb)		both	both	AR93138	Field
P. p. pusillus	Lake Eland, South Africa	MH364146(Cytb)		both	both	AR93139	Field
P. p. pusillus	Lake Eland, South Africa	MH364147(Cytb)		both	both	AR93140	Field
P. c. extoni	Nelspruit, South Africa	MH364148(Cytb)		both	both	AR93141	Field
P. c. extoni	Nelspruit, South Africa	MH364149(Cytb)		both	both	AR93142	Field

P. c. extoni	Nelspruit, South Africa	MH364150(Cytb)	both	both	AR93143	Field
P. c. extoni	Nelspruit, South Africa	MH364151(Cytb)	both	both	AR93144	Field
P. c. extoni	Nelspruit, South Africa	MH364152(Cytb)	both	both	AR93145	Field
P. c. extoni	Mawewe, South Africa	MH364153(Cytb)	both	both	AR93146	Field
P. p. pusillus	Mawewe, South Africa	MH364154(Cytb)	both	both	AR93147	Field
P. c. extoni	Mawewe, South Africa	MH364155(Cytb)	both	both	AR93148	Field
P. c. extoni	Mawewe, South Africa	MH364156(Cytb)	both	both	AR93149	Field
P. c. extoni	Mawewe, South Africa	MH364157(Cytb)	both	both	AR93150	Field
P. p. pusillus	Mawewe, South Africa	MH364158(Cytb)	both	both	AR93151	Field
P. c. extoni	Mawewe, South Africa	MH364159(Cytb)	both	both	AR93152	Field
P. p. pusillus	Mhlangatani, Swaziland	MH364160(Cytb)	both	both	AR93153	Field
P. c. extoni	Mhlangatani, Swaziland	MH364161(Cytb)	both	both	AR93154	Field
P. c. extoni	Mpofu, Swaziland	MH364162(Cytb)	both	both	AR93155	Field
P. c. extoni	Mpofu, Swaziland	MH364163(Cytb)	both	both	AR93156	Field
P. c. extoni	Mpofu, Swaziland	MH364164(Cytb)	both	both	AR93157	Field
P. c. extoni	Mpofu, Swaziland	MH364165(Cytb)	both	both	AR93158	Field
P. c. extoni	Mpofu, Swaziland	MH364166(Cytb)	both	both	AR93159	Field
P. c. extoni	Mpofu, Swaziland	MH364167(Cytb)	both	both	AR93160	Field
P. c. extoni	Mpofu, Swaziland	MH364168(Cytb)	both	both	AR93161	Field
P. p. pusillus	Mpofu, Swaziland	MH364169(Cytb)	both	both	AR93162	Field
P. c. extoni	Mpofu, Swaziland	MH364170(Cytb)	both	both	AR93163	Field
P. c. extoni	Mkhayeni, Swaziland	MH364171(Cytb)	both	both	AR93165	Field
P. p. pusillus	Mkhayeni, Swaziland	MH364172(Cytb)	both	Microsat	AR93166	Field

P. p. pusillus	Mkhayeni, Swaziland	MH364173(Cytb)	both	both	AR93167	Field
P. c. extoni	Mpofu, Swaziland	MH364174(Cytb)	both	both	AR93168	Field
P. c. extoni	Mpofu, Swaziland	MH364175(Cytb)	both	both	AR93169	Field
P. c. extoni	Mpofu, Swaziland	MH364176(Cytb)	both	both	AR93170	Field
P. c. extoni	Mpofu, Swaziland	MH364177(Cytb)	both	both	AR93171	Field
P. c. extoni	Mpofu, Swaziland	MH364178(Cytb)	both	both	AR93172	Field
P. p. pusillus	Mpofu, Swaziland	MH364179(Cytb)	both	both	AR93173	Field
P. c. extoni	Mpofu, Swaziland	MH364180(Cytb)	both	both	AR93174	Field
P. c. extoni	Mpofu, Swaziland	MH364181(Cytb)	both	both	AR93175	Field
P. p. pusillus	Manzini, Swaziland	MH364182(Cytb)	both	both	AR93176	Field
P. p. pusillus	Manzini, Swaziland	MH364183(Cytb)	both	both	AR93177	Field
P. p. pusillus	Manzini, Swaziland	MH364184(Cytb)	both	both	AR93178	Field
P. p. pusillus	Manzini, Swaziland	MH364185(Cytb)	both	both	AR93179	Field
P. p. pusillus	Manzini, Swaziland	MH364186(Cytb)	both	both	AR93180	Field
P. p. pusillus	Manzini, Swaziland	MH364187(Cytb)	both	both	AR93181	Field
Picumnus cirratus	GenBank		Biometrics		AY165819	GenBank
Ramphastos toco albigularis	GenBank				AY959852.1	GenBank
P. c. extoni	Nelspruit, South Africa	MH364216(Cytb), MH364271(ATP6/8)	Biometrics	Radseq	B34266	Field
P. c. extoni	Nelspruit, South Africa	MH364215(Cytb), MH364272(ATP6/8)	Biometrics	Radseq	B34267	Field
P. c. chrysoconus	Ghana	MH364214(Cytb), MH364273(ATP6/8)	Biometrics		B39241	Field
P. c. chrysoconus	Ghana	MH364213(Cytb), MH364274(ATP6/8)	Biometrics	Radseq	B39310	Field

P. subsulphureus	Ghana	MH364212(Cytb), MH364275(ATP6/8)	MH364323(Myo)	Biometrics		B39374	Field
P. subsulphureus	MtCameroon, Cameroon	MH364211(Cytb)		Biometrics		CAM14192	CUC
P. coryphaeus	MtCameroon, Cameroon	MH364210(Cytb)		Biometrics		CAM14349	CUC
P. c. chrysoconus	Kongelai, Kenya	MH364209(Cytb), MH364276(ATP6/8)		Biometrics	Radseq	J31301	Field
P. b. jacksoni	Kongelai, Kenya		MH364324(Myo)	Biometrics		J31302	Field
P. p. affinis	Kongelai, Kenya			Biometrics	Radseq	J31303	Field
P. p. affinis	Kongelai, Kenya	MH364208(Cytb), MH364277(ATP6/8)		Biometrics	Radseq	J31305	Field
P. p. affinis	Kongelai, Kenya			Biometrics	Radseq	J31306	Field
Tricholaema diademata	Awasi, Kenya	MG697232(Cytb), MG230178(ATP6/8)	MG576402(BFIB), MH364325(Myo)	Biometrics		J31308	Field
P. c. chrysoconus	Awasi, Kenya			Biometrics	Radseq	J31309	Field
P. c. chrysoconus	Awasi, Kenya	MH364207(Cytb), MH364278(ATP6/8)		Biometrics	Radseq	J31310	Field
P. c. chrysoconus	Awasi, Kenya			Biometrics	Radseq	J31311	Field
P. p. affinis	Awasi, Kenya	MH364206(Cytb), MH364279(ATP6/8)		Biometrics	Radseq	J31312	Field
P. p. affinis	Watamu, Kenya	MH364205(Cytb), MH364280(ATP6/8)		Biometrics	Radseq	J31313	Field
P. p. affinis	Watamu, Kenya			Biometrics	Radseq	J31314	Field
P. p. affinis	Diani, Kenya	MH364204(Cytb), MH364281(ATP6/8)		Biometrics	Radseq	J31315	Field
P. p. affinis	Diani, Kenya			Biometrics	Radseq	J31316	Field
P. p. affinis	Diani, Kenya			Biometrics	Radseq	J31317	Field
P. b. fischeri	Diani, Kenya	MG437424(Cytb)	MG576385(BFIB)	Biometrics		J31319	Field
P. c. chrysoconus	Kenya, Kenya			Biometrics	Radseq	J31320	Field
P. c. chrysoconus	Kenya, Kenya			Biometrics	Radseq	J31321	Field

P. p. affinis	Abuko, Kenya			Biometrics	Radseq	J31322	Field
P. p. affinis	Abuko, Kenya			Biometrics	Radseq	J31323	Field
P. p. affinis	Abuko, Kenya			Biometrics	Radseq	J31324	Field
P. p. affinis	Abuko, Kenya			Biometrics	Radseq	J31325	Field
P. p. affinis	Ruma NP, Kenya			Biometrics	Radseq	J31326	Field
P. c. chrysoconus	Awasi, Kenya			Biometrics	Radseq	J31327	Field
P. p. affinis	Kibwezi, Kenya			Biometrics	Radseq	J31328	Field
P. simplex	Arabuko-sokoke, Kenya		MH364326(Myo)	Biometrics		J31329	Field
P. p. affinis	Sokoke, Kenya			Biometrics	Radseq	J31330	Field
P. b. fischeri	Kilifi, Kenya	MG437425(Cytb)	MG576364(BFIB)	Biometrics		J31331	Field
P. b. fischeri	Kilifi, Kenya	MG437426(Cytb)	MG576365(BFIB)	Biometrics		J31332	Field
P. b. fischeri	Kilifi, Kenya	MG437427(Cytb)	MG576363(BFIB)	Biometrics		J31333	Field
P. b. conciliator	Kilifi, Tanzania		MG576400(BFIB)	Biometrics		J31334	Field
P. simplex	Kilifi, Kenya	MH364282(ATP6/8)		Biometrics		J31335	Field
P. p. affinis	Rukinga, Kenya			Biometrics	Radseq	J31336	Field
P. p. affinis	Rukinga, Kenya			Biometrics	Radseq	J31337	Field
P. p. affinis	Rukinga, Kenya			Biometrics	Radseq	J31338	Field
P. p. affinis	Kisamis, Kenya			Biometrics	Radseq	J31339	Field
P. p. affinis	Kisamis, Kenya			Biometrics	Radseq	J31340	Field
P. b. bilineatus	Karen Langata, Tanzania		MG576344(BFIB)	Biometrics		J31341	Field
P. b. bilineatus	Karen Langata, Tanzania		MG576343(BFIB)	Biometrics		J31343	Field
P. b. bilineatus	Dar es Salaam University, Tanzania	MG437433(Cytb)	MG576359(BFIB)	Biometrics		J31344	Field
P. b. bilineatus	Kinyonga, Saadani, Tanzania	MG437434(Cytb), MH364284(ATP6/8)	MG576360(BFIB), MH364309(Myo)	Biometrics		J31345	Field
P. c. extoni	Mikumi, Tanzania			Biometrics	Radseq	J31346	Field
P. p. affinis	Mikumi, Tanzania			Biometrics	Radseq	J31347	Field
P. c. extoni	Mikumi, Tanzania			Biometrics	Radseq	J31348	Field

P. c. extoni	Mikumi, Tanzania			Biometrics	Radseq	J31349	Field
P. c. extoni	Mikumi, Tanzania			Biometrics	Radseq	J31350	Field
P. p. affinis	Mikumi, Tanzania			Biometrics	Radseq	J31351	Field
P. c. extoni	Mikumi, Tanzania			Biometrics	Radseq	J31352	Field
P. b. conciliator	Udzungwa, Tanzania		MG576347(BFIB), MH364327(Myo)	Biometrics		J31353	Field
P. b. conciliator	Udzungwa, Tanzania	MG437479(Cytb), MH364285(ATP6/8)	MG576346(BFIB)	Biometrics		J31354	Field
P. b. bilineatus	Mchungu, Tanzania		MG576352(BFIB)	Biometrics		J31355	Field
P. b. fischeri	Mchungu, Tanzania	MG437428(Cytb)	MG576353(BFIB)	Biometrics		J31356	Field
P. b. bilineatus	Kilwa, Tanzania	MG437429(Cytb)	MG576354(BFIB)	Biometrics		J31357	Field
P. b. bilineatus	Kilwa Masoko, Tanzania	MG437430(Cytb)	MG576356(BFIB)	Biometrics		J31358	Field
P. simplex	Migeregere, Tanzania		MG576401(BFIB)	Biometrics		J31359	Field
P. c. extoni	Migeregere, Tanzania	MH364203(Cytb), MH364286(ATP6/8)		Biometrics	Radseq	J31360	Field
P. c. extoni	Migeregere, Tanzania	MH364202(Cytb), MH364287(ATP6/8)		Biometrics	Radseq	J31361	Field
P. c. extoni	Nainokwe, Tanzania			Biometrics	Radseq	J31363	Field
P. c. extoni	Nainokwe, Tanzania			Biometrics	Radseq	J31364	Field
P. c. extoni	Nainokwe, Tanzania			Biometrics	Radseq	J31365	Field
P. c. extoni	Nainokwe, Tanzania			Biometrics	Radseq	J31366	Field
P. c. extoni	Nainokwe, Tanzania			Biometrics	Radseq	J31367	Field
P. c. extoni	Selous, Tanzania	MH364201(Cytb), MH364288(ATP6/8)	MH364328(Myo)	Biometrics	Radseq	J31368	Field
P. p. affinis	Wami-Mbiki, Tanzania			Biometrics	Radseq	J31370	Field
P. p. affinis	Wami-Mbiki, Tanzania			Biometrics	Radseq	J31371	Field

P. p. affinis	Saadani, Tanzania			Biometrics	Radseq	J31372	Field
P. p. affinis	Saadani, Tanzania			Biometrics	Radseq	J31373	Field
P. p. affinis	Saadani, Tanzania			Biometrics	Radseq	J31374	Field
P. p. affinis	Saadani, Tanzania			Biometrics	Radseq	J31375	Field
P. p. affinis	Saadani, Tanzania			Biometrics	Radseq	J31376	Field
P. p. affinis	Saadani, Tanzania			Biometrics	Radseq	J31377	Field
P. p. affinis	Saadani, Tanzania			Biometrics	Radseq	J31378	Field
P. b. bilineatus	Amani, Tanzania	MG437420(Cytb)	MG576355(BFIB)	Biometrics		J31381	Field
P. b. bilineatus	Genda genda, Tanzania	MG437421(Cytb)	MG576357(BFIB)	Biometrics		J31382	Field
P. b. bilineatus	Genda genda, Tanzania	MG437422(Cytb)	MG576350(BFIB)	Biometrics		J31383	Field
P. b. bilineatus	Genda genda, Tanzania	MG437423(Cytb)	MG576351(BFIB)	Biometrics		J31384	Field
P. c. extoni	Mikumi, Tanzania			Biometrics	Radseq	J31385	Field
P. c. extoni	Mikumi, Tanzania			Biometrics	Radseq	J31386	Field
P. p. affinis	Iringa, Tanzania			Biometrics	Radseq	J31387	Field
P. p. affinis	Iringa, Tanzania			Biometrics	Radseq	J31388	Field
P. p. affinis	Iringa, Tanzania			Biometrics	Radseq	J31389	Field
P. p. affinis	Iringa, Tanzania			Biometrics	Radseq	J31390	Field
P. p. affinis	Iringa, Tanzania			Biometrics	Radseq	J31391	Field
P. c. extoni	Ruaha, Tanzania			Biometrics	Radseq	J31392	Field
P. c. extoni	Mbeya, Tanzania			Biometrics	Radseq	J31394	Field
P. c. extoni	Mbeya, Tanzania			Biometrics	Radseq	J31395	Field
P. c. extoni	Mbeya, Tanzania			Biometrics	Radseq	J31396	Field
P. c. extoni	Mbeya, Tanzania			Biometrics	Radseq	J31397	Field
P. c. extoni	Mbeya, Tanzania			Biometrics	Radseq	J31398	Field
P. c. extoni	Mbeya, Tanzania			Biometrics	Radseq	J31400	Field
P. b. bilineatus	Cabo Delgado, Mozambique	MG437476(Cytb)		Biometrics		JF2714	MVZ
P. b. bilineatus	Cabo Delgado, Mozambique	MG437475(Cytb)	MH364348(Myo)	Biometrics		JF2807	MVZ

P. p. pusillus	Table Farm, South Africa	MH364200(Cytb), MH364289(ATP6/8)		Biometrics		JF551	MVZ
P. p. pusillus	Morgan's Bay, Eastern Cape, South Africa	MH364292(ATP6/8)		Biometrics		JF790	MVZ
P. b. fischeri	Watamu, Kenya	MG437431(Cytb), MH364293(ATP6/8)	MG576374(BFIB)	Biometrics		K27792	Field
P. p. affinis	Watamu, Kenya			Biometrics	Radseq	K38709	Field
P. p. affinis	Mbeya, Tanzania			Biometrics	Radseq	K69301	Field
P. c. extoni	Katavi NP, Tanzania			Biometrics	Radseq	K69302	Field
P. c. extoni	Katavi, Tanzania			Biometrics	Radseq	K69303	Field
P. c. extoni	Uvinza, Tanzania	MH364199(Cytb), MH364294(ATP6/8)		Biometrics	Radseq	K69304	Field
P. c. extoni	Uvinza, Tanzania			Biometrics	Radseq	K69305	Field
P. c. extoni	Uvinza, Tanzania			Biometrics	Radseq	K69306	Field
P. c. extoni	Uvinza, Tanzania			Biometrics	Radseq	K69307	Field
P. c. extoni	Ruaha NP, Isunkavyula, Kilola valley, Tanzania	MH364198(Cytb), MH364295(ATP6/8)	MH364329(Myo)	Biometrics		K69309	Field
P. c. extoni	Ruaha NP, Isunkavyula, Kilola valley, Tanzania	MH364197(Cytb)	MH364330(Myo)	Biometrics		K69310	Field
P. p. affinis	Ruaha , Tanzania	MH364196(Cytb)	MH364349(Myo)	Biometrics	Radseq	K69311	Field
P. p. affinis	Fish Eaglepoint, Tanzania			Biometrics	Radseq	K69313	Field
P. p. affinis	Fish Eaglepoint, Tanzania			Biometrics	Radseq	K69314	Field
P. p. affinis	Pangani, Tanzania			Biometrics	Radseq	K69315	Field
P. p. affinis	Pangani, Tanzania	MH364195(Cytb)	MH364350(Myo)	Biometrics	Radseq	K69316	Field
P. b. bilineatus	Pangani, Tanzania	MG437432(Cytb)	MG576358(BFIB)	Biometrics		K69317	Field
P. b. bilineatus	Pangani, Tanzania	MG437435(Cytb)	MG576349(BFIB)	Biometrics		K69318	Field
P. b. fischeri	Zanzibar, Kiwengwa	MG437436(Cytb)		Biometrics		K69319	Field

P. b. fischeri	Zanzibar, Kiwengwa	MG437437(Cytb)		Biometrics		K69320	Field
P. b. fischeri	Zanzibar, Kiwengwa		MG576388(BFIB)	Biometrics		K69321	Field
P. b. fischeri	Zanzibar, Kiwengwa	MG437442(Cytb)		Biometrics		K69322	Field
P. simplex	Zanzibar, Bwejuu	MG437418(Cytb), MH364296(ATP6/8)	MG576389(BFIB), MH364331(Myo)	Biometrics		K69323	Field
P. b. fischeri	Zanzibar, Bwejuu	MG437443(Cytb)	MG576390(BFIB), MH364351(Myo)	Biometrics		K69324	Field
P. b. fischeri	Zanzibar, Bwejuu	MG437438(Cytb)	MG576391(BFIB)	Biometrics		K69325	Field
P. b. fischeri	Zanzibar, Bwejuu	MG437444(Cytb)	MG576392(BFIB)	Biometrics		K69326	Field
P. b. fischeri	Zanzibar, Bwejuu	MG437445(Cytb)		Biometrics		K69327	Field
P. b. fischeri	Zanzibar, Bwejuu	MG437446(Cytb)	MG576362(BFIB)	Biometrics		K69328	Field
P. b. fischeri	Zanzibar, Bwejuu	MG437440(Cytb)		Biometrics		K69329	Field
P. b. fischeri	Zanzibar, Bwejuu	MG437441(Cytb)	MG576393(BFIB)	Biometrics		K69330	Field
P. b. fischeri	Zanzibar, Bwejuu	MG437447(Cytb)	MG576394(BFIB)	Biometrics		K69331	Field
P. b. fischeri	Zanzibar, Bwejuu	MG437448(Cytb)	MG576395(BFIB)	Biometrics		K69332	Field
P. b. fischeri	Zanzibar, Bwejuu	MG437449(Cytb)	MG576396(BFIB)	Biometrics		K69333	Field
P. b. fischeri	Zanzibar, Bwejuu	MG437450(Cytb)	MG576397(BFIB)	Biometrics		K69334	Field
P. b. fischeri	Zanzibar, Masingini	MG437451(Cytb)	MG576398(BFIB)	Biometrics		K69335	Field
P. b. fischeri	Masing	MG437439(Cytb)		Biometrics		K69337	Field
P. b. fischeri	Diani, Kenya	MG437452(Cytb)	MG576366(BFIB)	Biometrics		K69339	Field
P. c. extoni	Uvinza, Tanzania	MH364194(Cytb), MH364297(ATP6/8)		Biometrics	Radseq	K69340	Field
P. b. fischeri	Buda Forest, Kenya	MG437453(Cytb)	MG576367(BFIB)	Biometrics		K69341	Field
P. b. fischeri	Buda Forest, Kenya	MG437454(Cytb)	MG576368(BFIB)	Biometrics		K69342	Field
P. b. fischeri	Shimoni, Kenya	MG437455(Cytb)	MG576369(BFIB)	Biometrics		K69343	Field
P. b. fischeri	Shimoni, Kenya	MG437456(Cytb)	MG576370(BFIB)	Biometrics		K69344	Field

P. b. fischeri	Shimoni, Kenya	MG437457(Cytb)	MG576371(BFIB)	Biometrics		K69345	Field
P. b. fischeri	Shimoni, Kenya	MG437458(Cytb)	MG576372(BFIB)	Biometrics		K69346	Field
P. b. fischeri	Shimoni, Kenya	MG437459(Cytb)	MG576373(BFIB)	Biometrics		K69347	Field
P. b. fischeri	Diani, Kenya	MG437460(Cytb)	MG576375(BFIB)	Biometrics		K69348	Field
P. b. fischeri	Diani, Kenya	MG437461(Cytb)	MG576376(BFIB)	Biometrics		K69349	Field
P. b. fischeri	Diani, Kenya	MG437462(Cytb)	MG576377(BFIB)	Biometrics		K69350	Field
P. b. fischeri	Diani, Kenya	MG437463(Cytb)	MG576378(BFIB)	Biometrics		K69351	Field
P. b. fischeri	Diani, Kenya	MG437464(Cytb)	MG576379(BFIB)	Biometrics		K69352	Field
P. b. fischeri	Diani Forest, Kenya	MG437465(Cytb)	MG576380(BFIB)	Biometrics		K69353	Field
P. b. fischeri	Tiwi Beach, Kenya	MG437466(Cytb)	MG576381(BFIB)	Biometrics		K69354	Field
P. b. fischeri	Tiwi Beach, Kenya	MG437467(Cytb)	MG576382(BFIB)	Biometrics		K69355	Field
P. b. fischeri	Tiwi Beach, Kenya	MG437468(Cytb)	MG576383(BFIB)	Biometrics		K69356	Field
P. p. affinis	Tiwi Beach, Kenya			Biometrics	Radseq	K69357	Field
P. p. affinis	Vipingo, Kenya			Biometrics	Radseq	K69358	Field
P. p. affinis	Watamu, Kenya	MG437478(Cytb), MH364298(ATP6/8)		Biometrics	Radseq	K69359	Field
P. p. affinis	Lamu, Kenya	MH364192(Cytb), MH364299(ATP6/8)		Biometrics	Radseq	K69360	Field
P. b. fischeri	Sokoke, Kenya	MG437469(Cytb)	MG576386(BFIB), MH364353(Myo)	Biometrics		K69361	Field
P. b. fischeri	Sokoke, Kenya	MG437470(Cytb)	MG576387(BFIB)	Biometrics		K69362	Field
P. b. fischeri	Sokoke, Kenya	MG437471(Cytb)		Biometrics		K69363	Field
P. b. fischeri	Watamu, Kenya	MG437472(Cytb)	MG576384(BFIB)	Biometrics		K69364	Field
P. p. pusillus	Tshaneni, Swaziland			Biometrics	Radseq	K69365	Field
P. b. bilineatus	Mbuluzi, Swaziland	MG437477(Cytb)		Biometrics		K69367	Field
P. scolopaceus		MH364300(ATP6/8)	MH364332(Myo)	Biometrics		KU8528	FMNH

Lybius dubius	GenBank					B39244	GenBank
P. makawai	Zambia	MG211673(Cytb), MG230187(ATP6/8)	MG673556(BFIB)			1964.33.1	NHM
P. subsulphureus	Ghana	MH364191(Cytb), MH364301(ATP6/8)	MH364333(Myo)	Biometrics		N05502	Field
P. b. sharpei	Ghana	MH364190(Cytb), MH364302(ATP6/8)		Biometrics		N05511	Field
Sasia ochracea	GenBank					NC028019	GenBank
P. p. affinis	Iringa, Tanzania			Biometrics	Radseq	115488	ZMUC
P. p. affinis	Wenge East, Kenya	MH364189(Cytb), MH364303(ATP6/8)		Biometrics	Radseq	T37337	Field
Melanerpes carolinus	GenBank					U89192	GenBank
P. b. jacksoni	mtkenya, Kenya	MH364188(Cytb), MH364304(ATP6/8)	MH364334(Myo)	Biometrics		X85463	FMNH

Table A4. Museums where we obtained some of our samples.

Abbreviation	**Museum**
LACM	Natural History Museum of Los Angeles County
FMNH	The Field Museum of Natural History
AMNH	The American Museum of Natural History
BMNH	The British Natural History Museum
NMNH	The National Museum of Natural History
Peabody	The Peabody Museum of Yale University
LSU	Museum of Natural Science at Louisiana State University
MVZ	Museum of Vertebrate Zoology
MNHN	Museum National d'Histoire Naturelle
ZMUC	Zoological Museum of the University of Copenhagen
Tring	Natural History Museum at Tring
CAM	Charles University Collections